



The
University
Of
Sheffield.

**COPPER, CYTOCHROMES AND
*CAMPYLOBACTER***

NITANSHU GARG

B.TECH. INDIAN INSTITUTE OF TECHNOLOGY ROORKEE

**THIS THESIS SUBMITTED IN PART
FULFILMENT FOR THE DEGREE OF DOCTOR OF
PHILOSOPHY.**

**DEPARTMENT OF MOLECULAR BIOLOGY AND
BIOTECHNOLOGY.**

THE UNIVERSITY OF SHEFFIELD

NOVEMBER 2018

Abstract

Campylobacter jejuni, a foodborne microaerophilic pathogen, is the commonest cause of bacterial gastroenteritis in many countries. It uses complex cytochrome-rich respiratory chains, which includes a pathway to a *cbb₃*-type cytochrome-*c*-oxidase (CcoNOQP). This oxidase has been shown to be crucial in host colonisation and represents a potential anti-microbial target. The oxidase contains a bi-nuclear haem-copper active site consisting of Cu(B). Insertion of Cu(B) requires an assembly system of copper transporters and chaperones. In *C. jejuni*, it was discovered that products of *cj0908 -cj0911* gene operon are responsible for assembly of Cu in CcoN, with Cj0911 and Cj0909 being Sco1 and PCu_AC homologs, respectively, and Cj0910 and Cj0908 being membrane bound novel proteins with thioredoxin-like motifs. *ccoGHIS* is a cluster of genes, located downstream to *ccoNOQP* in many bacteria, required for oxidase biogenesis. In *C. jejuni* *ccoGHIS* homologues are not clustered. Homology and mutant studies identified Cj0369 as CcoG, Cj1483 as CcoH, Cj1155 as CcoI and Cj1154 as CcoS in *C. jejuni*. *cj1484c*, *cj1485c* and *cj1486c* are directly downstream to *ccoNOQP*, with an unknown function. This study shows that *cj1486c* gene product is essential for oxidase activity, with *cj1484c* and *cj1485c* gene products playing an important role.

C. jejuni requires copper (Cu) as a cofactor for several metalloproteins, including cytochrome *c* oxidase. Therefore, Cu transportation and assembly is crucial for respiration, growth and host colonisation. However, copper is also being used as a growth supplement for poultry feed due to its antimicrobial effects, but how *C. jejuni* responds to excess copper is largely unknown. In *C. jejuni* NCTC 11168, this study shows that a cluster of genes (*cj1161c-cj1164c*) encode proteins needed for Cu homeostasis. Cj1161 is a CopA homologue and Cj1162 is homologous to CopZ. The precise roles of proteins encoded by the other genes are unknown. Our study give insight into the mechanisms for both copper acquisition and tolerance in this pathogen.

The Nap and Tor reductase mediated nitrate and TMAO reduction is widespread in Gram-negative bacteria and supports growth of *C. jejuni* in oxygen limited conditions. This study shows that the quinol-cytochrome *c* reductase complex

(QcrABC) mediates the transfer of electron from menaquinone pool to Nap and Tor reductases in an electrogenic, energy conserving manner.

Acknowledgement

First of all, I would like to thank Prof David J. Kelly for giving me the opportunity to pursue PhD in his lab and for his guidance and support throughout the period. His level of extreme patience, kind personality, immense scientific knowledge, communication skills, proper work-life balance and maintenance of professional and personal relations will always inspire me in every aspect of life. Dave, you are the example of a perfect PhD supervisor who is not only concerned with the progress of his students but also about their well-being. Thank you for everything. It's been a pleasure to work with you.

To all the past and present members of the Kelly lab, with whom I enjoyed every bit of working together, thank you very much for all your help and support. Our lab walks, Christmas meals, Friday socials, and everyday coffee breaks are some of the pleasant memories I would cherish all my life. Thank you for making the work environment cheerful with all the jokes, fun and leg pulling.

To all my friends in Sheffield, thank you for being there always. I will always cherish the memories of having fun together, all the dinners, parties, walks, concerts, celebrations, etc. Sheffield wouldn't be Sheffield without you. I don't have words to express my love and affection to all my Roorkee friends, who are more like family now. Thank you for your constant support and encouragement.

To my wonderful parents and life's first teachers, Jai Gopal and Geeta Gupta, and lovely sister, Trupti, because of whom I'm what I'm today and who taught me the high virtues of life and the quality of being humble and simple. I can never thank you enough for all your support and sacrifices for me. You inspire me to dream big and strive to achieve them. Thank you for always having my back. One day I'll make you proud.

Last but not least, I would like to thank all my previous teachers, be it school or university, for guiding me in the right direction and building my strong academic base.

Thank you University of Sheffield Vice-Chancellor India Scholarship for funding this project.

This thesis is dedicated to my Grandfather (Late) Mr. Pherumal Gupta, who always inspired me to focus on education. I wish you could see my achievement, you'd be so proud of your grandson.

“I promise to leave this world a better place to live than I found it”

N. Garg Nov 2018

Publications and presentations

Publications:

Garg, N., Taylor A.J., and Kelly D.J. (2018). Bacterial periplasmic nitrate and trimethylamine-N-oxide respiration coupled to menaquinol-cytochrome *c* reductase (Qcr): Implications for electrogenic reduction of alternative electron acceptors. *Sci Rep.* 8(1), 15478.

Guccione, E.J., Kendall, J.J., Hitchcock, A., Garg, N., White, M.A., Mulholland, F., Poole, R.K., and Kelly, D.J. (2017). Transcriptome and proteome dynamics in chemostat culture reveal how *Campylobacter jejuni* modulates metabolism, stress responses and virulence factors upon changes in oxygen availability. *Environ Microbiol.* 19(10), 4326-4348.

Presentations:

Garg, Nitanshu and Kelly, David J. (2018). Assembly of the Cytochrome *c* Oxidase in *Campylobacter jejuni*. Bacterial electron transfer processes and their regulation. Saint Tropez, France. (Poster presentation)

Garg, Nitanshu and Kelly, David J. (2018). Assembly of Cytochrome *c* Oxidase and Copper Homeostasis System in *Campylobacter jejuni*. University of Sheffield PhD symposium. Sheffield, UK. (Oral presentation)

Garg, Nitanshu and Kelly, David J. (2017). Assembly of the Cytochrome *c* Oxidase in *Campylobacter jejuni*. *Campylobacter, Helicobacter and relative Organisms*. Nantes, France. (Poster presentation)

Garg, Nitanshu and Kelly, David J. (2017). Copper management and transportation in *Campylobacter jejuni*. *Campylobacter, Helicobacter and relative Organisms*. Nantes, France. (Poster presentation)

Garg, Nitanshu and Kelly, David J. (2017). Assembly of the Cytochrome *c* Oxidase in *Campylobacter jejuni*. Microbiology Society Annual Conference. Edinburgh, UK. (Poster presentation)

Garg, Nitanshu and Kelly, David J. (2017). Assembly of Cytochrome *c* Oxidase and Copper Homeostasis System in *Campylobacter jejuni*. University of Sheffield PhD symposium. Sheffield, UK. (Poster presentation)

Garg, Nitanshu and Kelly, David J. (2016). Assembly of the Cytochrome *c* Oxidase in *Campylobacter jejuni*. M4 Midlands Microbiology Conference. Leicester, UK. (Oral presentation)

Garg, Nitanshu and Kelly, David J. (2015). Assembly of the Cytochrome *c* Oxidase in *Campylobacter jejuni*. Microbiology Society Annual Conference. Liverpool, UK. (Poster presentation)

Garg, Nitanshu and Kelly, David J. (2015). Assembly of the Cytochrome *c* Oxidase in *Campylobacter jejuni*. Microbiology Society Annual Conference. Nottingham, UK. (Poster presentation)

Abbreviations list

aa	Amino acid
Ab _{Sxxx}	Absorbance at xxx nm
Amp	Ampicillin
APS	Ammonium persulfate
ATP	Adenine triphosphate
bp	Base pair
BSA	Bovine serum albumin
°C	Degrees Celsius
Cam	Chloramphenicol
cat	Chloramphenicol acetyl transferase
cDNA	Complementary DNA
CFE	Cell free extract
Cio	Cyanide-insensitive oxidase
CO ₂	Carbon dioxide
Cu	Copper
Cyd	Cytochrome <i>bd</i> oxidase
Da	Dalton
dH ₂ O	Distilled water
DMSO	Dimethyl sulphoxide
DNA	Deoxyribonucleic acid
DNase	Deoxyribonuclease
DTT	Dithiothreitol
EDTA	Ethylenediamine tetra-acetic acid
ETC	Electron transport chain
Fdh	Formate dehydrogenase
Fe-S	Iron sulphur
fla	Flagellin
Fur	Ferric uptake regulator
g	Gram
GBS	Guillain-Barré syndrome

H ₂ O	Water
H ₂ O ₂	Hydrogen peroxide
HCl	Hydrochloric acid
HEPES acid	4-(2-hydroxyethyl)-1-piperazineethanesulfonic acid
HO·	Hydroxyl radical
hr	Hour
Hyd	Hydrogenase
ICP-MS	Inductively coupled plasma mass spectrometry
IM	Inner membrane
IPTG	Isopropyl β-D-1-thiogalactopyranoside
ISA	Isothermal assembly
kan	Kanamycin
kb	Kilobase
kDa	KiloDalton
l	Litre
LacZ	β-galactosidase
LB	Luria-Bertani
M	Molar
MeMα	Minimum Essential Medium Alpha
mg	Milligram
MH	Muller-Hinton
MHS	Muller-Hinton with 20 mM serine
min	Minutes
ml	Millilitre
mM	Millimolar
mm	Millimetre
mM	Millimolar
mRNA	Messenger ribonucleic acid
ms	Millisecond
MW	Molecular weight
NAD(P)	Nicotinamide adenine dinucleotide (phosphate)

NAD(P)H reduced	Nicotinamide adenine dinucleotide (phosphate)
ng	Nanogram
nm	Nanometer
nM	Nanomolar
NMR	Nuclear magnetic resonance
NO	Nitric oxide
O ₂ ⁻	Superoxide
OD _{xxx}	Optical density at XXX nm
OM	Outer membrane
Oor	2-oxoglutarate : acceptor oxidoreductase
ORF	Open reading frame
PAGE	Polyacrylamide gel electrophoresis
PBS	Phosphate buffered saline
PCR	Polymerase chain reaction
pH	Hydrogen potential
PMF	Proton motif force
Por	Pyruvate:acceptor oxidoreductase
psi	Pound force per square inch
QH ₂ O	Milli-Q water
qRT-PCR	Quantitative reverse transcriptase PCR
r.p.m.	Revolutions per minute
RNA	Ribonucleic acid
RNAse	Ribonuclease
ROS	Reactive oxygen species
RPM	Revolutions per minute
RT	Room temperature
s	Second
Sco	Synthesis of Cytochrome c Oxidase
SDS	Sodium dodecyl sulphate
TAE	Tris acetate EDTA solution
TCA	Tricarboxylic acid cycle

TEMED	N,N,N',N'-tetramethyl- ethane-1,2-diamine
TMA	Trimethylamine
TMAO	Trimethylamine-N-oxide
TMPD	<i>N,N,N',N'</i> -tetramethyl- <i>p</i> -phenylenediamine
Tris	Tris(hydroxymethyl)aminomethane
UV	Ultraviolet
v/v	Concentration, volume/volume
w/v	Concentration, weight/volume
WT	Wild-type
x g	Multiplied by gravitational force
μg	Microgram
μl	Microlitre
μM	Micromoles

Table of contents

Abstract	i
Acknowledgements	iii
Publications and Presentations	v
Abbreviations list	vii
Table of contents	xi
Chapter 1 Introduction	1
1.1 <i>Campylobacter jejuni</i> :	3
1.1.1 Discovery and taxonomy:	3
1.1.1.1 Brief introduction to the phylum <i>Epsilonproteobacteria</i> :	5
1.1.2 Genomic analysis and comparison of <i>Campylobacter jejuni</i> strains:	6
1.1.3 Pathogenicity and virulence factors of <i>Campylobacter jejuni</i> :	8
1.1.3.1 Epidemiology and transmission:	8
1.1.3.2 Motility and taxis:	11
1.1.3.3 Adhesion to host cells and invasion:	12
1.1.3.4 Toxin synthesis and secretion:	13
1.1.3.5 Protein glycosylation:	14
1.1.4 <i>C. jejuni</i> physiology:	15
1.1.4.1 Carbon catabolism:	16
1.1.4.1.1 Non-glycolytic nature of <i>C. jejuni</i> :	16
1.1.4.1.2 The tricarboxylic acid cycle and organic acid transport systems:	16
1.1.4.1.3 Amino acids/Organic acids are the main sources of carbon for <i>C. jejuni</i> :	17
1.1.4.1.4 Gluconeogenesis and anaplerotic reactions:	19
1.1.4.2 Microaerophily:	20
1.1.4.3 Capnophily:	23
1.2 Bacterial Electron transport chains:	23
1.2.1 Electron transport chains in <i>C. jejuni</i> :	24
1.2.2 The various electron donors to the ETC in <i>C. jejuni</i> :	25
1.2.2.1 Hydrogen and formate:	25
1.2.2.2 Malate:	26
1.2.2.3 Lactate:	27
1.2.2.4 Succinate:	27
1.2.2.5 Sulphite:	27

1.2.2.6 Gluconate:	28
1.2.2.7 Proline:	28
1.2.3 The quinone pool:	28
1.2.4 The menaquinol-cytochrome <i>c</i> reductase (Qcr) complex:	29
1.2.5 <i>c</i> -type cytochromes:	30
1.2.6 Terminal oxidases for oxygen dependent respiration:	31
1.2.6.1 <i>cbb</i> ₃ -type cytochrome <i>c</i> oxidase:	31
1.2.6.1.1 Assembly of <i>cbb</i> ₃ -type cytochrome <i>c</i> oxidase:	32
1.2.6.1.2 CcoGHIS:	33
1.2.6.2 CioAB oxidase:	34
1.2.7 Respiration with alternative electron acceptors under oxygen limited condition:	34
1.2.7.1 S- or N-oxide reductases:	35
1.2.7.2 Nitrate:	35
1.2.7.3 Nitrite reduction to ammonium:	36
1.2.7.4 Fumarate:	37
1.2.7.5 Hydrogen peroxide:	37
1.3 Role of metals in bacteria:	38
1.4 Copper:	39
1.4.1 Copper chemistry:	39
1.4.2 Role of Cu in bacterial physiology and as an antimicrobial	39
1.4.3 Cu as Fenton reagent:	39
1.4.4 Cu in humans:	40
1.4.5 Bacterial Copper Homeostasis:	40
1.4.6 Role of Cu in <i>C. jejuni</i> :	42
1.4.6.1 Cu acquisition in <i>C. jejuni</i> :	42
1.5 Aim of this project:	43
Chapter 2 Materials & Methods	45
2.1 Materials:	47
2.2 Organisms and growth media:	47
2.2.1 Organisms used in this study:	47
2.2.2 Growth media preparation:	49
2.2.2.1 Media preparation for <i>C. jejuni</i> growth:	49
2.2.2.2 Media preparation for <i>E. coli</i> growth:	49

2.2.2.3 Antibiotic Solutions:	49
2.3 Growth of Bacterial Cells:	50
2.3.1 Growth of <i>C. jejuni</i> in complex media:	50
2.3.2 Growth of <i>C. jejuni</i> in minimal media:	50
2.3.3 Oxygen-limited growth of <i>C. jejuni</i> :	50
2.3.4 Continuous chemostat culture of <i>C. jejuni</i> :	50
2.3.5 Growth of <i>E. coli</i> :	51
2.3.6 Culture growth measurement:	51
2.3.7 Check for contamination:	51
2.4 DNA preparation and manipulation:	52
2.4.1 Genomic DNA (gDNA) isolation:	52
2.4.2 Plasmid DNA isolation:	52
2.4.2.1 Plasmids used in this study:	53
2.4.3 Nucleotide concentration measurement:	55
2.4.4 Polymerase Chain Reaction (PCR):	55
2.4.4.1 PCR for Gene fragment amplification:	56
2.4.4.2 PCR for complementation gene amplification:	57
2.4.4.3 PCR for screening:	57
2.4.5 PCR primers used in this study:	58
2.4.6 Agarose gel electrophoresis:	63
2.4.7 PCR product clean up:	64
2.4.8 Digestion of DNA with Restriction Enzymes:	64
2.4.9 Alkaline Phosphatase Treatment:	65
2.4.10 DNA Ligation:	65
2.4.11 Isothermal Assembly (ISA) cloning:	66
2.5 Preparation and transformation of competent bacterial cells:	68
2.5.1 Preparation of <i>E.coli</i> competent cells	68
2.5.2 Transformation of competent <i>E.coli</i> cells:	69
2.5.3 Preparation of competent <i>C. jejuni</i> cells:	69
2.5.4 Transformation of competent <i>C. jejuni</i> cells:	70
2.6 RNA extraction and manipulation:	71
2.6.1 mRNA extraction from <i>C. jejuni</i> :	71
2.6.2 Real time quantitative reverse transcriptase PCR (qRT-PCR):	72

2.6.3 qRT-PCR primers used in this study:	73
2.7 Total and Inner membrane protein extraction from <i>C. jejuni</i> :	74
2.7.1 Preparation of <i>C. jejuni</i> cell-free extract:	74
2.7.2 Removal of metal contamination:	74
2.7.3 Total membrane protein extraction from <i>C. jejuni</i> :	75
2.7.4 Inner membrane protein extraction from <i>C. jejuni</i> :	75
2.7.5 Protein concentration measurement by Lowry assay:	75
2.8 Bacterial cell sample preparation for ICP-MS:	76
2.9 Growth curves:	76
2.9.1 Oxygen limiting growth curves and supernatant sample collection:	77
2.10 Microaerobic growth sensitivity assays:	77
2.10.1 Copper sensitivity assay:	77
2.10.2 Zinc sensitivity assay:	78
2.10.3 Cobalt sensitivity assay:	78
2.10.4 Nickel sensitivity assay:	78
2.11 Measurement of Cytochrome-c-oxidase activity:	78
2.12 Reductase activity assays:	79
2.12.1 TMAO reductase activity assay:	79
2.12.2 Nitrate reductase activity assay:	79
2.13 Measurement of Reactive Oxygen Species (ROS):	80
2.14 One-Dimensional sodium dodecyl sulfate polyacrylamide gel electrophoresis (SDS-PAGE):	80
2.15 Detection of c-type cytochromes by enhanced chemiluminescence (Haem blot) assay:	81
2.16 cytochrome <i>c</i> difference spectroscopy:	82
2.17 Prediction of transmembrane helices in protein sequences:	82
2.18 Western Blot:	83
Chapter 3 Cytochrome <i>c</i> Oxidase Assembly in <i>Campylobacter jejuni</i>	85
3.1 Introduction:	87
3.2 Results:	88
3.2.1 Gene arrangement in <i>C. jejuni</i> genome:	88
3.2.1.1 Putative genes expressing assembly proteins:	88

3.2.1.2 Genes expressing CcoGHIS proteins and genes downstream of <i>ccoNOQP</i> :	89
3.2.2 Bioinformatics analysis for finding homologous sequences:	91
3.2.3 Prediction of transmembrane helices in proteins:	93
3.2.4 Generation of Knock out mutants in <i>C. jejuni</i> 11168 by ISA:	98
3.2.4.1 Attempted complementation of $\Delta cj0908-cj0911$, $\Delta cj0369c$, $\Delta cj1154c$ and $\Delta cj1155c$ <i>C. jejuni</i> mutant strains:	103
3.2.5 Cytochrome <i>c</i> oxidase activity during microaerobic growth in batch culture of <i>C. jejuni</i> :	104
3.2.6 CcoNOQP abundance is not heavily regulated by oxygen availability:	105
3.2.7 Effect of formate on growth and oxidase activity in <i>C. jejuni</i> :	106
3.2.8 Cu sensitivity of growth of putative Cco assembly mutants:	108
3.2.9 Putative Cco assembly mutants show reduced, but not abolished Cytochrome <i>c</i> Oxidase activity:	109
3.2.10 <i>ccoG</i> , <i>ccoH</i> and <i>ccoI</i> mutants showed a growth defect with <i>ccoI</i> being Cu sensitive:	111
3.2.11 Cells lacking CcoGHIS show reduced or abolished Cytochrome <i>c</i> Oxidase activity:	113
3.2.12 Effect of <i>cj0908-11</i> operon, <i>cj1154c</i> and <i>cj1155c</i> deletion on biogenesis of cytochrome <i>c</i> oxidase subunits:	115
3.2.12.1 Deletion of <i>cj0908-11</i> operon, <i>cj1154c</i> and <i>cj1155c</i> does not affect biogenesis of the CcoO subunit of cytochrome <i>c</i> oxidase:	115
3.2.12.2 Attempts at Carbon monoxide difference spectroscopy to detect the active site Cu/b-heme centre in CcoN	116
3.2.12.3 Inductively coupled plasma mass spectrometry was inconclusive:	117
3.2.12.4 Attempt to detect CcoN using western blot:	118
3.2.13 Cu toxicity assay showed that cells lacking Cj1485 and Cj1486 are more sensitive to Cu with $\Delta cj1486c$ having a permanent growth defect:	119
3.2.14 Mutants lacking genes between <i>ccoP</i> and potential <i>ccoH</i> showed reduced or abolished Cco activity:	121
3.3 Disussion:	122
3.4 Conclusions and summary:	129

Chapter 4 Maintenance of Copper Homeostasis in *Campylobacter jejuni* **133**

4.1 Introduction:	135
4.2 Results:	137

4.2.1 Gene arrangement in <i>C. jejuni</i> genome:	137
4.2.2 Bioinformatics analysis for finding homologous sequences:	138
4.2.3 Prediction of transmembrane helices in proteins:	139
4.2.4 Generation of deletion mutants:	140
4.2.5 Copper toxicity assay:	144
4.2.6 Growth Curve Assays:	147
4.2.7 Quantification of the effect of Cu on gene expression:	149
4.2.8 Quantification of intracellular Cu content using ICP-MS:	151
4.2.9 Effect of copper homeostasis on cytochrome <i>c</i> oxidase activity:	153
4.2.10 Zinc, Cobalt and Nickel sensitivity of a putative Zn-Co-Ni transporter:	154
4.3 Discussion:	157
4.4 Summary and conclusion:	162
Chapter 5 Bacterial periplasmic nitrate and trimethylamine-N-oxide respiration coupled to menaquinol-cytochrome c reductase (Qcr): Implications for electrogenic reduction of alternative electron acceptors.	165
Preface:	165
Author contribution:	165
Manuscript inserted:	166
Chapter 6 General conclusions and future work	167
Chapter 7 References	173
Appendix	199

Chapter 1

Introduction

1.1 *Campylobacter jejuni*:

1.1.1 Discovery and taxonomy:

The discovery of *Campylobacter jejuni* can be traced back to 1886, when Theodor Escherich, the German bacteriologist who discovered *Bacterium coli* in the human colon in 1885 and which was later changed to *Escherichia coli* in 1919 in his honour, observed organisms resembling campylobacters in stool samples of children with diarrhea (Kist, 1985; Vandamme, 2000; King and Adams, 2008; Vandamme *et al.*, 2010). In 1906, Mcfadyean and Stockman observed that a *vibrio*-like bacterium was responsible for abortions in Devon longwoolled ewes in the UK (Skirrow, 2006; Zilbauer *et al.*, 2008), and similar observations of *vibrio*-like bacteria were reported by Smith and Taylor in 1918 for abortions in cattle in USA (Kist, 1985). Because of its morphological similarity to another *Vibrio* species, Smith and Taylor named it as *Vibrio fetus* (Smith, 1918). In 1927, Smith and Orcutt observed the same spiral shaped bacteria in the faeces of cattle with diarrhea and named them *Vibrio jejuni*. In 1947, Vinzent and co-workers reported the first confirmed *Campylobacter* human infection which caused abortion in two women suffering from fever. 10 years later, Elizabeth King isolated two *vibrio*-like bacteria from the blood of patients with diarrhea but failed to isolate them from feces of the patients because of limited growth technology at that time (Zautner and Masanta, 2016). In 1963, noticing the difference in DNA base composition, metabolism and respiration from other *vibrio* organisms, the genus *Campylobacter* was first proposed by Sebald and Véron (Etymologia: *Campylobacter*). The name *Campylobacter* came from two Greek words: *kampylos* (meaning curved) and *baktron* (meaning rod) because of its twisted rod like structure (Sebald and Veron, 1963). In 1968, *C. jejuni* was isolated from a human faeces sample for the first time by Dekeyser and Butzler using a filtration technique from a 20-year-old female suffering with severe diarrhea and fever in Brussels (Altekruse *et al.*, 1999). With the development of better techniques to isolate and identify *C. jejuni*, it was observed that this microorganism was actually an underreported endemic pathogen (Butzler *et al.*, 1973) and inspired microbiologists worldwide to understand this bacterium.

Campylobacter belongs to the family *Campylobacteraceae*, which also consists of the genera *Arcobacter* and *Sulfurospirillum*. The genus *Campylobacter*

comprises 25 species and 9 subspecies (Debruyne *et al.*, 2010). Different bacterial families, other than *Arcobacter* and *Sulfurospirillum*, like *Campylobacteraceae*, *Helicobacteraceae*, *Wolinella*, and *Thiovulum* species have been categorized into the *Campylobacterales* order based on their taxonomic studies and whole genome sequencing (Okoli *et al.*, 2007). They all come in the category of epsilonproteobacteria and have low G+C content (29 - 47 %) (Trust *et al.*, 1994; Debruyne *et al.*, 2008)

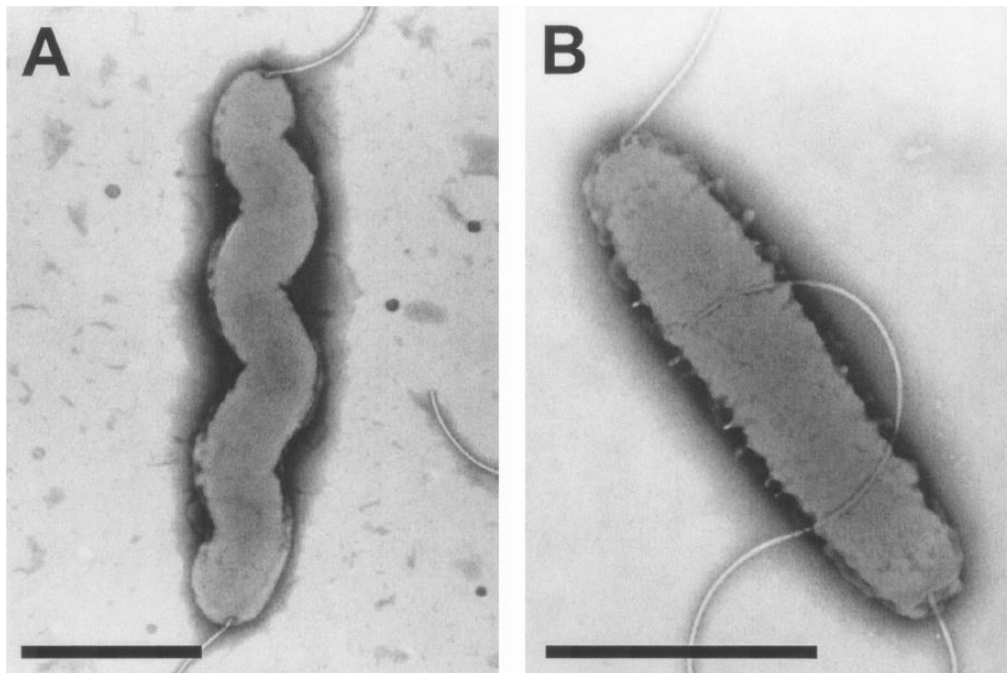


Figure 1.1: *Campylobacter jejuni* NCTC 11168 reference strain and original clinical isolate cell morphologies. (A) NCTC 11168-O the original clinical isolate of the wild type strain. (B) NCTC 11168-GS, a variant of the 11168-O strain used for producing the original 11168 genome sequence. The cells were negatively stained with 2% (w/v) phosphotungstic acid. The bars represent 1 μ M. Image adapted from (Gaynor *et al.*, 2004).

Campylobacter is a Gram-negative bacterium and its morphological characteristics include slender, curved, S-shaped or spiral rods, 0.5-5.0 μ m long and 0.2-0.8 μ m wide (Fig. 1.1). It is a non-spore forming microaerophilic bacterium which is highly motile due to presence of its single polar unsheathed flagella at one or both ends of the cell, which helps it in host colonisation as well. The first *C. jejuni* genome project was done with a reference strain *C. jejuni* NCTC11168 which was significantly different from the original clinical isolate, especially lack of distinctive spiral shape and reduced motility (Parkhill *et al.*, 2000; Gaynor *et al.*, 2004).

1.1.1.1 Brief introduction to the phylum *Epsilonproteobacteria*:

Most of the *Epsilonproteobacteria* are known for colonizing the deep sea thermal vents, unlike *Campylobacter* and *Helicobacter* species which prefer poultry (especially chicken) (Campbell *et al.*, 2006). *Epsilonproteobacteria* are supposed to be the second sub-group to diverge from the original proteobacteria group, which is estimated to have been diverged into 6 sub-groups, which thrive in diverse habitats (Gilbreath *et al.*, 2011). Their metabolically versatile nature makes them important for deep-sea chemical composition homeostasis, especially the Sulphur and Nitrogen cycles. The deep sea species are chemolithotrophs and oxidize reduced sulfur, formate, or hydrogen to meet their energy needs, coupled with the reduction of oxygen and nitrate (Takai *et al.*, 2005). They also help in fixing carbon dioxide into biomass by using the reverse Krebs cycle, which is significant for deep-sea marine life (Anbar and Knoll, 2002). Though on the basis of gross pathogenicity, *Campylobacter* is similar to other common enteric pathogens like *Salmonella* spp. and *Escherichia coli*, based on biological mechanisms involving biochemical processes, genetic regulatory pathways, and pathogenesis of disease, *Campylobacter* is very different from these distantly related enterobacteria

The closest genetically related genus to *Campylobacter* is *Helicobacter* (Vandamme, 2000). Previously known as *Campylobacter pylori*, *Helicobacter pylori* is linked with the development of duodenal ulcers and stomach cancer (Marshall *et al.*, 1988). More than half of the world's adult population is infected with *Helicobacter pylori*, colonising their upper gastrointestinal tracts (Amieva and Peek, 2016). However, frequency of infections vary from country to country. The helical shape of *H. pylori* has evolved to penetrate the mucoid lining of the stomach (Yamaoka, 2008) and it possess multiple virulence factors which can severely damage the epithelial layer (Kusters *et al.*, 2006). *Helicobacter* can also use molecular hydrogen as a respiratory substrate (Olson and Maier, 2002), a process which may have evolved in its deep-sea thermal vent ancestors. Another closely related species to *Campylobacter* is *Wolinella*, which has one third of the genome similar to *Campylobacter* and another one third to *Helicobacter* and together with *Helicobacter* form the family, Helicobacteraceae (Vandamme, 2000; Baar *et al.*, 2003). It can grow microaerobically and anaerobically, unlike *Campylobacter* and *Helicobacter*, using

hydrogen or formate as electron donors and a range of organic and inorganic compounds as electron acceptors (Kröger *et al.*, 2002).

1.1.2 Genomic analysis and comparison of *C. jejuni* strains:

The first *C. jejuni* NCTC11168 human isolate strain whole genome sequence was published in 2000 (Parkhill *et al.*, 2000; Fig. 1.2) and is constantly re-analyzed and re-annotated (Gundogdu *et al.*, 2007). The *C. jejuni* genome is relatively small with 1,641,481 base pair chromosome but compact with 1643 (revised from 1654 by Gundogdu *et al.*, 2007) open reading frames (ORFs), which makes it the densest prokaryotic genome sequence to date, with 94.3 % of the genome taken up with coding sequences (Parkhill *et al.*, 2000). Out of 1654, 19 are predicted to be pseudogenes. It consists of 54 stable RNA species and quite low G+C content (30.6 %). An interesting feature of the genome is phase variable switching of genes due to presence of 48 distinct poly-G/C tracts (Fouts *et al.*, 2005; Bayliss *et al.*, 2012), mostly found in genes for the biosynthesis or modification of surface structures. The whole genomic sequence availability facilitated research into the molecular physiology and pathogenicity of *C. jejuni* and also proposed potentially high metabolic versatility with a highly branched respiratory chain.

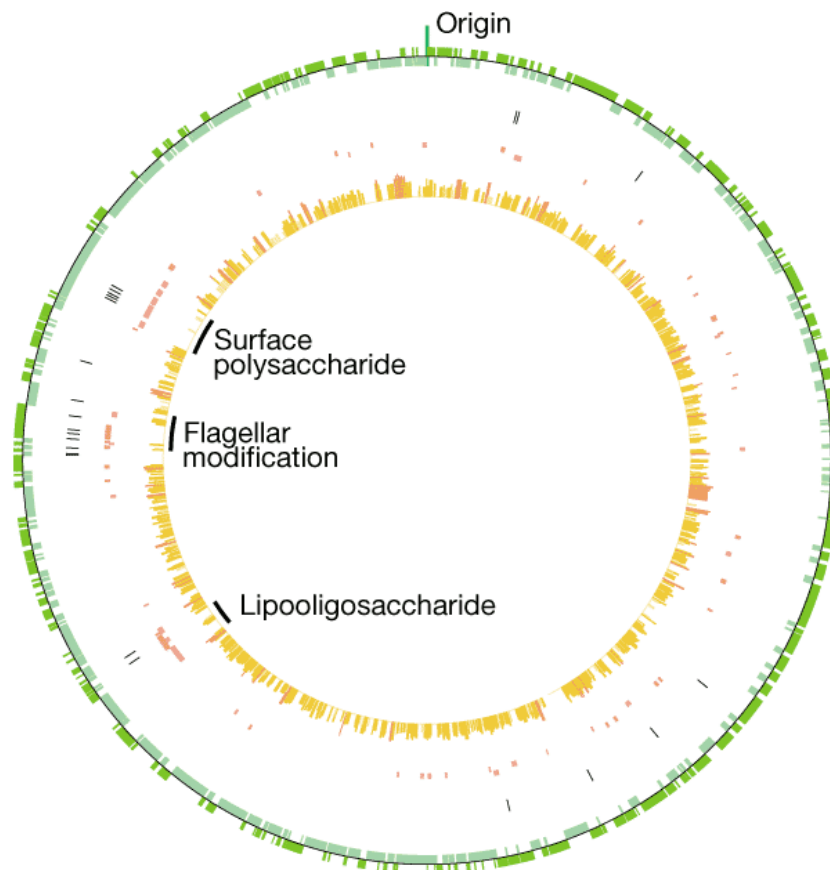


Figure 1.2: Circular genome sequence of *C. jejuni* NCTC 11168. Features of the 1,641,481 bp nucleotide sequence are represented by coloured concentric circles with the marked putative origin of replication. From the outside to the inside, the first circle shows coding sequences transcribed in the clockwise direction in dark green; the second shows coding sequences in the anticlockwise direction in pale green; the third shows the positions of hypervariable sequences in black, and the fourth and fifth show genes involved in the production of surface structures: clockwise in dark red and anticlockwise in pale red. The innermost histogram shows the similarity of each gene to its *H. pylori* orthologue, where present; the height of the bar, and the intensity of the colour, are proportional to the degree of similarity. Figure adapted from Parkhill *et al.*, 2000.

After NCTC11168, many other strains of *C. jejuni* were sequenced. Some commonly studied strains are: RM1221, sequenced in 2005, 81-176 in 2006, 81116 and CG8486 in 2007 (Fouts *et al.*, 2005; Hofreuter *et al.*, 2006; Pearson *et al.*, 2007; Poly *et al.*, 2007). The RM1221 strain of *C. jejuni* was isolated in 2000 and sequenced in 2005 (Miller *et al.*, 2000; Fouts *et al.*, 2005). Its genome is 1,777,831 bp long with 1884 potential ORFs, making 94 % of the genome taken up with coding sequences. It has an average G + C content of 30.31%, which is similar to that of 11168 reference strain (30.6 %). It contains 47 predicted pseudogenes, which is more than double that

in 11168 (contains only 20) and 12 of them are common in both (Gundogdu *et al.*, 2007). RM1221 has very low natural transformation efficiency, unlike 11168, potentially because of presence of two non-specific DNA/RNA endonucleases (Gaasbeek *et al.*, 2010). *C. jejuni* 81-176 strain is the strain with highest pathogenicity compared to other *C. jejuni* strains (Prendergast *et al.*, 2004). This makes it the most suitable known strain to be used in colonisation studies (Hofreuter *et al.*, 2006). Its genome is 1,594,651 bp long. Interestingly, it consists of 35 genes which are either absent or pseudogenes in both NCTC11168 reference strain and RM1221 (Hofreuter *et al.*, 2006; Gundogdu *et al.*, 2007). Some of them are: two DcuC homologues involved in succinate efflux, a dimethyl sulphoxide (DMSO) reductase, a glycerol-3-phosphate transporter (GlpT), cytochrome *c* and cytochrome biogenesis proteins and γ -glutamyltranspeptidase (*ggt*), having various roles in metabolism and pathogenicity. It also carries two plasmids containing important virulence factors: pVir, having components of a Type IV secretion system and a toxin-antitoxin system, where CjpT, a proteic toxin is inhibited at the RNA level by *cjpA*, a small non-coding RNA (Shen *et al.*, 2016); and pTet, confers tetracycline resistance and is a virulence factor in *C. jejuni* (Bacon *et al.*, 2002). Other than this, there are 51 genes which are present in 11168 but are absent in 81-176. The genome of another strain of *C. jejuni*, 81116 consists of 1,626 predicted ORFs with similar G+C content to 11168. It consists of only 17 poly-G tracts as compared to 30 in 11168 and is supposed to be both amenable to genetic manipulation as well as maintaining better genome fidelity (Manning *et al.*, 2001). The *C. jejuni* promoter regions differ from other bacteria, as instead of a -10 and -35 box region the *C. jejuni* promoters appear to contain only an extended -10 box (Petersen *et al.*, 2003).

1.1.3 Pathogenicity and virulence factors of *C. jejuni*:

1.1.3.1 Epidemiology and transmission:

C. jejuni, which was first recognized as a pathogen in 1977 (Byran and Doyle, 1995), is one of the most common causes of food borne illness and is a matter of great concern throughout the western world (Hofreuter, 2014). Consumption of uncooked or poorly cooked poultry (mainly chicken) and milk are the major source of infection in human beings (Blaser and Engberg, 2008; Allos, 2011, Figure 1.3). Untreated contaminated groundwater, cow or pig meat, mushrooms and shellfish as well as

domestic pets are some of the other sources (Dasti *et al.*, 2010). The most common hosts for *Campylobacter* are poultry birds, probably because of their 42 °C body temperature, which is the optimum growth temperature for *C. jejuni*. In general, *Campylobacter* colonizes 2-3 weeks old chickens with over 90% being colonized by 7 weeks. It has been reported that colonisation spreads rapidly among broiler chicken flocks and is almost impossible to eradicate once established in a flock (Evans and Sayers, 2000). In chickens and other poultry birds, *Campylobacter* species colonises the gastrointestinal tract, colon and caecum. From there they can reach the outer body of the bird during the process of washing and can be deposited in the feather follicles, where they remain viable at 4 °C for over 72 hours (Chantarapanont *et al.*, 2004).

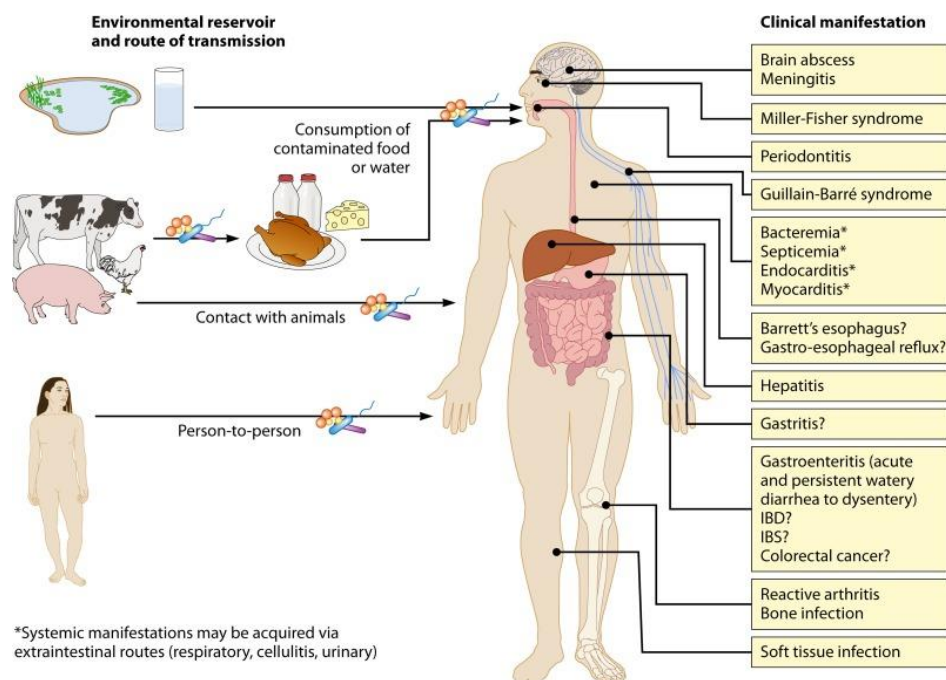


Figure 1.3: Sources and outcomes of *C. jejuni* infection. Several environmental reservoirs, like uncooked or poorly cooked poultry, contaminated groundwater, person to person, milk, cow or pig meat, can lead to human infection by *C. jejuni*. In humans, *C. jejuni* can invade the intestinal epithelial layer, resulting in inflammation and diarrhoea. Figure adapted from Kaakoush *et al.*, 2015.

C. jejuni colonises, reproduces and causes disease in the intestines of humans but is a commensal in birds (Elmi *et al.*, 2012, Figure 1.4). An infectious dose as low as 500 - 800 organisms is sufficient to cause illness in humans (Olson *et al.*, 2008). The optimum atmosphere for *C. jejuni* growth is 5 % CO₂, 10 % O₂ and 85 % N₂ and optimum temperature is 42 °C (Silva *et al.*, 2011). It is a leading cause of campylobacteriosis, a serious form of gastroenteritis in humans. *Campylobacter*

infection often leads to vomiting and diarrhea, which can be followed by bloody diarrhea for a few days and typically clears up in less than a week without treatment (Wassenaar and Blaser, 1999). The antibodies developed in the host body against the *C. jejuni* infection can result in autoimmunity against some neuronal cells. Therefore, in rare cases infection can be followed by acute paralysis, reactive arthritis or Guillain-Barré syndrome (GBS), ultimately leading to death (Ban Mishu Allos, 1998; Nachamkin *et al.*, 1998; Jacobs *et al.*, 2008).



Figure 1.4: *C. jejuni* colonisation in human. *C. jejuni* colonises, reproduces and causes disease in the intestines of humans

It has been suggested that reported *Campylobacter* infections are much lower in numbers than the actual level of infections, probably because of the similar symptoms shown with other food borne pathogens, like *E. coli* or *Salmonella*, which are better studied and easier to treat. In the United States, the infection rate is estimated about one in every 100 cases of food poisoning every year (Allos and Blaser, 1995). Surveys by the UK Food Standards Agency (FSA) have revealed that more than 70% of fresh chicken sold in UK supermarkets are contaminated with *C. jejuni* with 4.5% of chicken containing the highest level of contamination (containing more than 1000 colony forming units per gram, of campylobacter) in 2018. There is no doubt that *Campylobacter* infection is more common than expected and is the biggest cause of food poisoning in UK, responsible for 321,000 cases a year and around 100 deaths (2008 Defra Zoonoses report).

1.1.3.2 Motility and taxis:

One of the most important physiological characteristics of *C. jejuni* for its survival is its motility and chemotaxis, which enables host colonisation, virulence, protein secretion, host cell adhesion and invasion. It has flagellar motility, having a flagellum on each end of the rod shaped cell. It has been shown that *C. jejuni* cells lacking flagella, and subsequently its motility, were inefficient in chicken colonization and deficient in virulence in some animal models, including adhesion and invasion of human cells (Wassenaar *et al.*, 1991; 1993; Golden and Acheson 2002; Hendrixson and DiRita, 2004). This shows the importance of motility in the *C. jejuni* infection process. It is believed that the spiral shape and flagellar motility of *C. jejuni* facilitates the corkscrew motion, which helps it to penetrate the mucus of the small bowel of humans (Yao *et al.*, 1994; Golden and Acheson, 2002). *Campylobacter* swims with help of bipolar unsheathed flagellar, consisting of a basal body, a hook and filaments. These filaments are composed of FlaA (Cj1339) and FlaB (Cj1338) oligomers, which are close homologues of each other (91.9% sequence identity) (Guerry *et al.*, 1991).

Chemotaxis is motility under the influence of a chemical stimulation. It leads the bacterial cells towards or away with respect to a specific chemical (environmental attractants/repellants). Transmembrane methyl-accepting chemotaxis proteins (MCPs) are bacterial signalling proteins that sense these chemicals and transduce signals to the chemotaxis regulatory proteins; and influence the direction of cellular movement towards chemoattractants or away from chemorepellants. There are 10 methyl-accepting chemotaxis proteins, termed as Tlps (transducer-like proteins), predicted in the *C. jejuni* NCTC11168 genome (Marchant *et al.*, 2002). DocB (Cj0019) and DocC (Cj0262) are two examples of Tlps and it has been reported that cells lacking *docB* showed defects in chick gastrointestinal tract colonisation (Hendrixson and DiRita, 2004). *C. jejuni* showed a strong preference for amino acids and chemotaxis towards L-serine, L-fucose, L-glutamate, L-aspartate, L-cysteine, fumarate, pyruvate, succinate, malate, citrate and ketoglutarate (metabolic intermediates). Interestingly, most of them are found in high levels in the chick gastrointestinal tract (Hugdahl *et al.*, 1988). It also showed chemotactic motility towards mucins, which are secreted by epithelial cells. Some of the chemo-repellants to *C. jejuni* include deoxycholic acid, cholic acid and taurocholic acid (Hugdahl *et al.*, 1988). The *C. jejuni* chemotaxis

system is similar to that of *E. coli*. A set of *che* genes, namely, *cheA* (*cj0284*), *cheW* (*cj0283*), *cheY* (*cj1118*), *cheR* (*cj0923*), *cheB* (*cj0924*) and *cheZ* (potentially *cj0700*, but no direct homologue), are responsible for mediating chemotaxis.

Similar to chemotaxis, energy taxis is motility under the influence of energy stimulation, i.e. towards conditions of optimal metabolic activity by sensing the internal energetic conditions of cell. The presence of two energy taxis proteins CetA (Cj1190) and CetB (Cj1189) confers on *C. jejuni* the ability to move in response to localised energy levels, thought to be because of changes in the redox state of electron transport chain components/the proton motive force (Hendrixson *et al.*, 2001; Elliott and DiRita, 2008). CetB is a membrane-associated dimer, which serves as a signal sensing protein transmitting that signal to CetA, an integral membrane protein. Through CetA, this signal is directed to the chemotactic machinery, influencing it in deciding direction of movement (Elliott and DiRita, 2008). It has been established that both CetA and CetB are necessary for flagellar motility (Hendrixson *et al.*, 2001) and cells lacking CetB fail to invade human tissue culture cells (Golden and Acheson, 2002).

1.1.3.3 Adhesion to host cells and invasion:

For adhesion of bacterial cells to host cells, the bacterial cells require some specific components on the surface. The *C. jejuni* genome lacks genes encoding pili or fimbriae, which are a widely used structural mechanism by bacterial cells (well studied in *E. coli*) for host cell adhesion. Instead of this, *C. jejuni* cells adhere to host cells with the help of adhesins, including the flagellum, exposed on the surface of cells (Grant *et al.*, 1993). It has been shown that CapA (Cj0628/0629), CadF (Cj1478), FlpA (Cj1279c), and Cj1349c proteins produced by *C. jejuni* are responsible for adherence to chicken epithelial cells *in vitro* and PEB1 (Cj0921), CadF (Cj1478) and FlpA (Cj1279c) proteins play an important role in colonization of broiler chickens in *in vivo* (Flanagan *et al.*, 2009). CadF is an outer membrane fibrinectin binding protein (Konkel *et al.*, 1997) similar to FlpA (Flanagan *et al.*, 2009), CapA is an autotransporter protein (Ashgar *et al.*, 2007) and PEB1 is a periplasmic binding protein (Pei *et al.*, 1998), mediating interactions with epithelial cells (Leon-Kempis *et al.*, 2006). Other than these, the flagellar (Grant *et al.*, 1993), FlaC (Cj0720) (Song *et al.*, 2004), the major outer membrane protein (MOMP) PorA

(Cj1259) (Schroder and Moser, 1997), the surface capsular polysaccharide (Bacon *et al.*, 2001), lipooligosaccharide (LOS) (McSweegan and Walker, 1986), the surface exposed P95 (Kelle *et al.*, 1998) and the surface attached lipoprotein JlpA (Cj0983) (Jin *et al.*, 2001) also play an important role in host cell adhesion of *C. jejuni*.

C. jejuni promotes its uptake and to invade intestinal epithelial cells by altering host cell biology in a microtubule-dependent, actin-independent manner (Oelschlaeger *et al.*, 1993). In order to save itself from destruction in the lysosomes inside the host cells, *C. jejuni* produces its own membrane-bound compartment called the *Campylobacter*-containing vacuole (CCV) where it undergoes physiological changes in oxygen sensitivity and metabolism, allowing survival and replication (Watson and Galán, 2008). It is possible that caveolae markers are acquired by these CCVs in the early stages of uptake process, making Caveolin-1 protein essential for the efficient host cell entry of *C. jejuni* (Watson and Galán, 2008b). Nevertheless, the endocytic machinery associated with caveolae is energy intensive and seems unnecessary for bacterial uptake (Watson and Galán, 2008a). Therefore, it has been proposed that caveolae may be required for the assembly of a signal transduction pathway(s) that is exploited by *C. jejuni* to gain entry (Watson and Galán, 2008a). It has been shown that a series of invasion antigens known as *Campylobacter* invasion antigens (Cia) are produced and secreted by *C. jejuni* (Rivera-Amill *et al.*, 2001).

1.1.3.4 Toxin synthesis and secretion:

The transition of diarrhea from watery to bloody shows the capability of *C. jejuni* toxins to damage the epithelial lining of the intestines. This suggests that toxins are important for pathogenicity of *C. jejuni* and progression of disease. Different strains of *C. jejuni* are characterised with a variety of different types of toxins, some being studied better than others. In *C. jejuni* NCTC11168, the cytolethal distending toxins CdtABC (Cj0079-Cj0077) is the best-studied toxin (Dasti *et al.*, 2010; Lara-Tejero and Galán, 2001). *C. jejuni* NCTC11168 genome also encodes *pldA* (*cj1351*), a phospholipase producing gene (Ziprin *et al.*, 2001); *tlyA* (*cj0588*), encoding a putative contact dependent haemolysin; and *cj0183*, a novel gene potentially encoding a putative integral membrane protein with a haemolysin domain (Sałamaszyńska-Guz and Klimuszko, 2008). CDT is secreted to the surface of *C. jejuni* through outer membrane vesicles (Lindmark *et al.*, 2009) but the uptake mechanism for the

incorporation into the host's eukaryotic cells is not known yet. It has been established that presence and activity of all three subunits of Cdt proteins is essential for the CDT toxicity, which form an active tripartite holotoxin that exhibits full cellular toxicity (Lara-Tejero and Galán, 2001). CdtA and CdtC proteins, containing lectin like regions which are structurally similar to the toxin ricin (which recognise oligosaccharides), stays on the membrane of the target cell (Heywood *et al.*, 2005; Young *et al.*, 2007); whereas CdtB behaves as an active component of CDT system and exhibit a nuclease activity resulting in a rapid and specific cell cycle arrest (in HeLa and Caco-2 cells) (Whitehouse *et al.*, 1998). In other words, CdtA and CdtC work together to insert CdtB inside the target cell; where CdtB degrade DNA of host cell and lead to pre-programmed cell death (Lara-Tejero and Galán, 2001). Besides this, the role of CDT in the virulence process is unclear. *C. jejuni* cells lacking *cdt* were unaffected in host cell colonisation and adherence but showed inefficiency in invasiveness (Purdy *et al.*, 2000; Biswas *et al.*, 2006). Cells lacking *tlyA* showed defect in host cell invasion and lack hemolytic activity *in-vitro* as well; while deletion of *cj0183* does not abolish hemolytic activity (Sałamaszyńska-Guz and Klimuszko, 2008). Therefore, it can be concluded that some other un-annotated hemolytic proteins maybe responsible for haemolysis. Absence of *pldA* resulted in impaired chicken colonisation (Ziprin *et al.*, 2014).

1.1.3.5 Protein glycosylation:

Glycosylation is an important post-translational modification of proteins that determines protein structure, function and stability by covalently binding various sugar moieties to proteins. *C. jejuni*, despite having a small genome, possesses a complex glycosylation system to modify a range of target proteins, which includes both N- and O-linked glycans (reviewed in Gilbreath *et al.*, 2011). A glycan to the amide nitrogen of an asparagine residue is linked by N-linked glycosylation whereas a glycan to the hydroxyl group of threonine or serine is linked by O-linked glycosylation.

The N-linked glycosylation pathway in *C. jejuni* is used as a model system because this form of glycan addition had only been observed in eukaryotes and archaea before being discovered in *C. jejuni* (Szymanski *et al.*, 1999). Its biological function is still not well understood. The attachment of the N-acetylgalactosamine-

containing heptasaccharide (Young *et al.*, 2002; Kowarik *et al.*, 2006) to the asparagine residues of conserved sequence (D/E-X-N-Z-S/T, where N is the glycosylated asparagine and the X and Z are any amino acid; with the exception of proline) (Kowarik *et al.*, 2006) of some proteins and biosynthesis of N-linked glycans (Szymanski *et al.*, 1999) is mediated by the *pgl* gene cluster (*cj1119c-cj1130c*). It has been reported that cells lacking the *pgl* gene cluster showed impaired adherence/invasion of human intestinal epithelial cells and inefficient colonisation of animal models (Karlyshev *et al.*, 2004). It has also been observed that N-linked proteins also weaken the immune response in human (van Sorge *et al.*, 2009).

The O-linked glycosylation system is responsible for heavily modifying the flagellar FlaA protein (McNally *et al.*, 2006). It is also linked with adherence to and invasion of human epithelial cells (Szymanski *et al.*, 2002); filament formation and motility (Goon *et al.*, 2003); and animal models of infection colonization (Szymanski *et al.*, 2002). Its biological function is still not clear but O-linked glycosylation of exposed regions of the flagella suggest that glycans are immunogenic and may contribute to evasion of the host immune system (Power *et al.*, 1994; Thibault *et al.*, 2001). In *C. jejuni*, pseudaminic acid derivatives, produced by *pse* gene cluster, is a major O-linked glycan modification. Cells lacking *pse* genes lack motility, which suggest that O-linked glycosylation plays an important role in motility, and indirectly in efficient colonisation and adherence (McNally *et al.*, 2006, Nothaft and Szymanski, 2010).

1.1.4 *C. jejuni* physiology:

Bacterial physiology is the study of all the characteristics of a bacterium, which helps it to grow and survive. The physiology of *C. jejuni* plays an important role, directly or indirectly, in its colonization and virulence. This aspect of *C. jejuni* was highlighted by analysis of its genomic sequence. Before this (Parkhill *et al.*, 2000), it was very difficult to understand the metabolic pathways of *C. jejuni* as it always grows in complex environmental conditions with complex substrates. Therefore, more and more focus was just given to its colonisation and virulence mechanism.

1.1.4.1 Carbon catabolism:

1.1.4.1.1 Non-glycolytic nature of *C. jejuni*:

Glycolysis is a metabolic pathway, which is critical for carbon metabolism in many prokaryotic and eukaryotic cells. It converts glucose to pyruvate and releases ATP and NADH. ATP can be utilized by cells as an energy source directly while NADH is converted indirectly to ATP via the electron transport chain and ATPase utilising the proton-motive force. *C. jejuni*, on the other hand, is unable to utilize glucose because of absence of nonreversible glycolytic enzyme 6-phosphofruktokinase, which is an integral component of Embden-Meyerhof-Parnas (EMP) pathway (Parkhill *et al.*, 2000; Kelly, 2008). It has also been reported that BIOLOG phenotype microarray analyses showed no sign of stimulated respiratory activity of *C. jejuni* either by adding hexoses and pentoses like galactose, fructose, trehalose, rhamnose, ribose, or the presence of disaccharides maltose, lactose and sucrose (Line *et al.*, 2010; Gripp *et al.*, 2011; Muraoka and Zhang, 2011). However, in certain strains of *C. jejuni*, it has been discovered that L-fucose can be utilized as a carbon/energy source supporting growth (Stahl *et al.*, 2011; Muraoka and Zhang, 2011). It has also been observed that the 11168 strain contains fucose-inducible enzymes, which mediate sugar uptake and metabolism and helps in host intestinal colonisation as L-fucose is the predominant saccharide in mucins (particularly in the small intestine and cecum) (Stahl *et al.*, 2011).

1.1.4.1.2 The tricarboxylic acid cycle and organic acid transport systems:

The genome sequence of *C. jejuni* showed that homologues of most of the essential enzymes required for the operation of a complete oxidative tricarboxylic acid (TCA) cycle are expressed by it (Parkhill *et al.*, 2000). However, there is no direct homologue of 2-oxoglutarate dehydrogenase and pyruvate dehydrogenase produced by *C. jejuni* but homologues of other important enzymes like fumarate reductase complex (*frdABC*), NAD-linked malate dehydrogenase, the α and β subunit of succinyl-coA synthetase, and a malate:quinone oxidoreductase are produced (Kelly, 2001). It has been reported that Por, the flavodoxin/ferredoxin-dependent pyruvate:acceptor oxidoreductase encoded by *cj1476c* and Oor, the related 2-oxoglutarate:acceptor oxidoreductase complex encoded by *oorDABC* (*cj0535-cj0538* operon) replace pyruvate dehydrogenase and 2-oxoglutarate dehydrogenase in *C.*

jejuni with Por mediating oxidative decarboxylation of pyruvate to acetyl-CoA and Oor mediating the conversion of oxoglutarate to succinyl-CoenzymeA (Kelly, 2008). Iron-sulphur (Fe-S) clusters are present in both Por and Oor. These are highly sensitive to oxygen and Por and Oor are mostly found in obligate anaerobes. This might contribute to the microaerophilicity of *C. jejuni* (Kelly, 2008; Kendall *et al.*, 2014). In *H.pylori*, flavodoxin reduced by Por is re-oxidised by transfer of electrons mediated by an additional redox protein (Hughes *et al.*, 1998). In *C. jejuni* NCTC11168, Cj0559 is homologous to this protein (St Maurice *et al.*, 2007) but it has not been proved that whether it performs the same function or not. More likely, is that these electrons are donated to the respiratory complex I (Fig. 1.5).

1.1.4.1.3 Amino acids/Organic acids are the main sources of carbon for *C. jejuni*:

The *C. jejuni* genome has genes which enables this bacterium to transport and enzymatically catabolise several amino acids (Parkhill *et al.*, 2000), which are major sources of carbon and energy for *C. jejuni* (Fig. 1.5). Aspartate, glutamate, serine and proline are the amino acids efficiently utilised by most of the strains of *C. jejuni* for proliferation. For aspartate, glutamate (Leon-Kempis *et al.*, 2006; Guccione *et al.*, 2008) and serine (Velayudhan *et al.*, 2004), the enzyme mechanism for their uptake and catabolism has been elucidated; while Proline also supports *C. jejuni* proliferation, via the transporter PutP and proline dehydrogenase PutA (Guccione *et al.*, 2008; Hofreuter *et al.*, 2008). Interestingly, the amino acid composition of chicken excreta matches the amino acids utilized by *C. jejuni* (Parsons *et al.*, 1982; Leach *et al.*, 1997; Guccione *et al.*, 2008). Among these, serine is reported as the most favoured amino acid for *C. jejuni* growth because of the presence of SdaC (Cj1265c), an active serine transporter and SdaA (Cj1264c), a dehydratase and the cells' ability to efficiently convert serine to pyruvate which can be converted to acetyl-CoA by Por (section 1.1.4.1.2) and can enter directly into the TCA cycle (Velayudhan *et al.*, 2004). Only a few amino acids, like arginine and lysine, have been reported as chemorepellents (Rahman *et al.*, 2014). Proline is the least efficiently used amino acid in *C. jejuni*. It enters the TCA cycle through a sodium/proline symporter PutP (Cj1502) where it is converted to glutamate by a bifunctional enzyme PutA (Cj1503) in a two-step reaction (Stahl *et al.*, 2012). The amino acid catabolism plays an important role in process of colonisation as well and cells lacking enzymes catabolizing serine, aspartate or glutamine/glutamate showed inefficient colonisation

in infection of animal models (Hofreuter *et al.*, 2006; Barnes *et al.*, 2007; Guccione *et al.*, 2008; Novik *et al.*, 2010). *C. jejuni* entry and/or survival within host epithelial cells depends directly on its ability to utilise aspartate (Novik *et al.*, 2010) and genes involved in amino acid utilisation in the host cells are upregulated (Woodall *et al.*, 2005).

Gluconeogenesis is an important factor for the maintenance of physiological activities in *C. jejuni* and possibly this feature enables the substrates utilised in the cellular intermediary metabolism to fulfil the requirement for biosynthesis of carbohydrates, lipids and proteins. The genomic sequence of *C. jejuni* shows that it contains several systems for transportation of organic acids across the inner membrane (Parkhill *et al.*, 2000). It has been shown that *C. jejuni* is able to catabolise organic acids like lactate, pyruvate, acetate and intermediates of the TCA cycle (Westfall *et al.*, 1986; Elharrif and Megraud, 1986; Mohammed *et al.*, 2004; Guccione *et al.*, 2008; Hinton, 2006; Velayudhan and Kelly, 2002; Wright *et al.*, 2009). Other organic acids like succinate, fumarate, malate, pyruvate, lactate and 2-oxoglutarate acts as chemoattractants for *C. jejuni*, suggesting their role in cellular metabolic activities (Hugdhal *et al.*, 1988; Vegge *et al.*, 2009).

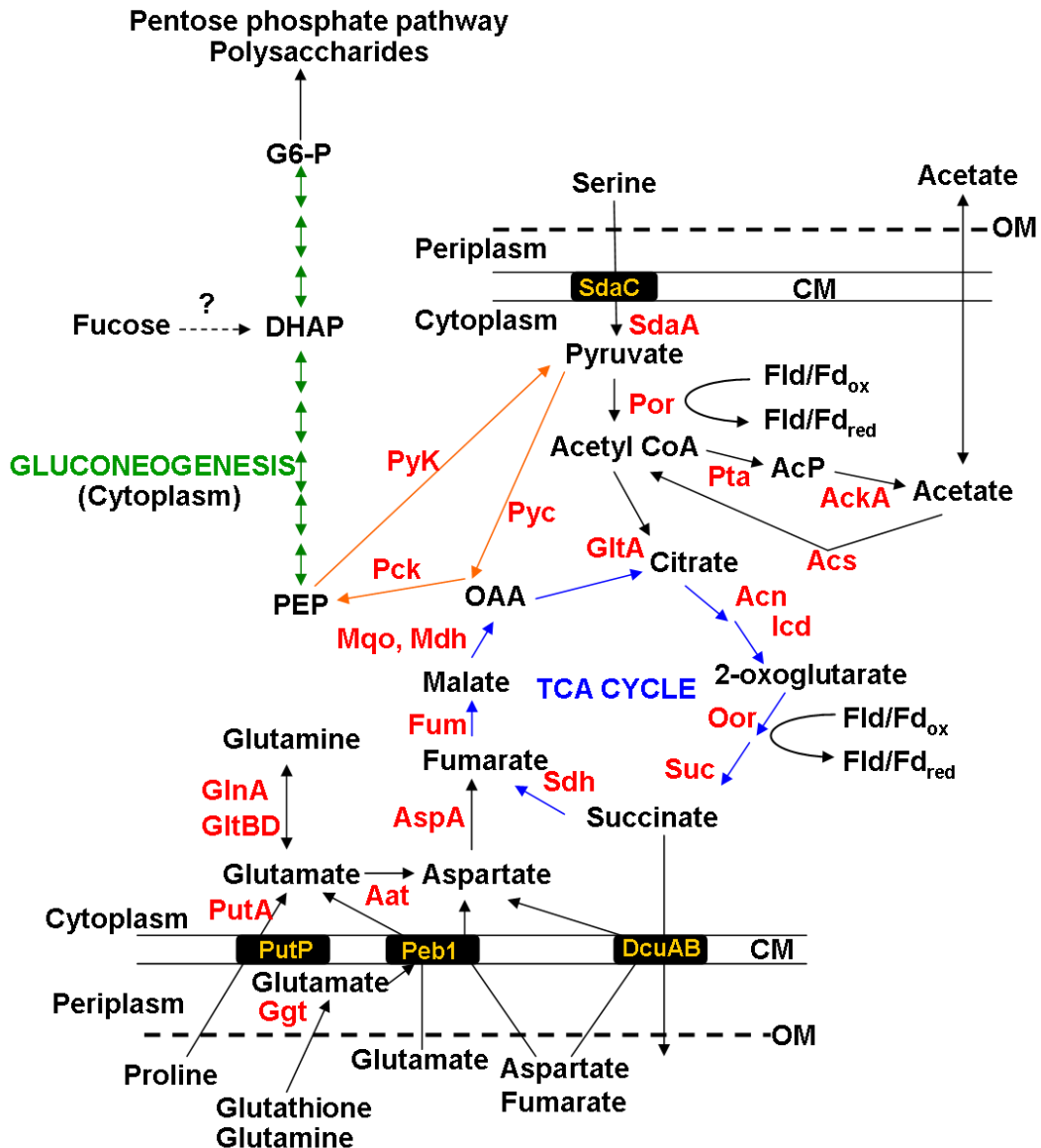


Figure 1.5: Amino acid utilisation and Central carbon metabolism in *C. jejuni*. TCA cycle is shown with **blue** arrows, gluconeogenesis with **green** and the anaplerotic reactions that link the two in **orange**. Enzymes are shown in **red** next to the reactions they catalyse. Transporters are shown in **yellow**. The predicted conversion of fucose to DHAP and subsequent entry into the lower half of the EMP pathway is shown with a dashed line. Figure adapted from Kelly, 2008.

1.1.4.1.4 Gluconeogenesis and anaplerotic reactions:

Several essential enzymes of Entner–Doudoroff pathway like, 6-phosphogluconate dehydratase and 2-keto-3-deoxyphosphogluconate aldolase, are absent in *C. jejuni* (Parkhill *et al.*, 2000; Fouts *et al.*, 2005). Homologues of phosphoenolpyruvate (PEP)-dependent phosphotransferase, a glucose uptake system

in *E. coli* is also absent (Gosset, 2005). This suggests its inability to catabolise glucose/hexose sugars (Velayudhan and Kelly, 2002) and the necessity of gluconeogenesis for the biosynthesis for glucose of various metabolic activities like the production of lipopolysaccharides and capsule and *O*-linked or *N*-linked glycosylation (Karlyshev *et al.*, 2005). There is no experimental evidence of gluconeogenesis in *C. jejuni* yet but homologues of various anaplerotic enzymes bridging the TCA cycle to the Embden-Meyerhof-Parnas (EMP) pathway have been discovered (Fig. 1.5). Pyruvate carboxylase PycA and PycB (Cj1037 and Cj0932), PckA (Cj0932) phosphoenolpyruvate carboxykinase and Pyk (Cj0392c) pyruvate kinase are a few examples of anaplerotic enzymes present in *C. jejuni*, which mediates phosphoenolpyruvate (PEP)-pyruvate-oxaloacetate conversion controlling the carbon flow. Inability to knock out *pckA* gene suggests that PckA, which catalyses the synthesis of PEP by the decarboxylation of oxaloacetate, is essential in NCTC11168 strain (Velayudhan and Kelly, 2002). Presence of irreversible pyruvate kinase (Pyk) in the absence of a functional forward EMP-pathway suggests a catabolic role for the lower part of the pathway as this normally catalyses the final step of glycolysis (conversion of PEP to pyruvate) (Velayudhan and Kelly, 2002). Malate oxidoreductase (Cj1287) also regenerates pyruvate by the oxidative decarboxylation of malate (Velayudhan and Kelly, 2002).

1.1.4.2 Microaerophily:

C. jejuni is a well-known microaerophilic bacterium, which means that it needs some amount of oxygen for various metabolic and catabolic activities but it cannot survive under the stress of normal atmospheric oxygen (which is 20.5 % oxygen by composition in atmosphere). This particular feature of this pathogen provides it the niche to grow in low oxygen environments, like the intestine (Kreig and Hoffman, 1986; Kelly *et al.*, 2001). The optimum amount of oxygen for the best cellular growth is 3-10 % (v/v), supplemented with 2–10% (v/v) CO₂ (Bolton and Coates, 1983) and both extreme conditions, the environmental level of oxygen or strictly anaerobic environment, are fatal for its survival. The life cycle of *C. jejuni* suggests that it has to survive through various oxygen levels, including sudden environmental oxygen shock during transmission from one host to another, but still its oxygen sensing mechanism and requirement of a microaerophilic growth environment is not clear, with one possible explanation for later being presence of various oxygen

dependent/sensitive enzymes. One interesting observation is that it contains various enzymes facilitating anaerobic respiration using alternative electron acceptors to oxygen but still it is unable to grow at all under strictly anaerobic conditions (Veron *et al.*, 1981).

The possible explanation behind the necessity of some amount of oxygen can be the requirement of oxygen for catalysis by class I-type ribonucleotide reductase (RNR), encoded in the *C. jejuni* genome, which is essential for the synthesis of deoxyribonucleotides in *C. jejuni* (Parkhill *et al.*, 2000; Sellars *et al.*, 2002). The widely accepted fact that *C. jejuni* cannot grow in strictly anaerobic environments was disputed by Weingarten *et al.* (2008). Weingarten *et al.* (2008) suggested that the sub-nanomolar amount of oxygen dissolved in cellular anaerobic vessels may be sufficient for generation of the tyrosyl radical required for RNR activity and also reported the anaerobic growth of *C. jejuni* in the presence of respiratory electron donors such as sulphite, formate or hydrogen complemented with electron acceptors such as nitrate or TMAO.

Like the oxygen requirement of *C. jejuni*, the inhibition of growth by oxygen is also not well understood. One possible explanation can be the presence of various oxygen sensitive enzymes, which can be damaged by oxygen and are crucial for various metabolic functions and ultimately for its survival. Many crucial proteins in *C. jejuni* contains iron-sulphur clusters, which makes them sensitive to oxygen, as reactive oxygen species permanently damages the iron-sulphur cluster. L-serine is the most favored source of carbon (Section 1.1.4.1.3) and the enzyme which catabolises L-serine to pyruvate, L-Serine dehydratase SdaA (Cj1624), is sensitive to atmospheric oxygen (Velayudhan *et al.*, 2004). One interesting feature of the SdaA enzyme in *C. jejuni* is, unlike most aerobes where it is pyridoxal 5'-phosphate (PLP)-dependent, it contains an oxygen labile Fe-S cluster like those typically found in most anaerobes (Velayudhan *et al.*, 2004). The presence of iron-sulphur clusters in the pyruvate and 2-oxoglutarate:acceptor oxidoreductase enzymes, Por and Oor (Section 1.1.4.1.2), of the TCA cycle can be the other potential reason behind oxygen sensitivity as their homologues in *H. pylori* have been observed as damaged by atmospheric oxygen (Hughes *et al.*, 1995, 1998). However, it has been reported that Por and Oor are partially protected by HerA (Cj0241c) and HerB (Cj1224), the oxygen binding hemerythrin proteins but cannot be repaired once exposed to atmospheric oxygen

concentrations (Kendall *et al.*, 2014). The rubredoxin oxidoreductase/rubrererythrin (Rbo/Rbr)-like Rrc protein (Cj0012c) is another example of an oxygen sensitive enzyme, which can be seriously damaged by reactive oxygen species (ROS) and aerobic stress (Yamasaki *et al.*, 2004). Both resistance and repair mechanisms are required for resisting this oxygen-mediated damage.

The fact that *C. jejuni* prefers the the mucus layer and the intestinal crypt close to the epithelium for colonisation instead of the intestinal lumen, which has a much lower amount of oxygen (Lee *et al.*, 1986; Beery *et al.*, 1988) and between the mid small intestine and the mid colon over the distal colon and rectum (He *et al.*, 1999) which again has a lower amount of oxygen, raises questions as to the explanation of the molecular basis for microaerophily due to oxidative stress. *C. jejuni* shows an ability to defend itself against ROS (reviewed by Atack and Kelly, 2009) to some extent. In response to bacterial infection, the host immune system generates various reactive oxygen species (ROS) (produced by stepwise one-electron reduction of O₂) like hydrogen peroxide (H₂O₂), Superoxide (O₂⁻) and hydroxyl radical (HO[·]) which targets DNA, proteins and membranes of the pathogen. *C. jejuni* produces various ROS-detoxifying enzymes which contradicts this as a hypothesis of the molecular basis for microaerophily. These ROS-detoxifying enzymes includes the the cytochrome *c* peroxidases (Cj0020c and Cj0358; Parkhill *et al.*, 2000), superoxide dismutase SodB (Cj0169; Pesci *et al.*, 1994), the catalase KatA (Cj1385; Day *et al.*, 2000), the alkyl hydroxide reductase AhpC (Cj0334; Baillon *et al.*, 1999), the thiol peroxidases Tpx (Cj0779; Atack *et al.*, 2008), the bacterioferritin comigratory protein Bcp (Cj0271; Atack *et al.*, 2008), and the methionine sulfoxide reductases MsrA and MsrB (Cj0637 and Cj1112; Atack and Kelly, 2009). *C. jejuni* responses to oxidative stress are not well understood as no direct oxygen sensing mechanism has been found so far and needs further investigation but PerR (Cj0322) is reported to be playing a crucial part as a peroxide sensor (Palyada *et al.*, 2009). Recently, the Regulator of Response to Peroxide (RrpA/B) proteins have been discovered which act as DNA-binding regulators and are believed to be a part of a novel oxidative stress response mechanism. Cells lacking *rrpB* showed stimulated sensitivity to oxidative stress and reduced expression of the the iron responsive peroxide response regulator *perR*, catalase gene *kataA* and the heat shock regulator *hspR* (Gundogdu *et al.*, 2011, Gundogdu *et al.*, 2015).

1.1.4.3 Capnophily:

Along with microaerophily, *C. jejuni* is also a capnophilic or CO₂ requiring bacterium. The optimum amount of carbon dioxide required for best growth is 5-10 % (v/v), which is much higher than the environmental amount (on an average ~0.04 %) (Bolton and Coates, 1983). The reason behind this is still unclear but a possible explanation can be the presence and inefficiency of various CO₂ utilizing enzymes, like acetyl-CoA carboxylase (Burns *et al.*, 1995), phosphoenolpyruvate carboxykinase (Kelly, 2001), carbonic anhydrase (Kelly, 2001) and phosphoenolpyruvate carboxykinase (Kelly, 2001). Acetyl-CoA carboxylase is essential for fatty acid biosynthesis and its homologue in *Helicobacter pylori* showed low affinity for CO₂ suggesting one reason behind high CO₂ requirement of *H. pylori* (Burns *et al.*, 1995). One of the two carbonic anhydrase enzymes encoded by *C. jejuni* 11168 genome to convert gaseous CO₂ to bicarbonate (Smith and Ferry, 2000), CanB (Cj0237) is also considered responsible for the capnophilic phenotype, as it has very low CO₂ affinity but is crucial for bacterial growth in low CO₂ concentrations, leading to poor CO₂ to bicarbonate conversion (Al-Haideri *et al.*, 2016).

1.2 Bacterial Electron transport chains:

Energy conservation by respiration (oxidative phosphorylation) is a fundamental metabolic mode for most aerobic, microaerobic and anaerobic prokaryotic and eukaryotic cells (Nicholls and Ferguson, 2002). Electron transport chains (ETCs) mediate cellular respiration with the help of series of enzymes by creating an ion (usually proton) gradient across the membrane that drives synthesis of ATP. The ETC is located in the cytoplasmic membrane and produce proton motive force (pmf) by proton pumping, by quinone/quinol cycling or by a redox loop. ETC transfers electron from electron donor to electron acceptor through a series of redox reactions. An individual bacterium can use multiple ETCs, employing a number of different electron donors, dehydrogenases, oxidases, reductases and electron acceptors, simultaneously.

Bacterial ETCs mostly consist of four parts: (i) the dehydrogenases for electron donors; (ii) the membrane soluble quinone pool which can carry electrons in the form of hydrogen atoms; (iii) the electron transfer enzymes which mediate the main flow of electrons coupled to proton-translocation; and (iv) a terminal oxidase or

reductase under aerobic conditions or oxygen-limited environments, respectively. A few factors determining the properties of ETCs in a bacteria are: (i) the degree of branching at both dehydrogenase and reductase ends of the chain determines the diversity of substrate utilisation and provides the growth advantage to bacteria; (ii) the competence of cells to utilize alternative electron acceptors to molecular oxygen; (iii) the presence of a variety of types of cytochromes as additional electron carriers and often more than one type of quinone; (iv) the proper interaction between electron pathways (the efficiency of electron transfer will be maximized if every reductant is able to be paired with a range of oxidants); and (v) the optimum degree of proton translocation and energy transduction which is contributed by each ETC.

1.2.1 Electron transport chains in *C. jejuni*:

The non-fermentative nature of *C. jejuni* means oxidative phosphorylation must meet the energy demands of the bacterium. Consequently, a network of electron transport chains has been predicted from the *C. jejuni* genome with most of them being experimentally tested (Smith *et al.*, 2000; Sellars *et al.*, 2002; Myers and Kelly, 2005a,b; Pittman *et al.*, 2007; Kelly, 2008; Weingarten *et al.*, 2008; Garg *et al.*, 2018). *C. jejuni* encodes a remarkably complex and branched electron transport chain for a fairly small genome (Fig. 1.10). This supports energy conservation and growth in a wide variety of environmental conditions. A variety of inorganic or organic electron donor substrates, including formate and sulphite, donates electrons to the quinone pool (Myers and Kelly, 2005a; Weerakoon *et al.*, 2009). Through the quinone pool, in presence of optimum amount of oxygen, these electrons are transferred to one of the two terminal oxidases, either *bd*-type CioAB oxidase or *cbb₃*-type cytochrome *c* oxidase. In extreme oxygen limitation, these electrons are transferred to several alternative electron acceptors including trimethylamine N-oxide (TMAO), nitrate, fumarate, nitrite, and dimethylsulphoxide (DMSO), supporting growth and energy conservation (Garg *et al.*, 2018)

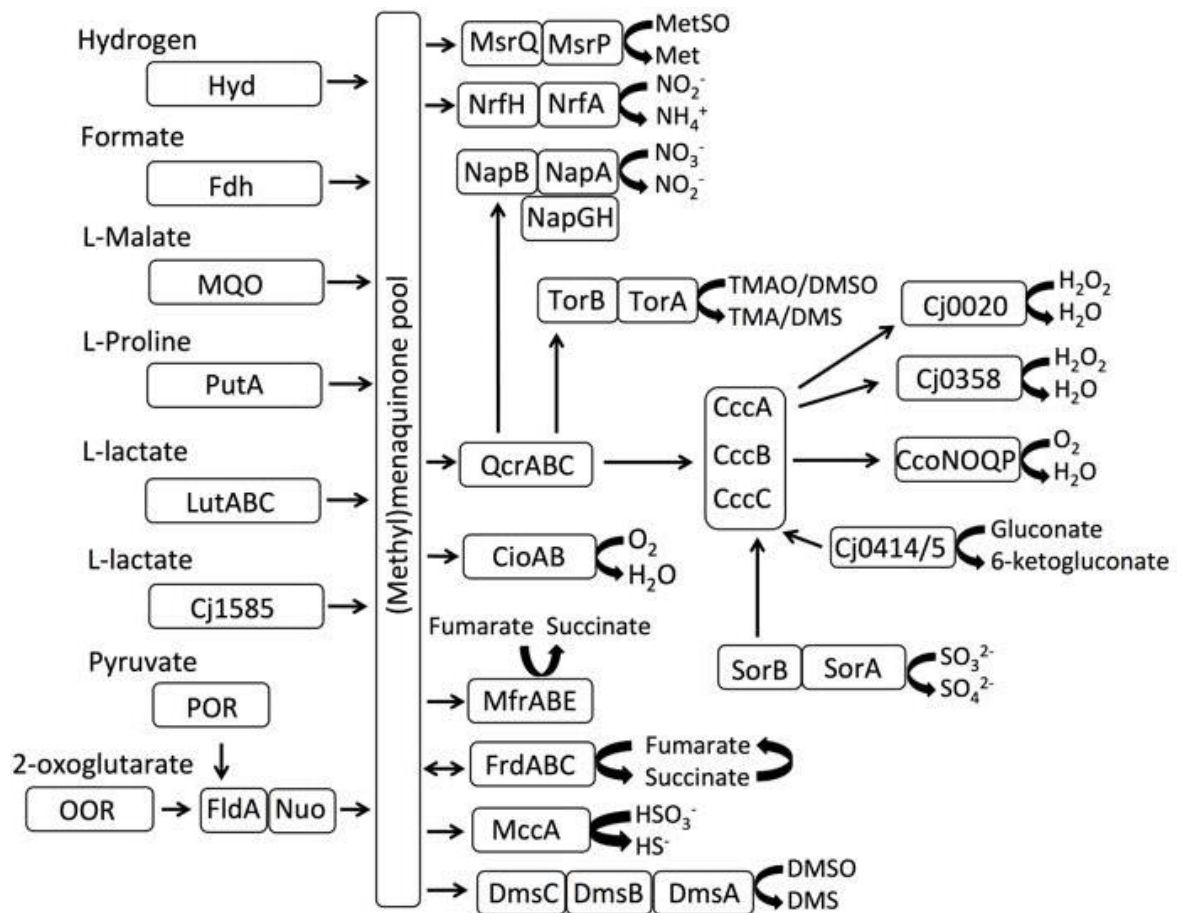


Figure 1.10: Major electron transport chains in *C. jejuni*. A variety of electron donors, including molecular hydrogen, amino acids and organic acids, are catalysed by a series of dehydrogenases, which transfer electrons to menaquinone pool in the lipid bilayer of the inner membrane. Under microaerobic conditions, menaquinol will further reduce the QcrABC complex which in turns reduces periplasmic *c*-type cytochrome(s). Cytochrome *c* is re-oxidised by one of the terminal oxidases, the high affinity *cb*-type cytochrome *c* oxidase. The cyanide-resistant, low affinity CioAB-type menaquinol oxidase is also present. Cytochrome *c* may also be re-oxidised by hydrogen peroxide in the periplasm through the activity of two separate CCPs. Besides, electrons can also be fed directly to some reductases, bypassing the menaquinone pool. Under oxygen-limited or extremely anaerobic conditions, several alternative electron acceptors to oxygen can terminate respiration. Note this is a composite figure; not all pathways exist in all strains. The individual components of the *C. jejuni* electron transport chains of NCTC 1168 are further discussed in the text.

1.2.2 The various electron donors to the ETC in *C. jejuni*:

1.2.2.1 Hydrogen and formate:

Both hydrogen and formate have a very low redox potential ($E_m \sim -420$ mV) and are produced as a by-product of gut-dwelling anaerobic fermentative bacteria in both the avian and human gut. This makes them the perfect candidates as the electron donors for *C. jejuni* (ETC) growth *in vivo*. Supporting this, it has been

reported that *C. jejuni* cells lacking both hydrogenase and formate dehydrogenase showed defects in chicken colonization (Weerakoon *et al.*, 2009).

Hydrogen has been reported as a major electron donor to the electron transport chain in *C. jejuni* with hydrogenase activity being observed in membrane fractions of *C. jejuni* (Hoffman and Goodman, 1982; Carlone and Lascelles, 1982). A *hydABC* operon (*cj1267c-cj1265c*), encoding HydA, HydB and HydC in *E. coli*, is present in *C. jejuni* genome (Thony-Meyer, 1997; Parkhill *et al.*, 2000). HydA, HydB and hydC are the subunits of a membrane bound Ni-Fe hydrogenase enzyme, which mediates the transfer of electrons from hydrogen to the quinone pool.

Formate is another excellent electron donor to the *C. jejuni* ETC and very high rates of formate dependent oxygen respiration have been reported (Myers and Kelly, 2005). *C. jejuni* genome encodes a *fdhABCD* operon (*cj1511c-cj1508c*), which encodes a formate dehydrogenase (Fdh) (Parkhill *et al.*, 2000; Weerakoon *et al.*, 2009). In the *C. jejuni* 81-176 strain, it has been reported that the strain showed more respiration and chemoattraction to formate than any other organic acid (Issmat *et al.*, 2017). Under microaerobic conditions, substitution of formate stimulated *C. jejuni*'s growth, motility, production of ribonucleotide reductase (RNR), biofilm formation and most importantly, the synthesis of alternative electron acceptor utilization facilitating proteins; but was reported to reduce oxidase activity (Issmat *et al.*, 2017). This suggests the important role of formate in supporting *in vivo* growth in oxygen-limited gastrointestinal tract of the host by encouraging transfer of electrons to alternate electron acceptors and conserving limited oxygen available for other essential functions, like DNA synthesis by RNR, etc.

1.2.2.2 Malate:

Malate can be a direct electron donor to the quinone pool and can stimulate respiration in *C. jejuni* with its relatively negative redox potential (E_m of malate/oxaloacetate couple = -166 mV) (Hoffman and Goodman, 1982). The soluble NAD-linked malate dehydrogenase (Mdh; Cj0532) and the NAD-independent, flavoprotein-type malate:quinone oxidoreductase (Mqo; Cj0393) are the enzymes responsible for malate oxidation in *C. jejuni*. Cj0393 (Mqo) is a membrane-bound, FAD-dependent and cytoplasmic-facing enzyme, which mediates direct electron

transfer from malate to quinone pool (Kather *et al.*, 2000) and is 49.3 % similar to malate:quinone oxidoreductase in *H. pylori*.

1.2.2.3 Lactate:

Lactate is also produced by various anaerobes colonizing the mammalian and avian gut, making it an important *in vivo* source of electrons for *C. jejuni* (Thomas *et al.*, 2011). *C. jejuni* NCTC 11168 genome encodes two novel NAD-independent membrane associated L-Lactate dehydrogenases (L-Ldh) which oxidise L-lactate to pyruvate (Thomas *et al.*, 2011). One L-Ldh consists of three subunits (Cj0073-Cj0075; LutABC) and the second is an unusual FAD and Fe-S containing oxidoreductase (Cj1585). Both transfer electrons derived from L-lactate to menaquinone (Thomas *et al.*, 2011).

1.2.2.4 Succinate:

C. jejuni does not possess a conventional succinate dehydrogenase. The fumarate reductase (FrdABC) present in *C. jejuni* performs a dual function by oxidising succinate to fumarate under aerobic conditions and reducing fumarate to succinate under oxygen-limited conditions (Weingarten *et al.*, 2009; Guccione *et al.*, 2010). The electrons released from succinate oxidation are transferred to the menaquinone pool. This reaction is a part of the tricarboxylic acid cycle.

1.2.2.5 Sulphite:

The characteristic property of sulphite to be more stable in low oxygen environments makes it a suitable source of electron for *C. jejuni* both inside and outside the host. A periplasmic sulphite:cytochrome *c* oxidoreductase (Sor) is present in *C. jejuni*, which mediates sulphite respiration with oxygen as the terminal electron acceptor (Hoffman and Goodman, 1982; Myers and Kelly, 2005). Sor consists of two subunits: a molybdopterin oxidoreductase, SorA (Cj0005) and a monohaem cytochrome *c* (Cj0004). It has been shown that Sor mediated sulphite oxidation donates electron directly to the cytochrome *c*, which transfers it to the high affinity *cb*-type cytochrome *c* terminal oxidase, bypassing the Qcr complex (Figure 1.10; Myers and Kelly, 2005). This suggests its role in respiration in low oxygen environments. Sulphite respiration can also be a mechanism for sulphite detoxification as it has been shown to inhibit the growth of many microorganisms including the closely related *H. pylori* (Jiang and Doyle, 2000). *C. jejuni* cells lacking

cj0005c have been reported as inefficiently adhering and invading host cells (Tareen *et al.*, 2011).

1.2.2.6 Gluconate:

The periplasmic gluconate dehydrogenase (GADH) synthesised by *C. jejuni* enables it to utilise gluconate, which is an oxidation product of glucose and a suitable source of electrons *in vivo* as it is present in abundance in intestinal mucus. GADH is encoded by a two-gene operon *cj0414-0415* (Pajaniappan *et al.*, 2008). The electrons derived from gluconate are predicted to enter the respiratory chain via the periplasmic cytochrome *c* (Kelly, 2008).

1.2.2.7 Proline:

The primary function of proline in *C. jejuni* is a source of carbon for supporting growth (Guccione *et al.*, 2008; Hofreuter *et al.*, 2008) but it can also act as a potential source of electrons as electrons are liberated during its catabolism. The putative proline transporter PutP (Cj1502) encoded by *C. jejuni* genome facilitates the uptake of proline into the cytoplasm. In the cytoplasm, the predicted bifunctional proline dehydrogenase PutA (Cj1503) oxidises proline and converts it to glutamate (Parkhill *et al.*, 2000; Kelly, 2008). The electrons liberated in this process can be transferred directly to the quinone pool via a bound flavin (FAD) in PutA (Kelly, 2008).

1.2.3 The quinone pool:

Menaquinone (MK; E_m -75 mV) is the sole respiratory quinone class present in *C. jejuni* and it does not contain the higher redox potential ubiquinone (E_m +90 mV). The role of MK is to transfer electrons produced by primary dehydrogenases to the Qcr complex, the cyanide-resistant quinol oxidase CioAB and to alternative electron acceptors in the ETC (Carlone and Anet, 1983; Ingledew and Poole, 1984; Collins *et al.*, 1984; Moss *et al.*, 1990; Jackson *et al.*, 2007). *C. jejuni* synthesizes two types of MK: (i) MK-6 (2-methyl, 3-farnesyl-farnesyl-1,4-naphthoquinone) and (ii) methyl-substituted MK-6 (MMK-6; 2,[5or8]-dimethyl, 3-farnesyl-farnesyl-1,4-naphthoquinone) (Carlone and Anet, 1983; Moss *et al.*, 1984). These have different midpoint redox potentials of -75 mV for MK-6 and -124 mV for MMK-6 (Juhnke *et al.*, 2009).

1.2.4 The menaquinol-cytochrome *c* reductase (Qcr) complex:

The membrane bound, proton-translocating, quinol cytochrome *c* reductase (Qcr) complex encoded by *C. jejuni* genome is a homolog of Complex III in eukaryotic mitochondria. It is highly conserved in phylogenetically diverse prokaryotes, showing an important role in oxygen-linked respiration (Dibrova *et al.*, 2013). It is present in most of the ubiquinone containing prokaryotes and eukaryotes, whether aerobic, anaerobic or photosynthetic, with *E. coli* being an exception (Ingeldew and Poole, 1984). In *C. jejuni*, it was believed that it transfers electrons from the quinone pool specifically to the terminal cytochrome *c* oxidase (Myers and Kelly, 2005) but recent work of Garg *et al.* (2018) showed that along with cytochrome *c*, it is also responsible for transporting electrons from the quinone pool to some alternate reductases, notably the nitrate reductase (NapAB) and the Trimethylamine N-oxide (TMAO) reductase (TorAB), under oxygen limitation. This suggests that the Qcr complex is an essential component of *C. jejuni* ETC which mediates proton translocation by transporting electrons either to the terminal oxidase or alternate reductases both in presence or absence of oxygen, supporting growth in wide range of environments.

C. jejuni Qcr complex consists of three subunits (QcrABC) with four redox centres in them. QcrABC are encoded by *cj1184c-cj1186c* operon in *C. jejuni* genome (Smith *et al.*, 2000; Parkhill *et al.*, 2000; Fig. 1.11). QcrA (Cj1186) contains a 2Fe-2S cluster and an N-terminal Tat signal sequence; QcrB (Cj1185) is a cytochrome *b* subunit consisting of a non-covalently bound *b*-type hems; and QcrC (Cj1184) is a cytochrome *c*₄ subunit consisting of 2 covalently attached *c*-type haems. Note that most bacteria have a monohaem cytochrome *c*₁ as part of the Qcr complex and these type of complexes are known as “*bc₁*” complexes. The *Epsilonproteobacteria* are an exception to this, but the complex is thought to work in a similar way (Fig. 1.11).

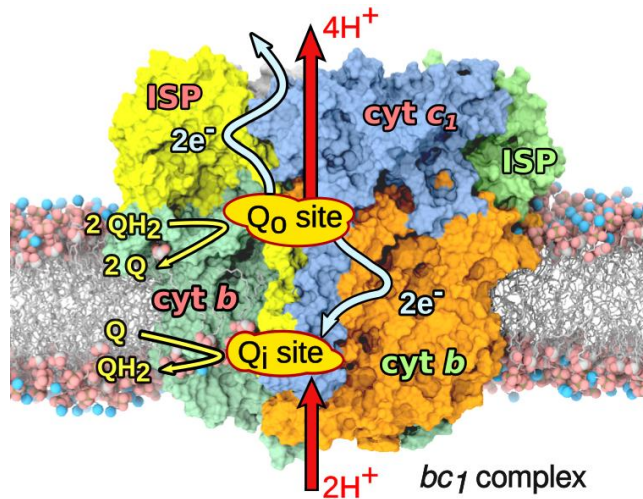


Figure 1.11: Reaction cycle of the bc_1 complex. bc_1 complex consists of three subunits and four redox centres. Two protons are absorbed from the negative side of the membrane and four protons are released to the positive side. This process is fueled by redox reactions with substrate quinol (QH₂) and quinone (Q) molecules from the membrane: two QH₂ are oxidized to Q at the Q_o binding site of the bc_1 complex, while one Q molecule is reduced to QH₂ at the negative side. The process is coupled to a series of internal electron transfers in the bc_1 complex. Figure adapted from The Quantum Biology and Computational Physics research group, University of Southern Denmark.

1.2.5 *c*-type cytochromes:

Soluble periplasmic *c*-type cytochromes are important components of ETC in many bacteria, including *C. jejuni* that transfer electrons from the Qcr complex to a terminal reductase. In *C. jejuni*, they receive electrons from the Qcr complex and transfer them to a *cbb*₃-type cytochrome *c* oxidase, which is a terminal oxidase (described in 1.2.6) ultimately transferring electrons to the oxygen. This makes them crucial for proton-translocation in presence of oxygen. In *C. jejuni*, *c*-type cytochrome proteins are present in abundance, either periplasmic soluble or anchored to the cytoplasmic membrane (Thony-Meyer, 1997), containing covalently bound haem(s) to the cysteines of the haem C binding motif, CXXCH (Ferguson, 2001). *cj1153* in *C. jejuni* encodes a periplasmic monohaem cytochrome *c*, homologous to the cytochrome C₅₅₃ of *H. pylori* and *Desulfovibrio vulgaris* (Koyanagi *et al.*, 2000). Cj1153 (CccA) is partly responsible for mediating electron transfer from the cytochrome bc_1 complex to a terminal oxidoreductase (Liu and Kelly, 2015). It may also directly accept electrons from the periplasmic dehydrogenases for sulphite and gluconate (Myers and Kelly, 2005; Kelly, 2008). Other soluble *c*-type cytochromes

which have a similar role are CccB (Cj1020) and CccC (Cj0037) (Liu and Kelly, 2015).

1.2.6 Terminal oxidases for oxygen dependent respiration:

There are two conserved oxidases in all strains of *C. jejuni*, a *cbb₃*-type cytochrome *c* oxidase and a cytochrome *bd*-type quinol oxidase (Parkhill *et al.*, 2000; Poly *et al.*, 2004; Fouts *et al.*, 2005; Hofreuter *et al.*, 2006). The presence of these two oxidases contributes to the microaerobic characteristics of *C. jejuni*. While the *cbb₃*-type cytochrome *c* oxidase is more energy efficient, sulphide inhibits it. On the other hand, the cytochrome *bd*-type quinol oxidase is reported to be sulphide resistant in *E. coli* (Korshunov *et al.*, 2016), which may partly explain the presence of two oxidases in *C. jejuni* as the concentration of sulphide is high in the intestine (Gong *et al.*, 2014). The presence of two oxidases makes it possible to knock out either of them for physiological characterisation.

1.2.6.1 *cbb₃*-type cytochrome *c* oxidase:

cbb₃-type cytochrome *c* oxidase has a high oxygen affinity and supports microaerobic bacterial growth (Jackson *et al.*, 2007). It is a heme-copper oxidase and catalyzes the reduction of O₂ to water (Pitcher *et al.* [2002](#)). The *cbb₃*-type cytochrome *c* oxidase in *C. jejuni* is homologous to the *cbb₃*-type cytochrome *c* oxidase in *Helicobacter pylori* (Thony-Meyer, 1997). This membrane bound cytochrome *c* oxidase complex consists of four subunits, namely, CcoN (Cj1490), CcoO (Cj1489), CcoQ (Cj1488) and CcoP (Cj1487) (Parkhill *et al.*, 2000). CcoN is a membrane-integral *b*-type cytochrome with a high-spin bi-nuclear haem-copper active site consisting of Cu(B) and a low-spin heme. CcoP and CcoO are two membrane anchored *c*-type cytochromes containing dihaem and monohaem, respectively. Their primary function is to transfer electron from cytochrome *c* to CcoN. Role of CcoQ is not well understood yet, probably it is just required for stabilising the complex (Oh and Kaplan 2002). Insertion of Cu(B) in CcoN subunit normally requires an assembly system of copper chaperones but these have not been identified in *C. jejuni* and are a major focus of this thesis. This oxidase has been reported to be necessary for normal growth of the bacteria and for colonization of the chick intestine. *C. jejuni* cells lacking CcoNOQP complex showed growth defects and an inability to colonize the chicken (Weingarten *et al.*, 2008).

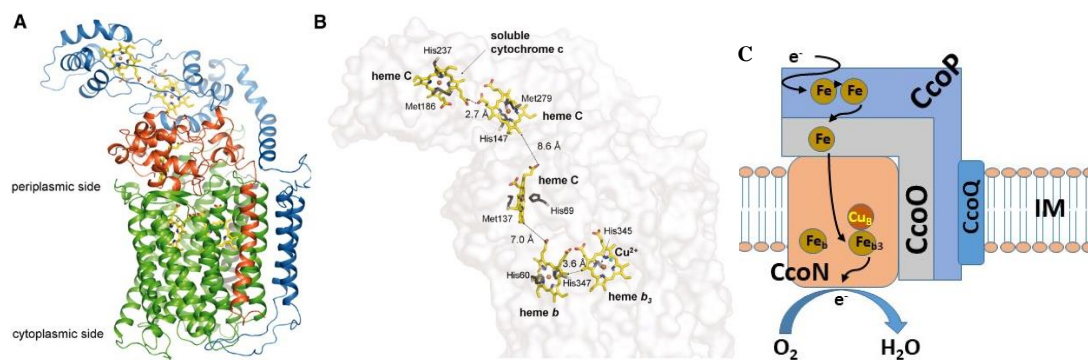


Figure 1.12: *cbb3*-type cytochrome *c* oxidase structure. (A) and (B) The *cbb3*-type cytochrome *c* oxidase protein structure has been derived from *Pseudomonas stutzeri* (Buschmann *et al.*, 2010). (C) The Cu_B, heme *b* and heme *b*₃ are present in CcoN subunit of the complex. CcoP and CcoO contains dihaem and monohaem, respectively. The electron from cytochrome *c* enters the complex through CcoP, which transfers it to CcoO. From CcoO, the electron is passed to CcoN, where it reduces the oxygen to water.

1.2.6.1.1 Assembly of *cbb3*-type cytochrome *c* oxidase:

cbb3-type cytochrome *c* oxidase is a metalloprotein, which uses Cu as a cofactor. The Cu needs to be transported to the Cu(B) site in CcoN with the help of Cu chaperones, and in reduced form. The Cu might be reduced with the help of thioredoxins. The necessity of Sco1 and Cox17 proteins for the correct assembly of cytochrome *c* oxidase in eukaryotic cells is well known (Dickinson *et al.*, 2000; Mattatall *et al.*, 2000). The Cox17 protein is believed to be the specific copper donor to membrane bound Sco1 (Horng *et al.*, 2004). In *Bacillus subtilis*, Mattatall *et al.* (2000) reported the discovery of YpmQ, a bacterial homolog of the inner mitochondrial membrane protein Sco1. Deletion of *ypmQ* in *B. subtilis* depressed the expression of cytochrome *c* oxidase and the level of cytochrome *c* oxidase was recovered on substituting the growth medium with additional Cu. Unlike Sco1, there is no known bacterial homolog of Cox17 protein. In *Deinococcus radiodurans* and *Caulobacter crescentus*, Banci *et al.* (2005) found a class of proteins of unknown function (referred as PCu_AC) displaying a conserved gene neighbourhood to bacterial *sco1* genes, all sharing a potential metal binding motif H(M)X₁₀MX₂₁HXM, and potentially taking the role of Cox17 in bacteria, involving copper delivery to the Cu(A) center in the oxidase. Both PCu_AC and Sco protein encoding genes are often found in the same bacterial operon (Abriata *et al.*, 2008). In *Rhodobacter sphaeroides* too, Thompson *et al.* (2012) reported the presence of a Sco homolog protein, PrrC,

and PCu_AC and have investigated their roles as copper chaperones in the assembly of the Cu centers of *cbb*₃-type cytochrome *c* oxidase. In *Rhodobacter capsulatus*, SenC, a Sco1-homologue and PccA, a PCu_AC-like periplasmic chaperone, have been identified. PccA has been demonstrated as a Cu-binding protein with a preference for Cu(I), which is required for efficient *cbb*₃-Cox assembly, in particular, at low Cu concentrations (Trasnea *et al.*, 2016). Cu is transferred from PccA to SenC and vice versa at similar levels, constituting a Cu relay system that facilitates Cu delivery to *cbb*₃-type Cco (Trasnea *et al.*, 2018). In the absence of PccA, SenC still obtains Cu that is exported by CcoI and facilitates Cco assembly, although with lower efficiency (Trasnea *et al.*, 2018). In *C. jejuni*, these assembly proteins have not been investigated yet, but this study hypothesises that products of *cj09008-cj0911* operon might be involved in assembly of *cbb*₃-type cytochrome *c* oxidase. This is further discussed in section 3.1.

1.2.6.1.2 CcoGHIS:

The necessity of the *ccoGHIS* gene products for the biogenesis of multisubunit enzymes encoded by the *ccoNOQP* operon and during the maturation of the *cbb*₃-type cytochrome *c* oxidase has been shown most convincingly in *Rhodobacter capsulatus* (Koch *et al.*, 2000). CcoG contains two cysteine-rich motifs which resembles those encountered in the (4Fe-4S) cluster containing ferredoxin molecules and supposed to have an oxidoreductase role (Preisig *et al.* 1996) and CcoI has a homology to Cu-translocating P-type ATPase (Preisig *et al.* 1996). CcoH and CcoS contains no characteristic motifs or homology to already characterised proteins (Koch *et al.* 2000). According to the model proposed by Kulajta *et al.* (2006) for the assembly of *cbb*₃-type cytochrome *c* oxidase in *R. capsulatus*, the process involves the formation of a stable but inactive sub-complex consisting of the subunits CcoNOQ and the assembly proteins CcoH and CcoS. Binding of CcoP, and subsequent dissociation of CcoH and CcoS, generates the active complex CcoNOQP. In a *ccoI* deletion strain, the sub-complex CcoNOQ was absent, although monomeric CcoP was still detectable. In the absence of CcoS, the complex was assembled but with no enzymatic activity. In a *ccoH* deletion strain, both the sub-complex CcoNOQ and monomeric CcoP were absent. Pawlik *et al.* (2010) demonstrated that biogenesis of CcoNOQP proceeds via CcoQP and CcoNO sub-complexes, which assemble into the active CcoNOQP and in absence of CcoH, neither the fully assembled CcoNOQP nor the CcoQP or CcoNO

sub-complex was detectable. CcoH binds to the CcoP with its transmembrane domain and not only interacts transiently with the Cco but also stays tightly associated with the active, fully assembled complex. In other words, CcoH is an essential part of the active Cco complex instead of just an assembly factor. In *C. jejuni*, these proteins have never been investigated before. They are further discussed in section 3.1.

1.2.6.2 CioAB oxidase:

There are two types of quinol oxidases: (i) the haem-copper oxidase type and (ii) cytochrome *d*-containing oxidase type. They receive electrons directly from the quinol pool. Homologs of the *cydAB* operon in *E.coli*, which encodes a cytochrome *bd*-type quinol oxidase, have been identified in the *C. jejuni* genome (Parkhill *et al.*, 2000). In *E. coli*, the oxidase synthesised by *cydAB* operon has high oxygen affinity and consists of haems *b₅₅₈*, *b₅₉₅* and *d* (Thony-Meyer, 1997). The *cydAB* operon (*cj0081-cj0082*) in *C. jejuni* encodes an enzyme that does not contain clear spectroscopic signals for *b₅₉₅* and *d*, typical characteristics of *bd*-type cytochromes. This makes it more similar to the CioAB enzyme of *Pseudomonas aeruginosa* homologous to the two subunits of bacterial cytochromes *bd*, but does not contain characteristic cytochrome *bd* features (Jackson *et al.*, 2007). This oxidase is poorly characterised in *C. jejuni* and renamed as CioAB (Jackson *et al.*, 2007). This oxidase is insensitive to cyanide and has lower oxygen affinity as compared to *cbb₃*-type cytochrome *c* oxidase (Jackson *et al.*, 2007). It supports growth under oxygen limitation. The *bd* oxidase in *E. coli* has been reported to be sulphide resistant, so it can support *in vivo* growth of *C. jejuni*, unlike *cbb₃*-type cytochrome *c* oxidase, which is inhibited by sulphide. The CioAB enzyme in *C. jejuni* receives electrons directly from the quinone pool, which provides an advantage against competing microorganisms that produce toxins inhibiting the Qcr complex (Trumpower, 1990).

1.2.7 Respiration with alternative electron acceptors under oxygen limited condition:

One of the important features of *C. jejuni* genome which allows it to grow in low oxygen environments is that it encodes several reductases that mediate respiration with number of alternative electron acceptors to oxygen (Parkhill *et al.*, 2000). These alternative electron acceptors might support growth and energy conservation *in vivo* as the avian and mammalian gut is likely to be oxygen-limited. Most strains of *C.*

jejuni can utilise trimethylamine-N-oxide (TMAO) (E_{m7} of TMAO/trimethylamine couple = +130 mV), nitrate (E_{m7} of nitrate/nitrite couple = +421 mV), dimethyl sulphoxide (DMSO) (E_{m7} of DMSO/dimethyl sulphide couple = +160 mV), nitrite (E_{m7} of nitrite/ammonium couple = +440 mV) and fumarate (E_{m7} of succinate/fumarate couple = +30 mV) for growth under oxygen limited conditions.

1.2.7.1 S- or N-oxide reductases:

Both TMAO and DMSO are abundant in aquatic environments and soil (McCrindle *et al.*, 2005). Many marine organisms excrete TMAO, which is an enzyme protective osmolyte and many algae produce DMSO as a cryoprotectant (McCrindle *et al.*, 2005). Therefore, it is more likely that *C. jejuni* encounter sufficient concentration of structurally similar compounds both outside the host and in the gut of species that predate aquatic prey. A wide range of bacteria carries out the reduction of TMAO to trimethylamine (TMA) and DMSO to dimethyl sulphide (DMS) through a single reductase or separate enzymes, especially in oxygen-limited environments. *Rhodobacter* spp. are the perfect example of bacteria having single enzyme using both TMAO and DMSO (Knablein *et al.*, 1997) while *E. coli* has separate enzymes. Dms and Tor in *E. coli* are DMSO reductase and TMAO reductase, respectively (Gennis and Stewart, 1996).

In *C. jejuni* NCTC 11168, both TMAO and DMSO reduction are catalysed by a single 93 kDa reductase encoded by *cj0264c* (Sellars *et al.*, 2002). A monohaem *c*-type cytochrome is produced by *cj0265c* (Parkhill *et al.*, 2000). The electrons from the quinone pool are transferred to Cj0265/Cj0264 through the Qcr complex (Garg *et al.*, 2018). It has been reported that cells lacking *cj0264c* colonise chickens similar to wild-type levels, which suggest TMAO/DMSO are not important electron acceptors in this host (Weingarten *et al.*, 2008).

1.2.7.2 Nitrate:

Nitrate respiration is widespread in many human pathogens because a higher nitrate concentration is observed in the host during intestinal inflammation and provides an advantage in growth to bacteria, which can utilise nitrate as electron acceptor under oxygen-limited conditions (Winter *et al.*, 2013; Sparacino-Watkins *et al.*, 2014). There are two major systems of nitrate reduction in bacteria: (i) the membrane bound complex Nar and (ii) the periplasmic-type Nap. All ϵ -

proteobacteria, including *C. jejuni*, contains the Nap system (Pittman *et al.*, 2007; Kern and Simon 2009a). In *E. coli*, both Nap and Nar systems have been reported with Nap having significantly higher affinity for nitrate and supporting nitrate reduction in low nitrate concentration and Nar being operational only in presence of high nitrate concentration (Potter *et al.*, 1999). The high affinity for nitrate makes Nap system more important for bacterial pathogenicity in the host where the nitrate concentration can be 10 to 50 μM (Potter *et al.*, 2001). It has been reported that cells lacking the *nap* operon showed compromised colonisation of the chickens (Weingarten *et al.*, 2008). The Nap system in *C. jejuni* is encoded by genes in the *napAGHBLD* operon. NapA is a molybdoenzyme (Smart *et al.*, 2009; Taveirne *et al.*, 2009) binding *bis*-molybdenum guanine dinucleoside cofactor and a [4Fe-4S] cluster in the cytoplasm before its translocation across the cytoplasmic membrane by TAT system (van Mourik *et al.*, 2008). NapB, a di-haem *c*-type cytochrome, forms the catalytic nitrate-reducing complex with NapA (Potter and Cole, 1999). In *C. jejuni*, it has recently been shown that electrons from the quinone pool are transferred to Nap system through the Qcr complex (Garg *et al.*, 2018). However, it has been shown that in *E. coli* NapG and NapH are putative Fe-S proteins forming an ubiquinol dehydrogenase to transfer electrons to NapA via NapC and NapB (Brondijk *et al.*, 2002; 2004). In *C. jejuni*, it was previously thought that the NapGH complex was the major route of electron transfer to NapA by forming a cytochrome *c* independent membrane bound menaquinol dehydrogenase complex (Pittman *et al.*, 2007, Kern and Simon, 2008). NapD mediates NapA maturation and supports growth by nitrate respiration (Potter and Cole, 1999; Kern *et al.*, 2007). The function of NapL is still unknown but *C. jejuni* cells lacking *napL* showed reduced NapA-dependent nitrate reduction (Pittman *et al.*, 2007).

1.2.7.3 Nitrite reduction to ammonium:

In *C. jejuni*, NrfH (Cj1356) and NrfA (Cj1357) forms the nitrite reductase (Nrf) system. NrfA, a periplasmic pentahaem cytochrome *c*, is a terminal reductase which receives electron from the quinone pool via NrfH, the tetrahaem NapC-like cytochrome *c* (Pitman *et al.*, 2007). The six electron dissimilatory reduction of nitrite to ammonia is catalysed by NrfA. It also reduces nitric oxide (NO) to ammonium (Costa *et al.*, 1990). Growth on nitrite can lead to nitrosative stress and it is well established that NO is an anti-microbial mechanism utilised by the mammalian

immune system in response to bacterial infection (Pitman *et al.*, 2007; Kern *et al.*, 2011a). In *C. jejuni*, NrfA acts as a defence mechanism against nitrosative stress along with the globin Cgb (Pittman *et al.*, 2007).

1.2.7.4 Fumarate:

The family of membrane bound multisubunit succinate:quinone oxidoreductases (SQORs) mediates the reduction of fumarate by catalysing the two-electron transfer between the succinate/fumarate and quinone/quinol couples (Lancaster, 2002). Fumarate is reduced to succinate by two different types of fumarate reductases encoded in the *C. jejuni* genome: (i) Frd encoded by the *frdABC* operon (*cj0408-cj0410*) and (ii) Mfr encoded by the *mfrABE* operon (*cj0437 - cj0439*) (Parkhill *et al.*, 2000). Both consist of a soluble domain attached to a cytoplasmic membrane protein, but while the FrdA active site subunit faces the cytoplasm, that of Mfr (MfrA) faces the periplasm. FrdABC complex performs a dual function of reducing fumarate in oxygen-limited conditions as well as oxidising succinate (to fumarate) aerobically (Weingarten *et al.*, 2009) unlike Mfr, which can only reduce fumarate. Mfr receives electrons from methylmenaquinol to reduce fumarate to succinate. Cells lacking *frdA* have been reported to show a growth defect when grown in oxygen-limited conditions on fumarate as electron acceptor, unlike an *mfrA* mutant, suggesting a more significant role of Frd in supporting growth under oxygen-limited conditions (Guccione *et al.*, 2010).

1.2.7.5 Hydrogen peroxide:

Hydrogen peroxide (H₂O₂) is a toxic intermediate formed during the incomplete reduction of molecular oxygen to water, which can be detoxified by cytochrome *c* peroxidases (CCPs). Bacterial CCPs are di-haemic periplasmic proteins, that play an important role in detoxifying H₂O₂ and converting it to H₂O with the help of reduced cytochrome *c* as an electron donor (Atack and Kelly, 2007). In *C. jejuni* NCTC 11168 strain, *cj0020c* and *cj0358* genes encode two putative CCPs (Parkhill *et al.*, 2000) and in the more pathogenic strain 81-176, *cjj0047c* and *cjj0382* genes encode the homologous products (Bingham-Ramos and Hendrixson, 2008). It has been reported that Cjj0047 is vital for chick colonization (Hendrixson and DiRita, 2004; Bingham-Ramos and Hendrixson, 2008) but none of them showed any significant contribution in detoxifying H₂O₂ *in vitro* (Bingham-Ramos and

Hendrixson, 2008). This along with the fact that the enzymes are not closely related phylogenetically, suggest that they perform non-redundant biological activities (Kelly, 2008). Cj0358/Cjj0382 shows some similarities within the four major classes of CCP while Cj0020/Cjj0047 have no similarities with that group (Atack and Kelly, 2007). The role of CCPs is not clear yet but studies to date indicate that protection against H₂O₂ is unlikely (Bingham-Ramos and Hendrixson, 2008) leading to postulate a role in respiratory metabolism. The periplasmic location of CCP enzymes might suggest that they are not energy conserving but reduction of H₂O₂ can contribute to generation of the proton motive force (PMF) if a proton translocating primary dehydrogenase and/or the Qcr complex containing respiratory chain is terminated by CCP during the process (Kelly, 2008). In *C. jejuni*, formate is an important *in vivo* source of electrons (section 1.2.2.1) but Fdh can also produce H₂O₂ as a periplasmic byproduct. Respiration with nitrate requires removal of H₂O₂ from the periplasm as it inhibits nitrate reduction (Richardson and Ferguson, 1995). This suggest CCPs function is important for growth on formate and nitrate and ultimately *in vivo* (Goodhew *et al.*, 1988).

1.3 Role of metals in bacteria:

Various transition metals have been identified which are essential micronutrients for bacteria. Over the course of time, various enzymes have been identified which are essential for growth, respiration, virulence, colonization, etc in many bacteria and require metal as cofactors (Barondeau and Getzoff, 2004). Some examples of these metals are Fe, Zn, Mn, Ni, Co, Cu, and Mo (Schaible and Kaufmann, 2005). When present in appropriate amount, these metals support growth but excess of them can be fatal for bacterial cells. They can initiate the Fenton reaction, which produce fatal amounts of reactive oxygen species and can ultimately lead to cell death (Stadtman, 1990).

In *C. jejuni*, the iron homeostasis mechanism has been characterised (Naikare *et al.*, 2013) but metabolism of other transition metals has been less well studied. It has been discovered that *C. jejuni* genome encodes a few key proteins using Cu as cofactor making it an essential micronutrient but excess of Cu has also been reported fatal for this pathogen, possibly via the Fenton reaction. This suggests that Cu

homeostasis must be a priority for this pathogen but it has never been studied in detail before.

1.4 Copper:

1.4.1 Copper chemistry:

Copper (Cu) is a transition metal, which exists as two stable and 9 radioactive isotopes, with atomic number 29 and atomic mass 63.546. It is the 26th most abundant metal found in the earth's crust. Atomic radius of Cu is 128 pm and covalent radius is 132 ± 4 pm. Cu^+ (reduced cuprous form) and Cu^{2+} (oxidized cupric form) are the two stable oxidised state of Cu.

1.4.2 Role of Cu in bacterial physiology and as an antimicrobial

Copper is both a blessing and a curse for microorganisms. It is an essential micronutrient required for the functioning of various enzymes that supports growth and on the other hand facilitates the initiation of Fenton's reaction, which is fatal for them. Essential enzymes like cytochrome c oxidase, the respiratory chain terminal electron acceptor, and Cu-Zn superoxide dismutase, required for defense against oxidative damage (Karlin, 1993), require Cu in sufficient amount for proper functioning. Its ability to kill bacteria made it a widespread antibacterial agent and text as old as 2400 BC (Smith Papyrus, an ancient Egyptian medical text) mention use of copper sulfate to sterilize water and treat infections (Dollwet and Sorenson, 1985). There are evidences suggesting use of Cu by Mesoamerican and Hellenistic civilizations to treat a variety of physical ailments, including microbial and parasitic infections. Even Hippocrates prescribed copper salts to treat leg ulcers in 400 BC. Faúndez *et al.* (2004) reported that metallic copper surfaces have an antibacterial activity against *C. jejuni*, so understanding the overall Cu homeostasis mechanisms in *C. jejuni* could be useful for application of Cu antimicrobial properties.

1.4.3 Cu as Fenton reagent:

In the presence of superoxide and/or hydrogen peroxide, Cu facilitates toxic hydroxyl radical formation by Fenton-like chemistry (See equation below; Liochev, 1999).



The hydroxyl radicals formed are extremely reactive and cannot be disposed of by enzymatic reactions. Mechanisms by which these ROS damage bacteria in the phagosome are unclear but their efficiency to kill bacteria make them the critical component of host anti-microbial activity. In *E. coli*, Cu has been reported to damage bacterial cells via non-fenton reactions too by destroying the cytoplasmic iron-sulfur enzymes (Macomber and Imlay, 2009).

1.4.4 Cu in humans:

Cu plays an important role in human growth and development as well with human blood containing approximately 10^{-13} M copper (Linder and Hazegh-Azam, 1996). Cu typically enters through food and is absorbed in the human body from the intestinal lumen. From there it is transferred to liver, which delivers it to various proteins, but also to the gut, where it acts against various gut bacteria, including *C. jejuni*.

1.4.5 Bacterial Copper Homeostasis:

While studying 268 *Gammaproteobacteria*, Hernández-Montes *et al.* (2012) observed that 95% of them had one or more proteins, belonging to a group of 14 proteins, maintaining intracellular Cu homeostasis. Only 3% of them had all 14 proteins. The most crucial and frequent functions for these proteins were Cu translocation from cytoplasm to periplasm by CopA and Cu export from cytoplasm to extracellular space by CusC, performed by co-ordinating with one or more of the other 12 proteins. This kind of study has never been done with *Epsilonproteobacteria* yet.

Cu chaperones are the class of proteins that covalently bind Cu, either to mediate its transportation or utilise it as a cofactor. They are characterised with a metal-binding motif, MXCXXC, in their structure. CopZ is a well-known Cu efflux chaperone. It is a small protein containing approximately 70 residues. Other known Cu chaperones are bacterial Sco1 and PCuAC proteins, responsible for transporting Cu to CcoN in Cu limiting conditions.

Cue and Cus are the two copper efflux systems, which maintain intracellular copper levels in *E. coli* (Rensing and Grass, 2003; Rademacher and Masepohl, 2012).

The Cue system is predominantly responsible for transport of Cu from cytoplasm to periplasm and consists of CueR, CopA and CueO. CueR, a MerR-like transcriptional regulator, controls the transcription of CopA and CueO proteins (Yamamoto and Ishihama, 2005). The Cus system is predominantly responsible for excretion of Cu from periplasm to outside the cell but also supports the Cue system in high copper concentrations under anaerobic conditions. It consists of CusRS and CusCFBA, with CusRS regulating the transcription of the *cusCFBA* genes (Rensing and Grass, 2003).

In *E. coli*, Rensing et al. (1999) discovered CopA as an Cu(I)-translocating P-type ATPase, playing a crucial role in maintaining intracellular Cu homeostasis. *E. coli* CopA acts as a Cu efflux pump. After this discovery, the Cu resisting CopA has been characterised in many bacteria (including pathogens) e.g. *Rubrivivax gelatinosus* (Durand et al. 2015), *Acinetobacter baumannii* (Williams et al., 2016), *Synechocystis* (Giner-Lamia et al., 2015). All the data suggests CopA is a Cu efflux protein essential for bacterial Cu resistance. CopA usually relies on the assistance of a metal chaperone CopZ, which is a putative cytoplasmic copper metallochaperone, responsible for trafficking Cu within the cytoplasm and which forms a complex with CopA for Cu efflux to the periplasm or extracytoplasmic region, for example in *Staphylococcus aureus* (Banci et al., 2001; Cobine et al., 1999; Palumaa, 2013; Corbett et al., 2011; Zhao et al., 2014; Quintata et al., 2017; Straw et al., 2018; Sitthisak et al., 2007). In *Bacillus subtilis*, the presence of a *copZA* operon was reported that encodes CopA and CopZ, with CopZ delivering Cu to CopA (Smaldone and Helmann, 2007). In *E. coli*, *copA* gene encodes both CopA and CopZ by undergoing a programmed frameshift (Meydan et al., 2017). The Cu⁺ effluxed by CopA is collected by multi-copper oxidase CueO in periplasm, which converts it to less toxic Cu²⁺ (Singh et al., 2004). Doku et al. (2013) reported that Cu(I) is a thermodynamically more favoured metal for binding, despite the known high Zn(II) affinity of zinc finger domains, suggesting that Cu(I)-substituted zinc finger domains might be relevant in the context of copper toxicity mechanisms. In *Rhodobacter sphaeroides*, the *cbb₃*-type cytochrome *c* oxidase assembly proteins, homologous to bacterial Sco1 and PCu_AC, were found responsible for maintaining intracellular Cu homeostasis too, with no reported system devoted only for maintaining intracellular Cu homeostasis (Thompson et al., 2012).

1.4.6 Role of Cu in *C. jejuni*:

C. jejuni requires copper (Cu) as a cofactor for a few metalloproteins, including cytochrome *c* oxidase (detailed in section 3.3), the Cj1516/CueO multi-copper oxidase and p19, a protein involved in Fe-transport in the periplasm. Therefore, Cu transportation and assembly is crucial for respiration, growth and host colonisation. However, an excess amount of Cu is toxic, as it can activate O₂ via the Fenton reaction to generate dangerous reactive oxygen radicals. This suggest that *C. jejuni* must encode an efficient Cu homeostasis system and precisely control Cu acquisition, trafficking and incorporation into the target proteins. (This Cu homeostasis system will be further discussed in section 4.1).

1.4.6.1 Cu acquisition in *C. jejuni*:

It has been reported that most of the alphaproteobacteria, including *Rhodobacter sphaeroides*, synthesise CcoA, a transport protein which facilitates the Cu acquisition by bacterial cells. Interestingly, there is no homolog of CcoA in *C. jejuni* and the mechanism of Cu uptake in *C. jejuni* is not known yet (Stahl *et al.*, 2012). *C. jejuni* cells grown in a Cu limited environment showed growth inhibition but deletion of non-essential copper containing proteins, like the p19 iron acquisition protein, partially relieved the growth defect (Chan *et al.*, 2010). Homologs of CueR or CusR, the Cu regulators, are not present in *C. jejuni* but it contains CopA (Cj1161) and CeuO (Cj1516) homologs (Hall *et al.*, 2008). The transmembrane CopA proteins belong to the family of Cu translocating proteins that pump excess Cu (Cuprous ions) from cytoplasm to periplasm, where CeuO oxidises it to less toxic cupric form (Osman and Cavet, 2008). It has been reported that *C. jejuni* cells lacking *copA* or *ceuO* showed severe Cu sensitivity (Hall *et al.*, 2008).

1.5 Aim of this project:

As described above, *C. jejuni* uses complex cytochrome-rich respiratory chains for growth and host colonisation. The respiratory chains are composed of many enzymes found in the inner membrane and periplasm, and includes pathways to two oxidases that transfer electrons to dioxygen; one is a simple quinol oxidase and the other is a more complex copper containing *cbb₃*-type cytochrome *c* oxidase. How *C. jejuni* acquires and manages copper and how it is assembled into this oxidase has not been investigated. The main aim of the project is to identify the genes and proteins responsible for oxidase assembly, with a focus on copper insertion (Chapter 3). In addition, the way in which *C. jejuni* manages the toxic effects of copper and achieves copper homeostasis will also be investigated (Chapter 4). Finally, the role of the Qcr complex in electron transport from the quinone pool to alternative electron acceptors will be investigated (Chapter 5).

Chapter 2

Materials & Methods

2.1 Materials:

All the chemicals, including growth media, used in this study were purchased from Sigma-Aldrich, Oxoid, Bio-Rad, Invitrogen, Life technologies, Promega, Fisher and Honeywell. All antibiotics were purchased from Apollo Scientific, Melford, Alfa Aesar and Sigma-Aldrich. Apparatus used were from Fisher Scientific, Don Whitley Scientific, Techne, Bio-Rad, Star Lab and Thermo Scientific. Gases were supplied by BOC.

2.2 Organisms and growth media:

2.2.1 Organisms used in this study:

All strains of *C. jejuni* and *E. coli* used in these studies are mentioned in Table 2.1. *C. jejuni* strain stocks were stored at -80 °C in Brain Heart Infusion (BHI) broth containing 15% [v/v] glycerol as cryoprotectant in cryogenic tubes. Strains of *E. coli* were stored at -80 °C in Luria-Bertani (LB) broth containing 15% [v/v] glycerol as cryoprotectant in cryogenic tubes.

Table 2.1: *C. jejuni* strains used in these studies:

<i>Campylobacter jejuni</i>	Description	Source / Reference
Wild type NCTC11168 (DJK)	Laboratory wild type strain, original human clinical isolate	Parkhill <i>et al.</i> , 2000
$\Delta cj0908-0911$	<i>C. jejuni</i> NCTC 11168 (DJK) <i>cj0911</i> , <i>cj0910</i> , <i>cj0909</i> and <i>cj0908</i> operon knock out deletion::kan	This study
$\Delta cj0911$	<i>C. jejuni</i> NCTC 11168 (DJK) knock out deletion:: kan	This study
$\Delta cj1490c-1487c$	<i>C. jejuni</i> NCTC 11168 (DJK) <i>cj1490c</i> , <i>cj1489c</i> , <i>cj1488c</i> and <i>cj1487c</i> operon knock out deletion::kan	This study
$\Delta cj1154c$	<i>C. jejuni</i> NCTC 11168 (DJK) knock out deletion:: kan	This study
$\Delta cj1155c$	<i>C. jejuni</i> NCTC 11168 (DJK) knock out deletion:: kan	This study
$\Delta cj0369c$	<i>C. jejuni</i> NCTC 11168 (DJK) knock out deletion:: kan	This study
$\Delta cj1483c$	<i>C. jejuni</i> NCTC 11168 (DJK) knock out deletion:: kan	This study

$\Delta cj1484c$	<i>C. jejuni</i> NCTC 11168 (DJK) knock out deletion:: kan	This study
$\Delta cj1485c$	<i>C. jejuni</i> NCTC 11168 (DJK) knock out deletion:: kan	This study
$\Delta cj1486c$	<i>C. jejuni</i> NCTC 11168 (DJK) knock out deletion:: kan	This study
$\Delta cj1161$	<i>C. jejuni</i> NCTC 11168 (DJK) knock out deletion:: kan	This study
$\Delta cj1162$	<i>C. jejuni</i> NCTC 11168 (DJK) knock out deletion:: kan	This study
$\Delta cj1163$	<i>C. jejuni</i> NCTC 11168 (DJK) knock out deletion:: kan	This study
$\Delta cj1164$	<i>C. jejuni</i> NCTC 11168 (DJK) knock out deletion:: kan	This study
$\Delta cj1165$	<i>C. jejuni</i> NCTC 11168 (DJK) knock out deletion:: kan	This study
$\Delta cj1166$	<i>C. jejuni</i> NCTC 11168 (DJK) knock out deletion:: kan	This study
$\Delta cj1186c-1184c$	<i>C. jejuni</i> NCTC 11168 (DJK) knock out deletion:: kan	This study
$\Delta cj0037$	<i>C. jejuni</i> NCTC 11168 (DJK) knock out deletion:: kan	This study
$\Delta cj1020$	<i>C. jejuni</i> NCTC 11168 (DJK) knock out deletion:: cam	This study
$\Delta cj0037+\Delta cj1020$	<i>C. jejuni</i> NCTC 11168 (DJK) <i>cj0037</i> and <i>cj1020</i> double knock out deletion:: kan+cam	This study

Table 2.2: *E. coli* strains used in these studies

<i>Escherichia coli</i>	Genotype	Source
DH5 α TM	F- Φ 80 <i>lacZ</i> Δ M15 Δ (<i>lacZ</i> YA- <i>argF</i>) U169 <i>recA1 endA1</i> <i>hsdR17</i> (rK-, mK+) <i>phoA</i> <i>supE44</i> λ - <i>thi-1 gyrA96 relA1</i>	Invitrogen
BL21 (DE3)	F- <i>omp</i> T <i>hsdSB</i> (rB-, mB-) <i>gal</i> <i>dcm</i> (DE3)	Invitrogen

2.2.2 Growth media preparation:

2.2.2.1 Media preparation for *C. jejuni* growth:

For making agar plates for growing *C. jejuni*, Columbia Blood Agar CM0331 (Oxoid, Basingstoke, UK) was dissolved in dH₂O, as per manufacturer instructions, and autoclaved for 20 minutes at 121 °C and 15 psi for sterilisation. At optimum temperature, 5% (v/v) lysed horse blood (SR0050C, Thermo Scientific) was added and mixed with heating at intervals until the media become chocolaty brown in colour. At optimum temperature 10 µg/ml vancomycin, 10 µg/ml amphotericin B and appropriate selective antibiotics were added and media was poured in plates. Liquid cultures of *C. jejuni* were grown in Mueller-Hinton broth (Oxoid) made by dissolving 21 g/L Mueller-Hinton broth (Oxoid) in dH₂O with 20 mM L-Serine (MHS) and autoclaved for 20 minutes at 121 °C and 15 psi for sterilisation.

2.2.2.2 Media preparation for *E. coli* growth:

Strains of *E. coli* were routinely grown on LB agar plates and LB broth. LB agar plates were made by dissolving 20g L⁻¹ LB broth granules (Oxoid) and 10 gL⁻¹ agar (Melford) in dH₂O and autoclaved for 20 minutes at 121°C and 15 psi for sterilisation. At optimum temperature, appropriate antibiotics were added and media was poured on plates. LB broth was made by dissolving 20 gL⁻¹ LB broth granules in dH₂O and autoclaved for 20 minutes at 121°C and 15 psi for sterilisation.

2.2.2.3 Antibiotic Solutions:

Antibiotics used in this study were vancomycin 10 µg ml⁻¹, amphotericin B 10 µg ml⁻¹, kanamycin 50 µg ml⁻¹, chloramphenicol 20 µg ml⁻¹ (for *C. jejuni*)/ 40 µg ml⁻¹ (for *E. coli*) and ampicillin/carbenicillin 50 µg ml⁻¹. All antibiotic solutions were made in sterile dH₂O except chloramphenicol, which was dissolved in ethanol. A few drops of concentrated NaOH (10 M) were added with Amphotericin B in dH₂O as it needs a basic solvent. 10x stock solutions of antibiotics were made and filter sterilised through 0.2 µm filters. Antibiotics were added to media after it had cooled down.

2.3 Growth of Bacterial Cells:

2.3.1 Growth of *C. jejuni* in complex media:

C. jejuni strains were routinely grown at 42 °C under microaerobic conditions [10% (v/v) O₂, 5% (v/v) CO₂ and 85% (v/v) N₂] in a MACS growth cabinet (Don Whitley Scientific, Shipley, UK). Bacterial cells, from frozen stocks, were streaked on Columbia plates (with appropriate antibiotics) and incubated over-night in MACS growth cabinet. Material from plates were used for inoculating 25-50 ml MHS and incubated on a shaker at 150 rpm in the MACS growth cabinet for 6-12 hours, depending on the growth stage required for the particular assay. Culture growth was monitored regularly (mostly hourly) by measurement of OD₆₀₀ against relevant media as control (Blank) with starting OD₆₀₀ ranging from 0.05 to 0.2, depending on the requirement of assay. MHS was routinely supplemented with 10 µg ml⁻¹ each of vancomycin and amphotericin B.

2.3.2 Growth of *C. jejuni* in minimal media:

To minimise the metal contamination, Minimum Essential Medium (MeM) α, (nucleosides added, no phenol red) minimal media (Life Science technologies) was used to grow *C. jejuni*. MeMα was supplemented with 40 µM FeSO₄, 20 mM Sodium Pyruvate and 20 mM L-Serine. FeSO₄, Sodium Pyruvate and L-Serine solutions were in MeMα and filter sterilised through 0.2 µm filters. Bacterial cells were grown in MeMα as described with MHS.

2.3.3 Oxygen-limited growth of *C. jejuni*:

C. jejuni cannot grow in completely anaerobic environments but was grown in severely oxygen-limited conditions with appropriate electron acceptors added where needed (20 mM final concentration). For oxygen-limited growth, cells harvested from starter cultures, were grown in 200ml MHS in 250ml conical flasks in the MACS growth cabinet as in 2.3.1 with starting OD₆₀₀ = 0.1, but without shaking.

2.3.4 Continuous chemostat culture of *C. jejuni*:

Cells were grown in a carbon (serine)- limited chemostat (Infors HT Labfors 3 monitored and controlled using Infors Iris 5 software; Infors, Switzerland) in the MEM- alpha minimal medium supplemented with 40 µM FeSO₄, 20 mM Sodium Pyruvate and 20 mM L-Serine.. The required input gas composition was obtained by

proportional mixing from a compressed air line plus a 90:10% v/v nitrogen/CO₂ gas cylinder. The input CO₂ concentration varied from ~2% v/v to 10% v/v over the range of oxygen inputs used. 2% v/v CO₂ is in excess of the cells growth requirements (Al- Haideri *et al.*, [2016](#)). The culture volume was 885 ml, the temperature was maintained at 37°C by a thermostatic water jacket, the gas sparging rate was 0.5 l min⁻¹ with a stirring rate of 350 rpm and the pH was maintained at 7 ± 0.1 with automatic addition of 1 M NaOH or H₂SO₄. The vessel was inoculated aseptically to an OD₆₀₀ of 0.1 with cells grown in MHS batch culture under standard microaerobic conditions. After inoculation, cells were initially grown as a batch culture for 6 h, reaching an OD₆₀₀ of ~0.6; at this point fresh media was fed into the vessel at a dilution rate of 0.2 h⁻¹ until steady- state was reached, defined by a stable optical density for five vessel volumes of fresh media supplied to the chemostat. Each steady- state was derived from an independent initial batch culture. Samples were taken from the steady- states for analyses. For the high to low oxygen temporal transition experiment, cultures initially grown to steady state with a gas mixture providing 150% perceived aerobiosis (7.5% v/v O₂, 6.4% v/v CO₂ & 85.7% v/v N₂) were switched to 40% aerobiosis (1.88% v/v O₂, 9.11% v/v CO₂ & 88.9% v/v N₂) at time zero. Samples were then taken when the culture reached the new steady state.

2.3.5 Growth of *E. coli*:

Strains of *E.coli* were routinely grown from frozen stocks on LB plates or in LB broth with appropriate antibiotics incubated overnight at 37 °C under aerobic condition. Liquid cultures were incubated continuously shaken at 250 rpm.

2.3.6 Culture growth measurement:

Growth in liquid media was measured by measuring optical density (OD) of cultures with a Jenway 6705 UV spectrophotometer at 600 nm wavelength (OD₆₀₀) against media as blank. 1 ml plastic cuvettes were used.

2.3.7 Check for contamination:

All *C. jejuni* cultures were checked for contamination before and/or after the assay, as the situation may require, by spreading a small amount of culture on LB agar plates and incubating 48 hours under fully aerobic conditions at 37 °C. Any growth on the plate indicates contamination.

2.4 DNA preparation and manipulation:

2.4.1 Genomic DNA (gDNA) isolation:

C. jejuni NCTC11168 cells were harvested by growing overnight on Columbia Blood Agar plates (section 2.3.1) and genomic DNA was extracted by using 5 Prime ArchivePure DNA Cell/Tissue Kit (Scientific Laboratory supplies). Manufacturer's instructions were followed. Harvested cells were resuspended in 1ml BHI broth and centrifuged at 9,000 x g for 1 minute at 4 °C. Supernatant was discarded and pellet was resuspended in 600 µl of Cell Lysis Solution (ArchivePure) by gentle pipetting. Sample was incubated at 80 °C for 5 minutes and 3 µl of RNase A solution (4 mg/ml) (ArchivePure) was added. Sample was mixed by inverting 25 times and incubated at 37 °C for 30 minutes. Sample was cooled to RT and 200 µl of protein precipitation solution (ArchivePure) was added. Sample was vortexed vigorously for 20 seconds and centrifuged at 12,550 x g for 3 minutes at 4 °C. Supernatant containing genomic DNA was transferred to a clean 1.5 ml microfuge tube containing 600 µl of 100% Isopropanol. Sample was mixed by inverting 50 times and incubated at RT for 5 minutes. After incubation, sample was centrifuged at 15,550 x g for 1 minute at 4 °C, supernatant was discarded and tube was drained on a clean absorbent paper. DNA pellet was washed with 600 µl of 70 % ethanol by inverting the tube several times and centrifuged at 15,550 x g for 1 minute at 4 °C. Supernatant was discarded and the pellet was air dried for 10-15 minutes. DNA was resuspended in 100 µl Nuclease-Free Water (Promega) by incubating at 65 °C for 1 hour with occasional mixing. gDNA concentration was measured by Nanodrop (Genova Nano-Jenway) (section 2.4.3) and stored at -20°C.

2.4.2 Plasmid DNA isolation:

Plasmid DNA were extracted from *E. coli* strains using Qiagen Miniprep (and sometimes midiprep) kits (Qiagen, UK). For miniprep, typically 5 ml of LB broth culture was grown in 20 ml falcon tubes incubated as in section 2.3.3. Manufacturer's instructions were followed. Cell pellet was resuspended in 250 µl of Buffer P1 (Qgen) and transferred to a microcentrifuge tube. 250 µl of Buffer P2 was added and mixed thoroughly by inverting. 350 µl of Buffer N3 was added and mixed immediately by inverting 4-6 times. Sample was centrifuged at 12,470 x g for 10 minutes. Resulting supernatant was transferred to QIAprep spin column (Qaigen) and centrifuged at

12,470 x g for 1 minute. Collection basket was emptied and spin column was washed with 0.75 ml Buffer PE (Qiagen) by centrifuging at 12,470 x g for 1 minute. Collection basket was emptied and column was centrifuged for 1 more minute to remove the residual wash buffer. Column was placed in a fresh 1.5 ml microcentrifuge tube, 50 µl of Nuclease-Free Water (Promega) was added to cover the whole membrane, let stand for 1 minute and centrifuged at 12,470 x g for 1 minute. Concentration was measured by Genova Nanodrop micro-volume spectrophotometer (Jenway) with Nuclease-Free Water (Promega) as reference (blank) as in section 2.4.3 and the plasmid was stored at -20°C.

2.4.2.1 Plasmids used in this study:

Table 2.3: Plasmids used in this study

Plasmid	Description	Resistance marker	Source
pGEM [®] 3Zf(-)	Standard cloning vector used for making mutagenesis constructs. MCS in frame with <i>lac</i> operon to allow blue/white colour selection	Amp ^R	Promega
pJMK30	Cloning vector containing the <i>aphAIII</i> gene encoding kanamycin resistance	Amp ^R Kan ^R	Van Vliet <i>et al.</i> , 1998
pAV35	Cloning vector containing the chloramphenicol acetyl transferase (<i>cat</i>) inserted at BamHI site	Amp ^R Cat ^R	Van Vliet <i>et al.</i> , 1998
p(K/C)46 (Metk / FdxA)	Group of vectors for complementation of <i>C. jejuni</i> mutants by insertion at the <i>cj0046</i> pseudogene locus	Kan ^R or Cat ^R	Gaskin <i>et al.</i> , 2007
pET21a(+)	Used for over-expression of proteins with C-terminal His-tag under control of IPTG inducible T7 promoter	Amp ^R	Novagen
StrepII-tag pET21a	Used for over-expression of proteins with C-terminal strepII-tag under control of IPTG inducible T7 promoter	Amp ^R	This study
pPRA	Group of vectors for complementation of <i>C. jejuni</i>	Apr ^R	Cameron <i>et al.</i> , 2014

	mutants by insertion at the <i>cj0046</i> pseudogene locus		
pGEM-cj0908-11	pGEM3Zf(-) containing the flanking regions of <i>cj0908-cj0911</i> around a Kan cassette	Amp ^R Kan ^R	This study
pGEM-cj0908	pGEM3Zf(-) containing the flanking regions of <i>cj0908</i> around a Kan cassette	Amp ^R Kan ^R	This study
pGEM-cj0909	pGEM3Zf(-) containing the flanking regions of <i>cj0909</i> around a Kan cassette	Amp ^R Kan ^R	This study
pGEM-cj0910	pGEM3Zf(-) containing the flanking regions of <i>cj0910</i> around a Kan cassette	Amp ^R Kan ^R	This study
pGEM-cj0911	pGEM3Zf(-) containing the flanking regions of <i>cj0911</i> around a Kan cassette	Amp ^R Kan ^R	This study
pGEM-cj1490c-87c	pGEM3Zf(-) containing the flanking regions of <i>cj1490c-cj1487c</i> around a Kan cassette	Amp ^R Kan ^R	Yang-Wei Liu
pGEM-cj1154c	pGEM3Zf(-) containing the flanking regions of <i>cj1154c</i> around a Kan cassette	Amp ^R Kan ^R	This study
pGEM-cj1155c	pGEM3Zf(-) containing the flanking regions of <i>cj1155c</i> around a Kan cassette	Amp ^R Kan ^R	This study
pGEM-cj0369c	pGEM3Zf(-) containing the flanking regions of <i>cj0369c</i> around a Kan cassette	Amp ^R Kan ^R	This study
pGEM-cj1483c	pGEM3Zf(-) containing the flanking regions of <i>cj1483c</i> around a Kan cassette	Amp ^R Kan ^R	This study
pGEM-cj1482c	pGEM3Zf(-) containing the flanking regions of <i>cj1482c</i> around a Kan cassette	Amp ^R Kan ^R	This study
pGEM-cj1484c	pGEM3Zf(-) containing the flanking regions of <i>cj1484c</i> around a Kan cassette	Amp ^R Kan ^R	This study
pGEM-cj1485c	pGEM3Zf(-) containing the flanking regions of <i>cj1485c</i> around a Kan cassette	Amp ^R Kan ^R	This study
pGEM-cj1486c	pGEM3Zf(-) containing the flanking regions of <i>cj1486c</i> around a Kan cassette	Amp ^R Kan ^R	This study
pGEM-cj1161	pGEM3Zf(-) containing the flanking regions of <i>cj1161</i> around a Kan cassette	Amp ^R Kan ^R	This study
pGEM-cj1162	pGEM3Zf(-) containing the flanking regions of <i>cj1162</i> around	Amp ^R Kan ^R	This study

	a Kan cassette		
pGEM-cj1163	pGEM3Zf(-) containing the flanking regions of <i>cj1163</i> around a Kan cassette	Amp ^R Kan ^R	This study
pGEM-cj1164	pGEM3Zf(-) containing the flanking regions of <i>cj1164</i> around a Kan cassette	Amp ^R Kan ^R	This study
pGEM-cj1165	pGEM3Zf(-) containing the flanking regions of <i>cj1165</i> around a Kan cassette	Amp ^R Kan ^R	This study
pGEM-cj1166	pGEM3Zf(-) containing the flanking regions of <i>cj1166</i> around a Kan cassette	Amp ^R Kan ^R	This study
pGEM-cj1186c-84c	pGEM3Zf(-) containing the flanking regions of <i>cj1186c-cj1184c</i> around a Kan cassette	Amp ^R Kan ^R	This study
pGEM-cj0037	pGEM3Zf(-) containing the flanking regions of <i>cj0037</i> around a Kan cassette	Amp ^R Kan ^R	Yang-Wei Liu
pGEM-cj1020	pGEM3Zf(-) containing the flanking regions of <i>cj1020</i> around a Cat cassette	Amp ^R Cat ^R	Yang-Wei Liu
pGEM-cj0037+1020	pGEM3Zf(-) containing the flanking regions of <i>cj0037</i> around a Kan cassette and <i>cj1020</i> around a Cat cassette	Amp ^R Kan ^R Cat ^R	Yang-Wei Liu
pCMetK46-Cj1490c-87c	pCMetK46 with the <i>cj1490c</i> , <i>cj1489c</i> , <i>cj1488c</i> and <i>cj1487c</i> ORF under the <i>metK</i> promoter	Cat	Yang-Wei Liu

2.4.3 Nucleotide concentration measurement:

RNA and DNA concentrations were measured by Genova Nano micro-volume spectrophotometer (Jenway) with ddH₂O as reference (blank). The concentration was determined according to manufacturer's instructions. For high quality RNA and DNA samples, the ratio of A₂₆₀/A₂₈₀ should be above 2.0 and 1.8 respectively.

2.4.4 Polymerase Chain Reaction (PCR):

Oligonucleotide sequences (primers) identical to starting of 5' and terminal 3' end of DNA segment were designed. Then purified DNA samples, both primers, deoxynucleoside triphosphates (dNTPs) and DNA polymerase (quantity as required by the reaction) were mixed together in a buffer (suitable for the respective reaction) in an Eppendorf to a final volume of 10 to 50 µl. Eppendorf is placed in a thermal cycler, which carries out the temperature cycles. There are 3 steps in each cycle: (i)

Denaturation in which the sample is heated at 95 °C. (ii) *Annealing* in which sample is heated from 55 °C to 65 °C, depending on the melting temperature of the primers. It anneals primers on both ends of the DNA segment; and (iii) *Extension* in which sample is heated at 72 °C. In this step DNA polymerase begins DNA formation. Conditions can be modified occasionally according to the requirement.

PCR reactions were used for screening *C. jejuni* knock out strains, clones of transformation *E coli*, amplification of desired gene fragments (500 bp both upstream and downstream of gene of interest), and amplification of antibiotic resistance cassette with adapters for restriction enzymes.

2.4.4.1 PCR for Gene fragment amplification:

Standard PCR reactions were done to amplify both the upstream and downstream gene fragments (of about 500 bp) of the desired gene. Primers were designed and ordered from Sigma-Aldrich. For upstream fragments, forward primers (F1F) were designed having 20 bp sequence aligning with the 5` end of DNA template with 30 bp adaptors homologous to pGEM3zf directly before the HincII restriction site. Reverse primers (F1R) were designed having 20 bp sequence of reverse complement of the 3` end of DNA template with 30 bp adaptors homologous to reverse compliment of the kanamycin antibiotic resistant cassette created with Kan+StyI 5` primers (Table: 2.8). For downstream fragments, forward primers (F2F) were designed having 20 bp sequence aligning with the 5` end of DNA template with 30 bp adaptor homologous to last 30 bp of kanamycin antibiotic resistant cassette created with Kan+StyI 3` primers. Reverse primers (F2R) were designed having 20 bp sequence of reverse complement of the 3` end of DNA template with 30 bp adaptor homologous to reverse compliment of pGRM3zf directly after the HincII restriction site.

In an eppendorf, all components of PCR as mentioned in table below were added together to a final volume of 50 µl. Phusion Flash (Thermo scientific) polymerase was used.

Table 2.4: Composition of PCR reactions

2X Phusion Flash polymerase mix	25 µl
dH ₂ O	22 µl
100 µM Primer solutions	1 µl each

Template DNA	1 μ l
--------------	-----------

Conditions were modified occasionally according to the requirements. PCR reactions were performed in a 60 well (Techne Flexigene) thermal-cycler using the settings described in Table 2.5 with Preheated lid and final hold at 4 °C.

Table 2.5: Standard PCR conditions

Stage	Temperature	Duration	Cycles	Description
1	98 °C	5 mins	1	Initial Denaturation
2	98 °C	10 seconds	30-35	Denaturation
	45-55 °C	10 seconds		Annealing
	72 °C	1 minute kb ⁻¹		Extension
3	72 °C	5 minutes	1	Final Extension
4	4 °C	Hold	1	Final Hold

2.4.4.2 PCR for complementation gene amplification:

Standard PCR reactions were done to amplify gene of interest with primers having first ~20 bp (minus ATG) and last ~20 bp of gene sequence and either BsmBI adaptors for p(C/K)46metK complementation vector or MfeI and XbaI restriction enzyme sites for pRRA complementation vector. Primers are listed in Table 2.4.5: Red coloured part of primers are BsmBI adaptors for p(C/K)46metK complementation vector and blue coloured part of primers are MfeI or XbaI restriction enzyme site for pRRA complementation vector with few random oligonucleotides in the beginning. Gene of interest was amplified according to section 2.4.4.1.

2.4.4.3 PCR for screening:

Standard PCR reactions were done to screen transformed DH5 α colonies and for putative *C. jejuni* mutants. Mostly cell material from colonies was used but in some cases plasmids or DNA extracted from cells were used. In an eppendorf, all components of PCR as mentioned in table below were added together to a final volume of 20 μ l. MyTaq (Bioline) was used as polymerase.

Table 2.6: PCR mixture for screening

2X MyTaq polymerase mix	10 μ l
dH ₂ O	7 μ l/8 μ l
100 μ M Primer solutions	1 μ l each

Colony/Template DNA	1/1 µl
---------------------	--------

Conditions were modified occasionally according to the requirements. PCR reactions were performed in a 60 well (Techne Flexigene) thermal-cycler using the settings described in Table with Preheated lid and final hold at 4 °C.

Table 2.7: PCR conditions for screening

Stage	Temperature	Duration	Cycles	Description
1	95 °C	10 mins	1	Initial Denaturation
2	95 °C	10 seconds	30-35	Denaturation
	50-60 °C	20 seconds		Annealing
	72 °C	1 minute kb ⁻¹		Extension
3	72 °C	5 minutes	1	Final Extension
4	4 °C	Hold	1	Final Hold

2.4.5 PCR primers used in this study:

All PCR primers were ordered from Sigma-Aldrich. Coloured sequences are adaptors.

Table 2.8:

<i>C. jejuni</i> NCTC 11168 knock out primers 5'-3'	
Cj0908 ISA F1 F	GAGCTCGGTACCCGGGGATCCTCTAGAGTC ACCTACTGGAGTTTTCAA ATCTCC
Cj0908 ISA F1 KR	AAGCTGTCAAACATGAGAACCAAGGAGAAT TATAGACAACCTTTTAA AACAAGCC
Cj0908 ISA F2 KF	GAATTGTTTTAGTACCTAGCCAAGGTGTGC AAAATTTTCAAATTTTAT ATTCAAATAAAA
Cj0908 ISA F2 R	AGAATACTCAAGCTTGCATGCCTGCAGGTC TTTAACTCTATGGTTTTGT GATTATTA
Cj0909 ISA F1 F	GAGCTCGGTACCCGGGGATCCTCTAGAGTC TTTATACATTATATGATA AAAAGAAAGAAAGTATATTT
Cj0909 ISA F1 KR	AAGCTGTCAAACATGAGAACCAAGGAGAAT ATTGTATCCTTATTTTAA TAATATTAATATTTGTTTC
Cj0909 ISA F2 KF	GAATTGTTTTAGTACCTAGCCAAGGTGTGC TTAATGAGAAAATTATT TTTATCCTAGC
Cj0909 ISA F2 R	AGAATACTCAAGCTTGCATGCCTGCAGGTC TAAAATAATGGCAACTAT AACTATAAACAAA
Cj0910 ISA F1 F	GAGCTCGGTACCCGGGGATCCTCTAGAGTC TCAAATTTTATATTCAA ATAAAAATATTTTTTT

Cj0910 ISA F1 KR	AAGCTGTCAAACATGAGAACCAAGGAGAATTAATTTAAAATTCTTTAG AATCAATATTTTTAACT
Cj0910 ISA F2 KF	GAATTGTTTTAGTACCTAGCCAAGGTGTGCAATAAACCCATAGGGTTT TATTTTG
Cj0910 ISA F2 R	AGAATACTCAAGCTTGCATGCCTGCAGGTC AATCGTTAATTTCTTTATA AAAATGACC
Cj0911 ISA F1 F	GAGCTCGGTACCCGGGGATCCTCTAGAGTC TTAATAATCACAAAACCA TAGAGTTAAAA
Cj0911 ISA F1 KR	AAGCTGTCAAACATGAGAACCAAGGAGAATTTTTTTAGCTCAAAATCA AAATAAAA
Cj0911 ISA F2 KF	GAATTGTTTTAGTACCTAGCCAAGGTGTGCTTATACTTAAGCAAAAAG ATCGGTT
Cj0911 ISA F2 R	AGAATACTCAAGCTTGCATGCCTGCAGGTC GTTTCTCAATTTGAAAAT ATTTCAAATA
CJ1154C ISA F1 F	GAGCTCGGTACCCGGGGATCCTCTAGAGTC AAGAGAAGGTGCAAAAAG AGC
CJ1154C ISA F1 R	AAGCTGTCAAACATGAGAACCAAGGAGAATTCATGATTATACTATTCA TTCTT
CJ1154C ISA F2 F	GAATTGTTTTAGTACCTAGCCAAGGTGTGCTTCTTAAAAAGAAAAGCC TT
CJ1154C ISA F2 R	AGAATACTCAAGCTTGCATGCCTGCAGGTC CACCGTCTCTATCTAAAA ATA
CJ1155C ISA F1 F	GAGCTCGGTACCCGGGGATCCTCTAGAGTC ATCGCTTCGATTTTTAAA AG
CJ1155C ISA F1 R	AAGCTGTCAAACATGAGAACCAAGGAGAATTGCAATGTTACATTTC TA
CJ1155C ISA F2 F	GAATTGTTTTAGTACCTAGCCAAGGTGTGCAAGGATTAAGAATGAATA GTATAA
CJ1155C ISA F2 R	AGAATACTCAAGCTTGCATGCCTGCAGGTC CACCGTCTCTATCTAAAA ATA
CJ0369C ISA F1 F	GAGCTCGGTACCCGGGGATCCTCTAGAGTC ACCTATCATACCAATTTG AATGATT
CJ0369C ISA F1 R	AAGCTGTCAAACATGAGAACCAAGGAGAATGTGTCCTTGCATTTTTAG ACC
CJ0369C ISA F2 F	GAATTGTTTTAGTACCTAGCCAAGGTGTGCAAAAATGAACTCAAATAG AACACCATCAC
CJ0369C ISA F2 R	AGAATACTCAAGCTTGCATGCCTGCAGGTC AGGAGCGTTAATTTAAAC ATTAAGAT
CJ1483C ISA F1 F	GAGCTCGGTACCCGGGGATCCTCTAGAGTC TTTTAATGAAAATATTTT AAGTCAAAAAGTAA
CJ1483C ISA F1 R	AAGCTGTCAAACATGAGAACCAAGGAGAATAATTATAGCCAAAAGTG AAAGCA
CJ1483C ISA F2 F	GAATTGTTTTAGTACCTAGCCAAGGTGTGCGAAACAGTGGGTTTTTTTT AGCT
CJ1483C ISA F2 R	AGAATACTCAAGCTTGCATGCCTGCAGGTC TACTTAAAAACCTTGCA AATCATAA
CJ1486C ISA F1 F	GAGCTCGGTACCCGGGGATCCTCTAGAGTC CAATGGGTCAAATATCT TTTTAGT
CJ1486C ISA F1 R	AAGCTGTCAAACATGAGAACCAAGGAGAATTCACCCCTTGAAAGAGA AAT
CJ1486C ISA F2 F	GAATTGTTTTAGTACCTAGCCAAGGTGTGCGTAAGGCTTTGGAATATT TAATTGTT
CJ1486C ISA F2 R	AGAATACTCAAGCTTGCATGCCTGCAGGTC GCAGCATTATAAATATCA CCTTTATTG

CJ1485C ISA F1 F	GAGCTCGGTACCCGGGGATCCTCTAGAGTC	ATGTAGCAAAGATCTTT CAGCT
CJ1485C ISA F1 R	AAGCTGTCAAACATGAGAACCAAGGAGAAT	TGTGCTTCCTTTATACTT CTATGATC
CJ1485C ISA F2 F	GAATTGTTTTAGTACCTAGCCAAGGTGTGC	AAAAAATATTACAAGATG GCTTTTTT
CJ1485C ISA F2 R	AGAATACTCAAGCTTGCATGCCTGCAGGTC	TATCACGATTTGCATTAC CTATAGA
CJ1484C ISA F1 F	GAGCTCGGTACCCGGGGATCCTCTAGAGTC	CCATGGAGAAGATGGAA AAG
CJ1484C ISA F1 R	AAGCTGTCAAACATGAGAACCAAGGAGAAT	CTAAAAAAAGCCATCT TGTAATATTTT
CJ1484C ISA F2 F	GAATTGTTTTAGTACCTAGCCAAGGTGTGC	ACAAAGAAGAATAAAGA GGAAAAAAA
CJ1484C ISA F2 R	AGAATACTCAAGCTTGCATGCCTGCAGGTC	GCCTTGAAGAGCTAAAAA TTCTT
CJ1482C ISA F1 F	GAGCTCGGTACCCGGGGATCCTCTAGAGTC	GAAACTAAAAAAAGTTTT TGGCC
CJ1482C ISA F1 R	AAGCTGTCAAACATGAGAACCAAGGAGAAT	TGAAGAGCTAAAAATTC TTAATTTCA
CJ1482C ISA F2 F	GAATTGTTTTAGTACCTAGCCAAGGTGTGC	ATAAACTCATTTATAAAA AGGAATTAATAATG
CJ1482C ISA F2 R	AGAATACTCAAGCTTGCATGCCTGCAGGTC	CAAGCTCGTTAAAAAAAT TTTCTT
CJ1161C ISA F1 F	GAGCTCGGTACCCGGGGATCCTCTAGAGTC	AGCTATTGTATTATCAAT CTTGCTTTT
CJ1161C ISA F1 R	AAGCTGTCAAACATGAGAACCAAGGAGAAT	ACGCAATTCTTCCATTAT AAACG
CJ1161C ISA F2 F	GAATTGTTTTAGTACCTAGCCAAGGTGTGC	AAGAATTTAAAAATTTAA TTTTTA
CJ1161C ISA F2 R	AGAATACTCAAGCTTGCATGCCTGCAGGTC	ACATTCCAAACCATTCTG CAA
CJ1162C ISA F1 F	GAGCTCGGTACCCGGGGATCCTCTAGAGTC	CATGATAATTGTAGCTAT TTTGGG
CJ1162C ISA F1 R	AAGCTGTCAAACATGAGAACCAAGGAGAAT	CAATTAACATTTTTTACT TTAAATTTTCATTTT
CJ1162C ISA F2 F	GAATTGTTTTAGTACCTAGCCAAGGTGTGC	TTTATAATGGAAGAATTG CGTATAAA
CJ1162C ISA F2 R	AGAATACTCAAGCTTGCATGCCTGCAGGTC	CTTCTTCTTTAAAAATTTG CAAATACA
CJ1163C ISA F1 F	GAGCTCGGTACCCGGGGATCCTCTAGAGTC	TTTGGCTCTAGCTATAGG AGTGAG
CJ1163C ISA F1 R	AAGCTGTCAAACATGAGAACCAAGGAGAAT	ATCTTATATCCTTTTTTG CTTGACAT
CJ1163C ISA F2 F	GAATTGTTTTAGTACCTAGCCAAGGTGTGC	AAGGAGTGAAAATGAAAT TTAAAGTAA
CJ1163C ISA F2 R	AGAATACTCAAGCTTGCATGCCTGCAGGTC	AAACATTTCAAATACAT AATAATCACACT
CJ1164C ISA F1 F	GAGCTCGGTACCCGGGGATCCTCTAGAGTC	GATTTGGCTTTGCTTATG CTT
CJ1164C ISA F1 R	AAGCTGTCAAACATGAGAACCAAGGAGAAT	AATCTACATTACAAACT GGACATAACA
CJ1164C ISA F2 F	GAATTGTTTTAGTACCTAGCCAAGGTGTGC	AGCTTTTTGACTTTTAATT TTTATAAAAAAT

CJ1164C ISA F2 R	AGAATACTCAAGCTTGCATGCCTGCAGGTCGGTTTTAGCGTCAATTC TTTT
CJ1165C ISA F1 F	GAGCTCGGTACCCGGGGATCCTCTAGAGTCGTGCTTTAAGCTGGGCTA TATATG
CJ1165C ISA F1 R	AAGCTGTCAAACATGAGAACCAAGGAGAATTAAAATAAATTCAATCA TCTTAAAATCCC
CJ1165C ISA F2 F	GAATTGTTTTAGTACCTAGCCAAGGTGTGC ACTAGACATGCAAAAAAA CATTAAAA
CJ1165C ISA F2 R	AGAATACTCAAGCTTGCATGCCTGCAGGTC TGGGAATGATGATGTTCA TG
CJ1166C ISA F1 F	GAGCTCGGTACCCGGGGATCCTCTAGAGTC GAACTATCCAAATTTGTT CCACTAC
CJ1166C ISA F1 R	AAGCTGTCAAACATGAGAACCAAGGAGAATTATATCAGGTTTTTCCAT ATTTAATAATCT
CJ1166C ISA F2 F	GAATTGTTTTAGTACCTAGCCAAGGTGTGC TTTTGGGATTTTAAGATG ATTGA
CJ1166C ISA F2 R	AGAATACTCAAGCTTGCATGCCTGCAGGTC GTTTTAATGTTTTTTTGC TGTCTAG
<i>C. jejuni</i> NCTC 11168 knock out mutant screening primers 5'-3'	
Cj0908 F screening	TTCCTTGACTTTATCAAGTAAATTTGG
Cj0908 R screening	TTTTGAGAATCTTTTATTACATAAAAAATCA
Cj0909 F screening	AATTTTTACAAATCATAAAGGCTTGT
Cj0909 R screening	TATCTCCTTTAAAATCTTTTAGGGTG
Cj0910 F screening	TTGAATTTTTAAACAATAATGCTCC
Cj0910 R screening	GGCTGAAAGATACCTCTCAACC
Cj0911 F screening	AAGCACAGAGCTTAAATCTGG
Cj0911 R screening	ACACTCTTTGGCGCTAGGTT
Cj1154c F screening	CAAGAAAAGGGTATTGTGGC
Cj1154c R screening	GCAAATAATTTCTAGCCAAAAAA
Cj1155c F screening	CATTGCATCGTATTCGAGTT
Cj1155c R screening	GCAAATAATTTCTAGCCAAAAAA
Cj0369c F screening	TTCTTCGATAATTACAAAAGCTCC
Cj0369c R screening	GGCTAATTATATCTTAATTTTGGTTAATAAAA
Cj1483c F screening	CTTCATATAGGATGAAAAAATATTACAAG
Cj1483c R screening	AATCAAGTTTTAAAAGATATTCAAGATTAAA
Cj1486c F screening	TTTTTCAAGTATAGGTCAATATAATGAAGA
Cj1486c R screening	ATAGTATCACGATTTGCATTACCTATAG
Cj1485c F screening	TTAAACATGGTTCAAAGGTATGA
Cj1485c R screening	TTAGTTTCTAACATTTTTTTTCTCTT
Cj1484c F screening	TGCTGCTTATGTAGCAAAGA
Cj1484c R screening	TGCTCAAACAACTTTATCTAAAAAT
Cj1482c F screening	CTATAGGTAATGCAAATCGTGATACT

Cj1482c R screening	TGAGTAAGACCCAAACAATAACTTC
Cj1161c F screening	TGTCAATATGAAGTCCGCTTT
cj1161c R screening	AAAATTAATCATCATTTTTAAGAGAGAT
Cj1162c F screening	GGCTTTTATCAATGCTTTAACCA
cj1162c R screening	ATATTTTCTAAAATTCTTTGATAATCTTG
Cj1163c F screening	TATCTTATTTCTTTTATACGCAGTGA
cj1163c R screening	TTTTAAAGCCTAAAAAAGCATG
Cj1164c F screening	TTTTGATTTGTTGTATAGCACTTG
cj1164c R screening	AAGCGGACTTCATATTGACAT
Cj1165c F screening	ATCATATTACTTTAAATGTTGTAGATATGG
cj1165c R screening	AAAGAATTTGAAAGGATTGAATAAAT
Cj1166c F screening	GTGCTGCAAACCTGAGAATCTC
cj1166c R screening	AACCAAATCTACATTACAAACTGGAC
CcoP F	GAAAGTAAAAGGAGTGCTTAATGC
CcoP R	CATCATTCACCCCTTGAAAG
<i>C. jejuni</i> NCTC 11168 knock out mutant complementation primers 5`-3`	
Cj0908/9/10/11 metK F	AATATTCGTCTCACATG ATAAGAAATTTTTTTATAGGAATGTCTTTTT
Cj0908/9/10/11 metK R	AATATTCGTCTCACATG TTATTGAGAATTTAGAAAAATTCTAAGTT
Cj0911 metK F	AATATTCGTCTCACATG AAAAAAAAATATTATTTGTTTATAGTTATAG
Cj0911 metK R	AATATTCGTCTCACATG TTATTGAGAATTTAGAAAAATTCTAA
Cj1161 metK F	AATATTCGTCTCACATG GGAAGAATTGCGTATAAAAAATAGGC
Cj1161 metK R	AATATTCGTCTCACATG TTAAATTCTTTTAAAGTCTTAAAGAATTAAGC
Cj1162 metK F	AATATTCGTCTCACATG AAATTTAAAGTAAAAAATGTTAATTGCA
Cj1162 metK R	AATATTCGTCTCACATG TTATAAACGCTCTACAATCTCAAAC
Cj1163 metK F	AATATTCGTCTCACATG TATAAATTTTTATCACACGAGCCTT
Cj1163 metK R	AATATTCGTCTCACATG TTAAATTTTCAATTTCACTCCTTATAGG
Cj1164 metK F	AATATTCGTCTCACATG TTATGTCCAGTTTGTAATGTAGATTTG
Cj1164 metK R	AATATTCGTCTCACATG TTAAAAGTCAAAAAGCTCGCC
Cj1165 metK F	AATATTCGTCTCACATG ATTGAATTTATTTAAGAGATATGTTTTTTG
Cj1165 metK R	AATATTCGTCTCACATG TTAATGTTTTTTTGCATGTCTAGTC
Cj1166 metK F	AATATTCGTCTCACATG GAAAAACCTGATATACAAAGATTAACTAATT
Cj1166 metK R	AATATTCGTCTCACATG TCATCTTAAAATCCCAAATCC
Cj1154 metK F	AATATTCGTCTCACATG AATAGTATAATCATGATGATGATAGGAGTT
Cj1154 metK R	AATATTCGTCTCACATG TTAAGAAAGCCTTTTTTTATCCA
Cj1155 metK F	AATATTCGTCTCACATG ATTATGAAATGTGAACATTGCAA

Cj1155 metK R	AATATTCGTCTCACATG TTCATTCTTTAATCCTTAAAGCATT
Cj0369 metK F	AATATTCGTCTCACATG CAAGGACACATTACAAACTATACAAAA
Cj0369 metK R	AATATTCGTCTCACATG CTATTTGAGTTCATTTTATCCTTTATAAGA
petABC_pRRA_native_F (MfeI)	<i>acac</i> CAATTG AGATTTGGCATTAAAAGAAT
petABC_pRRA_native_R (XbaI)	<i>acac</i> TCTAGA CCATTATCATTAATAATGGC
Primers (5`-3`) used in protein overexpression studies	
T7 forward	TAATACGACTCACTATAGGG
T7 reverse	GCTAGTTATTGCTCAGCGG
Strep tag reverse screening primer	TTTCAAAGTGC GGATGGC
Cj0908 nde1 F	<i>TATATT</i> CATATG GATAAAAAGAAAGAAAGTAT
Cj0908 xho1 R	<i>ATTTAT</i> CTCGAG ATGTGTGTACCTGTTTGAA
Cj0909 nde1 F	<i>TATATT</i> CATATG GAGGTAAAAAATGCCTTTGT
Cj0909 xho1 R	<i>ATTTAT</i> CTCGAG AAATTCTTTAGAATCAATAT
Cj0910 nde1 F	<i>TATATT</i> CATATG AAAGATTCTCAAAAAATAAC
Cj0910 xho1 R	<i>ATTTAT</i> CTCGAG TTTTTTTAGCTCAAAATCAA
Cj0911 nde1 F	<i>TATATT</i> CATATG AAAAATCATCAAAATTCTTA
Cj0911 xho1 R	<i>ATTTAT</i> CTCGAG TTGAGAATTTAGAAAAATTC

Bases* in italics represent random added bases. **Bases represent adaptor corresponding to pGRM3zf vector. **Bases** represent adaptor corresponding to kanamycin antibiotic resistant cassette. **Bases** represent adaptor corresponding to *metK* complementation vector. **Bases** represent MfeI restriction enzyme site. **Bases** represent XbaI restriction enzyme site. **Bases** represent NdeI restriction enzyme site. **Bases** represent XhoI restriction enzyme site.

2.4.6 Agarose gel electrophoresis:

1-Dimensional agarose gel, made by dissolving 1% agarose (Melford) in TAE (1 mM EDTA , 40 mM Tris-acetate pH 8.0) buffer, was used to analyse the amplified DNA for correct size. 1 kb DNA hyperladder-1 (Bioline) was used as a size marker. Ethidium bromide (0.1 µg ml⁻¹) was added to the gel to visualise DNA in ultraviolet light. 6X loading buffer dye (Bioline) was added to all DNA samples before loading to give them colour. Usually 5 µl samples were loaded in gel wells and separated by electrophoresis (Bio-Rad Powerpac 300) using a constant voltage of 100 V for 35-45 minutes. In this study, correct size of amplified DNA fragment is approximately 500 bp for all (section 2.4.4.1)

2.4.7 PCR product clean up:

All correct PCR products were cleaned by Quiagen QIAquick PCR purification kit. Manufacturer's instructions were followed. 5 volumes of Buffer PB (Quiagen) was added to 1 volume of the PCR reaction and mixed gently. The sample was transferred to QIAquick column (Quiagen) and centrifuged at 12,470 x g for 1 minute. 0.75 ml Buffer PE (Quiagen) was added to the column and centrifuged at 12,470 x g for 1 minute. Collection tube was emptied and column was centrifuged for 2 more minutes to remove residual wash buffer. Column was transferred to a fresh 1.5 ml microcentrifuge tube. 50 µl of Nuclease-Free Water (Promega) was applied to the column, making sure it covers the whole membrane and kept stand for 2 minutes. The column was centrifuged at 12,470 x g for 2 minutes and supernatant having plasmid DNA was stored in -20 °C. Concentration of final product was measured as in section 2.4.3.

2.4.8 Digestion of DNA with Restriction Enzymes:

PCR products and plasmid DNA sequences were checked for any internal digestion site for restriction enzymes. If there is no internal site, PCR products and plasmid DNA sequences were digested with enzyme according to manufacturer's instructions. In presence of internal site, partial digestion was carried out by varying the incubation time and checking the products by visual inspection on an agarose gel. In case of double digestion, either both restriction enzymes were added together with one or both compromising with buffer or incubation time, or one-by-one serial digestions were carried out. After digestion, enzyme was heat inactivated (if required) and digested products were cleaned from enzyme and buffers by QIAquick PCR Purification Kit (Qiagen) and concentration was measured according to section 2.4.3 and stored at -20 °C.

In a typical PCR products and plasmid DNA digestion in this study, 1 µl HincII and 2 µl 10X cutsmart buffer (NEB) was mixed with 17 µl of DNA in an Eppendorf and incubated for 1 hour at 37 °C but amount of DNA was varied according to concentration of sample. Restriction enzyme was heat inactivated by heating at 70 °C for 5 minutes.

For p(C/K)46metK plasmid DNA (complementation vector) and PCR products digestion in this study, 0.5 µl BsmBI (NEB) and 2 µl 10X 3.1 buffer (NEB)

was mixed with 0.5 µg of substrate (plasmid DNA and PCR products separately) and mixture was made final volume of 20 µl with dH₂O in an eppendorf. The mixture was incubated at 55 °C for 1 hour and then restriction enzyme was heat inactivated by heating at 80 °C for 5 minutes.

For digestion of pRRA plasmid DNA (complementation vector) and PCR products in this study, 1000 ng of plasmid DNA was double digested with 1 µl MfeI and 1µl XbaI, in 2 µl CutSmart, with 1 µl rSAP in a 20 µl reaction, at 37 °C for 1 hour. Then heat inactivate at 80 °C for 20 min, and gel extract (MfeI is not heat inactivated so it must be gel extracted). Similarly, single digest PCR products either with MfeI or XbaI respectively.

While making strepII-tag pET-21a from HIS-tag pET-21a, pET-21a and strepII-tag gblock were digested with BamH1 and Bpu1102. 100 ng of plasmid DNA and gblock each, separately, were double digested with 1 µl BamH1 and 1 µl Bpu1102, in 2 µl CutSmart, with 1 µl rSAP in a 20 µl reaction, at 37 °C for 1hour. Reaction was heat inactivated at 80 °C for 20 min

2.4.9 Alkaline Phosphatase Treatment:

The 5' phosphoryl termini of digested plasmid DNA are required by ligases. Therefore, Antarctic Phosphatase (NEB) was used to catalyse the removal of 5' phosphate groups from the ends. Plasmid DNA was phosphatase treated after digestion to prevent self-ligation of blunt sticky ends and decrease the vector-only background during cloning by adding 1 µl of Antarctic Phosphatase (NEB) and 2 µl 10 X Antarctic Phosphatase Buffer (NEB) in 17 µl of digested sample and incubated at 65 °C for 1 hour. Phosphatase enzyme was heat inactivated by heating at 80 °C for 5 minutes. Sample was PCR cleaned up using a QIAquick PCR purification kit (Qiagen) according to the manufacturer's instructions to remove excess enzyme and buffer. Concentration was measured according to section 2.4.3 and stored at -20 °C.

2.4.10 DNA Ligation:

Insert and vector concentrations were measured according to section 2.4.3 and DNA ligation method was carried out on insert and vector in a 10 µl reaction. Molar ratio of insert to vector:: 1:1, 3:1, 5:1 and 10:1 were used. Typically, 50-100 µg of

vector DNA was used per ligation reaction and amount of insert DNA required was calculated by following equation:

$$\frac{\text{amount of vector (ng)} \times \text{size of insert (kb)} \times \text{molar ratio of insert: vector}}{\text{size of vector (kb)}} \\ = \text{amount of insert (ng)}$$

For ligation reaction, appropriate amount of vector DNA and respective calculated amount of insert DNA were added along with 1 µl each of T4 DNA ligase (NEB) and 10 x T4 DNA ligase buffer (NEB) in an Eppendorf and made up to the total volume of 10 µl with ddH₂O. A control reaction with no insert was also done to analyse the level of un-cleaved plasmid/plasmid only re-ligation. The mixture was incubated at room temperature for 1 hour or overnight at 4 °C for both cohesive and blunt end DNA reactions. If the volume of vector or insert to be added in the reaction was less than 1 µl, serial dilutions were done with ddH₂O. The ligase enzyme was heat inactivated at 65 °C for 10 min prior to transformation of the reactions into chemically competent *E. coli* cells (see section 2.5.1).

2.4.11 Isothermal Assembly (ISA) cloning:

Isothermal assembly (ISA) cloning is a method used to generate constructs for *C. jejuni* mutagenesis by combining multiple overlapping DNA fragments together in vitro in a single reaction (Fig. 2.1). It was first explained by Gibson *et al* (2009). ISA mastermix was prepared by mixing 40 µl 5 X ISA buffer, 0.125 µl T5 exonuclease (Cambio), 2.5 µl Phusion polymerase (NEB) and 20 µl Taq ligase (NEB) and made to a total volume of 150 µl with dH₂O. 5 X ISA buffer consists of 25 % polyethylene glycol [PEG-8000], 500 mM Tris-HCl pH 7.5, 50 mM MgCl₂, 50 mM dithiothreitol [DTT], 1 mM of each dNTP and 5 mM NAD. ISA mastermix was divided into 15 µl aliquots for different reactions and stored at – 20 °C.

DNA fragments to be assembled in this study by ISA reaction to make a construct were pGEM3Zf(-) (vector), desired antibiotic resistance (Ab^R) cassette (mostly kanamycin (kan) or chloramphenicol (cat)) and amplified DNA fragments from each side of the gene of interest made by PCR as in section 2.4.4.1. pGEM3Zf (-) was digested with *HincII* as mentioned in section 2.4.8 and phosphatase treated according to section 2.4.9. The desired antibiotic resistance (Ab^R) cassette was PCR amplified using kan-ISA or cat-ISA primers followed by PCR clean up according to

section 2.4.7 and concentration measurement as in section 2.4.3. All fragments of the ISA reaction were combined in equimolar concentration with amounts ranging from 10-100 ng each, but in some cases the amount of Ab^R cassette and amplified DNA fragments were twice or thrice than amount of vector, with final volume of the mixture not exceeding 5 µl. A 15 µl ISA mastermix aliquot was thawed on ice and the mixture was added to it with the final volume made up to 20 µl with dH₂O. The reaction was incubated at 50 °C for 1 hour in a Techne Techgene Thermal Cycler (Techne Ltd). Preferably, the resulting DNA was immediately used to transform competent *E. coli* DH5α cells but, if necessary in given circumstances, it was stored at -20 °C for maximum 48 hours. After transforming, 0.5 ml LB broth was added to the cells and incubated, with shaking, at 37 °C for an hour. After this incubation, the *E.coli* DH5α cells were grown on LB solid media containing the appropriate selective antibiotic overnight in 37 °C. Colonies were screened by PCR (section 2.4.4.2) using M13 primers, which are homologous to the DNA sequence of the vector on both ends of the restriction enzyme site. Also correct assembly of plasmids was confirmed by automated DNA sequencing using same M13 primers (Core Genomic Facility, University of Sheffield Medical School, UK).

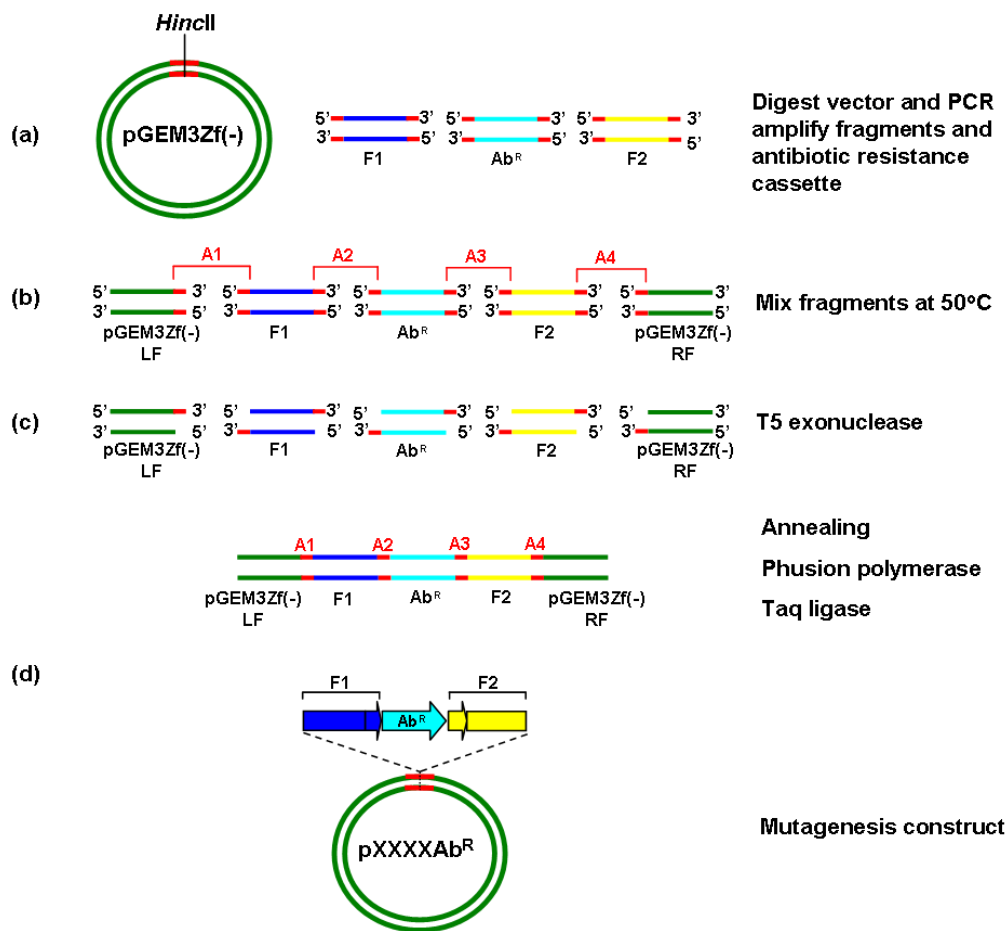


Figure 2.1: Isothermal assembly (ISA) cloning. (a) pGEM3Zf(-) was digested with restriction enzyme HincII. The flanking regions F1 and F2 and the resistance marker (AbR) were amplified by Phusion PCR. The regions highlighted in red are the overlapping adapter regions. (b) The vector and fragments were mixed together with the ISA reaction buffer and incubated for 1 hour at 50°C. (c) The T5 exonuclease removed nucleotides from the 5' end of each DNA fragment, the T5 enzyme, being heat labile, became inactive during the course of the reaction. (d) The homologous adapter regions annealed and the single strand nicks were filled in by Phusion polymerase. The final construct contained the flanking regions of the gene of interest with a resistance marker between them allowing for the gene of interest to be replaced with the resistance marker. Figure adapted from Gibson et al. (2009).

2.5 Preparation and transformation of competent bacterial cells:

2.5.1 Preparation of *E.coli* competent cells

Competent *E. coli* DH5a cells were made according to the Hanahan (1983) method. Two chemical solutions, RF1 and RF2 were made, filter (0.2 µm) sterilized and ice cooled. RF1 consists of 100 mM KCl, 50 mM MnCl₂·4H₂O, 30 mM

CH₃COOK, 10 mM CaCl₂·2H₂O, 15% [w/v] glycerol and adjusted to pH 5.8 with 0.2 M acetic acid. RF2 consists of 10 mM MOPS, 10 mM KCl, 75 mM CaCl₂·2H₂O, 15% [w/v] glycerol and adjusted to pH 6.8 with 5 M NaOH. *E. coli* cells were grown in 50 ml LB broth at 37 °C until they reached OD₆₀₀ ≈ 0.6 (mid-exponential phase) corresponding to a density of ≈ 4-7 x 10⁷ viable cells ml⁻¹. Cells were incubated on ice for 15 minutes and pelleted by centrifugation at 6000 x g for 20 min at 4 °C. The supernatants were discarded and pellets were resuspended by gentle pipetting in ice cold 50 ml RF1 solution. Cells were incubated on ice for 15 min, centrifuged as above and resuspended by gentle pipetting in 8 ml ice cold RF2 solution. Cells were incubated on ice for 20 minutes, divided into 100 µl aliquots in to pre-chilled eppendorfs for different transformations and stored at -80 °C for not more than 3 months. Competent cell viability and transformation efficiency were tested by transformation with uncut vector and growing on LB plates with appropriate antibiotics.

2.5.2 Transformation of competent *E.coli* cells:

One aliquot, 100µl of competent *E. coli* cells was freshly thawed on ice for each transformation. 10-20 ng plasmid or 2-5 µl of a ligation or ISA reaction was added to the cells and incubated on ice for 30minutes. The mixture was heat shocked by transferring to a 42 °C pre-heated water bath for 90 seconds. The mixture was immediately transferred to ice for 2 minutes. 0.5 ml 37 °C pre-heated sterile LB broth was added to the mixture and incubated with shaking at 37 °C for 1 hour. Cells were centrifuged (13000 x g 5 min), resuspended in 200 µl LB broth and plated out onto LB solid media having selective antibiotic and incubated overnight at 37 °C. To determine the level of background vector-only transformations, a no insert DNA control was always used.

2.5.3 Preparation of competent *C. jejuni* cells:

For making competent *C. jejuni* cells, cells were grown overnight on one or more plates, as required, according to section 2.3.1. Cells were harvested and resuspended in 1ml BHI broth. Cell suspension was centrifuged at 13000 x g for 5 minutes at 4 °C and resuspended in 1ml ice-cold wash buffer by gentle pipetting. Ice-cold wash buffer consists of 15% [v/v] glycerol and 9% [w/v] sucrose in dH₂O and filter (0.2 µm) sterilized. The cell suspension was again centrifuged similarly and

process was repeated three times. After the third time, cell pellet was resuspended in 0.3 ml buffer and divided in aliquots of 100 µl each. Preferably, cells were used immediately but, when required, were stored up to 1 month at -80 °C.

2.5.4 Transformation of competent *C. jejuni* cells:

100-1000 ng of plasmid DNA was added to freshly made (or thawed on ice) competent cells (not more than 10 µl plasmid DNA in 100 µl cell suspension) and incubated on ice for 30 minutes. The mixture was transferred to a pre-chilled electroporation cuvettes (Bio-Rad), electroporated with a pulse of 25 F. 2.5 kV and 200 Ω for 4 milliseconds in an *E. coli* pulser (Bio-Rad) and returned immediately to ice (Fig. 2.2). 100 µl BHI broth was added to the cells and mixed gently. The whole sample was plated out on a non-selective Columbia agar plate and incubated overnight in microaerobic conditions at 42 °C according to section 2.3.1. Cells were harvested and transferred to selective Columbia agar plates having appropriate antibiotics and incubated as above for 2-4 days for growth of Ab^r colonies. Colonies were checked by colony PCR with a combination of different screening and antibiotic cassette primers according to section 2.4.4.2.

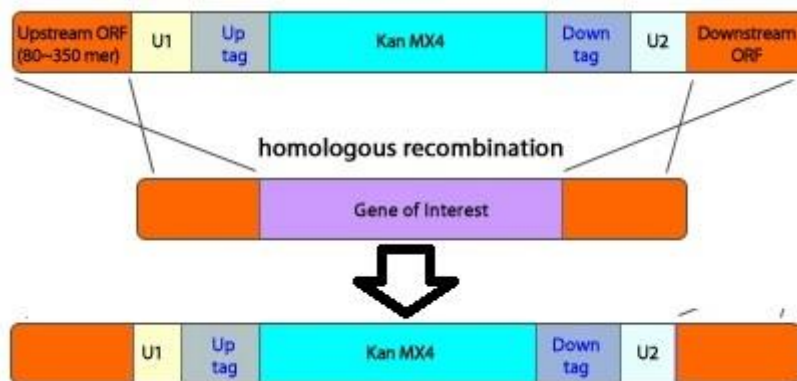


Figure 2.2: *C. jejuni* gene knock out mutant. Competent *C. jejuni* cells were transformed with plasmid DNA construct. The region highlighted in saffron are the overlapping flanking regions. The homologous flanking regions swapped, knocked out the gene of interest from bacterial DNA and replaced it with selective antibiotic resistance marker. Figure adapted AccuOligo®.

2.6 RNA extraction and manipulation:

2.6.1 mRNA extraction from *C. jejuni*:

SV Total RNA Isolation System (Promega) was used to extract RNA and manufacturer's instructions were followed with slight modifications. 1 ml culture of *C. jejuni* grown either in complex media or minimal media, with and without 0.25 mM excess copper (made by dissolving CuSO₄ (Sigma-Aldrich) in dH₂O and filter (0.2 µm) sterilised) was collected when the cells were in growth phase i.e. OD₆₀₀ = 0.5 ± 0.1 for complex media and 0.4 ± 0.05 for minimal media and centrifuged for 2 minutes at 12,470 x g at 4 °C. Supernatant was discarded and pellet was resuspended in 100 µl of freshly prepared TE (10 mM Tris, 1 mM EDTA and pH 8 with HCl) containing 1mg/ml lysozyme. Resuspended pellet was incubated at room temperature for 3-5 minutes and 75 µl of RNA Lysis Buffer (Promega) was added to it. 350 µl of RNA Dilution Buffer (Promega) was added to the sample and mixed by inversion. Cleared lysate solution was transferred to a fresh microcentrifuge tube by pipetting. RNase-free PCR tubes were used from here on. 200 µl of 95% ethanol was added to the cleared lysate and mixed by pipetting 3–4 times. This mixture was transferred to the Spin Column Assembly (Promega) and Centrifuged at 12,000–14,000 × g for one minute. Liquid in the Collection Tube was discarded and the Spin Basket inserted back into the Collection Tube. 600 µl of RNA Wash Solution (Promega), diluted with ethanol, was added to the Spin Column Assembly and centrifuged at 12,000–14,000 × g for one minute. DNase incubation mix was prepared by combining 40 µl Yellow Core Buffer (Promega), 5 µl 0.09 M MnCl₂ (Promega) and 5 µl of DNase I enzyme (thawed on ice) (Promega) per sample in a sterile tube (in this order) and mixing by gentle pipetting. 50 µl of freshly prepared DNase incubation mix was added directly to the membrane inside the Spin Basket, making sure that the solution is in contact with and thoroughly covering the membrane and incubated for 15 minutes at 20–25 °C. After this incubation, 200 µl of DNase Stop Solution (Promega) was added to the Spin Basket, and centrifuged at 12,000–14,000 × g for 1 minute. 600 µl RNA Wash Solution (Promega), with ethanol was added, and centrifuged at 12,000–14,000 × g for 1 minute. The Collection Tube was emptied, and 250 µl RNA Wash Solution (Promega) with ethanol was added, and centrifuged for 2 minutes. For each sample, 100 µl Nuclease-Free Water was added to the membrane, making sure to completely cover the surface of the membrane with the water. After centrifugation at 12,000–

14,000 × g for 1 minute the Spin Basket was removed and discarded. The Elution Tube containing the purified RNA was placed on ice temporarily or stored at -80 °C.

Purified RNA was checked for DNA contamination by running a PCR (section 2.4.4.1) with a pair of any *C. jejuni* gene primers. If any band is visible on agarose gel electrophoresis (section 2.4.6), the sample was treated with DNase (Ambion Turbo DNA-Free kit) according to manufacturer's instructions. Added 1 µl DNase and 5 µl of 10 X Turbo DNase buffer to 50 µl contaminated RNA sample and incubated at 37 °C for 30 minutes. After incubation, added 5.6 µl of inactivation reagent and incubated for 5 minutes at RT, mixing occasionally. After centrifugation at 10,000 x g for 2 minutes 45 µl of the aqueous RNA layer was transferred to a fresh tube without disturbing the pellet.

Concentration and ratio of A_{260}/A_{280} of RNA was measured according to section 2.4.3. Samples were diluted with Nuclease-Free Water to make final working concentration of $10 \pm 0.5 \mu\text{g}/\mu\text{l}$. Samples were divided in aliquots of 12 µl and stored at -80 °C.

2.6.2 Real time quantitative reverse transcriptase PCR (qRT-PCR):

18-22 bp long gene specific qRT-PCR primers were designed using PRIMER 3 software (Untergasser *et al.*, 2007) to amplify 200-300 bp long sequences within the gene of interest. The *C. jejuni gyrA* gene was used as the reference. All primers were diluted to 25 µM concentration in nuclease-free water (Fisher Scientific). qRT-PCR primers were checked for specificity and proper annealing temperature before use by performing a PCR reaction using *C. jejuni* genomic DNA as template according to section 2.4.4.1 and checked for correct size and performance efficiency by running agarose gel electrophoresis (section 2.4.6) and measuring nucleotide concentration (section 2.4.3), respectively.

qRT-PCR reactions (20 µl volumes) were carried out in a MX3005P thermal cycler (Agilent) in a MicroAmp® 96-well optical reaction plate (ABI prism). Reactions were performed using either the Sensifast SYBR Lo-ROX one step kit or Sensifast SYBR Hi-ROX one step kit (Bioline, UK). Each reaction contained 10 µl Sensifast SYBR 2x buffer (Bioline, UK), 0.2 µl of each gene specific qRT-PCR primer, 0.2 µl reverse transcriptase (Bioline, UK), 0.4 µl RNase inhibitor (Bioline, UK), 2 µl of matched RNA or DNA template and 7 µl nuclease free water (Bioline,

UK). Each reaction using RNA was replicated in triplicate and reactions using genomic DNA were replicated in duplicate for the standard curve. In the thermal cycler, qRT-PCR reactions were carried out at 45 °C for 10 min, 95 °C for 2 min, followed by 40 cycles of 95 °C for 20 s, 55 °C for 30 s and 72 °C for 20 s each. Data was collected with the associated MxPRO QPCR software (Agilent) and analyzed using Microsoft EXCEL. A standard curve for each gene was established using a series of *C. jejuni* genomic DNA dilutions to normalize for variation in primer annealing efficiency between different primer pairs. The relative expression levels of the target genes were calculated following the standard curve protocol described in the *User Bulletin #2 (ABI Prism 7700 Sequence Detection System, Subject: Relative Quantification of Gene Expression)* given by Applied Biosystems. Target gene expression was normalized to *gyrA* expression, which acts as an internal control. No-template control reactions were included as negative controls for each primer set being used.

2.6.3 qRT-PCR primers used in this study:

qRT-PCR primer is an oligonucleotide sequence designed in such a way that both primers of a reaction has similar melting temperature. All qRT-PCR primers were ordered from Sigma-Aldrich.

Table 2.9: primers used for RT-PCR

<i>C. jejuni</i> NCTC 11168 qRT-PCR primers 5`-3`	
GyrA RT-F	ATGCTCTTTGCAGTAACCAAAAAA
GyrA RT-R	GGCCGATTCACGCACTTA
Cj0908 RT_F	CCAACCTCTAACTTGTGACT
Cj0908 RT_R	ATCGGTAATGCTTCTACCTAT
Cj0909 RT_F	TTTGCTGTAAATCTTTGGGC
Cj0909 RT_R	GGTAACCTCCAGATTTAAGCT
Cj0910 RT_F	CCCATTGACTTGCGATCTTA
Cj0910 RT_R	AATTCTACCCTGAAACGCAT
Cj0911 RT_F	CTTAAAAGAGGAAACCACCC
Cj0911 RT_R	GTTCTCTTAAAATTTCTTGTGGA
Cj1161c RT_F	TTATGTGAATTCTAGCGGGG

Cj1161c RT_R	CCCAAAGCTACAAGGGTATT
Cj1162c RT_F	TAGAAGTGGATTTGGAGCAA
Cj1162c RT_R	CGCTCTACAATCTCAAAACC
Cj1163c RT_F	TGGCACTTTTAAGCGATACT
Cj1163c RT_R	TGCACCCTTAAACATCATCA
Cj1164c RT_F	AGTGATAGGAGTGGAGTTGA
Cj1164c RT_R	GCCTAGCCAACTTTCTTTCT
Cj1165c RT_F	GGGATTTGGCTTTGCTTATG
Cj1165c RT_R	CTAGAGCCAAAGTCACAGAA
Cj1166c RT_F	ATGCGTAGGAAGAATAGCTG
Cj1166c RT_R	AAAAGCCGAATTTGCCATAG

2.7 Total and Inner membrane protein extraction from *C. jejuni*:

2.7.1 Preparation of *C. jejuni* cell-free extract:

Biological triplicates of *C. jejuni* cells were grown in 500 ml to 1000 ml MHS broth according to section 2.3.1, depending on the amount of protein required. Given the facilities available to grow *C. jejuni*, two series of starter cultures were grown, first 25 ml which was back diluted to 100 ml. Cells were harvested during stationary phase by centrifuging at 17,700 x g for 20 minutes at 4 °C. Supernatant was discarded. Cell pellet was resuspended in 10 ml of ice-cold filter (0.2 µm) sterilised 10 mM HEPES buffer (pH 7.4) by gentle pipetting. The cell suspension was sonicated on ice for 6 x 15 sec pulses at a frequency of 16 amplitude microns using a Soniprep 150 ultrasonic disintegrator (SANYO) and cell debris/unbroken cells were removed by centrifugation at 12,470 x g for 20 minutes at 4 °C. Supernatant was carefully collected as the cell-free extract (CFE) in pre-chilled falcons and stored on ice for immediate use or at -20 °C.

2.7.2 Removal of metal contamination:

For removal of metal contamination, when required, cell pellets harvested from MHS as above was re-suspended in 10 ml wash buffer and centrifuged at 15,550 x g for 10 minutes at 4 °C. Wash buffer consists of 10 mM HEPES, 0.5 M Sorbitol and 100 µM EDTA in dH₂O with pH 7.5. Process was repeated three times but in the third wash, the wash buffer used was without any EDTA. Sample was centrifuged,

supernatant was discarded, and cell pellet was resuspended in 10 ml of ice-cold filter (0.2 µm) sterilised HEPES buffer (pH 7.4) by gentle pipetting for making cell free extract as in section 2.7.1.

2.7.3 Total membrane protein extraction from *C. jejuni*:

The cell free extract (section 2.7.1) was transferred to ultracentrifuge tubes. Ultracentrifuge tubes were filled completely and balanced to high precision within 0.1 g. Samples were centrifuged at 100,000 x g at 4 °C for 1 hour in benchtop ultracentrifuge (Beckman). Supernatant was removed carefully and discarded, and the pellet was washed by pouring off 10 mM HEPES buffer (pH 7.4) twice without disturbing the pellet, which was then re-suspended in 1 ml 25 mM phosphate buffer (pH 7.4) with gentle pipetting, transferred to a glass homogeniser and homogenised gently. Homogenised total membrane protein solution was stored at -80 °C and concentration was measured by Lowry assay (section 2.7.5).

2.7.4 Inner membrane protein extraction from *C. jejuni*:

To solubilise the inner membrane from homogenised total membrane protein solution, an equal volume of 2% sarkosyl (sodium N-lauryl sarcosinate dissolved in 10 mM HEPES buffer, pH 7.4) was added and mixture was incubated at 37 °C for 30 minutes. After incubation, the mixture was transferred to ultracentrifuge tubes. Ultracentrifuge tubes were filled completely with paraffin oil and balanced to high precision within 0.1 g. Samples were centrifuged at 100,000 x g at 4 °C for 1 hour in a bench top ultracentrifuge (Beckman) and supernatant was carefully collected with a syringe and transferred to a fresh pre-chilled falcon tube. Concentration was measured by Lowry assay according to section 2.7.5. Samples were divided in aliquots of 100µl and stored at -80 °C.

2.7.5 Protein concentration measurement by Lowry assay:

Lowry assay was used to measure the protein concentration in 96-well plates using BSA (Bovine serum albumin) as protein standard. Solutions A and B were made and stored as stock solutions and solution C and Folin- Ciocalteu Phenol (FCP) reagent were freshly made. Solution A consists of 2% Sodium carbonate, 0.4% Sodium hydroxide, 0.16% Sodium tartrate and 1% SDS in dH₂O. Solution B consists of 4% cupric sulphate (CuSO₄) in dH₂O. Solution C was made fresh on the day by mixing 100 parts of A and 1 part of B. Folin- Ciocalteu Phenol (FCP) reagent made

fresh on the day by diluting 2N reagent with equal volume of dH₂O. BSA was prepared in 10 ml water at 100 µg/ml as accurately as possible by making 10 mg/ml and diluting 100 times and filter (0.2 µm) sterilised. A series of 100, 80, 60, 40, 20 and 0 µg/ml dilutions were made for the standard curve. Protein samples were diluted 100 times with dH₂O in eppendorfs to a minimum of 200 µl. 50 µl each of Protein standards and diluted samples were added in triplicates in flatbottomed 96-well plates. 150 µl of solution C was added to each sample in wells and incubated at RT for 1 hour. 15 µl of 1x FCP reagent was added per well and incubated at RT for 45 minutes. Absorbance was measured at 600 nm using a 96-well plate reader and protein concentration was calculated according to BSA protein standard curve.

2.8 Bacterial cell sample preparation for ICP-MS:

Biological triplicates of *C. jejuni* cells were grown in 500 ml MHS broth according to section 2.3.1 and cells were harvested at stationary phase by centrifuging at 17,700 x g for 20 min at 4 °C. Cell pellet was re-suspended in 10 ml wash buffer and centrifuged at 11,000 rpm for 10 minutes at 4 °C. Wash buffer consists of 10 mM HEPES, 0.5 M Sorbitol and 100 µM EDTA in dH₂O with pH 7.5. Process was repeated three times but in the third wash, the wash buffer used was without any EDTA. Sample was centrifuged, supernatant was discarded and cell pellet was resuspended in 1 ml HNO₃ (65%) by thoroughly vortexing. Samples were left in acid overnight in the fume hood and then sent to University of Sheffield ICP-MS facility.

2.9 Growth curves:

C. jejuni cells were grown overnight on Columbia agar blood plates with appropriate antibiotics as in section 2.3.1. Cells were harvested and inoculated in 25 ml MHS broth, which was equilibrated overnight in microaerobic environment at 42 °C with shaking in 100 ml conical flasks for starter culture. OD₆₀₀ was measured (section 2.3.6) which should be in between 0.1 and 0.3. Starter cultures were incubated in microaerobic environment at 42 °C with shaking at 160 rpm (section 2.3.1) and cells were harvested by spinning at 12,000 x g for 4 min at 40 °C after 6-8 hours, i.e. when they reached mid-log phase, OD₆₀₀ between 0.6 to 0.8. For growth curves in MHS (complex) media, cells were resuspended in 5 ml MHS and added to 50 ml MHS (equilibrated overnight in microaerobic environment at 42 °C with shaking) in 250 ml conical flasks to make starting OD₆₀₀=0.1. For growth curves in

MeM α minimal media, cell pellet was washed by resuspending in 25 ml MeM α minimal media and centrifuged at 12,000 x g for 4 min at 40 °C. Cells were resuspended in 1 ml MeM α minimal media and added to 6 ml MeM α minimal media (equilibrated for 4 hours in microaerobic environment at 42 °C with shaking) in 6 well plates (Greiner) to make starting OD₆₀₀=0.1. Cultures were incubated in microaerobic environment at 42 °C with shaking at 160 rpm (section 2.3.1) and growth was measured hourly or otherwise by measuring OD₆₀₀ (section 2.3.6). For growth curve in MeM α minimal media, only 0.5 ml culture was collected and was diluted with 0.5 ml MeM α minimal media in cuvettes to make 1 ml for OD reading. All growth curves were done in biological triplicates.

2.9.1 Oxygen limiting growth curves and supernatant sample collection:

C. jejuni starter cultures were made as mentioned above. The starter culture was back diluted to 200 ml MHS broth in a 500 ml conical flask incubated in microaerobic environment at 42 °C with shaking at 160 rpm (section 2.3.1) for 12 hours. OD₆₀₀ was measured and cell culture was centrifuged at 12,000 x g for 4 min at 40 °C. Cell pellets were resuspended in 10 ml MHS broth and inoculated in 200 ml MHS (equilibrated for overnight in microaerobic environment at 42 °C) in 250 ml conical flask to OD₆₀₀=0.1. Cell cultures were incubated in a microaerobic environment at 42 °C without shaking (section 2.3.3). Where required, the electron acceptors sodium fumarate, sodium nitrate or TMAO were added to a final concentration of 20 mM from filter-sterilised stocks. 1 ml sample was collected every hour and OD₆₀₀ was measured (section 2.3.6). All growth curves were done in biological triplicates. Cells in 1 ml samples were separated from the media supernatant by centrifugation (13,800 x g, 5 min) and the supernatants removed and stored frozen at -20 °C until ready for analysis.

2.10 Microaerobic growth sensitivity assays:

2.10.1 Copper sensitivity assay:

C. jejuni starter cultures were grown and cells were harvested as in section 2.9. Cell pellets were washed by resuspending in 25 ml MeM α minimal media and centrifuged at 12,000 x g for 4 min at 40 °C. Cells were resuspended in 5 ml MeM α minimal media and added to 5 ml MeM α minimal media (equilibrated for 4 hours in microaerobic environment at 42 °C with shaking) in 6 well plates (Greiner) to make

starting OD₆₀₀=0.1. In 6-well plates, MeM α minimal media was supplemented with, 0.1 mM, 0.2 mM, 0.4 mM, 0.6 mM, 1.0 mM, 2.0 mM and 5.0 mM copper sulphate (CuSO₄) (Sigma-Aldrich) solution made in dH₂O and filter (0.2 μ m) sterilised. The 6 well plates were incubated in microaerobic environment at 42 °C with shaking at 160 rpm (section 2.3.1) for 12 hours, i.e. until cells reached stationary phase and OD₆₀₀ was measured (section 2.3.6). Assay was done with biological triplicates.

2.10.2 Zinc sensitivity assay:

Zinc sensitivity assays were performed similar to copper sensitivity assay (section 2.10.1), replacing copper sulphate solution (CuSO₄) with Zinc chloride (ZnCl₂) (Sigma-Aldrich) solution made in dH₂O and filter (0.2 μ m) sterilised.

2.10.3 Cobalt sensitivity assay:

Cobalt sensitivity assays were performed similar to copper sensitivity assay (section 2.10.1), replacing copper sulphate solution (CuSO₄) with Cobalt chloride (CoCl₂) (Sigma-Aldrich) solution made in dH₂O and filter (0.2 μ m) sterilised.

2.10.4 Nickel sensitivity assay:

Nickel sensitivity assays were performed similar to copper sensitivity assay (section 2.10.1), replacing copper sulphate solution (CuSO₄) with Nickel chloride (NiCl₂) (Sigma-Aldrich) solution made in dH₂O and filter (0.2 μ m) sterilised.

2.11 Measurement of Cytochrome-c-oxidase activity:

Rates of respiration were measured as the rate of oxygen consumption of cell suspensions in a Clark-type oxygen electrode using different substrates (0.25 mM TMPD with 1mM ascorbic acid or 10 mM sodium formate) as electron donor, calibrated using air-saturated 25 mM phosphate buffer (pH 7.4) (220 nmol dissolved O₂/ml at 42 °C). Electrodes were covered with saturated KCl and excess KCl was absorbed with a cigarette paper. Then a square shaped semipermeable membrane (permeable only for gases) was placed on it and the apparatus was assembled carefully with rubber ring to make it air tight. Oxygen electrode was assembled with 42 °C water circulation to keep sample at constant temperature throughout the oxygen consumption process. A zero-oxygen baseline was determined by the addition of sodium dithionite. 25 ml of *C. jejuni* cultures grown until exponential phase in MHS (section 2.3.1) without additions or with 0.25 mM excess copper (made by dissolving

CuSO₄ (Sigma-Aldrich) in dH₂O and filter (0.2 μm) sterilised) or 20 μM of BCS (made by dissolving Bathocuproinedisulfonic acid disodium salt (Sigma-Aldrich) in dH₂O and filter (0.2 μm) sterilised), as required by the experiment. Cells were pelleted and re-suspended in ice cold 1 ml 20 mM sodium phosphate buffer (pH 7.4) and kept on ice. For each experiment, 2 ml of 20 mM phosphate buffer was placed in the assembly and the plug inserted. After the reading became stable, 50 μl of cell solution was added using a Hamilton syringe, (the cell suspension in phosphate buffer was maintained in the electrode at 42 °C and stirred at a constant rate) followed by appropriate freshly made electron donor (20 μl of 25 mM TMPD with 0.1 M ascorbic acid in dH₂O or 20 μl of 0.1 M sodium formate in dH₂O) and took the oxygen consumption reading. Assay was done with biological triplicates. Total protein concentration of the cell suspension was determined by Lowry assay at 600 nm (section 2.7.5) and the specific rate of oxidation was calculated as nmol oxygen produced min⁻¹ mg⁻¹ total protein.

For growth vs cytochrome-c-oxidase activity, 50 ml culture was grown and 1ml sample was collected every hour. Sample growth was measured at OD₆₀₀ as in section 2.3.6, and cytochrome-c-oxidase activity was measured as above. It was done with biological triplicates.

2.12 Reductase activity assays:

2.12.1 TMAO reductase activity assay:

TMAO is reduced to TMA by TorA enzyme, and its reduction was followed by 1H-NMR spectroscopy. 10 μl of 100 mM tri-silyl propionate (TSP) was added to the 800 μl samples as a 0 ppm chemical shift reference and for quantitation. 500 μl of the mixtures were transferred to the NMR tubes. Then 50 μl of D₂O was added to the NMR tube. Tubes were mixed by inverting and then briefly centrifuged. TMA (and TMAO) concentration was measured by proton NMR on a mag4 Bruker NMR machine at 800 MHz with 10 second relaxation time (relaxation time for TSP).

2.12.2 Nitrate reductase activity assay:

Nitrate is reduced to nitrite by NapA enzyme. The formation of nitrite was measured in a colorimetric assay. Diluted culture supernatants (50 μl) from oxygen-limited growth experiments were added to 850 μl of 1% (w/v) sulphanilamide

(Sigma) dissolved in 1 M HCl and 100 μ l of 0.02% (w/v) naphthylethylenediamine (Sigma). After 15 min, the absorbance at 540 nm was measured using a Pharmacia Biotech Ultrospec 2000, and nitrite concentrations were determined by reference to a standard curve.

2.13 Measurement of Reactive Oxygen Species (ROS):

Cells were grown in MHS microaerobically until exponential phase (section 2.3.1) and harvested at mid-exponential growth level by centrifuging at 12,000 x g, 40 °C for 3 min. Cell pellets were washed and resuspended in 5 ml of 25 mM phosphate buffer (pH 7.4). 6 ml of 25 mM phosphate buffer (pH 7.4) in 6 well plates were inoculated with the cell suspension to a final OD₆₀₀ of 0.2. 10 μ M Dihydrodichlorofluorescein (H2DCFDA; Life Technologies, USA), dissolved in 1% DMSO, was added to the cell culture at time zero and plates were incubated microaerobically at 42 °C. 1 ml sample was collected every 10 min and Fluorescence was measured with a fluorescence spectrophotometer (Cary eclipse, Agilent) with excitation at 485 nm. Assay was done with biological triplicates. Total protein concentration of the cell suspension was determined by Lowry assay (section 2.7.5) and the data expressed as fluorescence intensity per mg protein.

2.14 One-Dimensional sodium dodecyl sulfate polyacrylamide gel electrophoresis (SDS-PAGE):

SDS-PAGE was performed with either whole cells or purified protein after appropriate processing using the Mini-Protean Tetra system (Bio-Rad). 10% or 12% acrylamide resolving gel, depending on protein size, was made by diluting a mixture of appropriate amount of 30% [w/v] acrylamide/0.8% [w/v] bis-acrylamide, 1 M Tris-HCl pH 8.8 and 10% [w/v] SDS in appropriate amount of dH₂O to make 12.5% acrylamide, 375 mM Tris-HCl pH 8.8 and 0.1 % [w/v] SDS solution, respectively. Polymerization was initiated by adding 0.1 % (w/v) ammonium persulphate (APS) and 0.01 % N,N,N',N'-Tetramethylethylenediamine (TEMED) in solution. Components were mixed thoroughly by gentle inverting. A gel cast was assembled and the solution was poured carefully leaving space equal to height of comb. That space was filled with a layer of 100% ethanol to ensure an even spread and no air bubble. When the gel was polymerised, the ethanol was completely removed by rinsing with water and any residual water was blotted from the gel surface with filter

paper prior to addition of the stacking gel. 5% Stacking gel was made by diluting a mixture of appropriate amount of 30 % (w/v) acrylamide/0.8 % (w/v) bisacrylamide, 1 M Tris-HCl pH 6.8, 10 % (w/v) SDS in appropriate amount of dH₂O to make 6 % acrylamide, 125 mM Tris-HCl pH 6.8 and 0.1 % (w/v) SDS, solution, respectively. Polymerization was initiated and components were mixed as above. The solution was poured carefully on top of the resolving gel and the loading comb was inserted in it without leaving any air bubble. Upon polymerisation, loading comb was removed and the gel set was assembled in a gel set holding gasket (with one more gel set or a plate). Assembly was placed in a gel tank and the inner pocket was filled completely and rest of the tank filled half with 1 x running buffer (25 mM Tris, 250 mM glycine, 0.1 % [w/v] SDS).

Loading samples were prepared by mixing protein samples or whole cells with equal volumes of of sample buffer (60 mM Tris-HCl pH 6.8, 2 % [w/v] SDS, 0.005 % [w/v] bromophenol blue, 5 % [v/v] β-mercaptoethanol, 10 % [w/v] glycerol) and boiling at 80°C for 5 minutes. Typically, 20 µl of the samples were loaded carefully in wells with Prestained EZ-Run protein ladder (Fisher) as a size marker.

The samples were separated by electrophoresis at 180 V until the tracking dye had migrated to the bottom of the gel. Gels were stained by shaking with Coomassie brilliant blue (50 % [v/v] methanol, 10 % [v/v] glacial acetic acid and 0.1 % [w/v] coomassie brilliant blue (Sigma-Aldrich)) solution overnight and de-stained by covering with (50 % [v/v] methanol, 10 % [v/v] glacial acetic acid) with continuous shaking until individual protein bands were resolved.

2.15 Detection of c-type cytochromes by enhanced chemiluminescence (Haem blot) assay:

Haem blot was performed with purified total membrane (section 2.7.3) proteins according to Vargas *et al.*, (1993) with some modifications. Loading samples were prepared by mixing protein samples with equal volumes of sample buffer (60 mM Tris-HCl pH 6.8, 2 % [w/v] SDS, 0.005 % [w/v] bromophenol blue and 10 % [w/v] glycerol) and mildly denaturing by boiling at 37 °C for 30-60 minutes in the absence of mercaptoethanol to preserve attachment of C-hemes to Cys residues. Proteins were separated by two separate SDS-PAGE (section 2.14) on 10% acrylamide gels. One was stained with Coomassie blue G250 (section 2.14) and other

was electroblotted onto nitrocellulose membrane (Hybond-C extra, GE Healthcare). SDS-PAGE and nitrocellulose membrane sandwich was made according to manufacturer's instructions and electroblotting was performed using Mini-Blot Electrophoretic Cell (Bio-Rad) in ice-cold transfer buffer (25 mM Tris, 190 mM glycine, 10 % [v/v] methanol) for 1 hour at constant 100 V. Then the membrane was washed with 20 mM Phosphate buffer for 5 minutes at RT to remove any residual SDS or methanol and covalently bound haem was detected as haem-associated peroxidase activity (Feissner *et al.*, 2003), using the enhanced chemiluminescence (ECL) kit from GE Healthcare according to manufacturer's instructions. Membrane was covered with pre-mixed solutions A and B, incubated for 1 minute at RT and developed by exposing for different times, as necessary, in ChemiDoc Imaging System (Bio-Rad).

2.16 cytochrome *c* difference spectroscopy:

Carbon monoxide difference spectroscopy was performed using total membrane proteins to detect the active site Cu/b-heme centre in CcoN. 1ml quartz cuvettes were filled with 1ml of 10 mg/ml protein and sparged thoroughly with carbon monoxide gas (CO) for 10 minutes under a fume hood. Spectra were measured at RT by using a Shimadzu UV-2401 dual wavelength scanning spectrophotometer (Shimadzu). Then the sample was reduced by adding appropriate amount of sodium dithionite and spectra was measured again. CO-reduced *minus* reduced scans were carried out from 400 to 700 nm. Assay was done with biological triplicates.

2.17 Prediction of transmembrane helices and signal peptides in protein sequences:

Transmembrane helices were predicted using the TMHMM program (<http://www.cbs.dtu.dk/services/TMHMM/>). The program takes an amino acid sequence in FASTA format. The prediction gives the most probable location and orientation of transmembrane helices in the sequence. It is found by an algorithm called N-best (or 1-best in this case) that sums over all paths through the model with the same location and direction of the helices. The plot shows the posterior probabilities of inside/outside/TM helix. The plot is obtained by calculating the total probability that a residue sits in helix, inside, or outside summed over all possible paths through the model. Sometimes it seems like the plot and the prediction

are contradictory, but that is because the plot shows probabilities for each residue, whereas the prediction is the over-all most probable structure. Therefore the plot should be seen as a complementary source of information. If the whole sequence is labelled as inside or outside, the prediction is that it contains no membrane helices. It is not advised to interpret it as a prediction of location (periplasmic or cytoplasmic).

Presence and location of signal peptides were predicted using SignalP 4.1 server (<http://www.cbs.dtu.dk/services/SignalP/>). It is a Bioinformatics tool which takes an amino acid sequence in FASTA format. It predicts the presence and location of signal peptide cleavage sites in amino acid sequences from different organisms. The method incorporates a prediction of cleavage sites and a signal peptide/non-signal peptide prediction based on a combination of several artificial neural networks.

2.18 Western Blot:

Total membrane (section 2.7.3) or inner membrane (section 2.7.4) protein fractions of strains were used to make loading samples and were separated by two separate SDS-PAGE as detailed in section 2.14). One was stained with Coomassie blue G250 (section 2.14) and the other was electroblotted onto nitrocellulose membrane (Hybond-C extra, GE Healthcare) as described in section 2.15. Tris-buffered saline with tween 20 (TBST) solution was made with 20 mM Tris (pH 7.5), 150 mM NaCl and 0.1% tween 20 in dH₂O. The sample was transferred to a nitrocellulose membrane was incubated with 10 ml TBST + 5% milk powder for 1 hour at RT on shaker for blocking followed by washing three times with 10 ml TBST for 5 to 10 minutes each. Then the membrane was incubated with primary antibody (1:1000 dilution in TBST + 5% skimmed milk powder) for 1 hour at RT on shaker followed by washing three times with 10 ml TBST for 5 to 10 minutes each. Then the membrane was incubated with secondary antibody (1:2000 dilution in TBST + 5% skimmed milk powder) for 1 hour at RT on shaker followed by washing as before. The processed membrane was developed as described in section 2.15.

Chapter 3

Cytochrome *c* Oxidase

Assembly

in

Campylobacter jejuni

3.1 Introduction:

C. jejuni is a Gram negative microaerophilic bacterium, which has a complex respiration system (Kelly, 2008) for its fairly small genome size of only ~1.7 Mb (Parkhill *et al.*, 2000). Various electron donors, like formate, malate, proline and many more donate electrons to the menaquinone pool from where they are transported to various terminal reductase enzymes (Sellars *et al.*, 2002; Kelly, 2008). It has two terminal oxidases, the Cyd-like CioAB quinol oxidase and *cbb*₃-type cytochrome *c* oxidase (Jachson *et al.*, 2007). The presence of two oxidases may be due to the fact that the Cyd-like CioAB quinol oxidase is more resistant to sulfide inhibition but has a low oxygen affinity, with a $K_m \sim 0.8 \mu\text{M}$ (Jachson *et al.*, 2007), which is necessary as *C. jejuni* is a gut bacterium and the concentration of sulfide is high in the intestine (Gong *et al.*, 2014), but the *cbb*₃-type cytochrome *c* oxidase is more energy efficient (proton pumping) and is necessary for normal growth of the bacterium and its host colonization (Liu *et al.*, 2013). *cbb*₃-type cytochrome *c* oxidase is further discussed in section 1.2.6.1. This chapter will focus on the assembly of the *cbb*₃-type cytochrome *c* oxidase, as in *C. jejuni* it is not known what genes and proteins are necessary for the biogenesis of this enzyme. As discussed in the General Introduction, this oxidase is an inner membrane protein complex consisting of CcoN, CcoO, CcoQ and CcoP subunits, collectively called CcoNOQP (Cosseau *et al.*, 2004).

In *C. jejuni* NCTC 11168 genes *cj1487c*, *cj1488c*, *cj1489c* and *cj1490c* collectively encode the CcoNOQP subunits of the *cbb*₃-type cytochrome *c* oxidase (Liu and Kelly, 2015). This type of oxidase contains two *c*-type cytochrome subunits and a bi-nuclear haem-copper active site consisting of Cu(B) and *b/b*₃ type haems. Insertion of Cu(B) normally requires an assembly system of copper chaperones but these have not been identified in *C. jejuni* (see section 1.2.6.1.1 for more details). This study hypothesised that genes *cj0911*, *cj0910*, *cj0909* and *cj0908* may encode proteins needed to transfer Cu from the periplasm to the CcoN subunit. Cj0909 is a putative Cu(I) binding protein and is homologous to mitochondrial Cox17 (Bacterial PCu_AC). Cj0911 is a protein belonging to Synthesis of cytochrome *c* oxidase 1 (Sco1) family. Members of this family are required in other bacteria for the proper assembly of cytochrome *c* oxidase. Cj0908 and Cj0910 are predicted to be transmembrane anchored but periplasmic facing proteins, having thioredoxin folds in the C-terminal domains. Recently a thiol-disulfide oxidoreductase DsbA was reported to be involved

in Cytochrome *c* oxidase biogenesis in *Rhodobacter capsulatus* (Onder *et al.*, 2017). Cells lacking DsbA showed low Cco activity, especially at low Cu concentration. Absence of DsbA perturbs cellular redox homeostasis required for the production of an active *cbb*₃-type Cco and also affects the incorporation of Cu into the catalytic subunit of *cbb*₃-type Cco. Cj0908 and Cj0910 have no homology with DsbA but they have thioredoxin folds. This study hypothesise that they may act to reduce Cu(II) to Cu(I), as the periplasm is highly oxidising.

Proteins encoded by the *ccoGHIS* operon also play an important role in biogenesis of the *cbb*₃-type cytochrome *c* oxidase in other bacteria (see section 1.2.6.1.2 for more details). In most bacteria, a *ccoGHIS* operon is situated downstream to *ccoNOQP*, but in *C. jejuni*, *ccoGHIS* genes seem to be scattered throughout the genome and do not make an operon (Fig. 3.2). In *C. jejuni*, this study found that Cj1155 could be equivalent to CcoI as it belongs to the same family of proteins of Cu-translocating P-type ATPase, which may have a copper translocating function, Cj1154 is a CcoS homologue which could be necessary for binding of copper in the CcoN subunit of cytochrome *c* oxidase and Cj0369 is a CcoG homologue (section 3.2.2). *cj1483c* may encode a CcoH homologue which in other bacteria is thought to be tightly associated with the oxidase. *cj1482c*, *cj1484c*, *cj1485c* and *cj1486c* are downstream of CcoNOQP, but with an unknown function and no clear homologues in other bacteria. These are included in this study because in the *C. jejuni* genome, they are in place of *ccoGHIS* in other bacterial genomes and having *ccoH* sandwiched between genes encoding unknown proteins.

3.2 Results:

3.2.1 Gene arrangement in *C. jejuni* genome:

3.2.1.1 Putative genes expressing assembly proteins:

Proteins potentially responsible for assembly of cytochrome *c* oxidase by capturing and transporting Cu(I) to CcoN subunit in *C. jejuni* are expressed by genes *cj0908*, *cj0909*, *cj0910* and *cj0911*, forming an operon (Fig. 3.1).

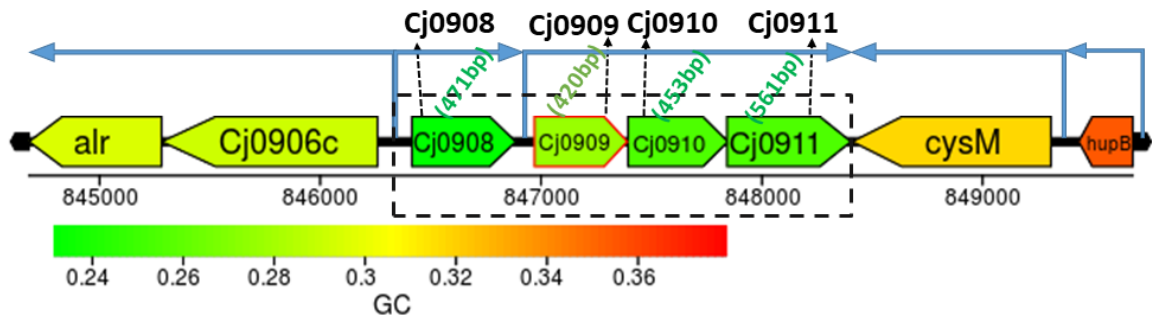


Figure 3.1: Putative assembly protein expressing gene arrangement in *C. jejuni*. Genes expressing potential cytochrome *c* oxidase assembly proteins in *C. jejuni* form an operon on the primary strand of DNA. The genes of interest are boxed. Arrows represent promoter sites. Genes are colour coded according to the scale (shown) based on GC content.

In *C. jejuni*, *cj0908* to *cj0911* genes form an operon on the primary strand of DNA, with *cj0909* to *cj0911* having the same promoter (Fig. 3.1). Upstream to this operon there are *cj0906c* and *cj0905c* (*alr*), having same promoter. Protein expressed by *cj0906c* is a putative periplasmic protein and by *cj0905c* is an alanine racemase which converts L-alanine to D-alanine which is used in cell wall biosynthesis. Downstream to this operon there are *cj0912c* (*cysM*) and *cj0913c* (*hupB*), having independent promoters. Protein expressed by *cj0912c* is cysteine synthase and by *cj0913c* is DNA-binding protein HU homolog. This showed that protein encoded by genes next to *cj0908-cj0911* gene operon on both sides have nothing to do with Cco assembly and are out of scope of this study.

3.2.1.2 Genes expressing CcoGHIS proteins and genes downstream of *ccoNOQP*:

In *C. jejuni*, BLAST searching and genome annotation suggests that the protein expressed by *cj1154c* is a CcoI homologue, by *cj1155c* is a CcoS homologue, by *cj0369c* is a CcoG homologue and by *cj1483c* may be a CcoH homologue. *cj1482c*, *cj1484c*, *cj1485c* and *cj1486c* are downstream of *ccoNOQP*, but with an unknown function and no clear homologues in other bacteria (Fig. 3.2).

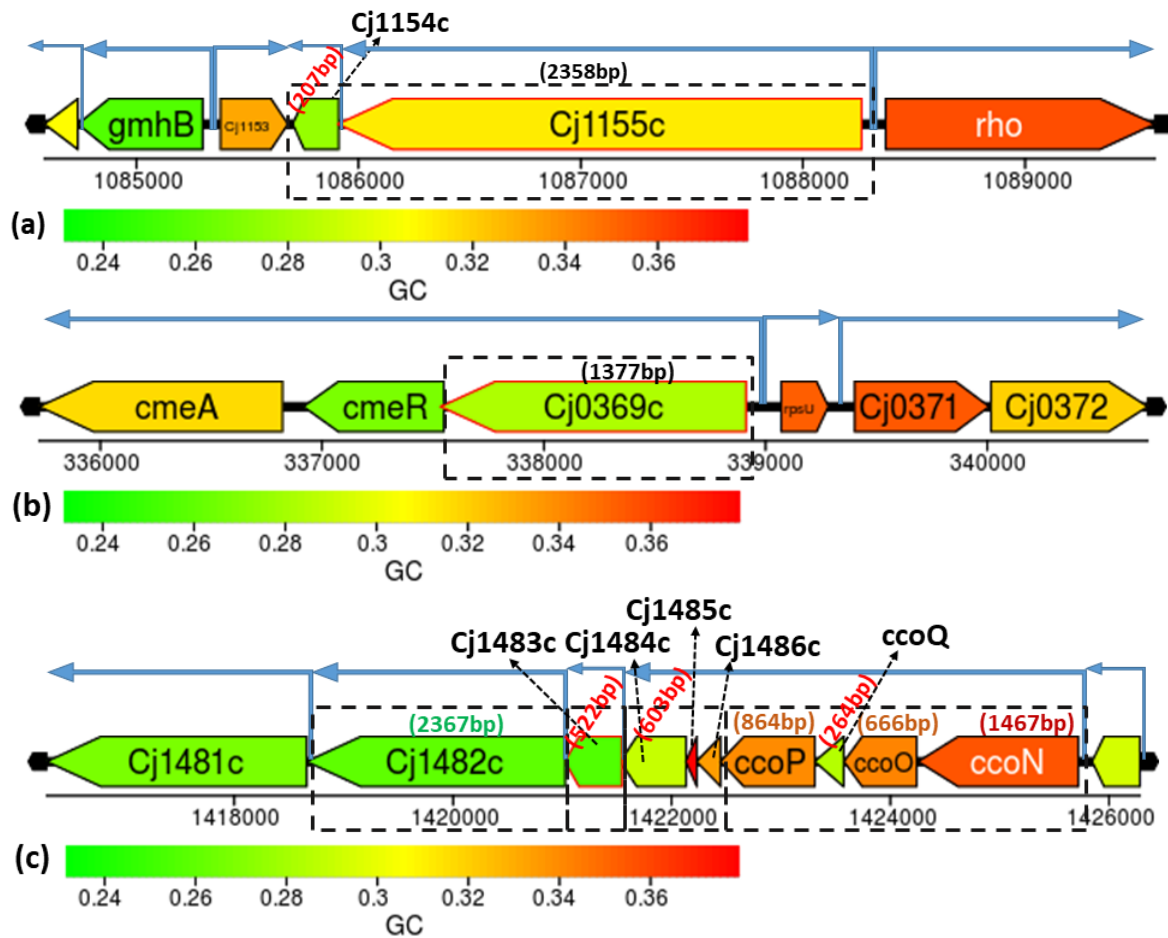


Figure 3.2: Arrangement of possible *ccoGHIS* genes and genes downstream of *ccoNOQP* in *C. jejuni*. Genes potentially expressing CcoGHIS proteins in *C. jejuni* are scattered throughout the genome. Gene arrangement of (a) *cj1154c* (*ccoI* homolog) and *cj1155c* (*ccoS* homolog), (b) *cj0369c* (*ccoG* homolog), (c) *cj1483c* (potential *ccoH* homolog), *cj1482c*, *cj1484c*, *cj1485c* and *cj1486c* (downstream to *ccoNOQP*) in *C. jejuni* genome. Genes of interest are in boxes. Arrows represent promoter sites. Genes are colour coded according to scale (shown) based on GC content.

In *C. jejuni*, *ccoGHIS* homologue genes are scattered throughout the genome on the complementary strand (Fig. 3.2). Genes *cj1154c* and *cj1155c* have the same promoter. Upstream of these genes, there are *cj1153* on the primary strand and the *cj1152c* on same strand. The protein expressed by *cj1153* is a periplasmic cytochrome *c* and *cj1152c* is a *gmhB* homologue, a putative D,D-heptose 1,7-bisphosphate phosphatase. Downstream of these genes, there is *cj1156* on primary strand, expressing a protein homologous to transcription termination factor Rho. *cj0369c* has *cj0367c* (*cmeA*) and *cj0368c* (*cmeR*) upstream and *cj0370* (*rpsU*) and *cj0371* downstream. Protein expressed by *cj0367c* is a putative periplasmic fusion protein

CmeA (multidrug efflux system CmeABC), by *cj0368c* is a putative transcriptional regulator CmeR (transcriptional repressor for CmeABC operon), by *cj0370* is homologues to 30S ribosomal protein S21 and by *cj0371* is a hypothetical protein. *cj1482c-cj1490c* cluster has *cj1481c* and *cj1491c*, downstream and upstream, respectively. *cj1481c* is encoding a putative recombination protein RecB and *cj1491c* is encoding a putative two-component regulator. This showed that proteins encoded by genes next to genes of interest in this study on both sides are not obviously related to Cco activity and are out of scope of this study, although the Cj1491 regulator could be of interest.

3.2.2 Bioinformatics analysis for finding homologous sequences:

C. jejuni Cj0908, Cj0909, Cj0910, Cj0911, Cj1154, Cj1155, Cj0369, Cj1482, Cj1483, Cj1484, Cj1485 and Cj1486 proteins were checked for any available characterised homologous protein by running protein BLAST in NCBI.

Protein	Homolog protein	% Identity	Other organisms with similar protein	Putative/predicted Function
Cj0908	-	-	-	CcoNOQP Cu Assembly protein Containing thioredoxin motif
Cj0909	Cu chaperone PCu _A C (Functionally similar to mitochondrial Cox17)	36 % (copper chaperone PCu(A)C in <i>Rhodobacter sphaeroides</i>)	<i>Deinococcus radiodurans</i> , <i>Caulobacter crescentus</i> , <i>Rhodobacter sphaeroides</i> , <i>Rhodobacter capsulatus</i>	CcoNOQP Cu Assembly Cytoplasmic protein containing metal binding motif
Cj0910	-	-	-	CcoNOQP Cu Assembly protein Containing thioredoxin motif
Cj0911	Sco family protein	31 % (SCO family protein in <i>Rhodobacter sphaeroides</i>)	<i>Bacillus subtilis</i> , <i>Rhodobacter sphaeroides</i> , <i>Rhodobacter capsulatus</i>	CcoNOQP Cu Assembly membrane bound protein containing Cu cheperon
Cj1154	CcoS	34 % (cbb3-type	<i>Rhodobacter capsulatus</i> , <i>E.</i>	Putative essential protein for

		cytochrome oxidase assembly protein CcoS in <i>Rhodobacter</i>)	<i>coli</i>	Biogenesis and maturation of CcoNOQP complex.
Cj1155	Cu-translocating P-type ATPase. (CcoI belongs to the same family)	29 % (copper-translocating P-type ATPase in <i>Rhodobacter sphaeroides</i>)	<i>Rhodobacter sphaeroides</i> , <i>Rhodobacter capsulatus</i> , <i>Helicobacter spp.</i> , <i>E. coli</i>	Putative essential protein for Biogenesis and maturation of CcoNOQP complex.
Cj0369	CcoG	29 % (CcoG in <i>E. coli</i>), 27 % (CcoG in <i>Rhodobacter capsulatus</i>)	<i>Rhodobacter capsulatus</i> ,	Putative essential protein for Biogenesis and maturation of CcoNOQP complex.
Cj1483	CcoH	40 % (putative CcoH in <i>Flavobacterium chungangense</i>)	<i>Rhodobacter capsulatus</i> , <i>Flavobacterium chungangense</i>	Putative essential protein for Biogenesis and maturation of CcoNOQP complex.
Cj1482	-	-	-	?
Cj1484	-	-	-	?
Cj1485	-	-	-	?
Cj1486	-	-	-	?

Table 3.1: Homologue searching. Proteins were checked for any available characterised homologous protein by running protein BLAST in NCBI.

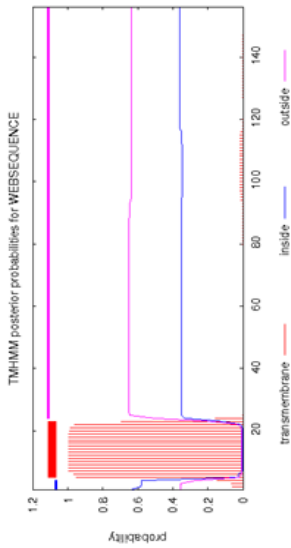
BLAST results showed that Cj0911 in *C. jejuni* has 31 % identity with a SCO family protein in *Rhodobacter sphaeroides*, which is essential for assembly of cytochrome *c* oxidase in Cu limited environment (Thompson *et al.*, 2012). Cj0909 has 36 % identity with the Cu chaperone PCu(A)C in *Rhodobacter sphaeroides* and 30% identity with bacterial analogue of COX17 protein. Cj1154 is 97% identity to CcoS in *E. coli*, Cj0369 is 29 % identical to CcoG in *E. coli* and 27 % identical to CcoG in *Rhodobacter capsulatus*. Cj1483 is 40% similar to putative CcoH in *Flavobacterium chungangense*, and has no characterised CcoH homolog. Cj1155 is 34 % identical to Cu translocating P-type ATPase in *E. coli*. There were no characterised homologues of Cj0908, Cj0910, Cj1482, Cj1484, Cj1485 and Cj1486 available, making those novel proteins.

3.2.3 Prediction of transmembrane helices in proteins:

C. jejuni Cj0908, Cj0909, Cj0910, Cj0911, Cj1154, Cj1155, Cj0369, Cj1482, Cj1483, Cj1484, Cj1485 and Cj1486 proteins were checked for their putative location with respect to the membrane by predicting soluble or membrane bound or transmembrane helices in proteins using TMHMM Server v.2.0 with amino acid sequence of proteins. As cytochrome *c* oxidase is an inner membrane protein complex, these predictions will help us to establish the pathway these proteins can interact with cytochrome *c* oxidase and use it to support or question the hypothesis established by the homology results. Signal sequences in proteins were predicted using SignalP 4.1 Server.

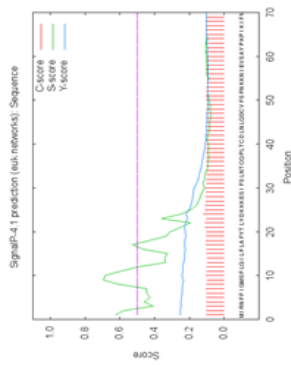
Protein

Predicted transmembrane helices

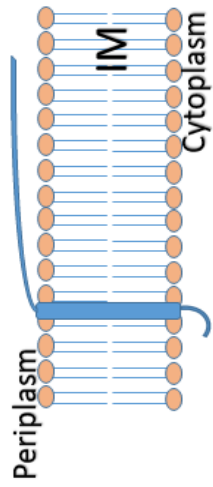


Cj0908

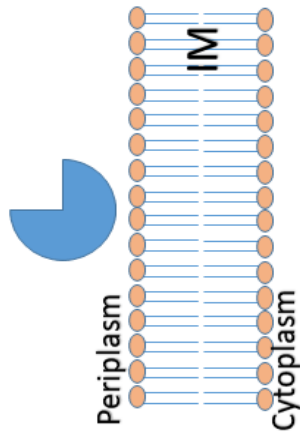
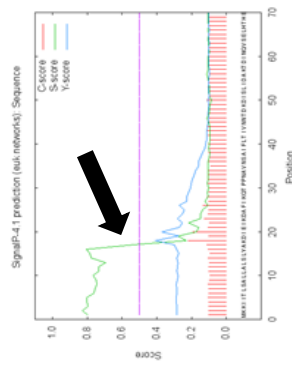
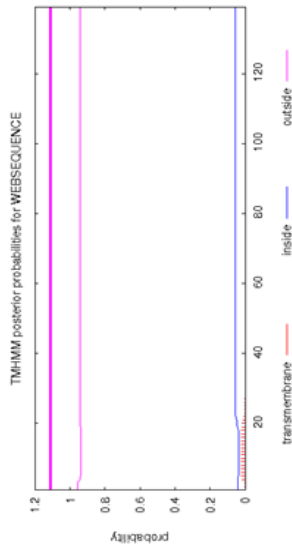
Predicted Signal sequence



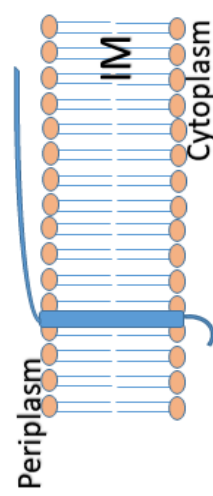
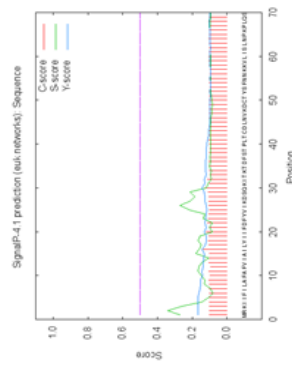
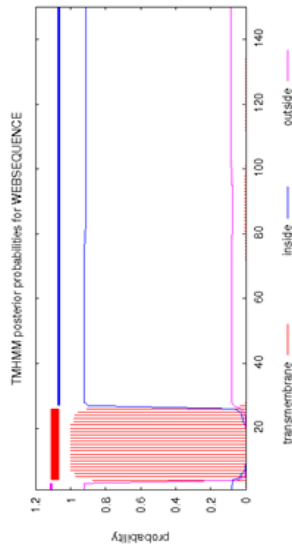
Predicted Protein Topology



Cj0909

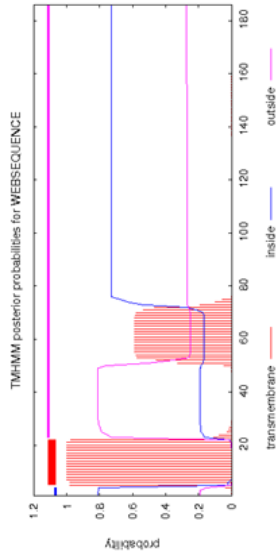


Cj0910



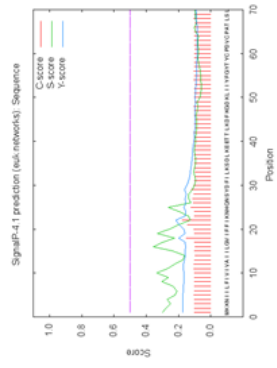
Protein

Predicted transmembrane helices

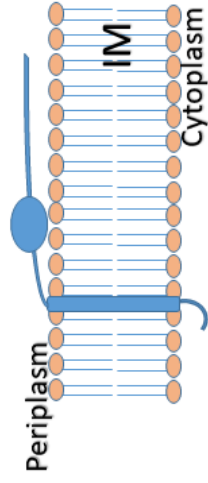


Cj0911

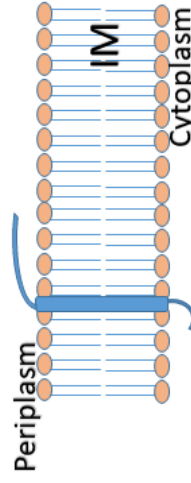
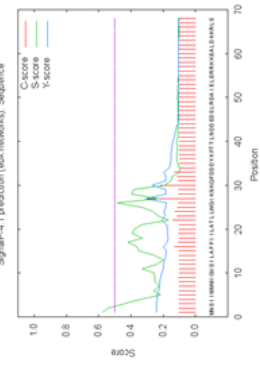
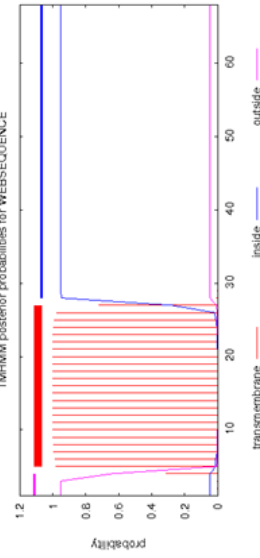
Predicted Signal sequence



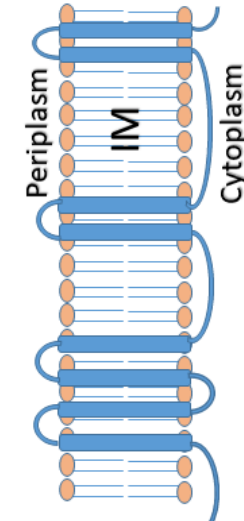
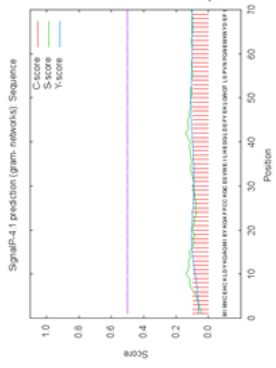
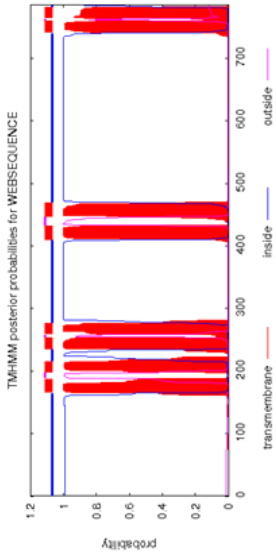
Predicted Protein Topology



Cj1154

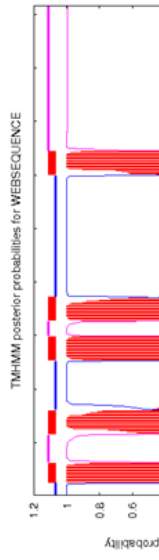


Cj1155



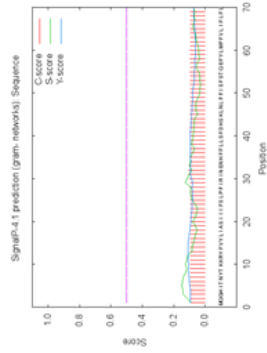
Protein

Predicted transmembrane helices

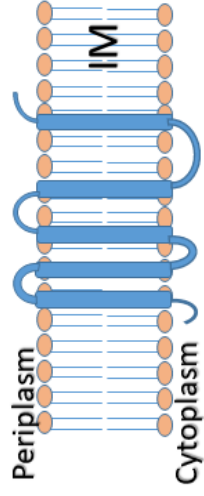


Cj0369

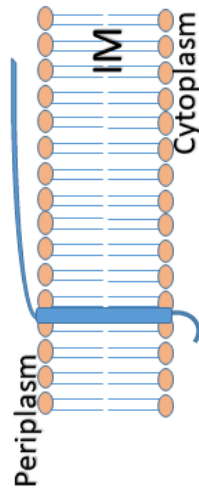
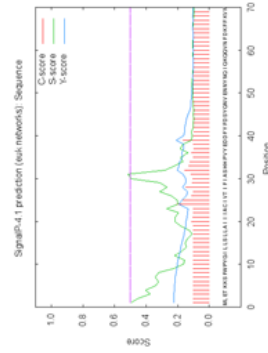
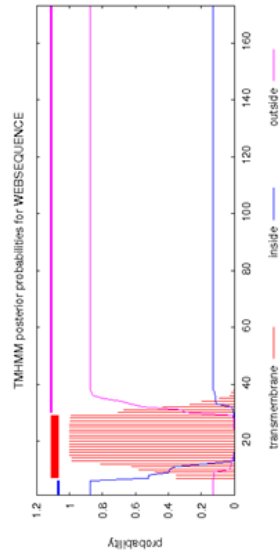
Predicted Signal sequence



Predicted Protein Topology



Cj1483



Cj1482

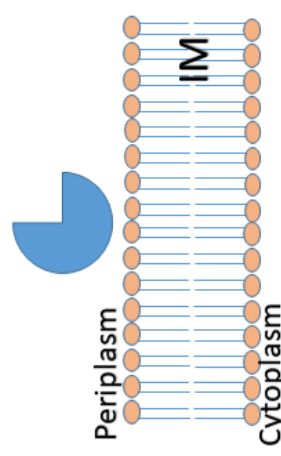
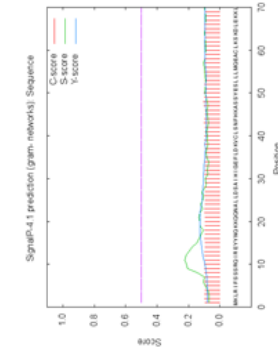
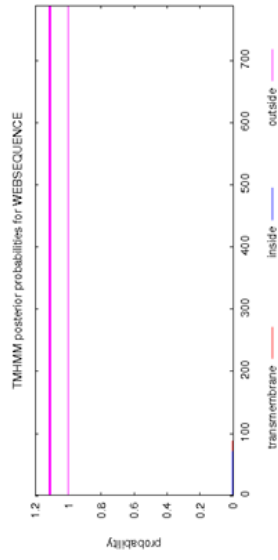


Figure 3.3: Prediction of transmembrane helices in proteins and subsequently their predicted topology. Protein amino acid sequences were submitted to TMHMM and SignalP 4.1 server individually. The plot shows the posterior probabilities of inside/outside/TM helix. The plot is obtained by calculating the total probability that a residue sits in helix, inside, or outside summed over all possible paths through the model. TMHMM result of (a) Cj0908, (b) Cj0909, (c) Cj0910, (d) Cj0911, (e) Cj1154, (f) Cj1155, (g) Cj0369, (h) Cj1483, (i) Cj1482, (j) Cj1484, (k) Cj1485 and (l) Cj1486. Plots were interpreted as directed by TMHMM Server v.2.0 website. If the whole sequence is labelled as inside or outside, the prediction is that it contains no membrane helices. It is probably not wise to interpret it as a prediction of location. Based on results, protein topology with respect to inner membrane are predicted and shown. Plots were interpreted as directed by TMHMM Server v.2.0 (<http://www.cbs.dtu.dk/services/TMHMM/>) and SignalP 4.1 server (<http://www.cbs.dtu.dk/services/SignalP/>).

TMHMM predictions, as described in section 2.17, suggests that Cj0908, Cj0910, Cj0911, Cj1154, Cj1483 and Cj1484 are membrane bound proteins, Cj1155, Cj0369, Cj1485 and Cj1486 transmembrane proteins, and Cj0909 and Cj1482 are non-membrane proteins (Fig. 3.3). Prediction of signal sequence can help in designing the protein over-expression primers to delete the sequence encoding the signal sequence part of the protein.

3.2.4 Generation of Knock out mutants in *C. jejuni* 11168 by ISA:

PrrC (Sco homologue) in *Rhodobacter sphaeroides* has been shown to be involved in assembly of copper center of *cbb₃*-type cytochrome *c* oxidase and in many bacteria, like *Rhodobacter capsulatus*, *ccoGHIS* gene products have been shown to have role in biogenesis of *cbb₃*-type cytochrome *c* oxidase. As *cbb₃*-type cytochrome *c* oxidase activity can easily be measured, it was decided to make knock out mutants by deleting genes encoding proteins potentially affecting cytochrome *c* oxidase activity and compare them with the wildtype strain.

Kanamycin resistant knock out mutants were made by deleting each gene individually and replacing it with a kanamycin resistance cassette by homologous recombination. Recombination plasmids were made (Fig. 3.4) using pGEM-3Zf(-) by isothermal assembly (section 2.4.11) and transformed to competent *C. jejuni* cells (section 2.5.3) to disrupt most of the genes of interest without affecting the neighbouring genes. As *cj0908*, *cj0909*, *cj0910* and *cj0911* in an operon, one mutant was made by deleting the whole operon as well as constructing individual gene

deletion mutants. The following section details how the mutant strains were produced in *C. jejuni* NCTC11168.

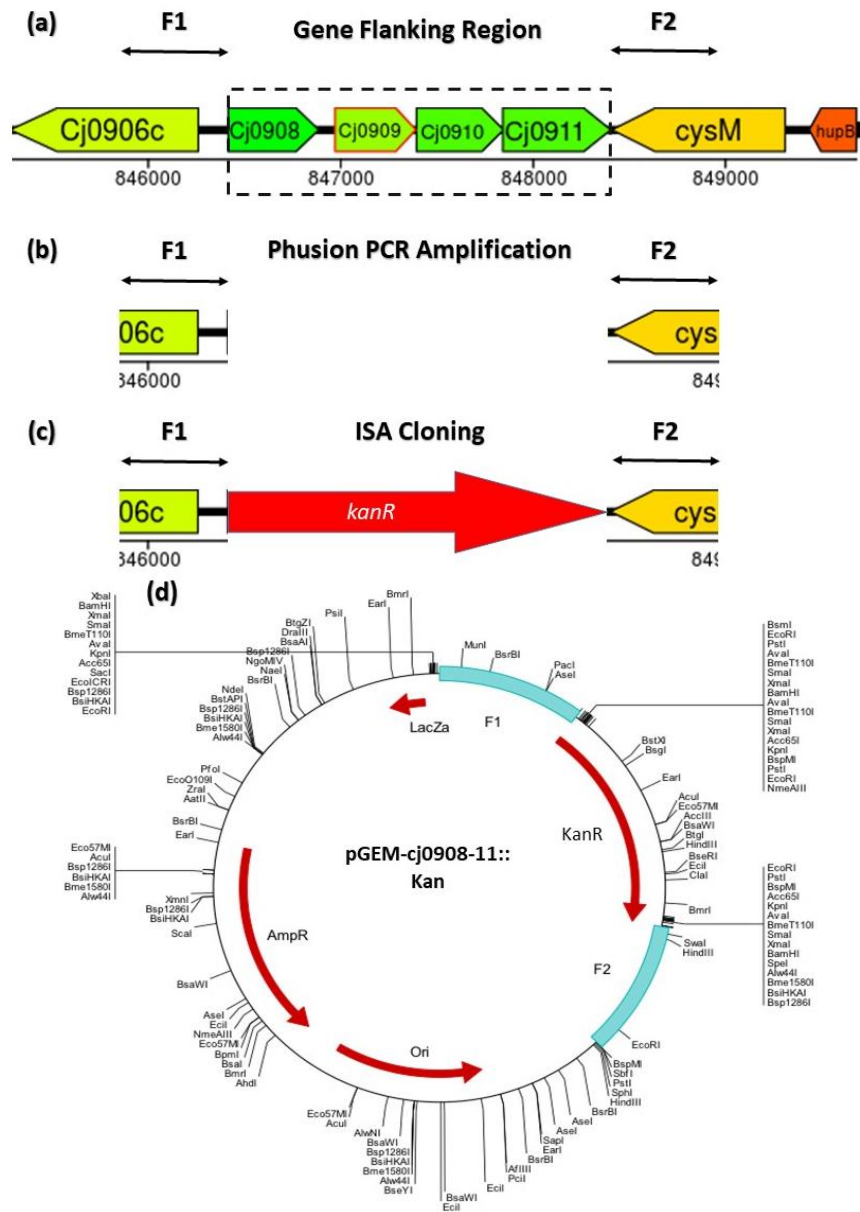


Figure 3.4: Generation of recombinant plasmid by ISA for *C. jejuni* mutation. (a) The flanking regions of genes of interest (*cj0908-cj0911*), 500 bp on each side (marked as F1 and F2). (b) F1 and F2 were amplified by high fidelity phusion PCR using forward and reverse primers removing the entire genes of interest without effecting the neighbouring gene sequence (c) The antibiotic resistant marker (kanamycin cassette in this case) is inserted between flanking regions into the pGEM-3Zf(-) vector by ISA cloning. (d) Completed recombinant plasmid containing the flanking regions with inserted resistance marker prior to transformation in to *C. jejuni*.

Recombinant plasmids for other knock out mutants (mentioned in 2.4.2.1) were made similarly as shown in above figure (Fig. 3.5). They are presented in appendix.

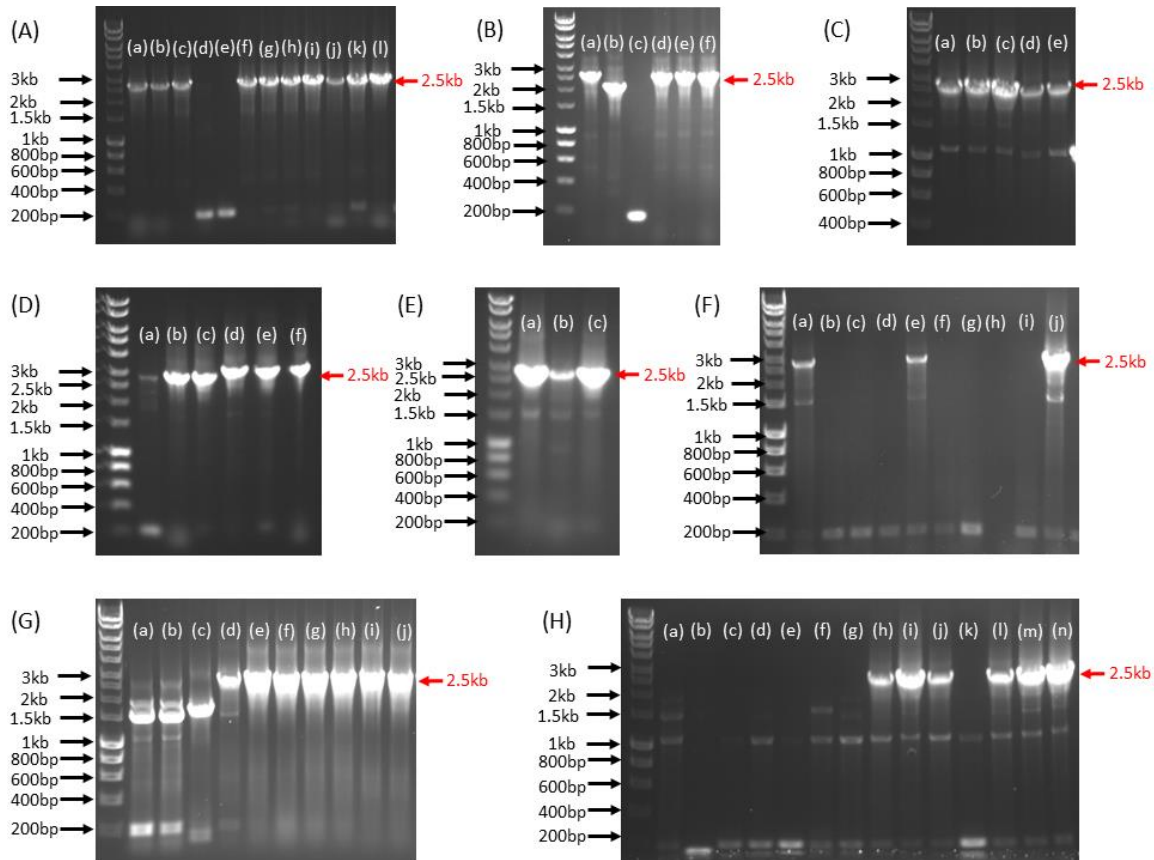


Figure 3.6: Recombinant plasmid confirmation by correct size using PCR. All recombinant plasmids made for knock out mutations were confirmed by PCR with M13 primers which anneal in the vector outside the cloned region. Correct size bands are 2.5 kb long (1.5 kb of kan cassette+500 bp of each flanks). All are different clones. (A) pGEM-cj0908-11 (a to l) (B) pGEM-cj0911 (a to f) (C) pGEM-cj1485c (a to e) (D) pGEM-cj1154c (b and c) and pGEM-cj1155c (d, e and f) (E) pGEM-cj0369c (a to c) (F) pGEM-cj1483c (j) (G) pGEM-cj1482c (d, e and f) and pGEM-cj1484c (g, h, i and j) (H) pGEM-cj1486c (h to n).

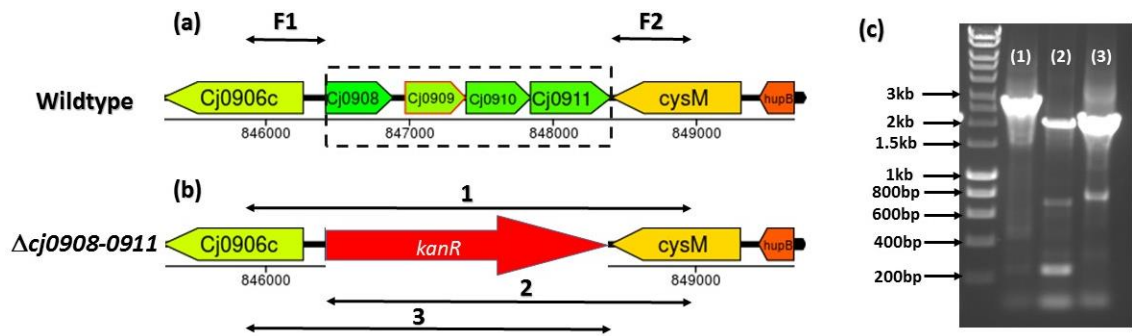


Figure 3.7: Mutagenesis of cytochrome *c* oxidase assembly operon in *C. jejuni*. The recombinant plasmid formed by ISA shown in figure 3.5 was transformed into *C. jejuni* to replace the gene of interest with kanamycin resistant cassette. **(a)** Shows the gene arrangement of *cj0908-cj0911* operon in wildtype strain. Arrows F1 and F2 indicates the flanking region. **(b)** Shows the gene arrangement in mutant with genes of interest replaced by kanamycin resistance cassette. The mutants were confirmed by PCR with a combination of screening and kan primers (section 2.4.5). Size of arrow corresponds to expected size of PCR product and number corresponds to PCR products on gel. **(c)** Gel containing PCR confirmation bands of different clones. Lane number and band size corresponds to number and size of arrows, respectively. Expected PCR product size are: 1-2.7 kb, 2-2.1 kb and 3-2.1 kb. First lane is ladder (HyperLadder 1 molecular weight marker, Bioline)

The knock out mutants formed by transformation of *C. jejuni* cells with recombinant plasmids were checked for correct mutation by running colony PCR with a combination of screening and kanamycin cassette primers (section 2.4.5) (Arrow 1: screening forward-screening reverse, arrow 2: Kan forward-screening reverse and arrow 3: screening forward-Kan reverse) according to section 2.4.4.3 (Fig. 3.7). Screening primers were designed 100 bp outside the flanking regions (which were 500 bp) on both sides to show that the construct was correctly inserted in the correct orientation and that the double recombination had removed the remaining vector DNA. Size of kanamycin resistant cassette is ≈ 1.5 kb. PCR products were checked for correct size by agarose gel electrophoresis according to section 2.4.6. Figure 3.7(c) confirmed correct mutation of *cj0908-cj0911* operon. All other mutants were made and checked similarly as follows (Fig. 3.8 to Fig. 3.11). *cj1486c* mutation was checked for intact *ccoP* (*cj1487c*) by running PCR according to section 2.4.4.3 for *ccoP* in *cj1486c* knock out mutant (Fig. 3.12).

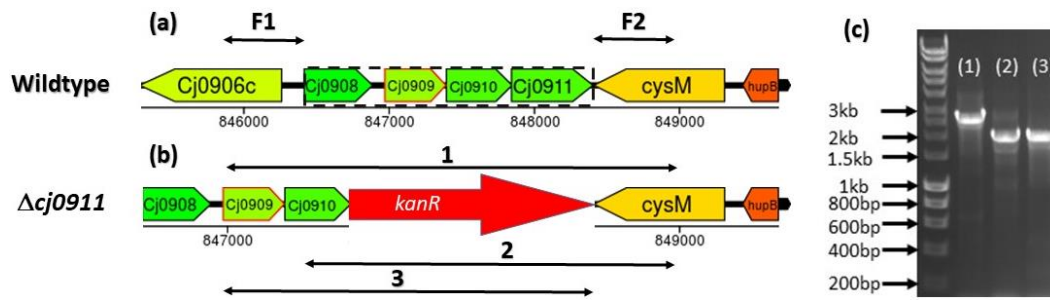


Figure 3.8: Mutagenesis of *cj0911* (encoding component of cytochrome *c* oxidase assembly proteins) in *C. jejuni*. (a) Shows the gene arrangement of *cj0911* in wildtype strain. (b) Shows the gene arrangement in mutant with *cj0911* replaced by kanamycin resistance cassette. (c) Gel containing PCR confirmation bands. Lane number and band size corresponds to number and size of arrows, respectively. See Figure 3.8 legend for detail description.

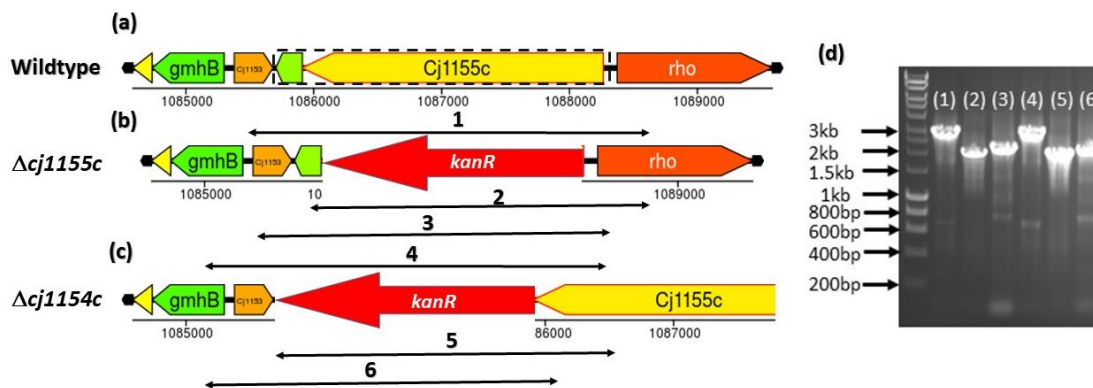


Figure 3.9: Mutagenesis of *cj1154c* and *cj1155c* (*ccoS* and *ccoI*) in *C. jejuni*. (a) Shows the gene arrangement of *cj1154c* and *cj1155c* in wildtype strain. (b) Shows the gene arrangement in mutant with *cj1154c* replaced by kanamycin resistance cassette. (c) Shows the gene arrangement in mutant with *cj1155c* replaced by kanamycin resistance cassette. (d) Gel containing PCR confirmation bands. Lane number and band size corresponds to number and size of arrows, respectively. See Figure 3.8 legend for detailed description.

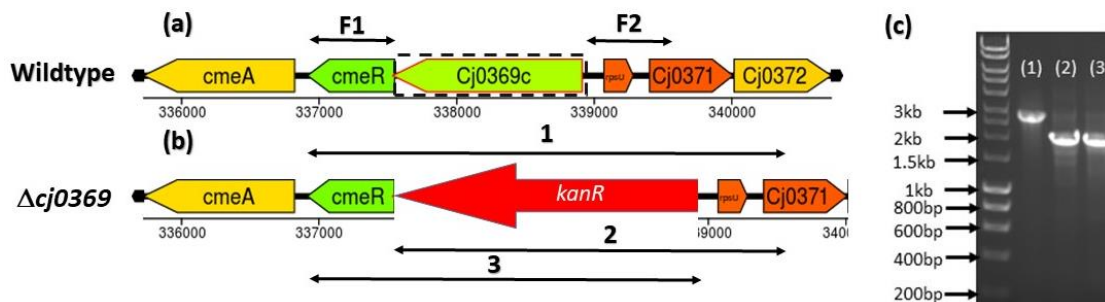


Figure 3.10: Mutagenesis of *cj0369c* (*ccoG*) in *C. jejuni*. (a) Shows the gene arrangement of *cj0369c* in wildtype strain. (b) Shows the gene arrangement in mutant with *cj0369c* replaced by kanamycin resistance cassette. (c) Gel containing PCR confirmation bands. Lane number and band size corresponds to number and size of arrows, respectively. See Figure 3.8 legend for detailed description.

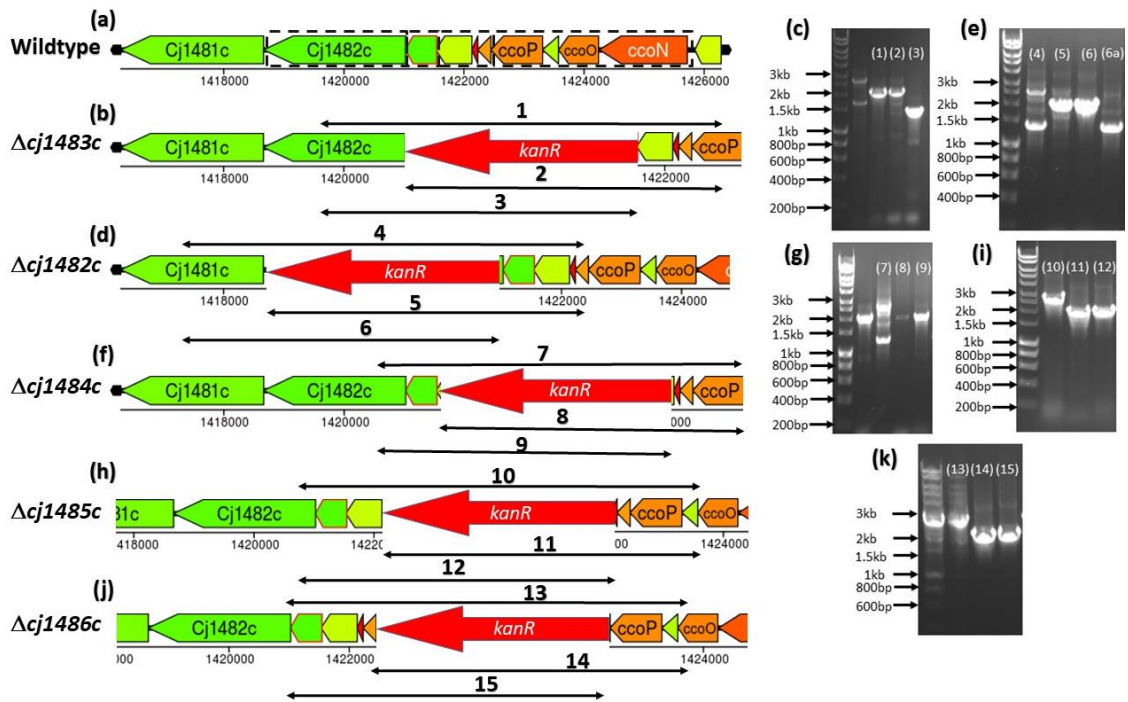


Figure 3.11: Mutagenesis of *cj1483c* (*ccoH*) and *cj1482c*, *cj1484c*, *cj1485c* and *cj1486c* in *C. jejuni*. (a) Shows the gene arrangement of *cj1482c*-*cj1486c* gene cluster in wildtype strain. Gene arrangement in mutant with (b) *cj1483c* (d) *cj1482c* (f) *cj1484c* (h) *cj1485c* and (j) *cj1486c* replaced by kanamycin resistance cassette. Gel containing PCR confirmation bands of (c) *cj1483c* (e) *cj1482c* (6a=PCR product with kan forward and kan reverse primers) (g) *cj1484c* (i) *cj1485c* and (k) *cj1486c* knock out mutants. Lane number and band size corresponds to number and size of arrows, respectively. See Figure 3.8 legend for detail description.

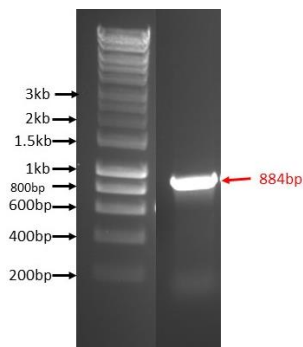


Figure 3.12: Intact *ccoP* in *cj1486c* knock out mutant. *cj1486c* mutant checked for intact *ccoP* (*cj1487c*) by running PCR. *ccoP* band is marked on gel. Size of *ccoP* gene is 884 bp.

3.2.4.1 Attempted complementation of $\Delta cj0908$ -*cj0911*, $\Delta cj0369c$, $\Delta cj1154c$ and $\Delta cj1155c$ *C. jejuni* mutant strains:

For attempted complementation of *cj0908*-*cj0911*, *cj1154* and *cj1155*, pCmetK complementation vector was used. Primers (section 2.4.5) were designed and *cj0908*-*cj0911*, *cj1154c* and *cj1155c* genes were amplified from genomic wild type DNA according to section 2.4.4.2. pCmetK plasmid and PCR products were digested (section 2.4.8) and ligated together (section 2.4.10). The resulting complementation plasmids, i.e. $\Delta cj0908$ -*cj0911*^{+/-} (Fig. 3.13), $\Delta cj0369$ ^{+/-}, $\Delta cj1154$ ^{+/-} and $\Delta cj1155$ ^{+/-},

were electrotransformed into the relevant mutant backgrounds and complemented transformants were selected for with both chloramphenicol and kanamycin.

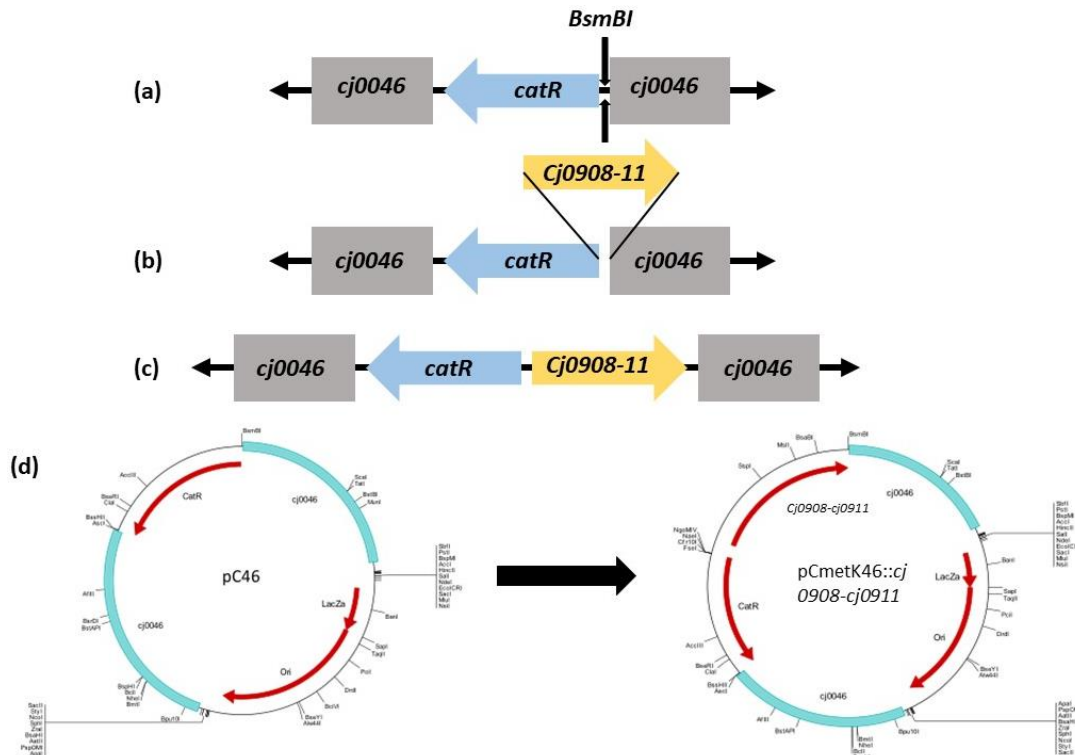


Figure 3.13: Generation of complementation construct by using pCmetK46 vector for *C. jejuni* mutants. (a) shows the location of the BsmBI restriction site and chloramphenicol acetyltransferase resistant cassette within the *cj0046* in pC46 plasmid. (b) Shows the plasmid and *cj0908-cj0911* operon PCR product after digestion with BsmBI. (c) Shows the gene arrangement in complementing plasmid construct after ligation step to insert *cj0908-cj0911* operon into the vector. (d) Shows the full length *cj0908-cj0911* complementation plasmid with *cj0908-cj0911* located downstream of the MetK promoter after cloning in empty pC46 plasmid. *cj0369c*, *cj1154c* and *cj1155c* complementation constructs were made similarly.

Despite numerous attempts, it was not possible to obtain *C. jejuni* $\Delta cj0908-cj0911^{+/-}$, $\Delta cj0369^{+/-}$, $\Delta cj1154^{+/-}$ or $\Delta cj1155^{+/-}$ complemented strains.

3.2.5 Cytochrome *c* oxidase activity during microaerobic growth in batch culture of *C. jejuni*:

Cytochrome *c* oxidase activity can be specifically measured in intact cells as the rate of oxygen consumption in an oxygen electrode using ascorbate as the electron donor and TMPD as a mediator, which directly transfer electrons into haems of the *c*-type cytochrome CcoP and hence into the active site subunit, CcoN. Initially, overnight cultures of wildtype and mutants were used for measuring the cytochrome *c*

oxidase activity but the measurements were not consistent every time. Among the potential factors responsible for this, one critical issue could have been that the cells were at different growth stages when harvested. Therefore, to see if cytochrome *c* oxidase activity changes with the growth phase of the bacteria, it was decided to measure the rate of respiration in wildtype cells with respect to growth.

In this experiment, *C. jejuni* wildtype cells were grown in starter culture till mid log phase (section 2.3.1) and then diluted to starting OD₆₀₀=0.1. The culture was grown according to section 2.3.1 and 1ml sample was collected every hour to measure culture growth (section 2.3.6) and rate of respiration (section 2.11). Protein concentration was measured by Lowry assay (section 2.7.5). Growth and rate of respiration were plotted together using GraphPad prism software. Measurement of activity in intact cells over the course of a batch growth curve for wild-type cells in complex media (Figure 3.14) showed that activity decreased rapidly as the cells entered stationary phase (probably due to loss of viability, although this was not measured in this experiment). Thus, in subsequent experiments, cells were harvested at mid-exponential phase to ensure maximal activity and correct comparisons between wild-type and mutant strains. .

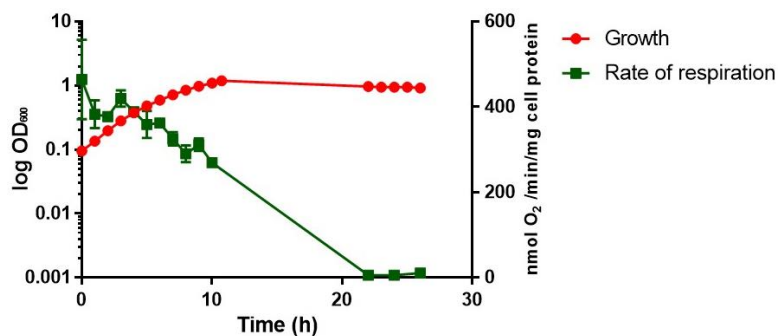


Figure 3.14: Cytochrome *c* oxidase activity vs growth. Cytochrome *c* oxidase activity measured as oxygen uptake in an oxygen electrode with ascorbate plus TMPD in wild type cells grown in Mueller-Hinton medium at different stages of growth phase. Oxidase activity decreases as cells enter stationary phase. The rate shown is $\text{nmol min}^{-1} \text{mg cell protein}^{-1}$ and is the average measured in triplicate cell samples. Error bars show SD.

3.2.6 CcoNOQP abundance is not heavily regulated by oxygen availability:

Another reason why activity may decrease as in Fig. 3.14 is that during growth the cells become progressively oxygen-limited and it is possible that this down regulates oxidase gene expression. To see if cytochrome *c* oxidase activity was different when cells were grown at high or low oxygen conditions, a chemostat was

used (section 2.3.4), where the cells are growing exponentially in minimal media (Serine as sole C source) at the same growth rate but where the oxygen availability can be varied. It was found that the rate measured was essentially the same at high or low oxygen, suggesting that CcoNOQP abundance is not heavily regulated by oxygen availability (Fig. 3.15). Differences were noted in the rates with some other electrons donors, particularly formate, reflecting oxygen regulation of formate dehydrogenase.

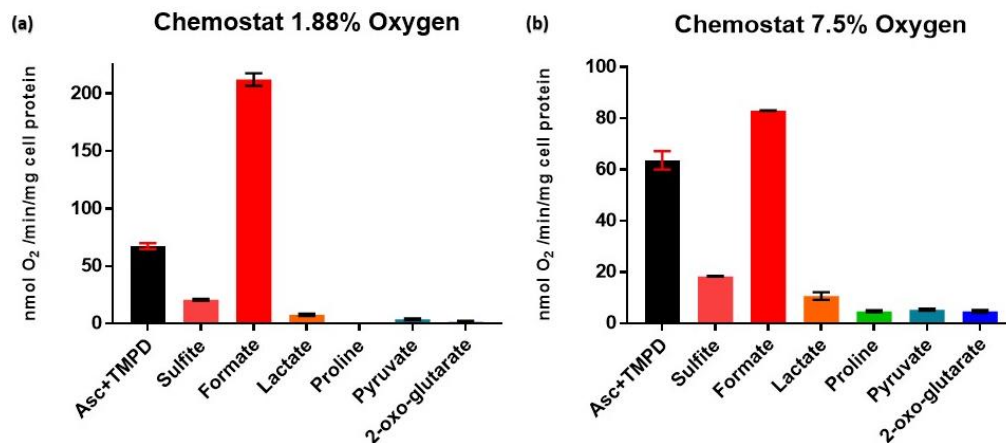


Figure 3.15: Cytochrome c oxidase activity at high or low oxygen. Cytochrome c oxidase activity (Asc/TMPD) was measured with cells grown continuously in chemostat culture at (a) low and (b) high oxygen concentration with different substrates as electron donors to see the effect of oxygen on CcO activity. Data shown are means and SD of three independent replicate cultures.

3.2.7 Effect of formate on growth and oxidase activity in *C. jejuni*:

As mentioned in section 1.2.2.1, Kassem *et al.* (2017) reported that addition of formate stimulated the growth of *C. jejuni* 81-176 strain but reduced the oxidase activity in microaerobic conditions. This does not comply with our observations, which suggests that optimum oxidase activity is necessary for proper growth in *C. jejuni* 11168 strain. Moreover, formate oxidised by formate dehydrogenase donates the electrons directly to the quinone pool, which, in microaerobic conditions, transfers electrons to cytochrome *c* oxidase via Qcr complex. Therefore, to analyse these conflicting observations, a growth curve assay comparing growth of wild type cells grown in MHS media with wildtype cells grown in MHS substituted with 10mM sodium formate was done (Fig. 3.16). The results do not show any stimulation of growth in the presence of formate.

Kassem *et al.* (2017) also reported that formate reduced the oxidase activity in *C. jejuni* 81-176 strain, when grown microaerobically. To check the effect of formate

on activities of both *cbb*₃-type cytochrome *c* oxidase and *bd*-type CioAB quinol oxidase in *C. jejuni* 11168 strain, the oxidase activity was measured (section 2.11) in wildtype, in Δ CcoNOQP (cells just having *bd*-type CioAB quinol oxidase) and in Δ CioAB (cells just having *cbb*₃-type cytochrome *c* oxidase) with TMPD only and with both TMPD and formate as electron donors. TMPD is specific e⁻ donor to *cbb*₃-type cytochrome *c* oxidase while formate donates electrons to quinone pool. Cells were grown microaerobically in MHS complex medium as described in section 2.3.1. Fresh cells harvested at mid exponential phase (as established by section 3.2.5) were used for measuring CcO activity. This study observed that formate cause higher oxidase activity in all three types of cells compared to TMPD (Fig. 3.17).

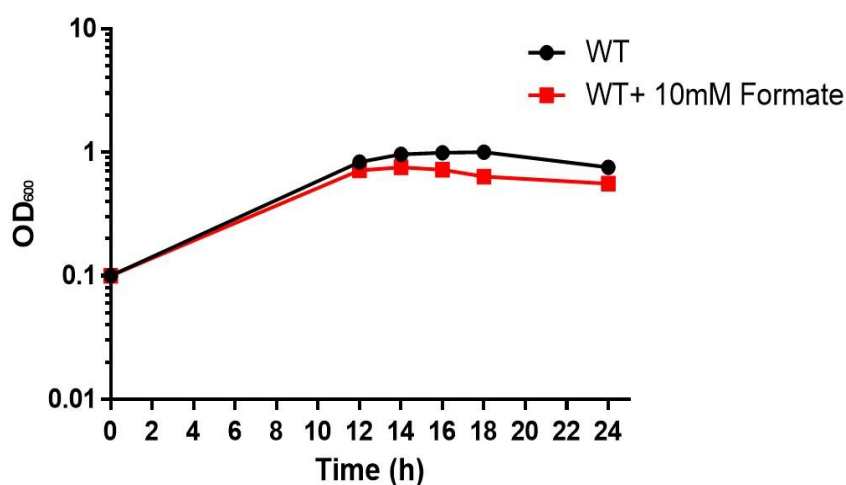


Figure 3.16: Effect of formate on *C. jejuni* 11168 growth. *C. jejuni* NCTC11168 wild type cells were grown in 50 ml MHS complex media with and without 10 mM excess formate in microaerobic cabinet at 42°C with continuous shaking at 200rpm. Stimulation in growth with additional formate cannot be seen. The data are the average of triplicate cultures with error bars showing SD.

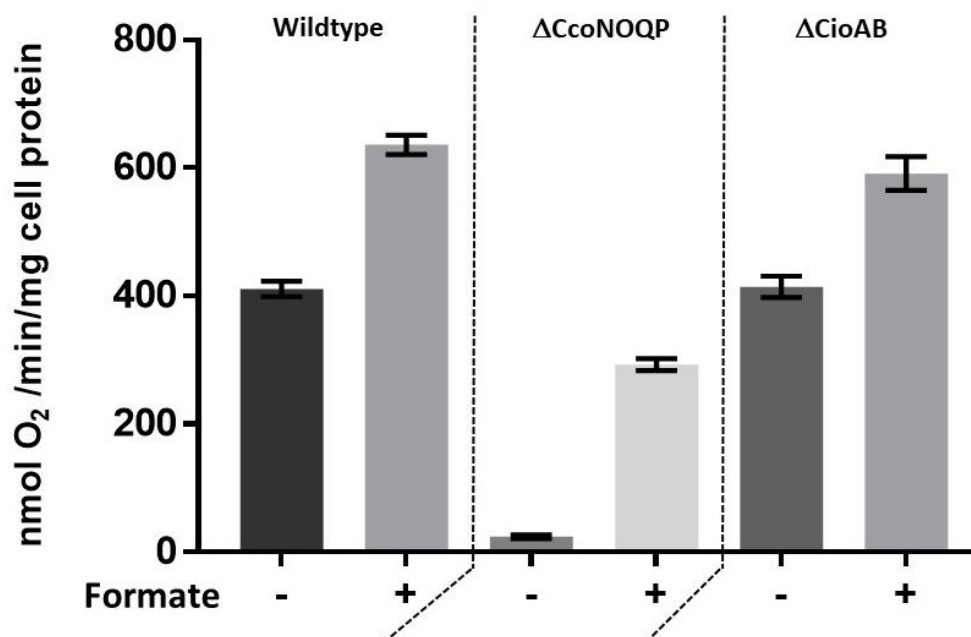


Figure 3.17: Cytochrome *c* oxidase activity of wildtype, Δ CcoNOQP and Δ CioAB with TMPD and Formate as electron donors. Cytochrome *c* oxidase activity measured with ascorbate/TMPD without (-) and with (+) 20mM Formate as electron donor (according to section 2.11). Wildtype, Δ ccoNOQP and Δ cioAB cells were grown in Mueller-Hinton medium. The data are the average of triplicate cultures with error bars showing SD. Formate can be seen stimulating the oxidase activity via both oxidases.

3.2.8 Cu sensitivity of growth of putative Cco assembly mutants:

As mentioned in section 3.1, it is important to know whether absence of potential assembly proteins has any effect on growth of cells in varying amounts of Cu as they are potentially involved in copper insertion into Cco and Cco activity is important for the normal growth of *C. jejuni*. It is also important to determine the maximum amount of Cu that can be added without making it toxic to the bacterial cells. Therefore, a Cu sensitivity assay was done (section 2.10.1). Cu can affect growth of these mutants in two potential ways, either these proteins are involved in intracellular Cu homeostasis, in which case the mutants will show poorer growth with respect to WT as Cu concentrations are increased, or these proteins are involved in Cco assembly and in their absence added Cu is interacting with CcoN directly (Trasnea et al., 2016), in which case added Cu might stimulate growth in the mutant (up to a point where Cu will become absolute toxic). In the latter case, there may be a growth defect in mutants with no added Cu.

WT and $\Delta cj0908-cj0911$ cells were grown in MHS complex media as described in section 2.3.1 up to mid exponential phase and back diluted to $OD_{600}=0.1$ in equilibrated 5ml MHS complex media in 6-well plates with varying concentration of added Cu (Cu solution made as described in section 2.10.1) as shown in figure 3.18. The cells were grown overnight as described in section 2.10.1 and final growth was measured according to section 2.3.6.

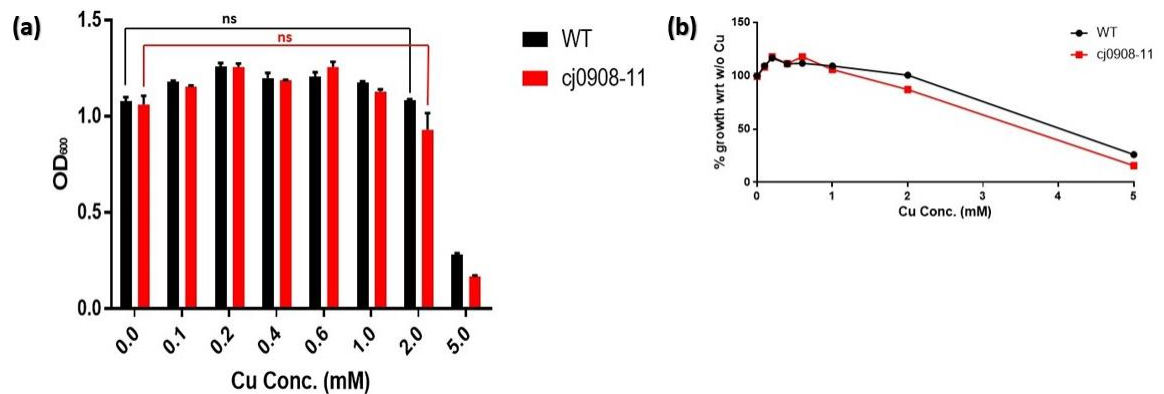


Figure 3.18: Cu sensitivity assay for putative CcO assembly mutants. (a) WT and $\Delta cj0908-cj0911$ cells were grown at different concentrations of $CuSO_4$ (0, 0.1, 0.2, 0.4, 0.6, 1.0, 2.0 and 5.0 mM) in Mueller-Hinton medium (section 2.3.1) until stationary phase and the final ODs were measured (section 2.3.6). (b) Growths at different concentrations of Cu normalised with growth without Cu being the control, i.e. 100%. The data are the average of triplicate cultures with error bars showing SD. T-tests were performed to check significance in difference. ($p>0.05$, ns; $0.05>p>0.01$, *; $0.01>p>0.001$, **; $0.001>p>0.0001$, ***; $0.0001>p$, ****)

Figure 3.18 showed that the $\Delta cj0908-cj0911$ operon mutant is insensitive to varying amount of Cu with respect to WT. This suggests that proteins encoded by components of $cj0908-cj0911$ operon are probably not involved in intracellular Cu homeostasis. There is no growth defect at no added Cu so the second case cannot be rejected. There is some stimulation in growth on adding up to 0.2 mM of Cu in both wild-type and mutant. This can be due to the lack of the optimum amount of Cu in unsupplemented MHS medium. Results also showed that adding more than 2 mM Cu is toxic for the bacterial cells but up to ~1 mM Cu has no significant toxicity.

3.2.9 Putative CcO assembly mutants show reduced, but not abolished Cytochrome *c* Oxidase activity:

CcoNOQP is a metalloprotein which needs Cu(I) to be assembled in CcoN subunit for its function and assembly of Cu(I) needs a system of Cu chaperones and

thioredoxins for transportation and reduction. Therefore, absence of any of these proteins should have an adverse effect on *ccb3*-type cytochrome *c* oxidase activity, which can be measured. In *C. jejuni*, proteins encoded by the operon *cj0908-cj0911* are potentially responsible for Cu(I) insertion in CcoN, the mutants made by knocking out these genes should have lower or perhaps no cytochrome *c* oxidase activity. Therefore, the cytochrome *c* oxidase activities of $\Delta cj0908-cj0911$ and $\Delta cj0911$ were measured (section 2.11) to compare them to CcO activity in wildtype cells. A *ccoNOQP* deletion mutant was used as a negative control.

WT, $\Delta cj0908-cj0911$ and $\Delta cj0911$ cells were grown in MHS complex medium as described in section 2.3.1 without any added copper (ICP-MS analysis showed this medium contains approx. 0.05 μ M copper) and also with copper added to 0.6 mM (an excess but non-toxic level; see Fig. 3.20) and with MH medium plus 20 μ M of BCS which is a specific copper II chelator (see 3.1 for explanation). Fresh cells harvested at mid exponential phase (as established by section 3.2.5) were used for measuring CcO activity with ascorbate and TMPD as electron donor (according to section 2.11)

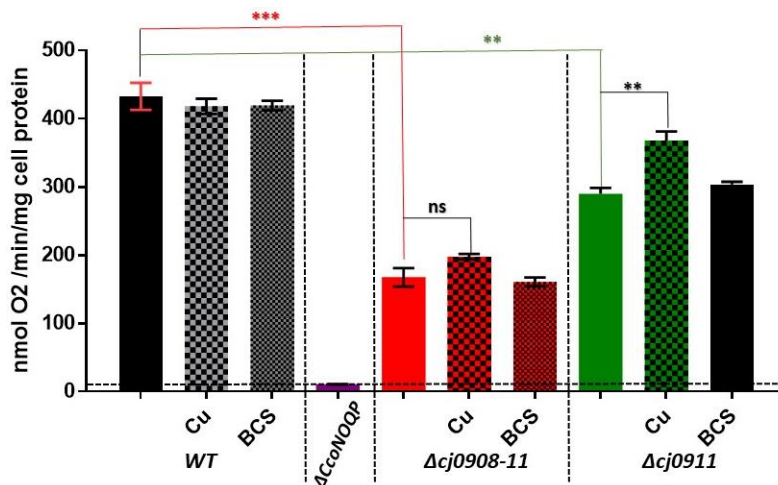


Figure 3.19: Cytochrome *c* oxidase activity of assembly mutants. Cytochrome *c* oxidase activity measured with ascorbate/TMPD as electron donor (according to section 2.11). Wildtype, $\Delta ccoNOQP$, $\Delta cj0908-cj0911$ and $\Delta cj0911$ cells were grown in Mueller-Hinton medium without any added copper (ICP-MS analysis showed this medium contains approx. 0.05 μ M copper) and also with copper added to 0.6 mM (an excess but non-toxic level; see Fig. 3.20) and with MH medium plus 20 μ M of BCS which is a specific copper II chelator (section 2.3.1). The data are the average of triplicate cultures with error bars showing SD. T-tests were performed to check significance in difference. ($p > 0.05$, ns; $0.05 > p > 0.01$, *; $0.01 > p > 0.001$, **; $0.001 > p > 0.0001$, ***; $0.0001 > p$, ****)

The data in Figure 3.19 shows that products of gene operon *cj0908-cj0911* and *cj0911* are clearly affecting cytochrome c oxidase activity. As expected, there is no activity in the *ccoNOQP* deletion mutant. In the Δ *cj0908-cj0911*, activity is highly reduced (over 50% lower activity) but was not abolished, suggesting that these gene products are involved in CcO assembly but are not essential. Cu may be able to insert into CcoN to an extent without additional proteins or assembly occurs by some alternate pathway as well. In the Δ *cj0911* mutant, lacking the Sco1 homologue, activity is reduced but not as much as in the entire operon mutant, showing the importance of the other gene products in Cu assembly. A significant stimulation in activity on adding excess Cu suggests a direct involvement of Cj0911 with handling Cu. No significant effect of the copper chelator BCS could be demonstrated in these experiments.

3.2.10 *ccoG*, *ccoH* and *ccoI* mutants showed a growth defect with *ccoI* being Cu sensitive:

For the reasons described in section 3.2.7, Cu sensitivity assay was performed with wildtype and Δ *cj1154c*, Δ *cj1155c*, Δ *cj0369c* and Δ *cj1483c* strains in the same way as in section 3.2.7.

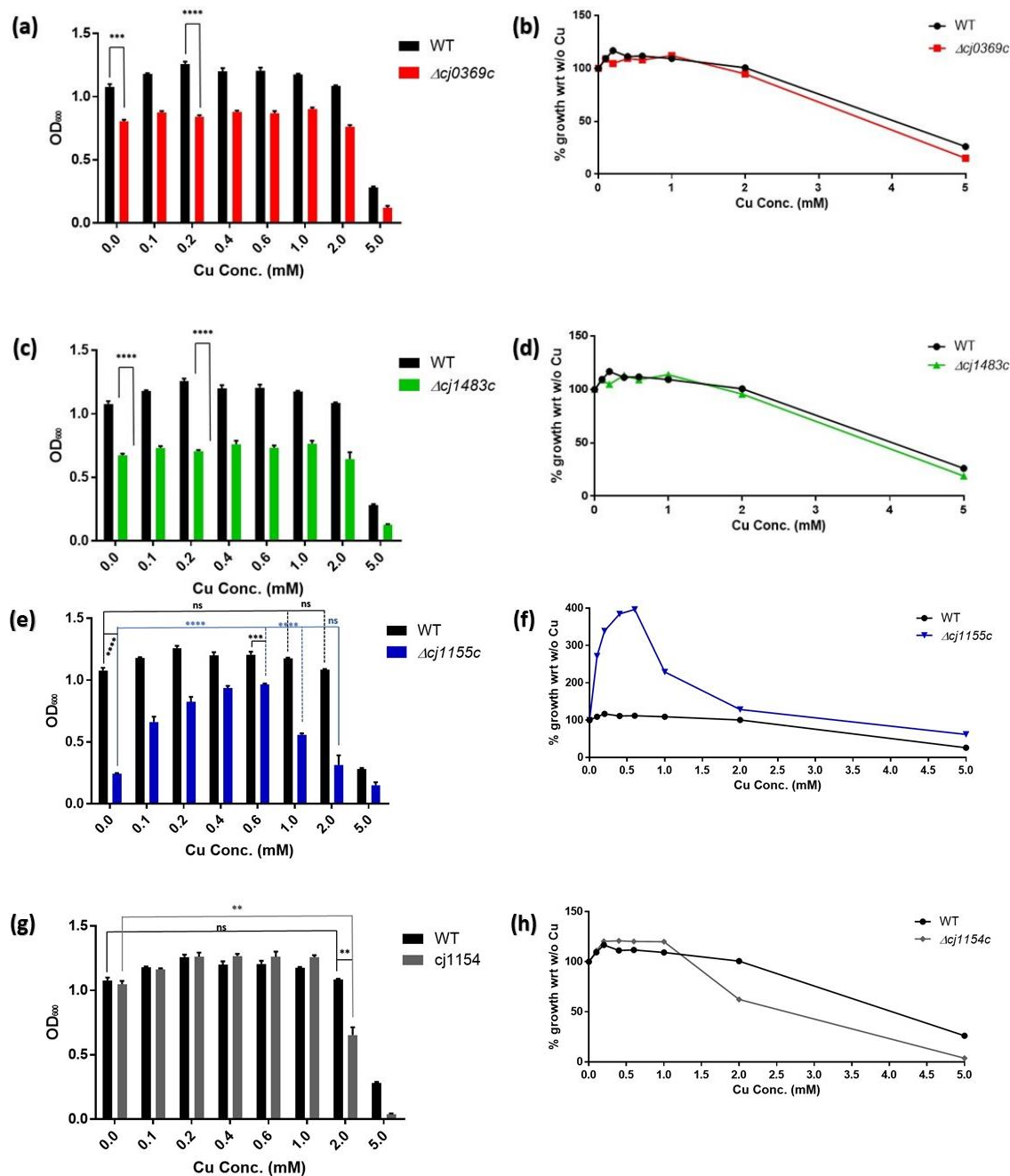


Figure 3.20: Cu sensitivity assay for *ccoGHIS* mutants. WT, $\Delta cj0369c$ (a); $\Delta cj1483c$ (c); $\Delta cj1155c$ (e); and $\Delta cj1154c$ (g) cells shown were grown at different concentrations of CuSO₄ (0, 0.1, 0.2, 0.4, 0.6, 1.0, 2.0 and 5.0 mM) in Mueller-Hinton medium (section 2.3.1) until stationary phase and the final ODs were measured (section 2.3.6). $\Delta cj0369c$ (b); $\Delta cj1483c$ (d); $\Delta cj1155c$ (f); and $\Delta cj1154c$ (h) grown at different concentrations of Cu normalised with growth without Cu being the control, i.e. 100%, respectively. The data are the average of triplicate cultures with error bars showing SD. T-tests were performed to check significance in difference. ($p > 0.05$, ns; $0.05 > p > 0.01$, *; $0.01 > p > 0.001$, **; $0.001 > p > 0.0001$, ***; $0.0001 > p$, ****)

The assay (Fig. 3.20) showed that the cells lacking Cj1155 (CcoI homolog) have a large growth defect but are highly sensitive to varying Cu concentrations. Increases in Cu concentration up to 0.6 mM can almost substitute for the absence of the *cj1155c* gene product, giving high final cell densities, consistent with its suggested role as a copper translocator. It probably delivers copper directly to the assembly proteins to be transported to CcoN. Cells lacking Cj1154 (CcoS homolog) don't have a growth defect but are sensitive to Cu at concentrations above 1 mM. Cells lacking Cj0369 and Cj1483 proteins (CcoG and CcoH homologue respectively) showed a consistent growth defect but are insensitive to varying copper concentration compared to WT, except perhaps a very slight effect at 2-5 mM Cu. The fact that $\Delta cj0369c$ and $\Delta cj1483c$ mutants have a consistent growth defect irrespective of Cu concentration is possibly because *cj0369c* and *cj1483c* gene products are necessary for normal functioning of cytochrome *c* oxidase, which is in turn necessary for normal growth of the bacterial cells. This assay also showed that the maximum amount of excess Cu is 0.6 mM, which is non-toxic and can be consistently used with all strains of *C. jejuni* while growing them for measuring CcO activity.

3.2.11 Cells lacking CcoGHIS show reduced or abolished Cytochrome *c* Oxidase activity:

As mentioned in section 3.1, CcoGHIS proteins are necessary for normal Cytochrome *c* oxidase activity in other bacteria and in *C. jejuni*, *cj0369c*, *cj1483c*, *cj1155c* and *cj1154c* potentially encodes CcoG, CcoH, CcoI and CcoS proteins, respectively. Therefore, cells lacking *cj0369c*, *cj1483c*, *cj1155c* and *cj1154c* gene products should have reduced or abolished CcO activity. WT, $\Delta cj0369c$, $\Delta cj1483c$, $\Delta cj1155c$ and $\Delta cj1154c$ cells were grown and harvested as described in section 3.2.8. CcO activity of knock out mutants was measured with ascorbate and TMPD as electron donor (section 2.11) to compare it to CcO activity in wildtype cells. *ccoNOQP* deletion mutant was used as a control.

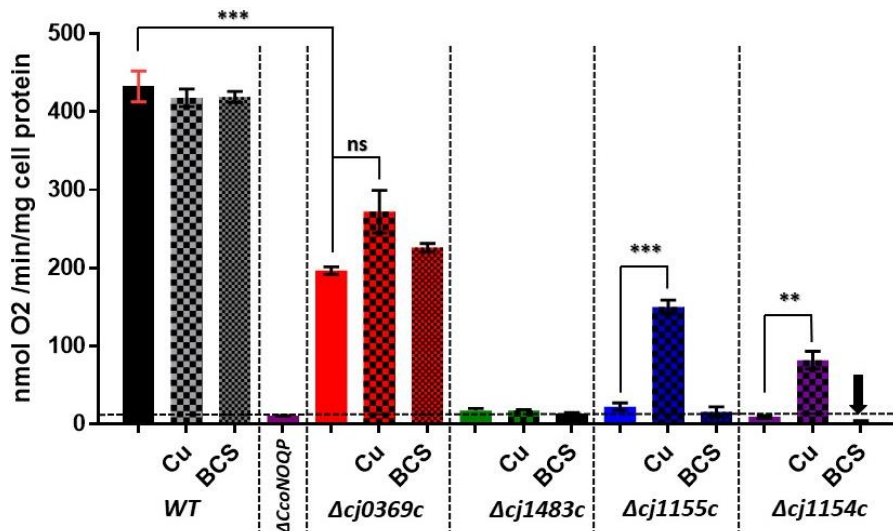


Figure 3.21: Cytochrome *c* oxidase activity of *ccoGHIS* mutants. Cytochrome *c* oxidase activity measured with ascorbate/TMPD as electron donor (according to section 2.11). Wildtype, $\Delta ccoNOQP$, $\Delta cj0369c$, $\Delta cj1483c$, $\Delta cj1155c$ and $\Delta cj1154c$ cells were grown in Mueller-Hinton medium without any added copper (ICP-MS analysis showed this medium contains approx. 0.05 μ M copper) and also with copper added to 0.6 mM (an excess but non-toxic level; see Fig. 3.21) and with MH medium plus 20 μ M of BCS which is a specific copper II chelator (section 2.3.1). The data are the average of triplicate cultures with error bars showing SD. T-tests were performed to check significance in difference. ($p > 0.05$, ns; $0.05 > p > 0.01$, *; $0.01 > p > 0.001$, **; $0.001 > p > 0.0001$, ***; $0.0001 > p$, ****)

The data in Figure 3.21 shows that products of genes *cj0369c*, *cj1483c*, *cj1155c* and *cj1154c* are clearly affecting cytochrome *c* oxidase activity. As expected, there is no activity in the *ccoNOQP* deletion mutant. In the *cj0369c* deletion mutant, lacking the *ccoG* homologue, activity is reduced by ~30% and is not stimulated by adding excess Cu. Reduction in activity but not abolition suggest that it's not necessary for the biogenesis or maturation of CcoNOQP complex and no significant difference on adding excess Cu indicates that it's not assembling Cu as Cu assembly proteins are only required in limited Cu condition. Along with these, presence of thioredoxin motif suggest that Cj0369 may be acting as a thioredoxin, which reduce Cu to be assembled to CcoNOQP. In the *cj1483c* deletion mutant, the putative *ccoH* homologue, there is no oxidase activity at all and also there is no effect on adding excess copper, suggesting an absolutely essential role in activity or biogenesis of *ccoNOQP* subunits. In *cj1155c* and *cj1154c* deletion mutants, lacking the *ccoI* and *ccoS* homologues respectively, there is no oxidase activity after growth in standard media but a significant stimulation in activity was found after growth with excess

copper, which suggests their potential involvement in copper supply to CcoNOQP. CcoI is thought to be a copper pump (Fig. 3.20); adding excess copper in the medium may thus circumvent its deletion.

3.2.12 Effect of *cj0908-11* operon, *cj1154c* and *cj1155c* deletion on biogenesis of cytochrome *c* oxidase subunits:

I wanted to find out how mutation of the putative assembly genes was affecting individual subunits of the oxidase. Heme blotting (section 3.2.12.1) only detects covalently bound heme and so can be used to look at the C-heme containing subunits CcoP and CcoO. This will tell us whether CcoP and CcoO subunits are produced in the assembly mutants or not. Size of CcoP is 31.17 kDa and CcoO is 24.95 kDa. As Heme blotting only detects covalently bound heme, it cannot be used to detect CcoN subunit (which has a non-covalently bound b-type heme). Therefore, carbon monoxide difference spectroscopy (section 3.2.12.2) was used to detect the CcoN subunit in cells as CO binds to the active site Cu/b-heme centre in CcoN. CO-binding *b*-type haems show a feature at about 560 nm in CO-reduced *minus* reduced spectra. CcoN is the only Cu containing protein which is in abundance in the inner membrane. Furthermore, the amount of Cu in the total membrane fractions of strains lacking CcoN should be lower than that of wildtype and this can be measured by Inductively Coupled Plasma Mass Spectrometry (ICP-MS) (section 3.2.12.3).

3.2.12.1 Deletion of *cj0908-11* operon, *cj1154c* and *cj1155c* does not affect biogenesis of the CcoO subunit of cytochrome *c* oxidase:

This experiment was done using total membrane preparations of wild-type, Δ *ccoNOQP*, Δ *ccoNOQP*^{+/+}, Δ *cj0908-cj0911*, Δ *cj1154c* and Δ *cj1155c* cells. Total membrane preparations were made as described in section 2.7.3 and total membrane protein concentration was measured by Lowry assay (section 2.7.5). Loading samples were prepared according to section 2.15 and equivalent to 20 µg of total membrane protein were loaded in each well of 10% SDS-PAGE. Heme blotting was performed as detailed in section 2.15. Coomassie stained gel was used to ensure similar amount of protein in loading samples.

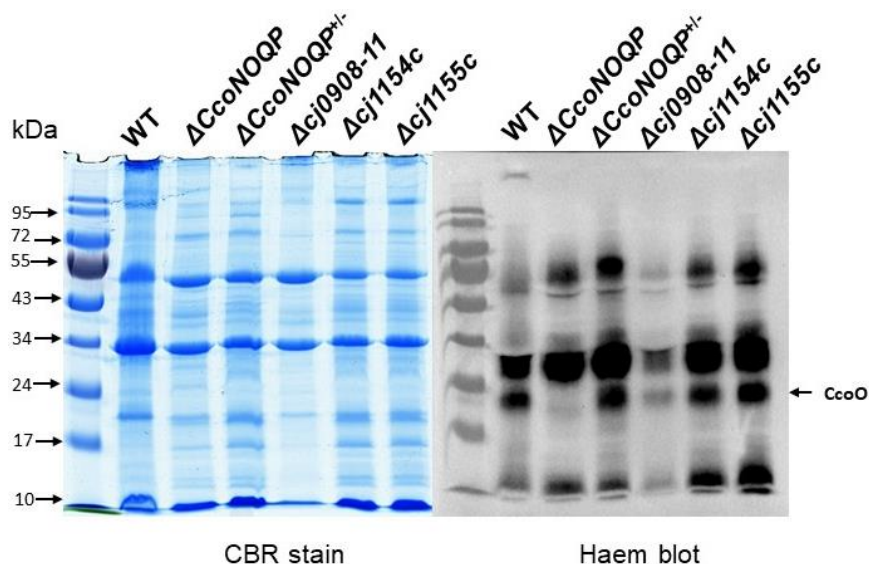


Figure 3.22: Total Membrane Heme Blot. Heme-associated peroxidase activity was detected using the standard enhanced chemiluminescence kit (section 2.15). Loading samples (section 2.15), consisting of 20 μ g of total membrane protein of wild-type, $\Delta ccoNOQP$, $ccoNOQP^{+/-}$, $\Delta cj0908-cj0911$, $\Delta cj1154c$ and $\Delta cj1155c$ (section 2.7.3), were mildly denatured in the absence of mercaptoethanol to preserve attachment of C-hemes to Cys residues and were loaded on 10% SDS-PAGE. CcoO band is missing in $\Delta ccoNOQP$ only. Unable to see CcoP because of intense bands of a similar size.

The heme blot clearly shows that deletion of *cj0908-11* operon, *cj1154c* or *cj1155c* does not affect biogenesis of the CcoO cytochrome c subunit of cytochrome-*c*-oxidase, supporting their specific role in assembly of the Cu containing CcoN subunit. Fainter band of CcoC in $\Delta cj0908-11$ lane is because of less amount of protein in its loading sample, which is also confirmed by Coomassie stained gel. Unfortunately, the CcoP subunits are not visible because of intense bands of other cytochromes at their potential position on the gel.

3.2.12.2 Attempts at Carbon monoxide difference spectroscopy to detect the active site Cu/b-heme centre in CcoN

This experiment was done using total membrane preparations of wild-type, $\Delta ccoNOQP$, $\Delta cj0908-cj0911$, $\Delta cj1154c$ and $\Delta cj1155c$ cells. Total membrane preparations were made as described in section 2.7.3 and total membrane protein concentration was measured by Lowry assay (section 2.7.5). 1 ml of 10 μ g/ml protein sample was used to measure spectra as detailed in section 2.16. CO-binding *b*-type haems should show a feature at about 560 nm in CO-reduced *minus* reduced spectra.

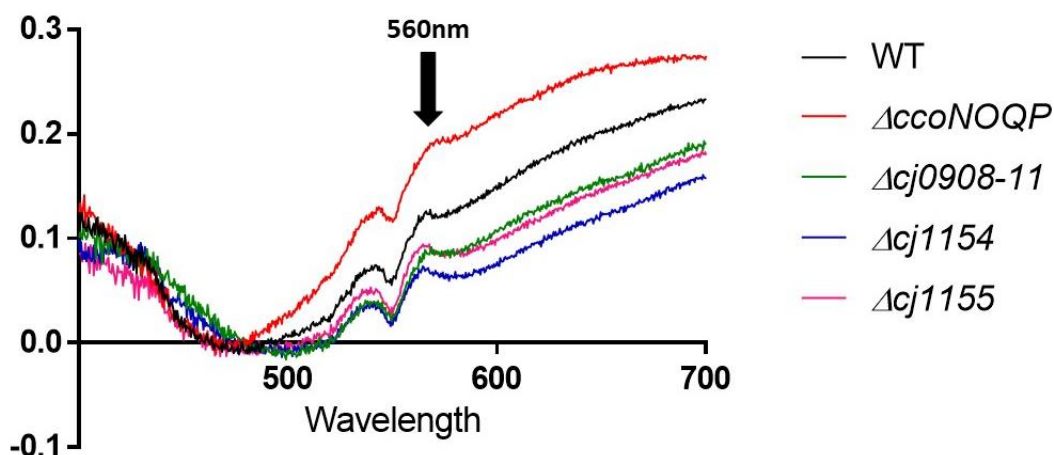


Figure 3.23: Carbon monoxide difference spectroscopy. Total membrane proteins of wild-type, $\Delta ccoNOQP$, $\Delta cj0908-cj0911$, $\Delta cj1154c$ and $\Delta cj1155c$ cells were reduced with sodium dithionite, a spectrum recorded and then the sample reacted with carbon monoxide by bubbling through the sample. The positive going feature at 560 nm may represent the CO-heme b adduct in the CcoN subunit but further confirmation will be necessary.

In wildtype, a peak near 560 nm was observed that was shifted in the CcoNOQP deletion mutant, but little difference was observed for the other mutants (Fig. 3.23). It is difficult to conclude from this if CcoN assembly is being affected or not, as the oxidase deletion mutant still showed the feature.

3.2.12.3 Inductively coupled plasma mass spectrometry was inconclusive:

500ml of Wild-type, $\Delta ccoNOQP$, $\Delta ccoNOQP^{+/+}$, $\Delta cj0908-cj0911$, $\Delta cj1154c$ and $\Delta cj1155c$ cultures were grown to make the *C. jejuni* cell free extracts (section 2.7.1) and metal contaminations were removed according to section 2.7.2. The total membrane protein fractions were prepared from these metal-free cell free extracts according to section 2.7.3 and were used to make the ICP-MS samples (section 2.8). The protein concentration was measured just before adding nitric acid by Lowry assay (section 2.7.5). Handling of the samples was done to try to keep them as metal free as much as possible (used new salts, glass spatulas, etc.).

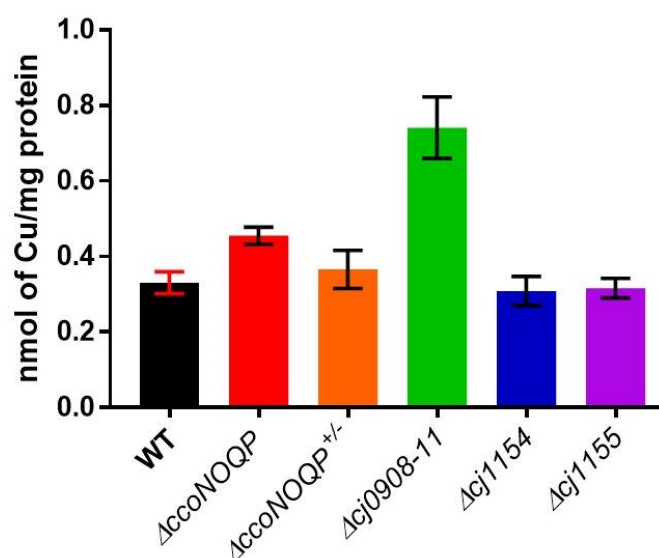


Figure 3.24: Inductively coupled plasma mass spectrometry of total membrane protein fractions. Amount of Cu per milligram protein of total membrane protein fractions of wild-type, $\Delta ccoNOQP$, $\Delta ccoNOQP^{+/-}$, $\Delta cj0908-cj0911$, $\Delta cj1154c$ and $\Delta cj1155c$. No consistent difference can be seen, potentially because of presence of metal contamination in ICP-MS samples.

Results were calculated in terms of n moles of Cu per mg of protein in samples. The data (Fig. 3.24) showed that the amount of Cu in total membrane protein fractions of $\Delta ccoNOQP$, $\Delta ccoNOQP^{+/-}$, $\Delta cj1154c$ and $\Delta cj1155c$ is similar to that of wildtype, unlike $\Delta cj0908-cj0911$, which surprisingly showed higher amount of Cu. Total membrane protein fraction of $\Delta ccoNOQP$ having amount of Cu equal to wildtype is only possible if the samples are contaminated with Cu as this is thought to be the only major Cu containing protein complex in the inner membrane.

3.2.12.4 Attempt to detect CcoN using western blot:

The anti-bodies raised against CcoN in *Rhodobacter* were used for detecting CcoN in *C. jejuni* wild-type, $\Delta ccoNOQP$, $\Delta ccoNOQP^{+/-}$, $\Delta cj0908-cj0911$, $\Delta cj1154c$ and $\Delta cj1155c$ strains using western blotting (section 2.18). 20 μ g of inner membrane proteins (section 2.7.4) were used to make loading samples (section 2.14) and were separated by 10% SDS-PAGE (section 2.14).

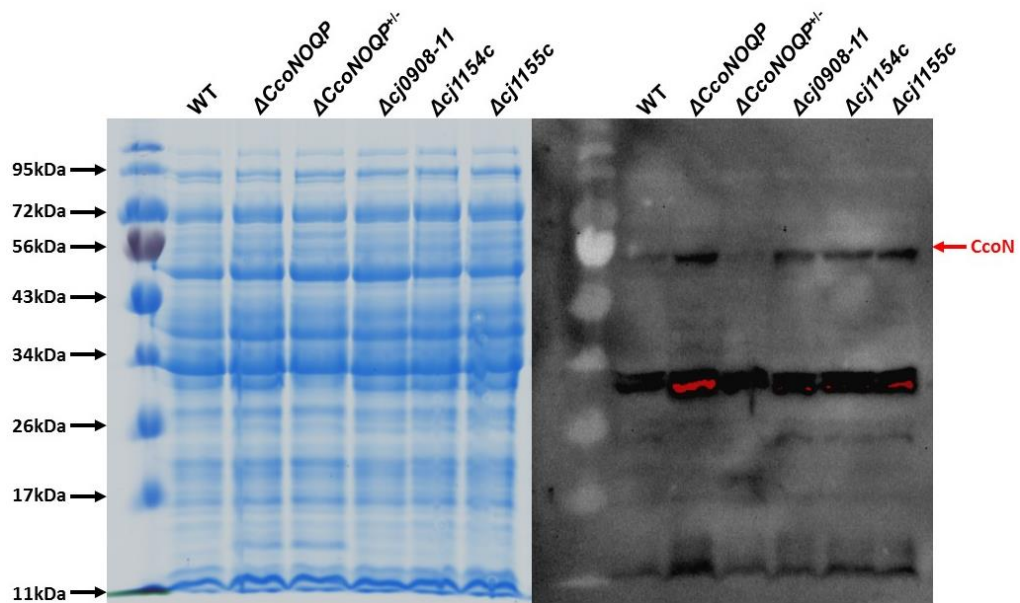


Figure 3.25: Western blot for CcoN. Antibodies against *Rhodobacter* CcoN were used as primary antibodies and anti-mouse HRP conjugate were used as secondary antibodies. Loading samples (section 2.15), consisting of 20 μ g of total membrane protein of wild-type, Δ *ccoNOQP*, Δ *ccoNOQP*^{+/-}, Δ *cj0908-cj0911*, Δ *cj1154c* and Δ *cj1155c* (section 2.7.3), were denatured with β mercaptoethanol and were loaded on 10% SDS-PAGE. Unable to see anything.

Despite multiple attempts, no specific band corresponding to CcoN can be seen, as a band of similar size is present in the oxidase deletion mutant (Fig. 3.25). This suggests that the antibodies raised against CcoN in *Rhodobacter* do not bind to CcoN in *C. jejuni*.

3.2.13 Cu toxicity assay showed that cells lacking Cj1485 and Cj1486 are more sensitive to Cu with Δ *cj1486c* having a permanent growth defect:

A Cu sensitivity assay was performed with wildtype, Δ *cj1486c* and Δ *cj1485c* cells in the same way as in section 3.2.7.

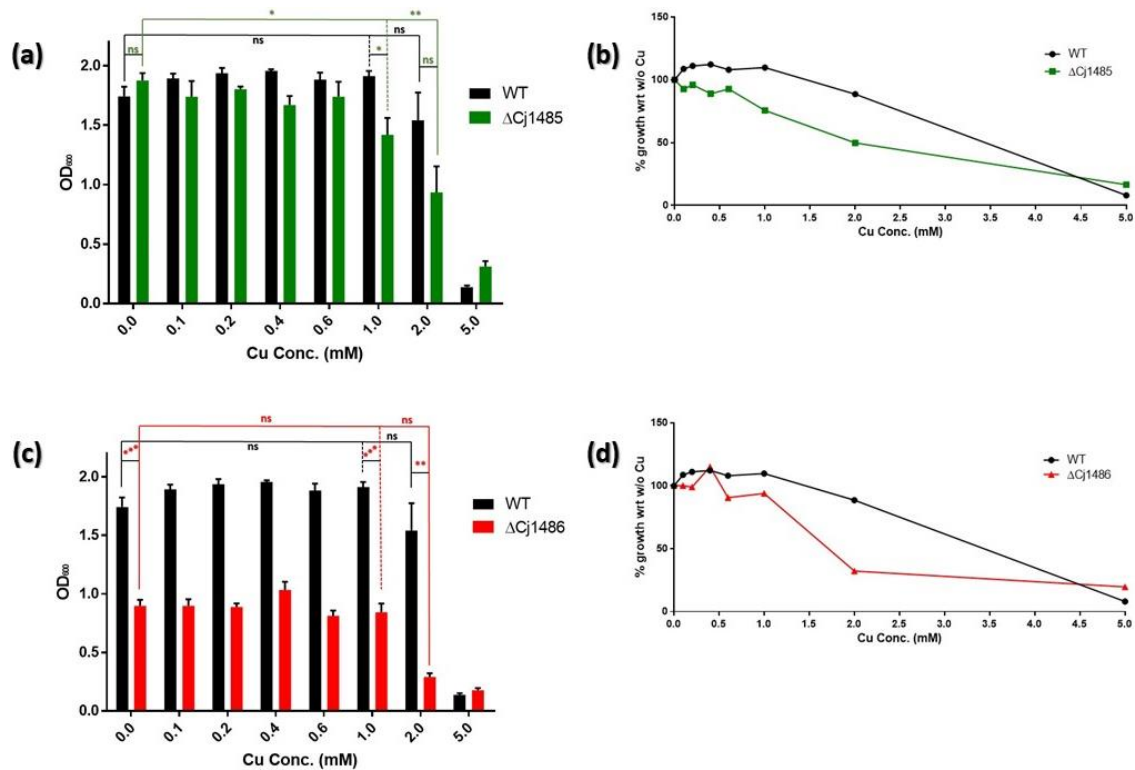


Figure 3.26: Cu sensitivity assay for $\Delta cj1486c$ and $\Delta cj1485c$ mutants. (a) WT and $\Delta cj1485c$; and (c) WT and $\Delta cj1486c$ cells shown were grown at different concentrations of CuSO₄ (0, 0.1, 0.2, 0.4, 0.6, 1.0, 2.0 and 5.0 mM) in Mueller-Hinton medium (section 2.3.1) until stationary phase and the final ODs were measured (section 2.3.6). (b) WT and $\Delta cj1485c$; and (d) WT and $\Delta cj1486c$ cells grown at different concentrations of Cu normalised with growth without Cu being the control, i.e. 100%. $\Delta cj1486c$ has a permanent growth defect and insensitive to Cu. $\Delta cj1485c$ is more Cu sensitive after 0.1 mM Cu. The data are the average of triplicate cultures with error bars showing SD. T-tests were performed to check significance in difference. ($p > 0.05$, ns; $0.05 > p > 0.01$, *; $0.01 > p > 0.001$, **; $0.001 > p > 0.0001$, ***; $0.0001 > p$, ****)

The assay (Fig. 3.26) showed that cells lacking *cj1485c* gene product does not have a growth defect but became more sensitive to Cu with respect to wildtype above 0.1 mM Cu. The $\Delta cj1486c$ has a definite growth defect and showed more sensitivity to Cu than wildtype above ~1 mM Cu. These data suggest that these genes may be involved in normal bacterial growth and Cu sensitivity of *C. jejuni*, including *cbb3*-type cytochrome *c* oxidase activity, which is tested in the next section.

3.2.14 Mutants lacking genes between *ccoP* and potential *ccoH* showed reduced or abolished CcO activity:

To see whether *cj1486c*, *cj1485c*, *cj1484c* and *cj1482c* gene products have any role in the cytochrome *c* oxidase activity of *C. jejuni*, *cj1486c*, *cj1485c*, *cj1484c* and *cj1482c* knock out mutants were made and their CcO activity was measured and compared with CcO activity of wildtype. Wildtype, $\Delta cj1486c$, $\Delta cj1485c$, $\Delta cj1484c$ and $\Delta cj1482c$ cells were grown and harvested as described in section 3.2.8. *ccoNOQP* deletion mutant was used as a control.

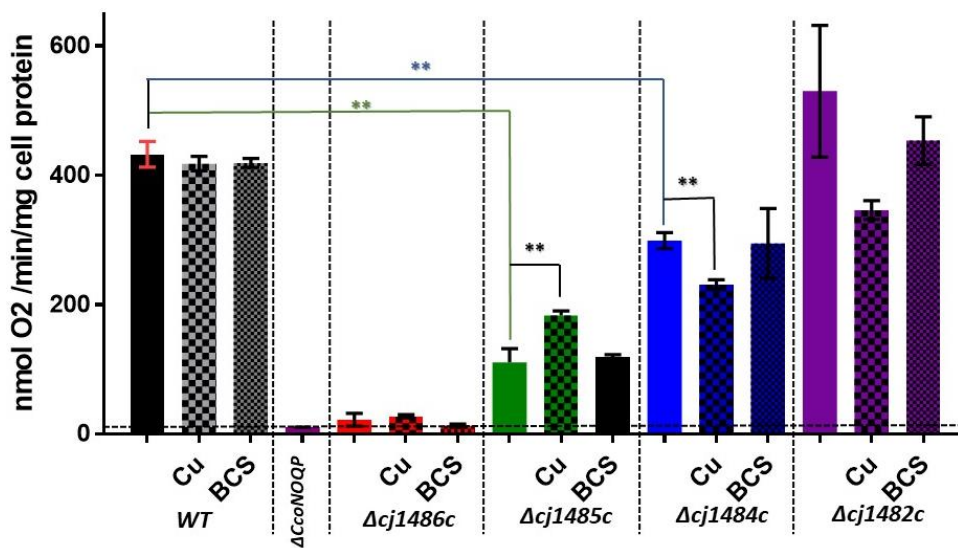


Figure 3.27: Cytochrome *c* oxidase activity of *cj1486c*, *cj1485c*, *cj1484c* and *cj1482c* mutants. Cytochrome *c* oxidase activity measured with ascorbate/TMPD as electron donor (according to section 2.11). Wildtype, $\Delta ccoNOQP$, $\Delta cj1486c$, $\Delta cj1485c$, $\Delta cj1484c$ and $\Delta cj1482c$ cells were grown in Mueller-Hinton medium without any added copper (ICP-MS analysis showed this medium contains approx. 0.05 μ M copper) and also with copper added to 0.6 mM (an excess but non-toxic level; see Fig. 3.18) and with MH medium plus 20 μ M of BCS which is a specific copper II chelator (section 2.3.1). The data are the average of triplicate cultures with error bars showing SD. T-tests were performed to check significance in difference. ($p > 0.05$, ns; $0.05 > p > 0.01$, *; $0.01 > p > 0.001$, **; $0.001 > p > 0.0001$, ***; $0.0001 > p$, ****)

The results (Fig. 3.27) showed that products of gene *cj1484c*, *cj1485c* and *cj1486c* are clearly affecting cytochrome *c* oxidase activity, unlike *cj1482c* gene product. This is interesting because of the fact that *cj1484c*, *cj1485c* and *cj1486c* are the only genes sandwiched between *ccoP* and *ccoG*, and are in place where *ccoH*, *ccoI* and *ccoS* should be. In the $\Delta cj1484c$, CcO activity is reduced by approx. 30%

and is not stimulated by excess Cu. This suggests a potential role in assembly/activity of CcO. In the *cj1485c* deletion mutant, the gene next to *ccoP*, activity is reduced but there is a (non-significant) slight stimulation in activity on adding excess Cu which might suggest its potential involvement in oxidase biogenesis. Finally, and perhaps most surprisingly, in the *cj1486c* deletion mutant, also next to *ccoP*, oxidase activity is abolished and also there is no effect on adding excess copper. To be sure that this result was not just an artefact of *ccoP* gene being affected while knocking out *cj1486c*, Δ *cj1486c* strain was checked for intact *ccoP* by running colony PCR for *ccoP* (Fig. 3.12), which showed the gene was intact. Given the genomic position of *cj1485c* and *cj1486c*, this study hypothesise that the proteins they encode might be part of the oxidase complex itself.

3.3 Disussion:

The aim of this study was to obtain a deeper understanding of the assembly of *cbb3*-type cytochrome *c* oxidase and factors affecting the formation of active CcoNOQP complex, an important virulence factor, in *C. jejuni* NCTC 11168. This study attempted to characterise genes encoding proteins that might be essential for assembly of cytochrome *c* oxidase complex, its activity and transport of Cu to the heme-Cu_B binuclear centre of *cbb3*-type Cco. For this, mutant strains of *C. jejuni* NCTC 11168 knocking out genes encoding proteins of interest were made. Appropriate assays were done to compare properties of these mutant strains with the wild type cells to analyse the effects of missing protein on bacterial cells.

It was already established that *C. jejuni* cells lacking cytochrome *c* oxidase had a micro aerobic growth defect compared to wildtype (Liu and Kelly, 2015) which indicated the necessity of Cco activity for normal growth. But the decrease of cytochrome *c* oxidase activity (per mg protein) rapidly with the culture growth is a surprising phenomenon which is difficult to explain with the current knowledge about effect of cytochrome *c* oxidase activity on *C. jejuni* growth. This phenomenon has never been reported in any other organism yet. The possibility that the dissolved oxygen in the medium is becoming limiting with cultural growth and affecting the expression of the oxidase is rejected by section 3.2.6, showing that the Cco activity is not regulated by oxygen availability. Another possibility is Cco activity per viable cell protein is same but while measuring the amount of protein in the samples, the dead

cells were also contributing, making the Cco activity per mg protein lower. After many failed attempts to get the consistent Cco activity for any strain, this finding gave me the insight to be consistent with the cultural growth while harvesting the cells in mid exponential phase, not only for measuring the Cco activity but for every assay.

As expected, any stimulation in growth of *C. jejuni* 11168 on adding 10 mM excess formate was not found (Fig. 3.16), contrary to the stimulation reported in 81-176 strain (Kassem *et al.*, 2017). It was also observed that formate is, in fact, stimulating oxidase activity in all three (WT, Δ CcoNOQP and Δ CioAB) types of cells with ascorbate/TMPD, unlike the inhibition reported in 81-176 strain by Kassem *et al.* (2017). In fact, the formate activity in cells just having the *cbb*₃-type cytochrome *c* oxidase is almost equal to its activity in wild type cells having both oxidases. This suggests that formate is not inhibiting activity of *cbb*₃-type cytochrome *c* oxidase at all. On the other hand, the formate activity in cells just having the *bd*-type CioAB quinol oxidase is much lower than in other two strains, suggesting that formate mediates *cbb*₃-type cytochrome *c* oxidase activity more efficiently than *bd*-type CioAB quinol oxidase activity. These results supports our initial theory that electrons donated by formate to the quinone pool helps the oxidase activity in microaerobic conditions, not inhibits it and if a compound inhibits the *cbb*₃-type cytochrome *c* oxidase activity, it cannot stimulate the *C. jejuni* 11168 growth as *cbb*₃-type cytochrome *c* oxidase activity is essential for optimum growth (Liu *et al.*, 2013).

In *C. jejuni*, *cj0911* encodes a protein homologous to other bacterial ScoI proteins. In 2005, Banci *et al.* reported the presence of *scoI* genes with a common neighbouring gene of unknown function in eight different bacteria, including *B. subtilis*, with a conserved metal binding motif in the protein: H(M)X₁₀MX₂₁HXM. Later that gene of unknown function was termed as PCu_AC and recognised as the bacterial gene equivalent to mitochondrial Cox17. In *C. jejuni*, *cj0909* is homologous to PCu_AC (69% identity). *cj0909* and *cj0911* forms an operon with *cj0908* and *cj0910* genes of unknown function. *cj0908* and *cj0910* have conserved thioredoxin motif: two vicinal cysteines in a CXXC motif. Presence of thioredoxins in operon containing the Cco assembly genes in Gram negative bacteria is in accordance with the fact that periplasm is a highly oxidised environment and Cco assembly need Cu to be in reduced form {Cu(I)}. The observation that Δ *cj0908-cj0911* growth was insensitive to different amounts of Cu showed that *cj0908-cj0911* gene products are not involved in

the overall intracellular Cu homeostasis. The Cco assembly proteins, SenC and PrrC, characterised in *Rhodobacter capsulatus* are crucial for maintaining intracellular Cu homeostasis as well (Trasnea *et al.*, 2016), which makes assembly proteins in *C. jejuni* distinct from already studied homologues. Both $\Delta cj0908-cj0911$ and $\Delta cj0911$ showed significantly reduced Cco activity indicating the crucial role of *cj0908-cj0911* gene products in Cco activity, which is consistent with the hypothesis that *cj0908-cj0911* gene products are potentially involved in assembly of Cco. There is more reduction of Cco activity in $\Delta cj0908-cj0911$ (~40% activity then of WT) than in $\Delta cj0911$ (~60% activity then of WT), suggesting the importance of *cj0908*, *cj0909* and *cj0910* gene products in activity, *cj0908* and *cj0910* being novel. One can argue that $\Delta cj0911$ still contains Cj0909 (PCu_AC homologue), which is assembling Cco rescuing the absence of Cj0911, unlike $\Delta cj0908-cj0911$. But assembly proteins are required by the bacteria under conditions of low copper availability only and excess of Cu in the medium rescues the absence of either PCu_AC or Sco1 or both (Trasnea *et al.*, 2016). When grown with excess Cu in medium, $\Delta cj0911$ showed stimulated Cco activity but there was no difference in $\Delta cj0908-cj0911$. This suggests that it is not just the absence of both PCu_AC and Sco1 homologues in $\Delta cj0908-cj0911$ but also the absence of *cj0908* and *cj0910* novel genes, which is affecting the Cco activity. Excess Cu in the medium is unable to rescue the absence of *cj0908* and *cj0910*, which is in accordance to the observation that they both contain a thioredoxin motif and are potentially reducing Cu(II) to Cu(I) in the oxidised environment of periplasm, making it suitable to be captured by *cj0909* and *cj0911* Cu chaperones to be delivered to the CcoN subunit. Cco assembly requires Cu in the reduced form for its ability to lose an electron and PCu_AC prefers Cu in Cu(I) form (Trasnea *et al.*, 2016). Homology, Cu sensitivity and Cco activity results gave the preliminary data that suggests that the $\Delta cj0908-cj0911$ gene products are involved in assembly of Cco in *C. jejuni* but they raised a few questions as well. For example, are Cj0908 and Cj0910 actually working as thioredoxins? If yes, what is the need for two such proteins? If both Cj0909 and Cj0911 participate in assembly of Cu center in Cco, are their functions unique or redundant? Further investigation needs to be done with purified proteins and individual mutants. For this the pET21a protein overexpression vectors have been designed for each individual protein with strepII-tag for purification but time constraints didn't allow us to further investigate them for this study.

Unlike most other *cbb₃*-type Cco containing bacteria which have *ccoGHIS* genes next to *ccoNOQP*, this study found potential *ccoGHIS* homologous genes scattered throughout the genome in *C. jejuni* (Fig. 3.2). This study of these genes in *C. jejuni* is focused on establishing their possible roles in oxidase assembly and activity. Cj0369 is a membrane bound protein, homologous to CcoG. Δ *cj0369c* has a growth defect which is expected in *C. jejuni* cells if their Cco activity is hindered. Δ *cj0369c* is not sensitive to Cu rejecting a role of Cj0369 in Cu homeostasis. Absence of Cj0369 reduced the Cco activity (by ~50%) but not as much as the absence of other proteins of the cluster (no activity). In *Rhodobacter capsulatus* too, deletion of CcoG had only minor effects on the activity of the *cbb₃*-type Cco (Kulajta *et al.*, 2005). The loss of activity wasn't rescued by growing cells with excess Cu in the medium suggesting Cj0369 is not handling Cu at any stage for Cco assembly. On the basis of homology, Cu sensitivity and Cco activity results, it can be said that Cj0369 is CcoG in *C. jejuni*. Cj1483 is a CcoH homologue based on BLAST searches. Δ *cj1483c* has a growth defect which is expected in *C. jejuni* cells if their Cco activity is hindered and is not sensitive to Cu rejecting role of Cj1483 in Cu homeostasis. Δ *cj1483c* has no Cco activity at all, irrespective of amount of Cu in the medium. This suggests that Cj1483 is absolutely essential for activity or biogenesis of CcoNOQP subunits. This observation is in accordance with the model suggested by Pawlik *et al.* (2010) in which biogenesis of *cbb₃*-type Cco proceeds via CcoQP and CcoNO subcomplexes in *R. capsulatus*, neither the fully assembled *cbb₃*-type Cco nor the CcoQP or CcoNO subcomplex was detectable in cells lacking CcoH. They also claimed that CcoH remains tightly associated with the active, fully assembled CcoNOQP complex.

Cj1155 has significant identity with Cu-translocating P-type ATPases. Δ *cj1155c* showed a large growth defect as well as high sensitivity to Cu. The growth defect is rescued by Cu when added up to 0.6 mM above which the Cu became toxic. Similarly, Δ *cj1155c* didn't show any Cco activity but the activity was partially rescued on growing cells with 0.6 mM excess Cu. This means that excess of Cu can partially substitute the absence of Cj1155. In *R. capsulatus*, the CcoNOQP complex was absent in strain lacking *ccoI* but CcoP was still detectable (Kulajta *et al.*, 2005). It is also possible that like CcoP, the other subunits, CcoN, CcoO and CcoQ were also produced but the CcoNOQP complex was unable to be assembled. One convincing reason can be unavailability of Cu as assembly of Cco needs Cu. That is why the

effect of the absence of Cj1155 was diminished on adding excess Cu. Given that Cj1155 is likely to be a Cu-translocating P-type ATPase, it may be transporting Cu from cytoplasm to periplasm to be transported to CcoN with the help of Cu chaperones for the assembly of CcoNOQP and while doing this it's also affecting the overall intracellular Cu homeostasis. Interestingly, Cj1155 is also similar to CtpA, a copper-translocating P1B-type ATPase, in *Rubrivivax gelatinosus*, which is homologous to (35 %) and reported to be CcoI-like (Hassani *et al.*, 2010). Like *cj1155c*, *ctpA* in *Rubrivivax gelatinosus* is not encoded next to *ccoNOQP* (Hassani *et al.*, 2010). *R. gelatinosus* cells lacking *ctpA* showed a growth defect, which was complemented with increasing the amount of Cu in the media (Hassani *et al.*, 2010), as in *C. jejuni*. Crucially, *ctpA* mutants not only showed reduced cytochrome *c* oxidase activity, which was partially restored by adding excess Cu in the media, but were also deficient in another Cu-requiring oxidase and also NosZ, a Cu-containing nitrous oxide reductase (Hassani *et al.*, 2010). CtpA is thus supplying copper for several periplasmic enzymes. The large growth defect and marked copper stimulation observed, suggests that Cj1155 in *C. jejuni* may be functionally similar to CtpA in *R. gelatinosus*. Further work is needed to determine if it also supplies copper to e.g. CueO and p19. Cj1154 is 97% identical to CcoS in *E. coli*. $\Delta cj1154c$ showed no growth defect but no Cco activity was detected in cells lacking Cj1154 (knock out mutant confirmed for intact *cj1155c*), which was surprising. Koch *et al.* (2000) reported the necessity of CcoS for the presence of heme *b*, heme *b*₃, and Cu_B cofactors of the CcoN subunit, which explains the absence of Cco activity in $\Delta cj1154c$. In *R. capsulatus* cells lacking CcoS, CcoNOQP complex was detected but inactive (Kulajta *et al.*, 2005). $\Delta cj1154c$ is sensitive to high concentration of Cu and the addition of 0.6 mM excess Cu to the growth medium partly rescued the Cco activity, but to only ~20% of that in *C. jejuni* wildtype cells. This suggests that Cj1154 is required for the presence of Cu_B cofactor of the CcoN subunit. $\Delta cj1154c$, showing no Cco activity and no growth defect; sensitive to Cu and slight stimulation in Cco activity with excess Cu, is difficult to explain with the limited knowledge available at the moment and needs further investigation.

In most of the bacteria that have been studied for *cbb*₃-type cytochrome *c* oxidase, it has been reported that activity is dependent on proper working of CcoNOQP, CcoGHIS, PCu_AC and Sco1 homologue proteins only. *C. jejuni*, already

being an exception by not having *ccoGHIS* cluster next to *ccoNOQP*, proved to be exceptional again. It was found that the products of genes next to *ccoNOQP* (in between *cj1487c* and *cj1483c*) are playing a role in Cco activity too. *cj1486c*, *cj1485c* and *cj1484c* are expressed by the same promoter expressing *ccoNOQP* and Cj1486, Cj1485 and Cj1484 are unknown proteins with no presently characterised protein homologue. Cj1486 is a transmembrane (Fig. 3.3) putative periplasmic protein of unknown function. Δ *cj1486c* showed no sensitivity to Cu, confirming that *cj1486c* gene product is not affecting the intracellular Cu homeostasis (Fig. 3.26). No Cco activity was observed in Δ *cj1486c* cells and it wasn't rescued by addition of excess Cu in growing medium (Fig. 3.27). This suggests that *cj1486c* gene product is either involved in activity of CcoNOQP subunits or the assembly of complex and is not handling Cu to be delivered to CcoN. It has a severe growth defect which is expected from *C. jejuni* cells lacking Cco activity (Fig. 3.26). *cj1486c* is next to *ccoP* with similar GC% content. Our finding indicates that *cj1486c* may be an uncharacterised protein essential for oxidase activity that interacts with CcoP, which needs to be further investigated as this would be a novel feature of bacterial Cco oxidase assembly and structure. Presence of intact *ccoP* was confirmed in the Δ *cj1486c* strain to rule out any mistake while knocking out *cj1486* (Fig. 3.12). Cj1485 is a very small (33 amino acids long) transmembrane protein of unknown function. Δ *cj1485c* didn't show any growth defect and sensitivity to Cu. But the Cco activity is severely reduced with slight stimulation with excess Cu. Similar results were shown by Cu assembly mutant, suggesting that *cj1485c* gene product might be involved in assembly of Cu in CcoNOQP complex. But it is too small to have a metal binding motif as 20 of its aa are embedded in membrane. This suggests that instead of being an assembly protein, it is potentially interacting with the assembly proteins and its presence is crucial for their activity. Cj1484 is a membrane bound protein of unknown function. In Δ *cj1484c*, Cco activity is significantly reduced, suggesting role of *cj1484c* gene product in CcoNOQP activity. An interesting observation was that the Cco activity was further reduced by adding excess Cu in medium. It suggests that Cj1484 is playing a dual role by supporting Cco activity in presence of low Cu but acting like a barrier for Cu to reach CcoN in presence of excess Cu. It probably is a part of some sort of *C. jejuni* protecting mechanism to protect CcoNOQP complex in case of excess Cu, which needs further investigation. Δ *cj1482c*, being a neighbour of *ccoH*

on the other side, was also analysed for having a role in Cco activity, which appeared to be negative.

The role and necessity of assembly proteins and CcoGHIS proteins for Cco activity has been extensively studied in many bacteria. Therefore, for a bacterial protein to be homologous to any of them and affecting the Cco activity, with or without Cu homeostasis, should provide evidence to consider it as an assembly protein. What is more interesting is to understand the role of assembly proteins and CcoGHIS proteins in the biogenesis of CcoNOQP subunits and complex; and mechanism of CcoNOQP active complex formation. In *C. jejuni*, this study started with investigating the effect of absence of assembly, CcoI and CcoS proteins on biogenesis of CcoNOQP subunits. CcoO and CcoP contain active C-heme sites which were used to detect them in $\Delta cj0908-cj0911$, $\Delta cj1154c$ and $\Delta cj1155c$ by heme blotting (Fig. 3.22). In figure 3.22, a CcoO band can be seen in all strains except $\Delta ccoNOQP$ strain (which was used as a control). In *R. capsulatus*, Kulajta *et al.* (2005) reported the absence of CcoNOQ complex in cells lacking CcoI but didn't comment on the individual CcoO subunit. They also reported presence of CcoNOQ complex in cells lacking CcoS. This suggest that CcoO subunit is produced even in absence of assembly, CcoI and CcoS proteins. There are very intense bands in all strains, including $\Delta ccoNOQP$, near CcoP size which made it impossible to visualize CcoP using this technique. The carbon monoxide difference spectroscopy used to detect CO-binding *b*-type haems in CcoN subunit gave a hint of presence of CcoN subunit in all strains except $\Delta ccoNOQP$, but the peak height near 560 nm is too low to make any firm conclusion from it (Fig. 3.23). And it has been reported that purified CcoP from *B. japonicum* and *P. stutzeri* also binds CO along with CcoN with CO binding specifically to CcoP in *P. stutzeri* under low CO concentration (Pitcher and Watmough, 2003). Therefore, it is difficult to comment whether CO in section 3.2.11.2 is interacting with CcoN or CcoP subunit of *C. jejuni* wild type and mutants and the result cannot be interpreted for CcoN alone. Assuming that CcoN is the only Cu containing protein present in abundance in inner membrane, the amount of Cu in inner membranes of all strains was measured using ICP-MS to detect Cu containing CcoN (Fig. 3.24). The cells lacking CcoN should have low amount of Cu in their inner membrane than wildtype. The assay did not work as anticipated. Most probable reason is metal contamination at various stages of sample preparation followed by

very small difference between Cu amounts which are beyond the ICP-MS machine's detection range. The antibodies against CcoN in *Rhodobacter* didn't prove to be specific to CcoN in *C. jejuni*. This study found that CcoO is produced in *C. jejuni* cells lacking assembly, CcoI and CcoS proteins but biogenesis of CcoN, CcoQ and CcoP subunits in *C. jejuni* cells lacking the assembly and CcoGHIS proteins still needs further investigation. Further efforts should also be directed to understand the role of novel genes in *C. jejuni*, between *ccoP* and *ccoH*, in biogenesis of CcoNOQP active complex.

3.4 Conclusions and summary:

This study provides evidence that proteins encoded by *cj0911* is ScoI homologue (membrane bound protein having Cu binding motif), by *cj0909* is PCu_AC homologue (periplasmic protein having Cu binding motif), by *cj0369c* is CcoG homologue (membrane bound protein having thioredoxin motifs), by *cj1483c* is CcoH homologue (membrane bound protein, believed to be closely attached to active Cco complex), by *cj1155c* is CcoI homologue (transmembrane protein having Cu translocating function) and by *cj1154c* is CcoS homologue (membrane bound protein, essential for Cco activity) in *C. jejuni* NCTC11168. This study also provides evidence of presence of novel genes in *C. jejuni* NCTC11168 encoding proteins playing crucial role in the Cco activity, some of which being essential for the activity. Cj0908 and Cj0910 are membrane bound proteins having thioredoxin motifs with two cysteines on periplasmic side, potentially having role in reducing Cu to be transported to CcoN by Cj0909 and Cj0911. Cj1486 is a membrane bound protein essential for the Cco activity, potentially a sub part of CcoP, attached to the active Cco complex even after maturation. Cj1485 is an inner membrane protein with most part embedded inside the membrane and affecting the Cco activity. Cells lacking this protein showed the same characteristics showed by the cells lacking the assembly proteins, giving evidence that Cj1485 might be acting as assembly protein, potentially as a thioredoxin. Cj1484 is a membrane bound protein which is required for the normal activity of the Cco but the abnormal behaviour of cells lacking Cj1484 in presence of excess Cu made it difficult to draw any conclusion about it. Findings in this study for cytochrome *c* oxidase

assembly and activity in *C. jejuni* NCTC11168 can be summarised in the model in Figure 3.28:

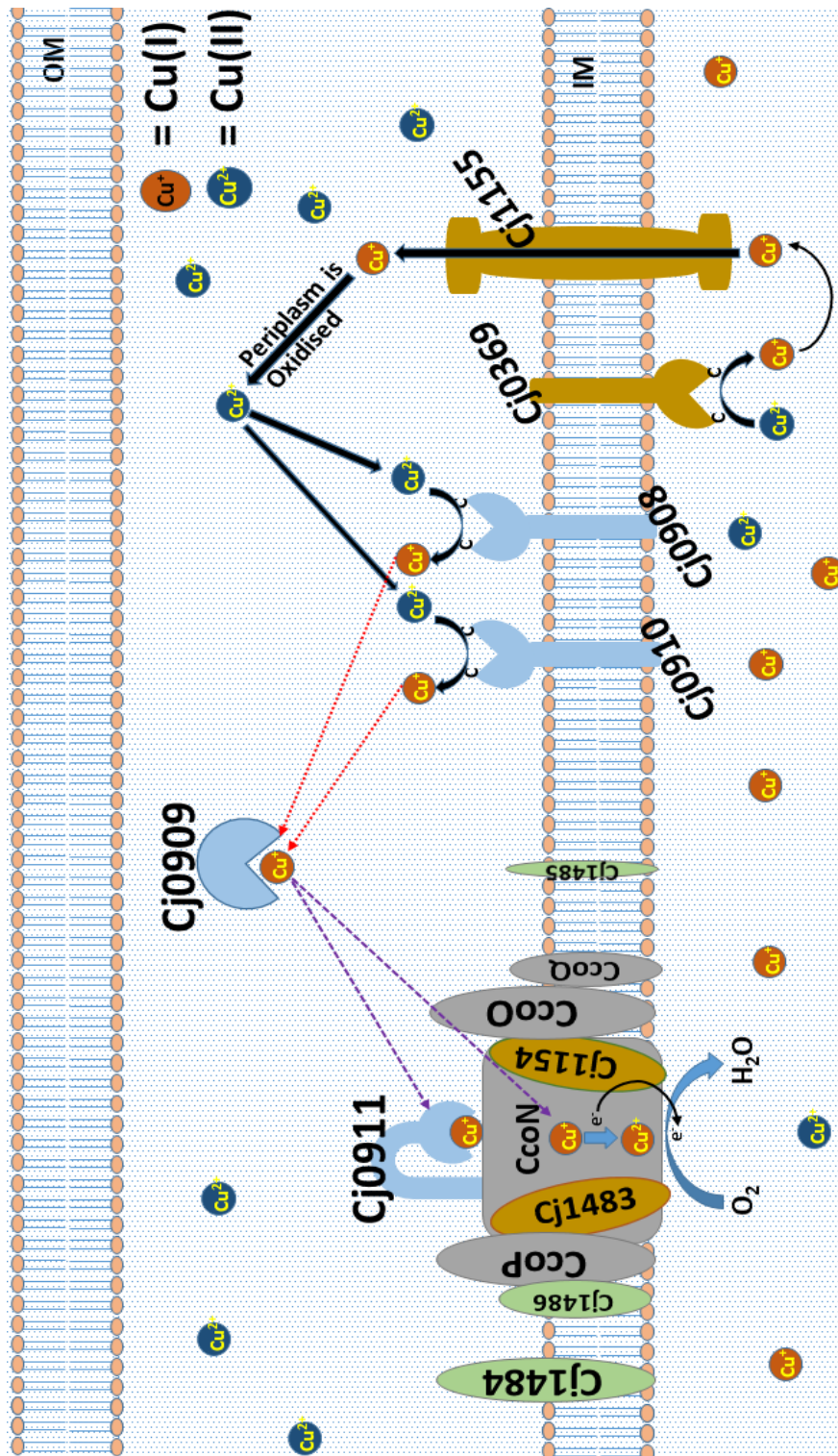


Figure 3.28: A working model from this study. Proteins encoded by same operon/cluster of genes are represented by same colour. “C” on thioredoxins represent cysteine. Cj0369 reduce Cu in cytoplasm to be captured by Cj1155. Cu is transported from cytoplasm to periplasm through Cj1155, where it is oxidised to Cu(II). Cu(II) is reduced to Cu(I) by Cj0908 and Cj0910 and collected by Cj0909. Cu(I) from Cj0909 is either transported to CcoN or to Cj0911, which ultimately transfers it to CcoN. Cj1483 is an integral part of Cco complex. Cj1154, is responsible for presence of cofactors in CcoN, may or may not stay with complex after maturation. Cj1486 is sub-part of CcoP. Further analysis is required to predict anything about Cj1484.

Based on all results, this study proposed a working model for cytochrome *c* oxidase activity in *C. jejuni* (Fig. 3.28). The Cu(II) in cytoplasm is reduced to Cu(I) by Cj0369 and transported to periplasm through Cj1155. Most of the Cu is in Cu(II) form due to highly oxidised environment of periplasm. This Cu(II) is reduced to Cu(I) by Cj0908 and Cj0910 from where it is collected by Cj0909 and transported to either Cj0911, which assembles it in Cu centre in CcoN, or to Cu centre in CcoN directly. At CcoN, heme b-Cu(I) reduces oxygen to a water molecule. Cj0911 is membrane bound and is near the CcoNOQP complex so that it can transfer Cu to CcoN. Cj1483 is an integral part of Cco complex. Cj1154 is responsible for presence of cofactors in CcoN but whether it remain with the complex after maturation or not is not clear. It is shown to stay with the complex as an integral protein in this model. It is not necessary, but it must be with the complex at some point during the maturation. Cj1486 is attached to CcoP, acting as an interacting protein. Cj1485 is a very small transmembrane protein, absence of which is similar to the absence of assembly proteins in the *C. jejuni* cells. In this diagram, Cj1485 has been shown as a membrane bound protein but it maybe interacting with thioredoxins, Cj0909 or Cj0911. There is no evidence of any of this and more experiment of protein-protein interaction is required. Cj1484 is a membrane protein which is affecting the Cco activity, but no certain prediction about its function can be made at the moment.

Chapter 4

Maintenance of Copper Homeostasis in *Campylobacter jejuni*

4.1 Introduction:

It is already established that copper is an essential but highly toxic nutrient (section 1.4.2). Therefore, its uptake and precise intracellular distribution is crucial for all cells.

C. jejuni requires copper (Cu) as a cofactor for a few metalloproteins, including the *cbb₃*-type cytochrome *c* oxidase (Chapter 3), the Cj1516/CueO multi-copper oxidase and p19, a protein involved in Fe-transport (Bannister and Bannister, 1987; De la Cerda *et al.*, 1997; Iwata, 1998; Nakamura and Go, 2005). Cu transportation and assembly to *cbb₃*-type cytochrome *c* oxidase is crucial for respiration, growth and host colonisation (Liu and Kelly, 2015). However, an excess amount of Cu is toxic, as it can activate O₂ via the Fenton reaction to generate dangerous reactive oxygen radicals (Storz *et al.*, 1999; Rensing and Grass, 2003; Gardner and Olson, 2018; section 1.4.3). Therefore, bacterial cells need to precisely control Cu acquisition, trafficking and incorporation into the target proteins. In Gram-negative bacteria, all cuproenzymes are located within the inner membrane and the periplasm, which implies transport of copper from the medium or from the cytoplasm to these cell compartments. Copper diffuses through nonspecific outer membrane porins into the periplasm and transits to the cytoplasm (Durand *et al.*, 2015). In all subcellular compartments, copper presents a threat to the cell integrity; therefore, it has to be handled by specific copper homeostasis systems to avoid its toxicity. Very little is known about Cu homeostasis in *C. jejuni*.

In *E. coli*, transcription of genes providing immunity against excess Cu invasion is regulated by CusR and CueR regulators, with CueR, a MerR-like transcriptional regulator, affecting the transcription of *copA* and *cueO* (Yamamoto and Ishihama, 2005; section 1.4.5). Interestingly, both CueS and CueR regulators are absent in *C. jejuni* 11168 genome (Hall *et al.*, 2008). However, the regulatory role maybe fulfilled by Cj1563, which is a MerR-like protein in *C. jejuni* genome but there is no evidence yet (Hall *et al.*, 2008) and need further investigation. Maintenance of Cu homeostasis by cytochrome *c* oxidase assembly proteins, like in case of *Rhodobacter sphaeroides*, was also not observed in *C. jejuni* (section 3.2.7). However, both CopA and CueO are present in *C. jejuni* (Hall *et al.*, 2008). *C. jejuni* cells lacking CopA, CueO, or both have been reported to be more Cu sensitive and

more prone to copper-mediated oxidative stress (Hall *et al.*, 2008; Gardner and Olson, 2018). CopA and CueO were also observed to be necessary for efficient chicken colonisation and this colonisation deficiency was further stimulated by high Cu containing diet (Gardner and Olson, 2018).

In *C. jejuni*, Cj1161c is homologous to bacterial CopA proteins (Hall *et al.*, 2008), known to be P-type ATPases that have a copper transporting functions. Cj1162c is a cytoplasmic protein believed to have a putative heavy metal associated protein domain and is a CopZ homologue. Cj1163c is a potential Zn-Co-Ni transporter and Cj1164c is homologous to Zn finger proteins. Cj1165c and Cj1166c are unknown proteins. This study hypothesised that in *C. jejuni* the gene cluster *cj1161c*, *cj1162c*, *cj1163c*, *cj1164c*, *cj1165c* and *cj1166c* may encode proteins needed to efflux excess Cu from the cytoplasm to the periplasm.

In this study, to characterise the phenotypic profiles of genes encoding proteins potentially involved in maintaining *C. jejuni* intracellular Cu homeostasis within the wild type strain, deletion mutants were made by knocking out genes *cj1161c*, *cj1162c*, *cj1163c*, *cj1164c*, *cj1165c* and *cj1166c* individually by homologous recombination. Absence of any of the encoded proteins should disrupt the Cu homeostasis in bacterial cells, especially the Cu efflux, resulting in more than normal Cu accumulation inside the cells. As a high amount of Cu is toxic for bacterial cells, this should make bacterial cells more Cu sensitive and should have effects on normal bacterial growth. This disruption in intracellular Cu homeostasis might have some effect on other Cu associated metalloproteins like cytochrome *c* oxidase. As these proteins are solely responsible for getting rid of all excess Cu, the amount of Cu present in the media should have effect on their expression. Therefore, wild type and knock out mutants were checked for copper sensitivity, growth defects, intracellular Cu content and cytochrome *c* oxidase activity. The effect of Cu on gene expression was also studied. As Cj1163c is a potential Zn-Co-Ni transporter, zinc, cobalt and nickel sensitivity assays were performed on *cj1163c* knock out mutant along with *cj1161c* knock out mutant as control.

4.2 Results:

4.2.1 Gene arrangement in *C. jejuni* genome:

Potential Cu-homeostasis maintenance proteins in *C. jejuni* are expressed by genes *cj1161c*, *cj1162c*, *cj1163c*, *cj1164c*, *cj1165c*, and *cj1166c* in a cluster.

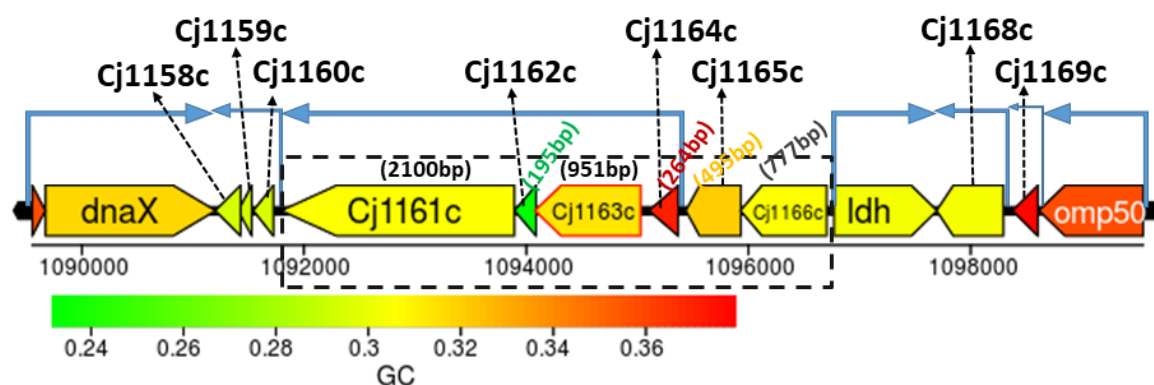


Figure 4.1: Gene arrangement in *C. jejuni*. Genes expressing potential Cu-homeostasis proteins in *C. jejuni* forms a cluster on complementary strand of DNA. These genes of interest are in box. Arrows represent promoter sites. Genes are colour coded according to scale (shown) based on the GC content.

cj1166c to *cj1161c* genes form a cluster on the complementary strand of DNA, with *cj1164c* to *cj1161c* having the same promoter (Fig. 4.1). The promoter site for *cj1166c* and *cj1165c* is not clear. Downstream of this cluster, there are *cj1160c*, *cj1159c* and *cj1158c*, having the same promoter and unknown function. They encode small hydrophobic proteins with *cj1160c* and *cj1159c* products having one probable transmembrane helix and *cj1158c* having one probable transmembrane helix. Next to this cluster, there is *cj1157*, which is on the primary strand and denoted by *dnaX*, the probable DNA polymerase III subunits gamma and tau. Next to *cj1157*, there is *cj1156*, which is homologous to a transcription termination factor in *E. coli*. Upstream of *cj1166c-cj1161c* cluster, there is *cj1167*, which is on the primary strand and encodes a probable L-lactate dehydrogenase. *cj1167* is followed by *cj1168*, which is on the complementary strand and encodes a putative integral membrane protein (DedA homologue) with four probable transmembrane helices predicted by TMHMM2.0. This showed that proteins encoded by genes next to *cj1166c-cj1161c* gene cluster on both sides are not obviously associated with Cu homeostasis and so were not further studied.

4.2.2 Bioinformatics analysis for finding homologous sequences:

C. jejuni Cj1161, Cj1162, Cj1163, Cj1164, Cj1165 and Cj1166 proteins were checked for any available characterised homologous protein by running protein BLAST in NCBI.

Table 4.1: BLAST results of Cj1161 to Cj1166 proteins:

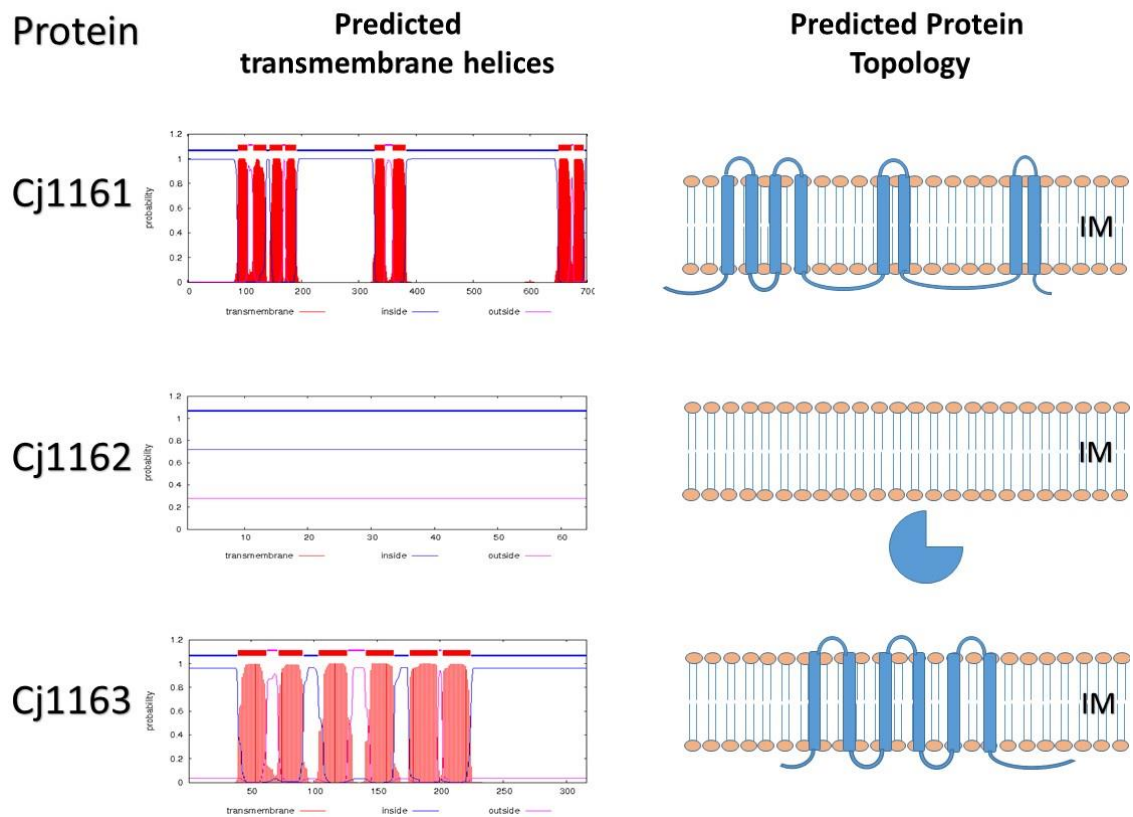
Protein	Homolog protein	% Identity	Other organisms with similar protein	Putative Function
Cj1161	Copper-translocating P-type ATPase (CopA)	35 % (copper-translocating P-type ATPase in <i>E. coli</i>)	<i>E. coli</i> , <i>Rubrivivax gelatinosus</i> , <i>Acinetobacter baumannii</i> ,	Cu translocation from cytoplasm to periplasm
Cj1162	Cu chaperone (CopZ)	44 % (copper chaperone in <i>Wolinella succinogenes</i>)	<i>Wolinella succinogenes</i> , <i>Staphylococcus aureus</i>	Cu transportation to CopA
Cj1163	Cation transporter; CDF family zinc transporter ZitB	33 % (cation transporter in <i>E. coli</i>); 36 % (CDF family zinc transporter ZitB in <i>E. coli</i>)	<i>E. coli</i> , <i>Arcobacter cryaerophilus</i>	Co-Ni-Zn transporter. Cu translocation from cytoplasm to periplasm.
Cj1164	hypothetical protein	99 %	<i>E. coli</i>	?
Cj1165	-	-	-	?
Cj1166	-	-	-	?

BLAST results showed that Cj1161 has 35% identity with Cu-translocating P-type ATPase in *E. coli*, which indicates Cj1161 potentially has a Cu-translocating function. Cj1162 has 43% identity with a potential Cu-chaperone in *Wolinella succinogenes* and 40% identity with a possible heavy metal transporter in *Sulfurimonas*, which suggested its potential role as binding unwanted intracellular excess Cu and transporting it to Cu efflux pump i.e. Cu-translocating P-type ATPase. Cj1163 is 47% identical to a cation transporter in *Denitrovibrio*. Therefore, Cj1163 may be acting as Cu transporter. Cj1164 is most similar to a hypothetical protein in *E.*

coli but it has a combination of cysteine and histidine residues that may bind Cu/Zn. There were no characterised homologues of Cj1165 and Cj1166 available, making those novel proteins.

4.2.3 Prediction of transmembrane helices in proteins:

To be a Cu-translocator, protein has to be a transmembrane protein and for a protein to be a Cu chaperone for transporting Cu to the Cu-translocating protein, it has to be a cytoplasmic protein. Therefore, whether the potential Cu-translocating proteins in this study qualifies as a transmembrane protein or not were predicted by predicting transmembrane helices in proteins using TMHMM Server v.2.0 with amino acid sequence of proteins. These predictions were used to predict the topology of proteins and it further added to the hypothesis established by the homology results.



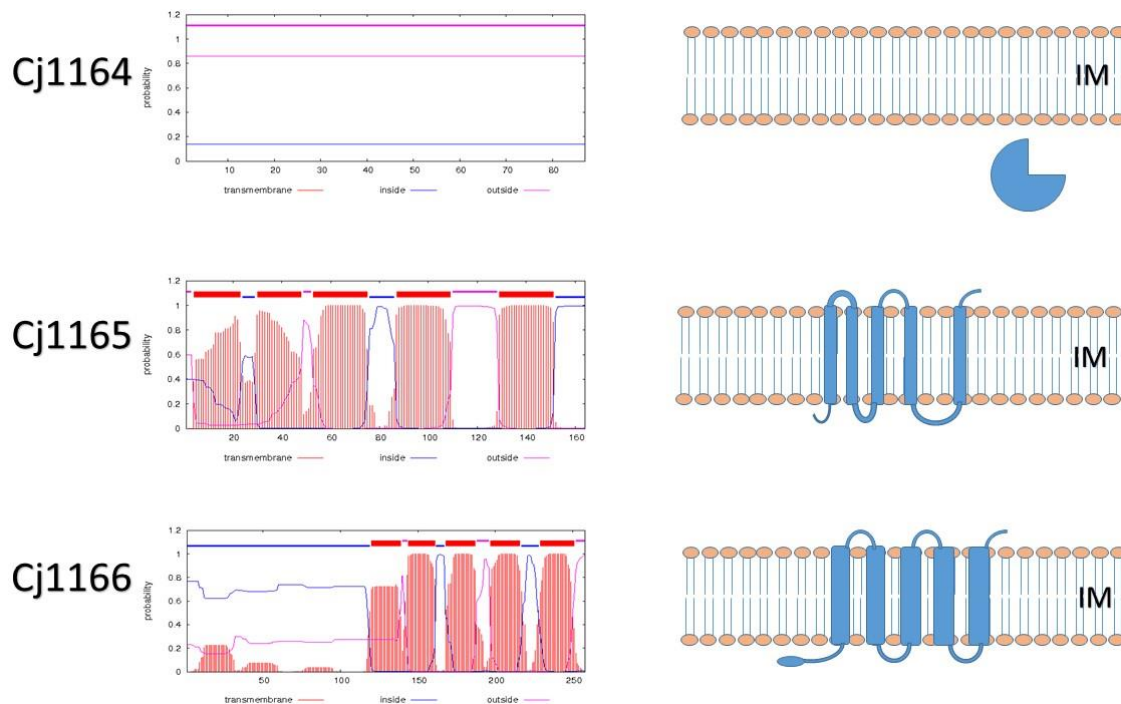


Figure 4.2: Prediction of transmembrane helices in proteins and subsequently their predicted topology. Protein amino acid sequences were submitted to TMHMM server individually. The plot shows the posterior probabilities of inside/outside/TM helix. The plot is obtained by calculating the total probability that a residue sits in helix, inside, or outside summed over all possible paths through the model. However, if the whole sequence is labelled as inside or outside, the prediction is that it contains no membrane helices. It is probably not wise to interpret it as a prediction of location. Based on results, protein topology with respect to inner membrane are predicted and shown. Plots were interpreted as directed by TMHMM Server v.2.0 (<http://www.cbs.dtu.dk/services/TMHMM/>).

TMHMM predictions, as described in 2.17, suggests that Cj1161, Cj1163, Cj1165 and Cj1166 are transmembrane proteins and Cj1162 and Cj1164 are non-membrane proteins (Fig. 4.2). Given Cj1161 as CopA homologue, Cj1162 as CopZ homologue, Cj1163 as potential Zn-Co-Ni transporter and Cj1164c as homologous to Zn finger proteins, this prediction of protein localisation further added to our preliminary hypothesis that proteins expressed by gene cluster *cj1161c* to *cj1166c* may be responsible for maintaining Cu homeostasis in *C. jejuni*.

4.2.4 Generation of deletion mutants:

Kanamycin resistant deletion mutants were made by knocking out each gene individually and replacing it with a kanamycin resistance cassette by homologous

recombination. Recombination plasmids were made using pGEM-3Zf(-) by isothermal assembly (section 2.4.11) and transformed to competent *C. jejuni* cells (section 2.5.3) to disrupt most of the genes of interest without effecting the neighbouring genes. All genes of interest were knocked out individually. The following section details how the mutant strains were produced in *C. jejuni* NCTC11168.

20-22 bp primers were designed for amplifying both \approx 500 bp upstream and downstream DNA fragments of the gene of interest (section 2.4.5; Fig. 4.3). Both DNA fragments and kanamycin resistant cassette were amplified by PCR (section 2.4.4.1) and digested with HincII restriction enzyme (section 2.4.8). pGEM[®]3Zf(-) cloning vector was isolated from *E. coli* (section 2.4.2), digested with HincII restriction enzyme (section 2.4.8) and phosphatase treated with Antarctic Phosphatase (section 2.4.9). Both DNA fragments, kanamycin resistant cassette and cloning vector were PCR cleaned up (section 2.4.7), followed by concentration measurement (section 2.4.3) and ran on agarose gel to check for correct size and digestion (section 2.4.6).

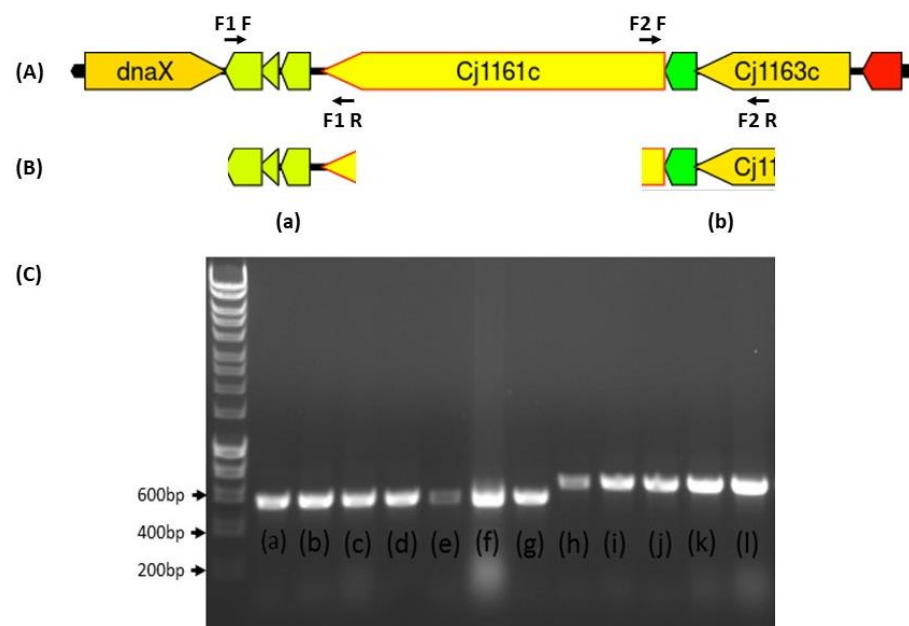
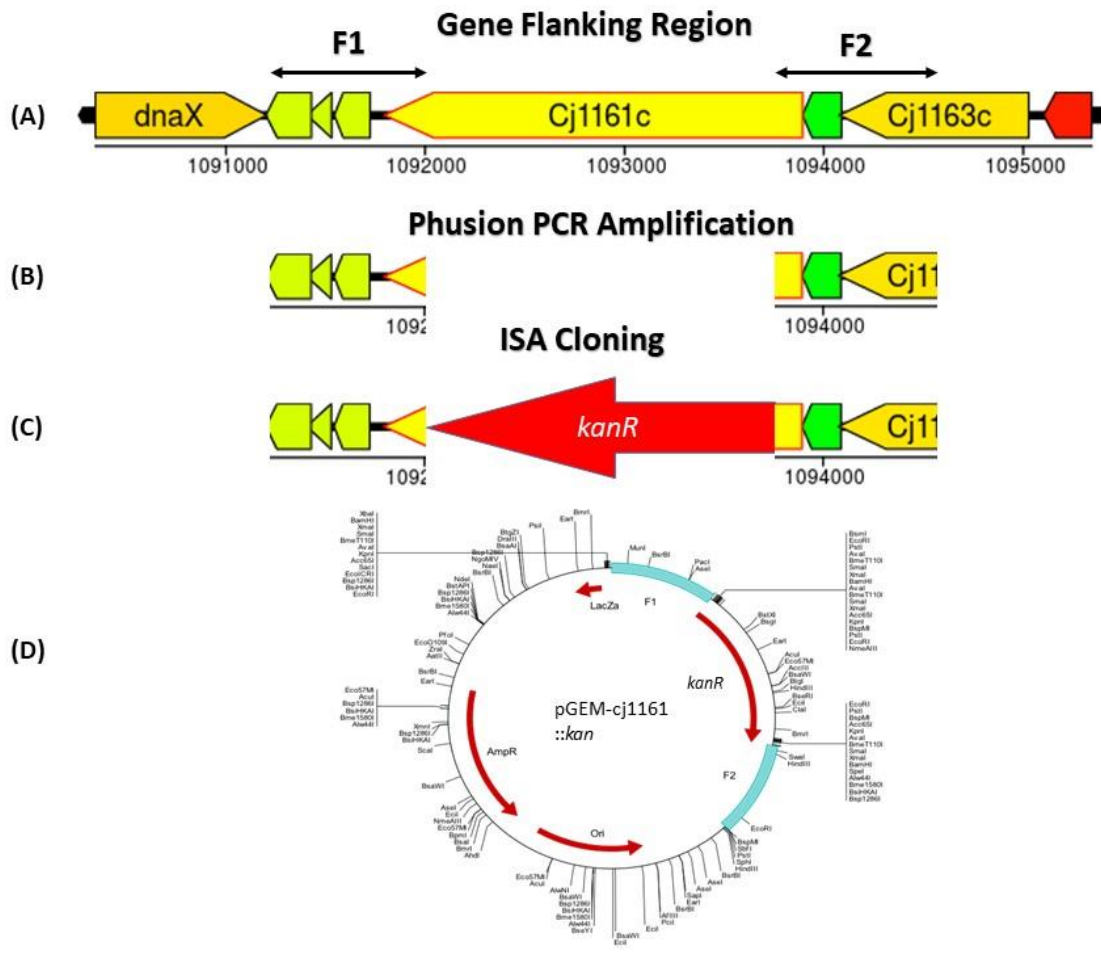


Figure 4.3: PCR amplification of upstream and downstream DNA fragments and size confirmation by agarose gel electrophoresis. (A) Location of primers designed for amplification of neighbouring fragments of gene of interest. (B) Amplified fragments for *cj1161c*. (C) Gel containing PCR amplified bands. Lane name corresponds to name of fragment. Expected PCR product size is 500 bp. First lane is 1 kb DNA ladder (Thermo scientific). Flanking region: (a) Upstream *cj1161c* (b) Downstream *cj1161c* (c) Upstream *cj1162c* (d) Downstream *cj1162c* (e) Upstream

cj1163c (f) Downstream *cj1163c* (g) Upstream *cj1164c* (h) Downstream *cj1164c* (i) Upstream *cj1165c* (j) Downstream *cj1165c* (k) Upstream *cj1166c* and (l) Downstream *cj1166c*. All correct size.

Both DNA fragments, kanamycin resistant cassette and cloning vector were ligated together by ISA according to section 2.4.11 and the resulting DNA was immediately used to transform competent *E.coli* DH5 α cells as described in section 2.5.2. Colonies were screened by colony PCR (section 2.4.4.2) using M13 primers (section 2.4.5) followed by agarose gel electrophoresis (section 2.4.6; Fig. 4.4) and extracted plasmid was confirmed by automated DNA sequencing using same M13 primers (Core Genomic Facility, University of Sheffield Medical School, UK).



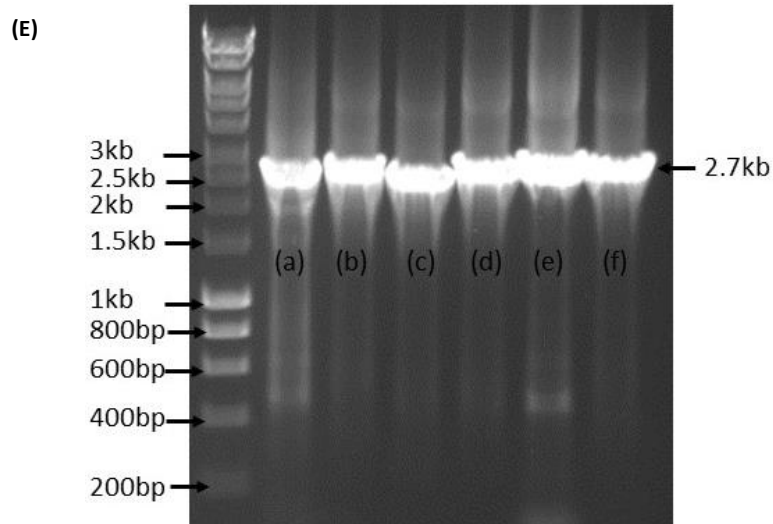


Figure 4.4: Recombinant plasmid construction and confirmation by correct size using PCR. (A) The flanking regions of genes of interest (*cj1161c*), 500 bp on each side (marked as F1 and F2). (B) Amplified F1 and F2. (C) The antibiotic resistant marker (kanamycin cassette in this case) is inserted between flanking regions into the pGEM-3Zf(-) vector by ISA cloning. (D) Completed recombinant plasmid containing the flanking regions with inserted resistance marker prior to transformation in to *C. jejuni*. All recombinant plasmids made for knock out mutations were confirmed by PCR with M13 primers. Correct size bands are 2.5 kb long (1.5 kb of kan cassette+500 bp of each flanks). First lane is 1 kb DNA ladder (Thermo scientific). (a) pGEM-cj1161 (b) pGEM-cj1162 (c) pGEM-cj1113 (d) pGEM-cj1164 (e) pGEM-cj1165 (f) pGEM-cj1166. Recombinant plasmids for other knock out mutants (mentioned in section 2.4.2.1) were made similarly.

Competent *C. jejuni* cells were transformed with recombinant plasmids by electroporation (section 2.5.4) and were checked for correct mutation by running colony PCR with combination of screening and kanamycin cassette primers (section 2.4.5) (Arrow 1: screening forward-screening reverse, arrow 2: Kan forward-screening reverse and arrow 3: screening forward-Kan reverse) according to section 2.4.4.3 (Fig. 4.5). Screening primers were designed 100 bp outside the flanking regions (which were 500 bp) on both sides to show that the construct was correctly inserted in the correct orientation and that the double recombination had removed the remaining vector DNA. Size of kanamycin resistant cassette is \approx 1.5 kb. PCR products were checked for correct size by agarose gel electrophoresis according to section 2.4.6. Figure 4.6(c) confirmed correct mutation of *cj1161c*. All other mutants were made and checked similarly.

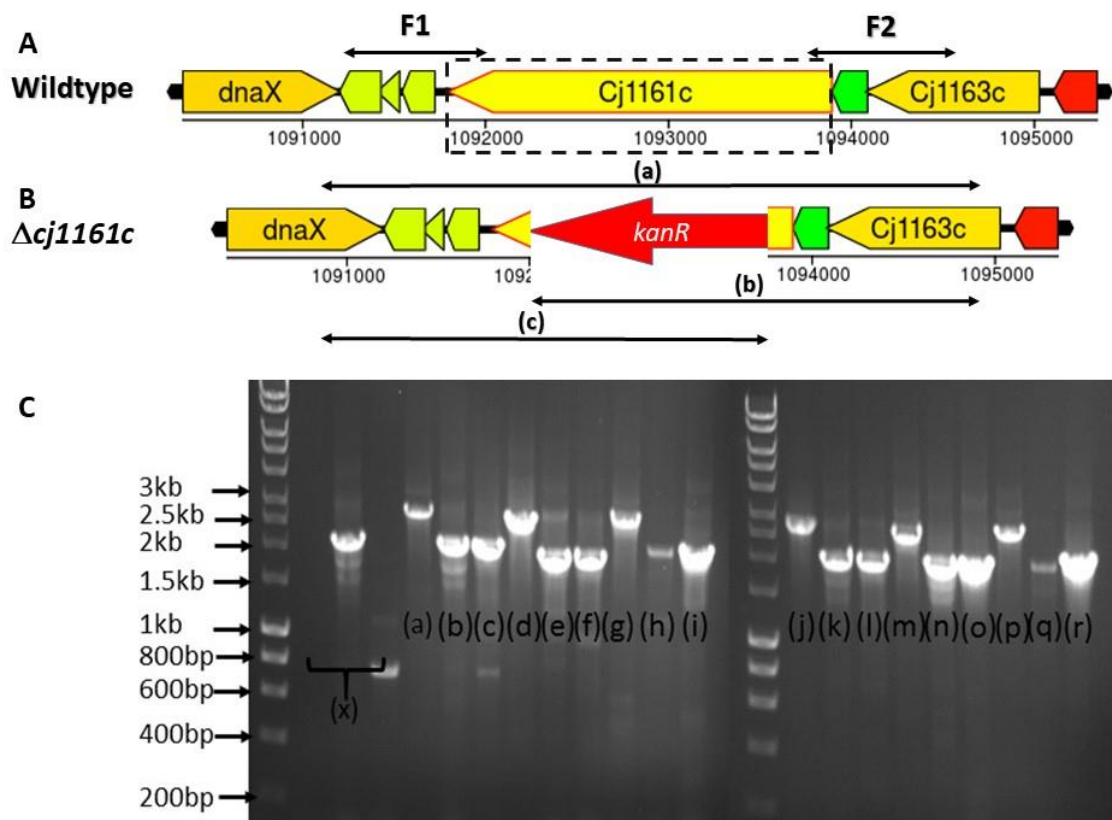


Figure 4.5: Mutagenesis of Cu homeostasis genes in *C. jejuni*. The recombinant plasmids formed by ISA shown in figure 4.4 were transformed into *C. jejuni* to replace the gene of interest with kanamycin resistant cassette. **A** Shows the gene arrangement of *Cj1161c* in wildtype strain. Arrows F1 and F2 indicates the flanking region. **B** Shows the gene arrangement in mutant with genes of interest replaced by kanamycin resistance cassette. The mutants were confirmed by PCR with combination of screening and kan primers (section 2.4.5). Size of arrow corresponds to expected size of PCR product and name corresponds to PCR products on gel. **C** Gel containing PCR confirmation bands of all mutants. Lane name and band size corresponds to name and size of arrows, respectively. Expected PCR product size are: (a)-2.7 kb, (b)-2.1 kb and (c)-2.1 kb. All other mutants were made similarly and their PCR products are represented on the gel in same way as of *Cj1161c*. First lane is ladder (HyperLadder 1 molecular weight marker, Bioline) and x is random PCR product, irrelevant to this study.

4.2.5 Copper toxicity assay:

In *C. jejuni* NCTC11168, Cj1161, Cj1162, Cj1163, Cj1164, Cj1165 and Cj1166 proteins were identified as potential Cu homeostasis maintenance proteins and absence of any of these proteins should make the bacterial cells more sensitive to Cu. This was measured as the effect on the final cell density in batch cultures. Wildtype, Δ *Cj1161c*, Δ *Cj1162c*, Δ *Cj1163c*, Δ *Cj1164c*, Δ *Cj1165c* and Δ *Cj1166c* cells were grown in 25 ml MHS broth (section 2.3.1) until mid exponential phase. Cells were harvested,

washed and inoculated in 6-well plates with 5 ml MeM α minimal media (equilibrated) (section 2.3.2) substituted with varying amounts of Cu as described in section 2.10.1. All experiments were done in triplicates. Cells in 6-well plates were grown for 12 hours according to section 2.10.1 and final ODs were measured according to section 2.3.6. Results were plotted in terms of culture growth (OD₆₀₀) vs Cu concentration. They were also analysed by normalising culture growths at different concentrations of Cu with respect to growth without any additional Cu. Culture growth without any additional Cu was set as 100% growth. (Fig. 4.6).

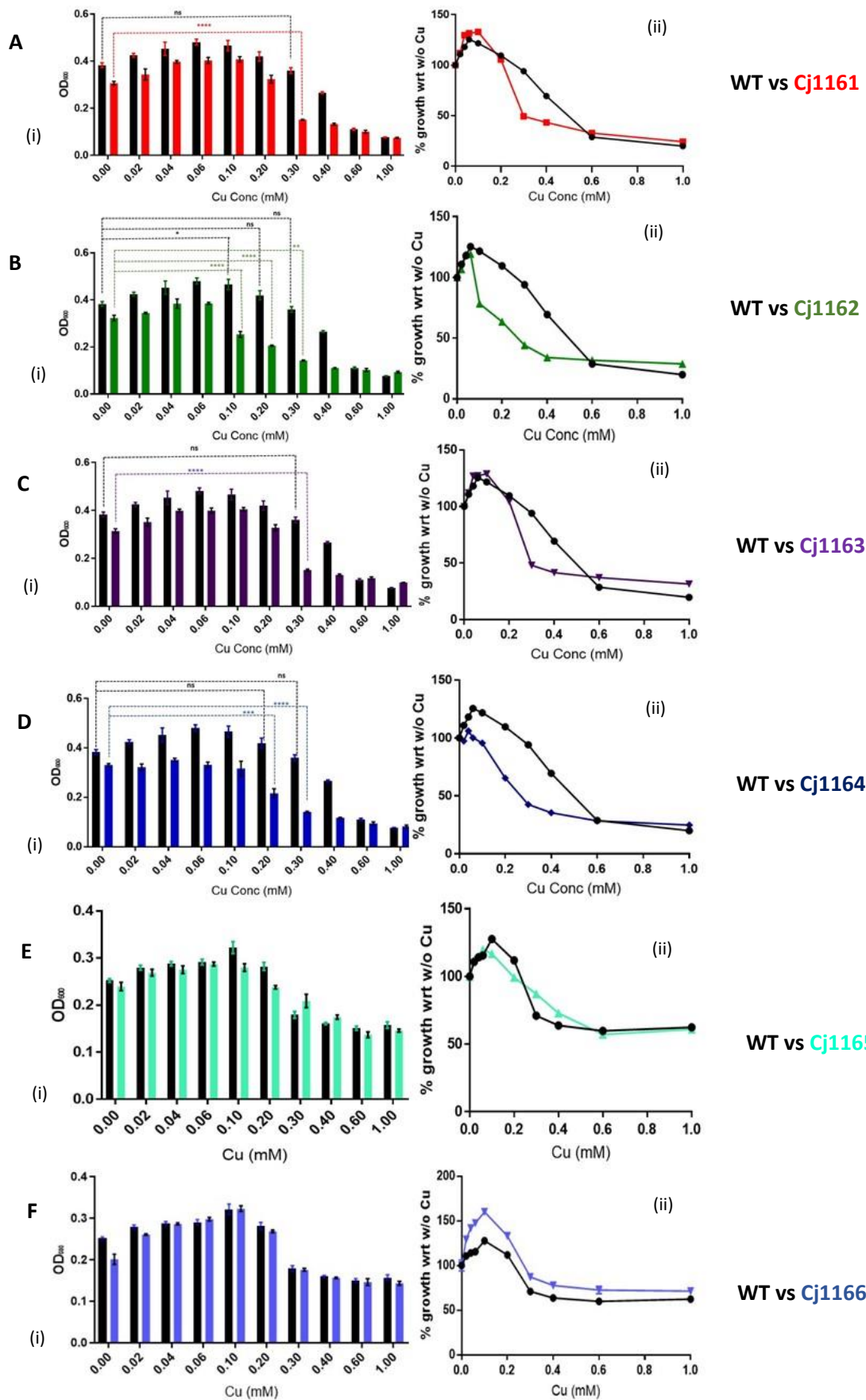


Figure 4.6: Cu toxicity assay for putative Cu homeostasis maintenance mutants. Assay was performed by growing *C. jejuni* wild type $\Delta cj1161c$, $\Delta cj1162c$, $\Delta cj1163c$, $\Delta cj1164c$, $\Delta cj1165c$ and $\Delta cj1166c$ strains in 5 ml MeM α minimal media in 6-well plates substituted with different concentrations of Cu (0.0, 0.02, 0.04, 0.06, 0.1, 0.2, 0.3, 0.4, 0.6, 1.0 mM) for 12 hours (section 2.10.1) and culture growths were measured (section 2.3.6). (i) Growth of **A** WT vs $\Delta cj1161c$, **B** WT vs $\Delta cj1162c$, **C** WT vs $\Delta cj1163c$, **D** WT vs $\Delta cj1164c$, **E** WT vs $\Delta cj1165c$ and **F** WT vs $\Delta cj1166c$. (ii) Growths at different concentrations of Cu normalised with growth without Cu being the control, i.e. 100%, respectively. The data are the average of triplicate cultures with error bars showing SD. T-tests were performed to check significance in difference. ($p > 0.05$, ns; $0.05 > p > 0.01$, *; $0.01 > p > 0.001$, **; $0.001 > p > 0.0001$, ***; $0.0001 > p$, ****)

Cu stimulated growth up to a concentration of 0.1 mM in all cases. This is in accordance with the fact that a small amount of Cu supports growth as it is necessary for certain enzyme activities and suggests Cu is in a limiting amount in MHS. The assay showed that $\Delta cj1161c$, $\Delta cj1162c$, $\Delta cj1163c$ and $\Delta cj1164c$ are more sensitive to Cu, but unequally, than wild type (Fig. 4.6). This suggested that cells lacking proteins expressed by these genes are unable to efficiently manage intracellular Cu and these proteins have a potential role in maintaining Cu homeostasis in the bacterial cells. The assay also gave us the threshold amount of Cu above which the mutants become more Cu sensitive. $\Delta cj1162c$ is most sensitive (at 0.1 mM Cu), followed by $\Delta cj1164c$ (at 0.2 mM Cu), which is followed by $\Delta cj1161c$ and $\Delta cj1163c$ (at 0.3 mM Cu), being equally sensitive. The results also showed that $\Delta cj1165c$ and $\Delta cj1166c$ are not significantly differently sensitive to Cu with respect to wild type. Therefore, proteins expressed by them may not be involved in maintaining Cu homeostasis in the bacterial cells. They are novel proteins, with no present homologous characterised protein available.

4.2.6 Growth Curve Assays:

As maintaining copper homeostasis is important for the normal growth of the bacteria, deleting any of the genes should have effects on growth rate as well as final cell density. Therefore, a growth curve assay was done to check for growth defects. The above Cu sensitivity assay showed that 0.25 mM excess Cu is the approximate threshold amount of Cu above which most of the mutants become more sensitive to Cu than wild type. The wild type, $\Delta cj1161c$, $\Delta cj1162c$, $\Delta cj1163c$, $\Delta cj1164c$, $\Delta cj1165c$ and $\Delta cj1166c$ cells were grown in Mem alpha minimal media on its own and also with 0.25 mM excess copper.

The starter cultures of wild type, $\Delta cj1161c$, $\Delta cj1162c$, $\Delta cj1163c$, $\Delta cj1164c$, $\Delta cj1165c$ and $\Delta cj1166c$ cells were grown in MHS till mid-exponential phase (section 4.2.5) and inoculated in 6-well plates with 6 ml MeM α minimal media (section 2.3.2) substituted with and without 0.25 mM Cu (CuSO₄ dissolved in dH₂O and filter sterilised) up to OD₆₀₀=0.1 according to section 2.9. Cells in 6-well plates were grown according to section 2.3.2. 0.5 ml samples were collected every 2 hours and mixed with 0.5 ml fresh MeM α media in a 1 ml cuvette and OD₆₀₀ were measured according to section 2.3.6. All experiments were done in triplicates. Results were plotted in terms of culture growth (OD₆₀₀) vs time (in hours) on a XY graph using GraphPad prism software for each mutant with wild type. Wild type or mutant name with “Cu” represents growth with 0.25 mM excess Cu in media.

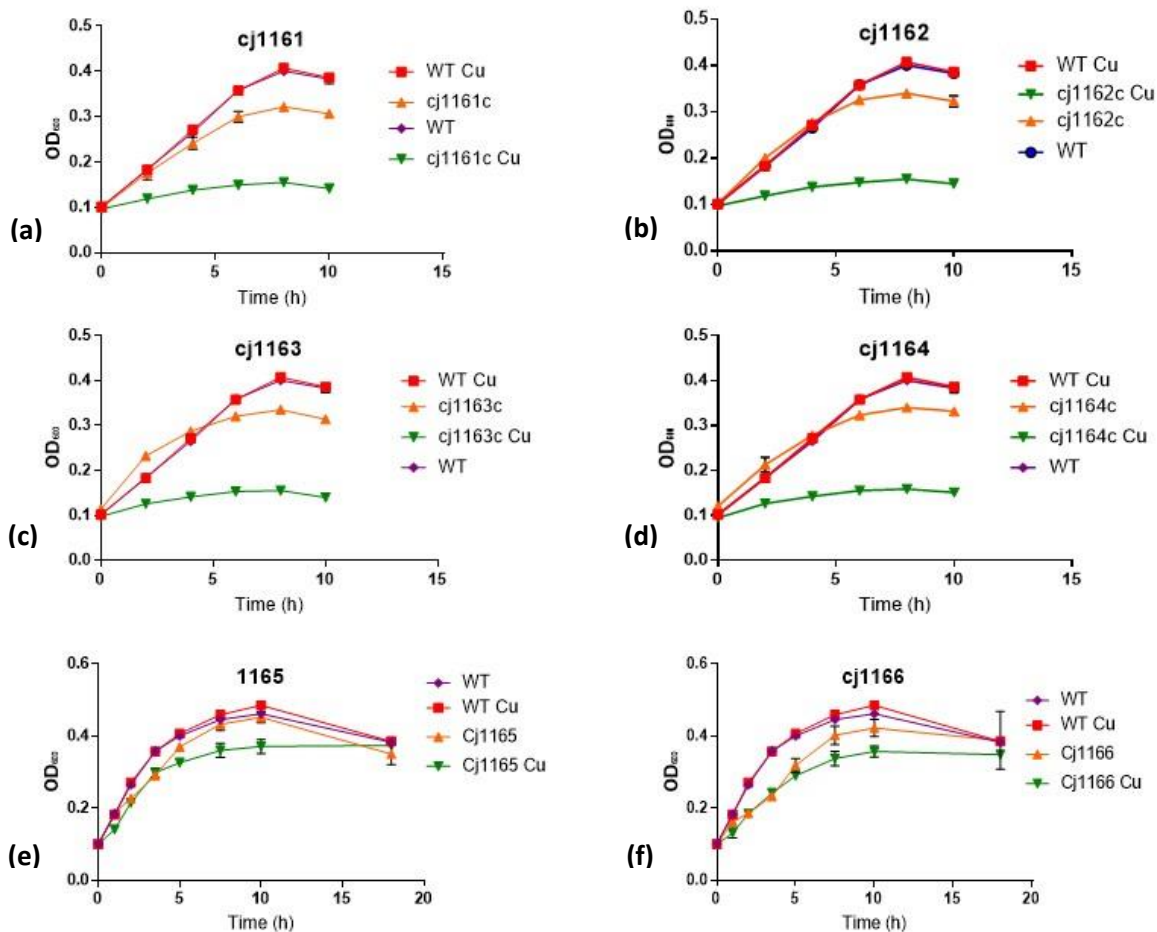


Figure 4.7: Effect of copper on growth. *C. jejuni* wild type, $\Delta cj1161c$, $\Delta cj1162c$, $\Delta cj1163c$, $\Delta cj1164c$, $\Delta cj1165c$ and $\Delta cj1166c$ cells were grown in 6 ml MeM α minimal media with and without 0.25 mM excess Cu in 6-well plates in microaerobic cabinets at 42°C with continuous shaking at 200rpm. Growth of (a) WT vs $\Delta cj1161c$, (b) WT vs $\Delta cj1162c$, (c) WT vs $\Delta cj1163c$, (d) WT vs $\Delta cj1164c$, (e) WT vs $\Delta cj1165c$ and (f) WT vs $\Delta cj1166c$, with and without 0.25 mM excess Cu. “Cu” represents

growth with 0.25 Mm excess Cu in media. The data are the average of triplicate cultures with error bars showing SD. T-tests were performed to check significance in difference. ($p > 0.05$, ns; $0.05 > p > 0.01$, *; $0.01 > p > 0.001$, **; $0.001 > p > 0.0001$, ***; $0.0001 > p$, ****)

The results (Fig. 4.7) showed that $\Delta cj1161c$, $\Delta cj1162c$, $\Delta cj1163c$, $\Delta cj1164c$, $\Delta cj1165c$ and $\Delta cj1166c$ knock out mutants have a slight growth defect compared to the wild type, even in the absence of copper. Presence of excess Cu had no effect on growth of wildtype, but it clearly suppressed the growth of $\Delta cj1161c$, $\Delta cj1162c$, $\Delta cj1163c$ and $\Delta cj1164c$, suggesting their inability to handle Cu efficiently and maintaining the Cu homeostasis, which is in accordance to Cu sensitivity assay result. This can be due to the fact that Mem α minimal media on its own is copper deficient but when copper is present in excess, the bacterial cells have to pump out excess copper, which is more difficult in these knock out mutants, suggesting a role of these gene products in copper homeostasis. $\Delta cj1165c$ and $\Delta cj1166c$ had only slight growth defects, but excess of Cu had no significant effect on their growth, suggesting their ability to handle Cu efficiently, which is again in accordance to Cu sensitivity assay result. This suggests that products of *cj1161c*, *cj1162c*, *cj1163c* and *cj1164c* genes in *C. jejuni* bacterial cells have roles in maintaining intracellular Cu homeostasis.

4.2.7 Quantification of the effect of Cu on gene expression:

If these gene products are involved in copper homeostasis, the amount of copper present in the medium should influence gene expression as well. The presence of excess Cu may increase the gene expression as more gene product would be required to pump out excess Cu to maintain intracellular Cu homeostasis. Therefore, expression of *cj1161*, *cj1162*, *cj1163* and *cj1164* genes were quantified by using RT-PCR to see effect of copper on gene expression.

Starter cultures were grown to mid-exponential phase and 5 ml MeM α minimal media was equilibrated in each well of 6-well plates, 3 with and 3 without 0.25 mM excess Cu, as described in section 4.2.5. Cells were spun down, washed, inoculated in a 6-well plate to an initial OD₆₀₀ \approx 0.05 and incubated till OD₆₀₀ \approx 0.15, as described in section 4.2.5. Cells were harvested and RNA was extracted from each sample as described in section 2.6.1. qRT-PCR was done as described in section 2.6.2.

Results were calculated as fold change in gene expression in excess Cu with respect to gene expression without addition of excess Cu, which was used as a control value, i.e. 1-fold. *gyrA* gene was used as an internal control (Fig. 4.8)

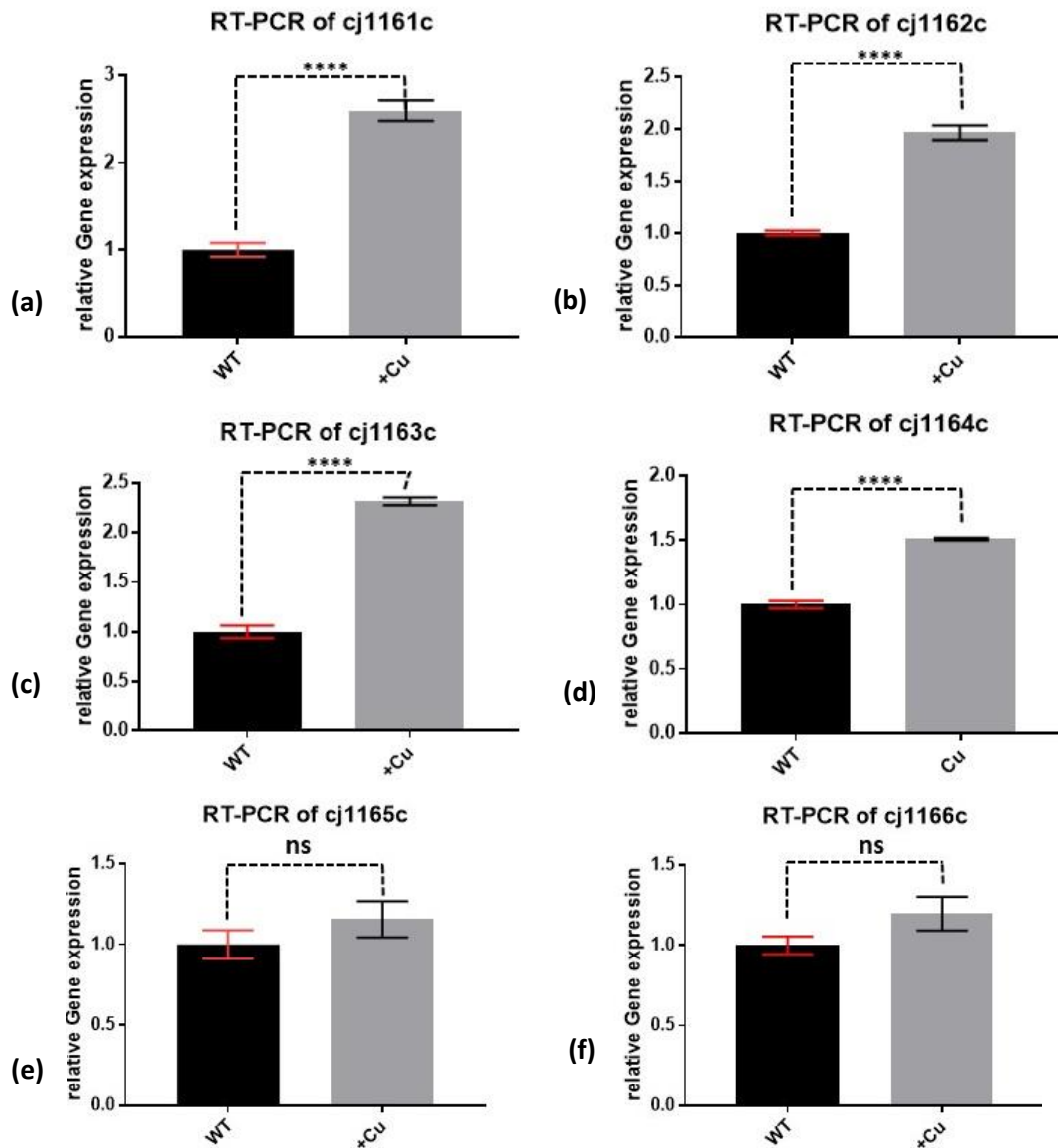


Figure 4.8: Quantification of gene expression using qRT-PCR. *C. jejuni* cells were grown with and without 0.25 mM excess Cu. RNA were extracted according to section 2.6.1 and matched to 10 ng μl^{-1} in nuclease free water. qRT-PCR was done on *cj1161c*, *cj1162c*, *cj1163c* and *cj1164c* genes using RT-PCR primers (section 2.6.3) with the *gyrA* gene used as an internal control. (a) Plot shows 2.5-fold change in *cj1161c* gene expression in excess Cu with respect to without excess Cu. (b) Plot shows 2-fold change in *cj1162c* gene expression in excess Cu with respect to without excess Cu. (c) Plot shows 2.25-fold change in *cj1163c* gene expression in excess Cu with respect to without excess Cu. (d) Plot shows 1.5-fold change in *cj1164c* gene expression in excess Cu with respect to without excess Cu. (e) and (f) Plot shows no significant change in *cj1165* and *cj1166* gene expression, respectively. The data are the average of triplicate cultures with error bars showing SD. T-tests were performed

to check significance in difference. ($p > 0.05$, ns; $0.05 > p > 0.01$, *; $0.01 > p > 0.001$, **; $0.001 > p > 0.0001$, ***; $0.0001 > p$, ****)

qRT-PCR result showed that *cj1161c*, *cj1162c*, *cj1163c* and *cj1164c* are increased modestly in expression in presence of excess copper, which suggests that Cu is stimulating their expression. This is again in accordance with the hypothesis that *cj1161c*, *cj1162c*, *cj1163c* and *cj1164c* gene products are involved in Cu efflux for maintaining intracellular Cu homeostasis and for cellular growth in presence of excess Cu. *cj1165c* and *cj1166c* did not show any difference in their expression.

4.2.8 Quantification of intracellular Cu content using ICP-MS:

As our hypothesis is that the products of some of these genes are responsible for maintaining Cu homeostasis by pumping out Cu, the absence of any of them should have effects on the amount of intracellular Cu. Therefore, intracellular Cu was measured in wild type, $\Delta cj1161c$, $\Delta cj1162c$, $\Delta cj1163c$, $\Delta cj1164c$, $\Delta cj1165c$ and $\Delta cj1166c$ cells grown with and without 0.25 mM excess Cu using inductively coupled plasma mass spectrometry (ICP-MS). Absence of potential Cu efflux proteins should result in more intracellular Cu accumulation in mutants than wild type.

Wild type, $\Delta cj1161c$, $\Delta cj1162c$, $\Delta cj1163c$, $\Delta cj1164c$, $\Delta cj1165c$ and $\Delta cj1166c$ cells were grown in 50 ml MHS in 250 ml conical flasks to make starter culture according to section 2.3.1. 50 ml MeM α minimal media in 250 ml conical flasks were also equilibrated in microaerobic cabinet at 42 °C shaken, 6 for each strain (3 without excess Cu and 3 with 0.25 mM excess Cu). When the starter culture reached mid exponential phase, i.e. $OD_{600} \approx 0.6$, cells were harvested and cell pellets were washed with 5 ml MeM α minimal media (equilibrated micro-aerobically in cabinets for 6 hours at 42 °C with shaking) each by gentle pipetting followed by similar centrifugation. The cell pellets were re-suspended in 6 ml MeM α minimal media (equilibrated similarly) and 1 ml was inoculated in respective MeM α minimal media containing equilibrated flask making initial $OD_{600} \approx 0.1$. Cultures were grown for 12 hours according to section 2.3.1 and growths were measured according to section 2.3.6. Cells were harvested, and ICP-MS samples were made according to section 2.8. 100 μ l of the cell suspensions were stored at 4 °C and later used to measure protein concentration by Lowry assay as described in section 2.7.5. All chemicals were freshly opened and glass spatulas used to minimise metal contamination. Samples

were left in acid overnight in fume hood and then sent to University of Sheffield ICP-MS facility to quantify amount of Cu present in the samples.

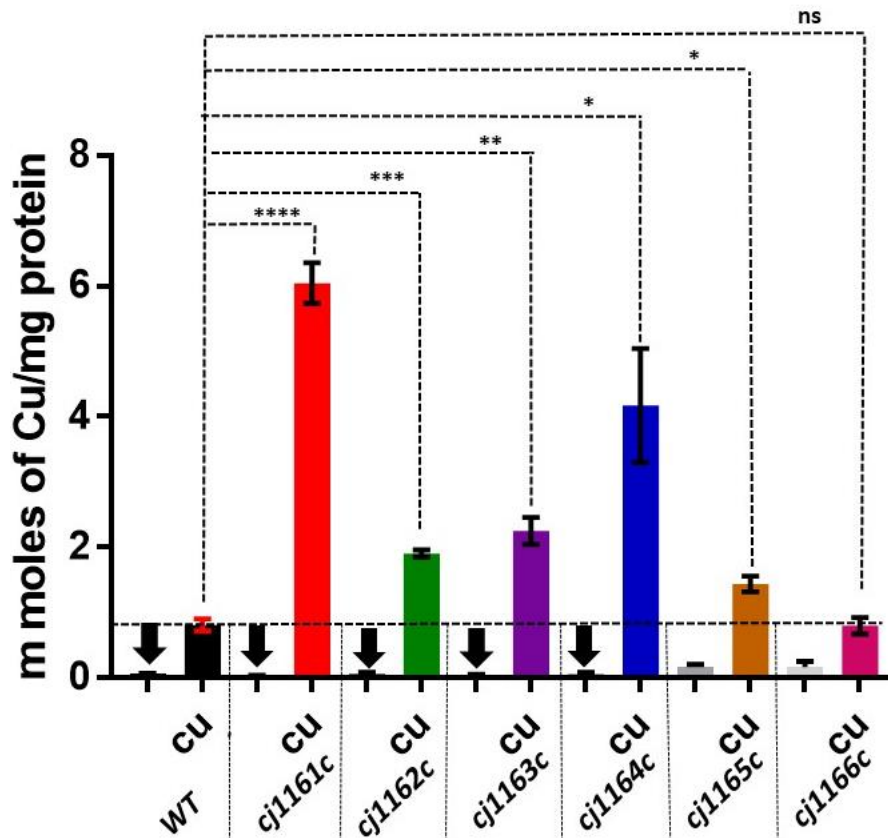


Figure 4.9: Intracellular Cu accumulation. *C. jejuni* wild type, $\Delta cj1161c$, $\Delta cj1162c$, $\Delta cj1163c$, $\Delta cj1164c$, $\Delta cj1165c$ and $\Delta cj1166c$ cells were grown separately in two conditions, either without excess Cu or with 0.25 mM excess Cu. And intracellular Cu content was measured by ICP-MS. Excess Cu condition is represented by “cu” in the plot. Protein concentration was measured by lowry assay (section 2.7.5) and results were expressed as mmoles of Cu per mg of protein. The data are the average of triplicate cultures with error bars showing SD. T-tests were performed to check significance in difference. ($p > 0.05$, ns; $0.05 > p > 0.01$, *; $0.01 > p > 0.001$, **; $0.001 > p > 0.0001$, ***; $0.0001 > p$, ****)

ICP-MS (Fig. 4.9) shows that there is no significant difference in intracellular Cu concentration of wild type and knock out mutants when cells were grown in a Cu limiting environment and that these concentrations were very low. But when cells were grown with 0.25 mM excess Cu, the intracellular Cu concentrations in *cj1161c*, *cj1162c*, *cj1163c* and *cj1164c* knock out mutants were significantly higher (by 2-6-fold) than wild type grown in a similar environment, unlike *cj1165c* and *cj1166c*

knock out mutants. This suggested that $\Delta cj1161c$, $\Delta cj1162c$, $\Delta cj1163c$ and $\Delta cj1164c$ either have no or less efficient Cu efflux system(s). This again suggested the role of $cj1161c$, $cj1162c$, $cj1163c$ and $cj1164c$ gene products in maintaining Cu homeostasis by pumping out unwanted excess Cu, which is in accordance to our hypothesis.

4.2.9 Effect of copper homeostasis on cytochrome *c* oxidase activity:

As already known, Cu is essential for bacterial cells as it is required as a co-factor for various metalloproteins (section 3.1). It was decided to check whether disruption in intracellular Cu homeostasis has any effect on cytochrome *c* oxidase (Cco) activity, which is a metalloprotein which requires Cu as a co-factor. Therefore, Cco activity was measured in wild type and $\Delta cj1161c$, $\Delta cj1162c$ and $\Delta cj1163c$ cells by measuring rate of respiration using Clark-type oxygen electrode as described in section 2.11 using TMPD as mediator and ascorbic acid as electron donor..

Clark-type oxygen electrode was assembled on the day of assay and zero-oxygen baseline was determined by the addition of sodium dithionite, as described in section 2.11. Cells were grown as described in section 4.2.5 to mid exponential phase, i.e. $OD_{600} \approx 0.15$, in 5 ml MeM α minimal media in 6-well plates with and without 0.25 mM excess Cu. 2 ml cell cultures were harvested and re-suspended in 200 μ l filter sterilised ice cold 20 mM Sodium Phosphate buffer (pH 7.4) by gentle pipetting (section 2.11). Samples were made fresh on the day of experiment and stored on ice throughout the assay. All experiments were done in biological triplicates. Whole cells were used for measuring rate of respiration and protein concentrations in cells were determined by Lowry assay (section 2.7.5) for normalisation.

Readings were recorded using LabScribe v3 software, which took readings in form of volts vs time on a XY plane. Slope for each samples were calculated ($V_2 - V_1 / T_2 - T_1$) and Lowry assay gave the protein concentration for each samples. Results were calculated as nmol of O₂ consumed per minute per mg of protein in samples.

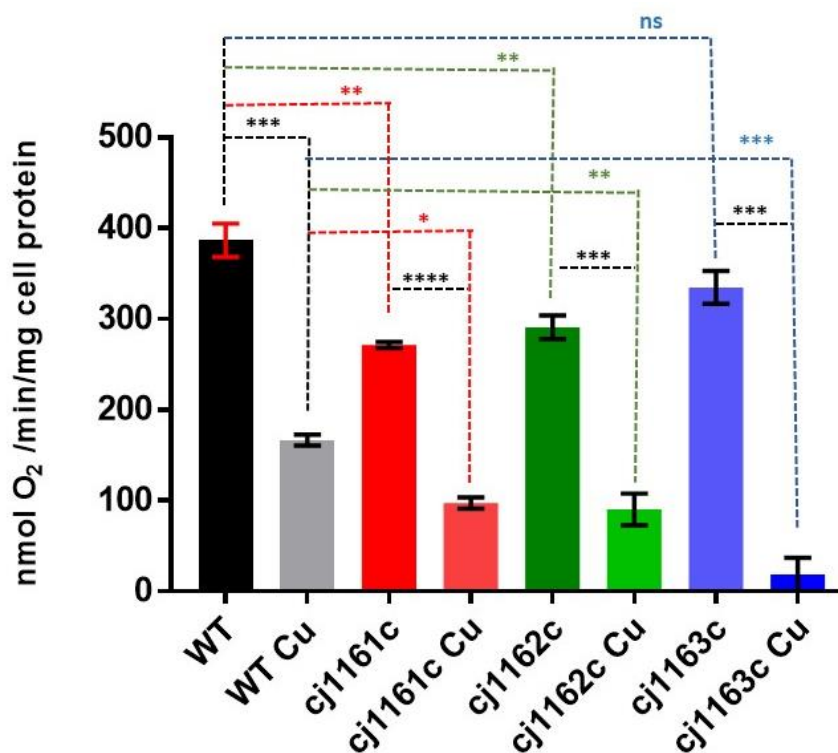


Figure 4.10: Cytochrome *c* oxidase activity. *C. jejuni* wild type, $\Delta cj1161c$, $\Delta cj1162c$ and $\Delta cj1163c$ cells were grown in 5 ml MeM α minimal media in 6-well plate, 3 wells with and other 3 wells without excess 0.25 mM Cu till OD₆₀₀≈0.15 (section 4.2.5) and cytochrome *c* oxidase activity was measured with 25 μ M TMPD and 100 μ M ascorbic acid. Excess Cu condition is represented by “Cu” in the plot. Protein concentration was measured by lowry assay (section 2.7.5) and results were expressed as m moles of Cu per mg of protein. The data are the average of triplicate cultures with error bars showing SD. T-tests were performed to check significance in difference. ($p > 0.05$, ns; $0.05 > p > 0.01$, *; $0.01 > p > 0.001$, **; $0.001 > p > 0.0001$, ***; $0.0001 > p$, ****)

Assays (Fig. 4.10) showed that *cj1161c*, *cj1162c* and *cj1163c* knock out mutants have significantly lower *cbb₃*-type oxidase activity (which uses Cu as co-factor) than wild type cells. Also, the activity is significantly reduced in wild type and all mutants when the cells were grown in high Cu containing environment. This suggested that disruption in intracellular Cu homeostasis as well as availability of Cu in the bacterial growth environment affects the activity of this Cu-containing metalloprotein.

4.2.10 Zinc, Cobalt and Nickel sensitivity of a putative Zn-Co-Ni transporter:

As Cj1163 is homologous to potential Zn-Co-Ni transporters, $\Delta cj1161c$ and $\Delta cj1163c$ mutants were also characterised for zinc, cobalt and nickel sensitivity with

respect to wild type. If Cj1163 belongs to a family of Zn-Co-Ni transporters and has role in intracellular Zn, Co and Ni homeostasis then cells lacking this protein should show more sensitivity to Zn, Co and Ni.

50 mM stock solutions of each of zinc, cobalt and nickel, were made by dissolving zinc sulphate, cobalt sulphate and nickel sulphate, respectively, in dH₂O and filter sterilised. *C. jejuni* wild type, $\Delta cj1161c$ and $\Delta cj1163c$ cell starter cultures were grown in MHS till mid exponential phase ($OD_{600}=0.6$) as described in section 4.2.5. Cells were harvested and inoculated in equilibrated 5 ml MeM α minimal media (section 2.3.2) in 6-well plates substituted with 0, 0.02 mM, 0.04 mM, 0.06 mM, 0.1 mM, 0.2 mM, 0.3 mM, 0.4 mM, 0.6 mM and 1.0 mM of Zn, Co or Ni making initial $OD_{600}\approx 0.1$. All experiments were done in triplicates. Cells in 6-well plates were grown for 12 hours according to section 2.10.1 and growths were measured according to section 2.3.6.

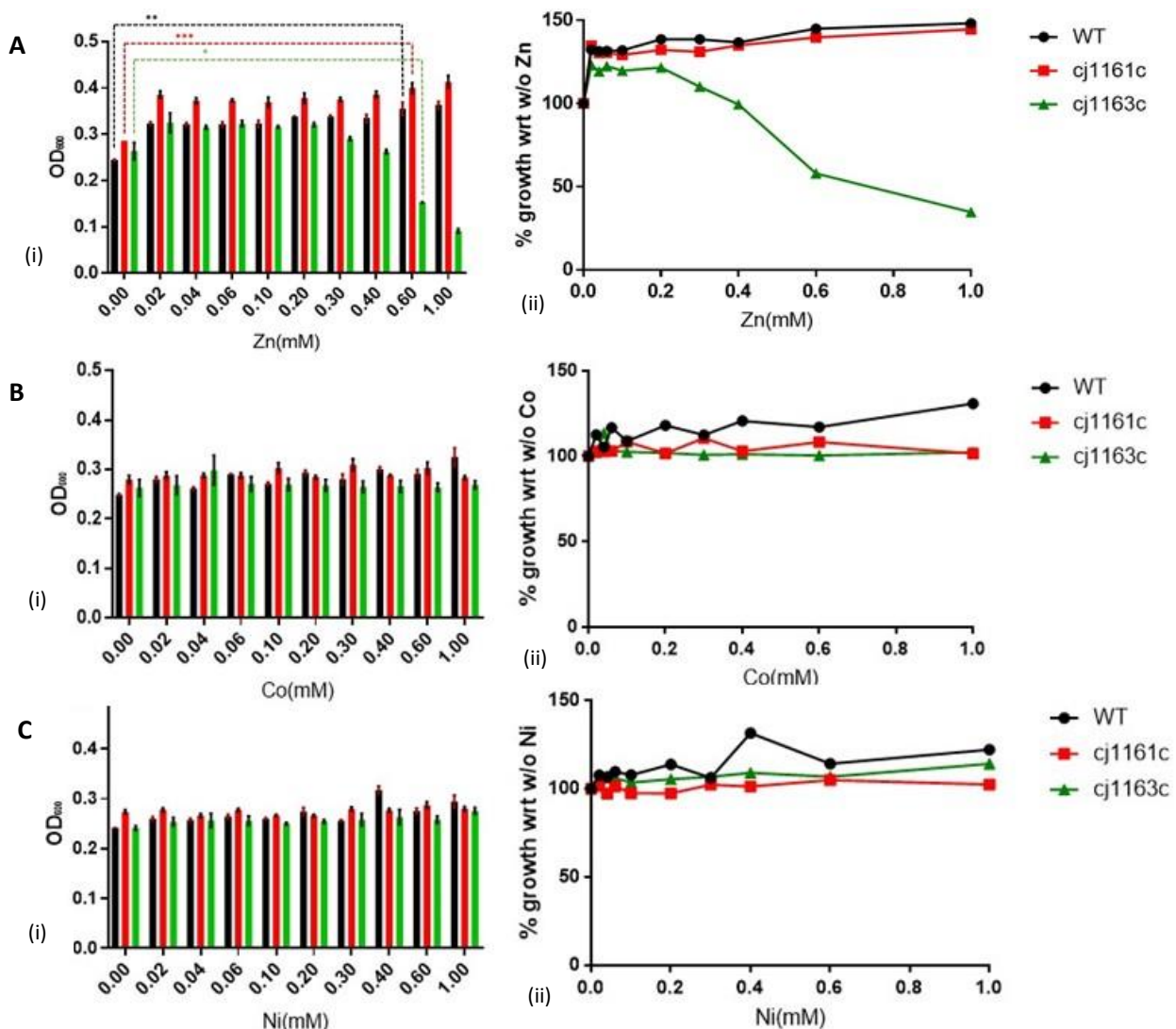


Figure: 4.11: Zn-Co-Ni sensitivity assay for mutant lacking Cj1163. Assay was performed by growing *C. jejuni* wild type, $\Delta cj1161c$ and $\Delta cj1163c$ strains in 5 ml MeMa minimal media in 6-well plates substituted with different concentrations (0.0, 0.02, 0.04, 0.06, 0.1, 0.2, 0.3, 0.4, 0.6, 1.0 mM) of Zn, Co or Ni for 12 hours in microaerobic cabinet at 42 °C. Culture growths were measured by measuring OD₆₀₀. (i) Growth of WT, *cj1161c* and *cj1163c* knock out mutant at different concentrations of **A** Zn, **B** Co and **C** Ni. (ii) Growth of WT, *cj1161c* and *cj1163c* knock out mutants normalised with growth without **A** Zn, **B** Co and **C** Ni being the control, i.e. 100%, at different concentration of **A** Zn, **B** Co and **C** Ni, respectively. The data are the average of triplicate cultures with error bars showing SD. T-tests were performed to check significance in difference. ($p > 0.05$, ns; $0.05 > p > 0.01$, *; $0.01 > p > 0.001$, **; $0.001 > p > 0.0001$, ***; $0.0001 > p$, ****).

Growth is stimulated in all cases initially because minimal media lacks optimum amount of Zn, Co or Ni required by the bacteria for various metabolic activities (Fig. 4.11). The *cj1163c* knock out mutant is much more sensitive to Zn than wild type, but not to Co and Ni. This mutant is more sensitive to Cu as well

(section 4.2.5). This suggested that the protein expressed by this gene has a potential role in maintaining Cu as well as Zn homeostasis in bacterial cells. ICP-MS result also showed high amount of Zn in *C. jejuni* cells lacking Cj1163 (Figure 4.12).

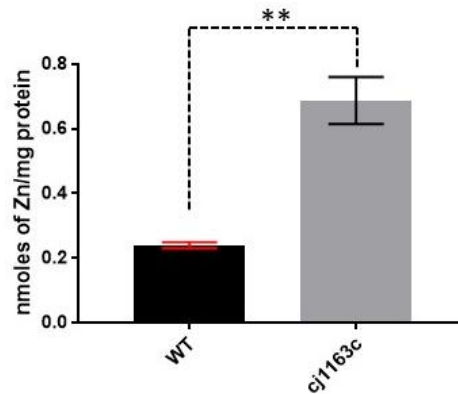


Figure 4.12: Intracellular Zn accumulation. *C. jejuni* wild type and $\Delta cj1163c$ cells were grown separately in MeM α minimal media and intracellular Zn content was measured by ICP-MS. Protein concentration was measured by lowry assay (section 2.7.5) and results were expressed as nmoles of Zn per mg of protein. The data are the average of triplicate cultures with error bars showing SD. T-tests were performed to check significance in difference. ($p > 0.05$, ns; $0.05 > p > 0.01$, *; $0.01 > p > 0.001$, **; $0.001 > p > 0.0001$, ***; $0.0001 > p$, ****)

4.3 Discussion:

In many bacteria, including Gram-negative *Rhodobacter sphaeroides*, it was reported that the *cbb₃*-type cytochrome *c* oxidase assembly proteins, homologous to bacterial Sco1 and PCu_AC, were playing role in maintaining intracellular Cu homeostasis as well (Thompson *et al.*, 2012). This was not observed in *C. jejuni* (section 3.2.7). This led to the idea that there might be some independent mechanism present in *C. jejuni* for maintaining Cu homeostasis as Cu management is crucial for the bacteria. In Hall *et al.* (2008), evidence was obtained from mutant studies that Cj1161 is a CopA homologue and a major component of the Cu homeostasis system of *C. jejuni*, but the overall Cu homeostasis mechanism has not been characterised until now. On observing the genes around *cj1161c*, it was noticed that genes from *cj1164c* to *cj1161c* were expressed by the same promoter, with all gene products containing the Cu binding motif (except Zn finger, which thermodynamically prefers to bind Cu(I)). The homology of *C. jejuni* protein Cj1161 to CopA (P-type ATPases that have a copper transporting function), Cj1162 to CopZ (containing a putative heavy metal associated protein domain), Cj1163 to potential Zn-Co-Ni transporters and Cj1164c to Zn finger proteins, inspired this study to characterise them as

potentially having role in intracellular Cu homeostasis maintenance protein system in *C. jejuni*. Cj1165c and Cj1166c are novel proteins but cells lacking these proteins didn't show any clear results regarding their role in Cu homeostasis. Therefore, this discussion is mainly focused on the phenotypes associated with *cj1161c*, *cj1162c*, *cj1163c* or *cj1164c* gene knock out mutants. It should be noted that a lower overall growth of *C. jejuni* cells in this chapter is apparent in the growth studies compared to the previous chapter 3, because cells were grown in MeMa minimal media here, unlike MHS complex media in previous chapter, and most of the essential nutrients required by cells are only available in limited amount.

In *E. coli*, disruption of *copA* made it more sensitive to Cu (Rensing *et al.*, 1999). The *Pseudomonas aeruginosa* and *Streptococcus mutans* cells lacking *copZ* were reported to be more Cu sensitive (Quintana *et al.*, 2017; Singh *et al.*, 2015). The *Streptococcus pyogenes* and *Staphylococcus aureus* cells lacking CopA or CopZ homologs were reported to be more Cu sensitive (Young *et al.*, 2015; Sitthisak *et al.*, 2007). In *C. jejuni*, Hall *et al.* (2008) has already reported that cells lacking Cj1161 were more sensitive to Cu than wildtype. In this study, the copper toxicity assays (section 4.2.5) showed that *C. jejuni* cells lacking proteins expressed by not only just *cj1161c*, but also by *cj1162c*, *cj1163c* and *cj1164c* genes (individually) were more sensitive to increasing amount of Cu in media (Figure 4.6). Increasing amount of Cu in the media should facilitate more Cu uptake of the bacterial cells growing at the constant temperature through unspecified transporters (Stahl *et al.*, 2012, Faúndez *et al.*, 2004). As the amount of Cu in the media was increased, mutants started dying at lower concentrations as compared to wildtype cells and it is already known that excess of Cu is toxic for bacterial cells and its poor management kills them by initiating the Fenton reaction by making reactive oxygen species (Section 4.1). This suggested that mutants lacking those proteins were having difficulty in efficiently processing the excess intracellular Cu. This clearly indicated, if not exclusively proved, that those proteins were necessary for maintaining the intracellular Cu homeostasis by and pumping out the unwanted excess Cu. There is no evidence of anyone exploring the effect of absence of Zn-Co-Ni transporters and Zn finger proteins on bacterial copper sensitivity. *cj1165c* and *cj1166c* knock out mutants didn't show any difference, suggesting no role of Cj1165 and Cj1166 in Cu homeostasis.

cj1162c knock out mutant showed the highest sensitivity to Cu as compared to the other mutants. It maybe because its (potential) function is to chelate unwanted Cu in the cytoplasm and transport it to Cu translocating proteins to export. It is in accordance to the fact that Cj1162 is homologous to CopZ, a metal binding Cu chelator and in absence of this Cu chelator, Cu translocating proteins will not be getting enough Cu to pump out efficiently. Hence, the cells lacking this gene are having the highest sensitivity to varying amount of Cu.

The other thing to be observed from this assay was cells lacking Cj1161, Cj1162, Cj1163 or Cj1164 did not die abruptly on increasing the Cu amount of the medium. They showed lesser and lesser growth gradually with respect to increasing amount of Cu. If the only available Cu efflux route is disrupted, then cells should die instantly at any increased amount of Cu unless they escalate their defence systems against reactive oxygen or there is an alternate protein available to substitute. This gives the hint that potentially Cj1161 and Cj1163; and Cj1162 and Cj1164 are having the similar functions, given their similar locations in the cells. This assay also gave us the threshold amount of Cu, 0.25mM, at and above which all mutants die. As the amount of Cu increases in the media, there is some stimulation in growth initially in wildtype and all mutants. This is due to the fact that MeM α minimal media doesn't have any Cu containing compound in its constituents. Theoretically, there is only contaminating Cu available for bacteria unless it is added and small amount of Cu is essential for the growth of bacteria. Whatever Cu the bacterial cells obtain in media without adding any additional Cu is actually from metal contamination, and is lower than the optimum amount of Cu needed by the bacteria.

Growth curve assays (section 4.2.6) showed that when grown in minimal media without any additional Cu, mutants showed slight growth defects compared to wildtype. But in media containing 0.25 mM additional Cu, mutants actually showed a significant growth defect, whilst there was no effect on growth of wildtype cells (Figure 4.7). This suggested that the mutants lacking Cj1161, Cj1162, Cj1163 or Cj1164 proteins were struggling to cope with excess of Cu entering the cells throughout growth. They were not as efficient as wildtype cells in managing excess Cu and the only difference being absence of one of these proteins. This again proved the involvement of these proteins in bacterial Cu resistance by managing intracellular Cu and maintaining its homeostasis. *cj1165c* and *cj1166c* knock out mutants didn't

show any significant growth defect with excess Cu, again suggesting no role of Cj1165 and Cj1166 in Cu homeostasis.

If the amount of Cu is becoming toxic to the bacteria, it should increase the expression of genes producing proteins maintaining Cu homeostasis. Rensing *et al.* (1999) showed that in *E. coli* CopA was induced by increased amount of Cu. In *Halobacterium salinarum*, Pang *et al.* (2013) reported the increased transcription of a P1-type ATPase efflux pump (VNG0700G), and two metallochaperones (VNG0702H and VNG2581H) with Cu binding sites in presence of high amount of Cu. Increase in expression of CopA and CopZ homologs were also reported in *Pseudomonas aeruginosa* (Quintana *et al.*, 2017). Hall *et al.* (2007) reported no difference in expression of *cj1161c* in *C. jejuni* on growing cells in MeM α minimal media with 50 μ M excess Cu. Quantification of gene expression by qRT-PCR (section 4.2.7) showed that *C. jejuni* cells expressed more Cj1161, Cj1162, Cj1163 and Cj1164 proteins when grown in media with additional Cu (Figure 4.8). Change in expression of these genes only by changing one factor, i.e. amount of Cu, again suggested their relationship with amount of Cu and increase in their expression on increasing amount of Cu indicated their role as working against Cu, i.e. Cu efflux. Expression of Cj1165 and Cj1166 were not affected, which is in accordance with results of previous assays.

We hypothesised that Cj1161-Cj1164 proteins are maintaining Cu homeostasis by pumping out unwanted Cu. If that is the case, in absence of any of these proteins, the intracellular Cu amount should be higher than the wildtype. Therefore, intracellular Cu amount was measured by ICP-MS. In various bacteria, like *E. coli*, *Neisseria gonorrhoeae*, *Pseudomonas aeruginosa*, *Streptococcus pyogenes*, *Halobacterium salinarum*, it was observed that the amount of intracellular Cu dramatically increased in the absence of the efflux pump, CopA (Peterson *et al.*, 2000; Djoko *et al.*, 2012; Quintana *et al.*, 2017; Young *et al.*, 2015; Pang *et al.*, 2013). In *Staphylococcus aureus*, absence of CopA or CopZ both increased the amount of intracellular Cu (Purves *et al.*, 2018). ICP-MS results (section 4.2.8) showed that when grown in similar Cu excess media, the amount of Cu in bacterial cells lacking genes expressing Cj1161, Cj1162, Cj1163 or Cj1164 was much higher than the wild type cells having all those proteins (Figure 4.9). This proved that the system responsible for pumping out excess toxic Cu from the cells was either missing or highly inefficient in mutants than wild type. Cj1161, Cj1162, Cj1163 or Cj1164 being

the only ones missing in the mutants suggested they are necessary for pumping out excess toxic Cu and maintain the intracellular homeostasis. No significant difference was observed in Cj1165 and Cj1166.

When grown in media without addition of excess Cu, we can hardly see any Cu detectable in any strain. This is due to the limitation of mass spectroscopy to detect small amounts of Cu in the sample. Similar effect was reported in *Streptococcus mutans* by Singh *et al.* (2015) and in *Streptococcus pyogenes* by Young *et al.* (2015) but without any explanation. Both *S. mutans* and *S. pyogenes*, when grown without excess Cu, no Cu was observed in wildtype or $\Delta copA$ mutant strain but when grown with 1mM excess Cu, a significantly larger amount of intracellular Cu was observed in wildtype and ~2-fold increase in the amount of intracellular copper was observed in the *copA* homolog deletion strain compared with the amount in the wild-type strain.

The relationship between Cu importers and Cco activity has been analysed in some bacteria, like *Rhodobacter capsulatus*, but there is little evidence of exploration of the relationship between Cu exporters (or homeostasis maintaining proteins) and Cco activity (Ekici *et al.*, 2015). In this study, measurement of Cco activity (Section 4.2.9) by measuring oxygen consumption showed reduced Cco activity in cells lacking Cj1161, Cj1162 or Cj1163 than wildtype (Figure 4.10). When grown with 0.25mM excess Cu, Cco activity is reduced in all, which is an interesting observation as increase in Cu concentration makes more Cu available for Cco. There must be some other phenomena working with Cco activity in this situation which needs further analysis.

The idea behind checking zinc, cobalt and nickel sensitivity was the fact that Cj1163 is homologous to Zn-Co-Ni transporters. Therefore, *cj1163c* knock out mutant was characterised against the wild type and *cj1161c* knock out mutant was used as a control as it is a part of the protein cluster investigated in this study yet not having any homology with Zn-Co-Ni transporters. The assay showed that, as expected, *cj1161c* knock out mutant has no different sensitivity to zinc, cobalt or nickel than wildtype. *cj1163c* knock out mutant has no sensitivity to cobalt or nickel with respect to wildtype, unlike zinc. The assay showed that cells lacking Cj1163 protein are more sensitive to zinc than wild type. It suggests that Cj1163 has dual role in cell. It is

involved in Cu homeostasis as well as Zn homeostasis, which is not a big surprise given their size is very similar (Cu atom has 145pm radius while Zn has 142pm radius). This leads to several questions, like how Zn and Cu compete each other for Cj1163, how efficiently Cj1163 differentiate between them to maintain their respective homeostasis, therefore, further analysis is required.

4.4 Summary and conclusion:

- Cj1161 is homologous to CopA, Cj1162 to CopZ, Cj1163 to potential Zn-Co-Ni transporters and Cj1164c to Zn finger proteins.
- TMHMM predictions showed Cj1161 and Cj1163 are transmembrane proteins and Cj1162 and Cj1164 are non-membrane proteins.
- *cj1161c*, *cj1162c*, *cj1163c* and *cj1164c* knock out mutants showed more sensitivity to Cu than wildtype.
- *cj1161c*, *cj1162c*, *cj1163c* and *cj1164c* knock out mutants showed more growth defect in presence of excess Cu than wildtype than without added Cu.
- *cj1161c*, *cj1162c*, *cj1163c* and *cj1164c* knock out mutants showed more intracellular Cu than wildtype.
- *C. jejuni* cells expressed more Cj1161, Cj1162, Cj1163 and Cj1164 proteins in presence of excess Cu.
- Above observations in this study led to the conclusion that proteins expressed by *cj1161c*, *cj1162c*, *cj1163c* and *cj1164c* in *C. jejuni* are responsible for maintain intracellular homeostasis by pumping out excess unwanted Cu. This helped me to develop a *C. jejuni* intracellular Cu homeostasis model as follows:

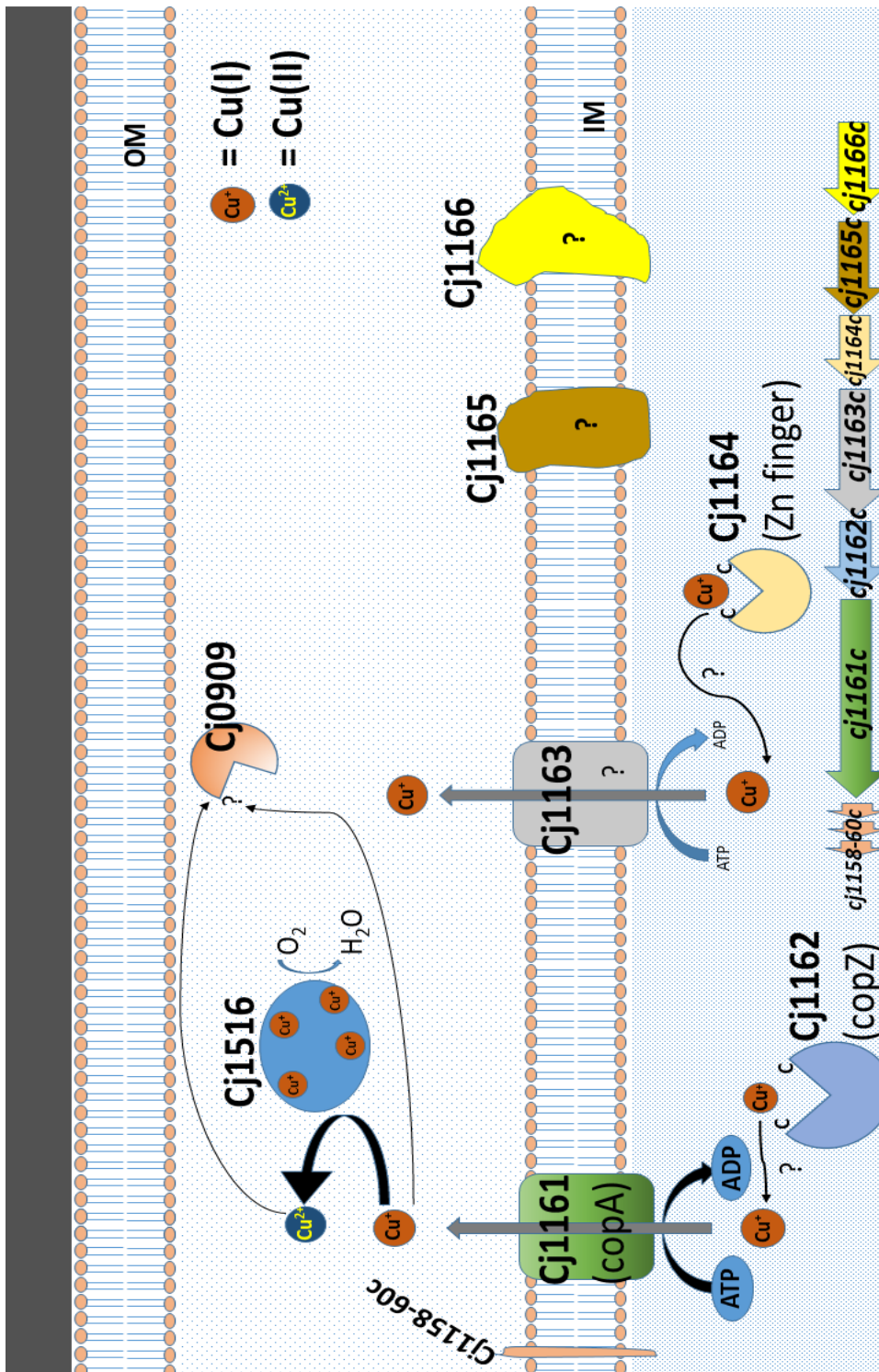


Figure 4.13: Copper homeostasis system in *C. jejuni*. Cj1161 and Cj1163 are the transmembrane Cu translocating proteins. Cj1162 and j1164 are the cytoplasmic Cu chaperons. Cj1165 and Cj1166 are the inner membrane proteins with unknown functions. Cj1162 and Cj1164 capture unwanted excess Cu in the cytoplasm and transport it to Cj1161 and Cj1163, where it gets pumped out. This pumped out Cu may be captured by multicopper oxidase, Cu chaperons working for some metalloproteins, etc in periplasm. OM stands for outer membrane. IM stands for inner membrane.

Fig. 4.13 shows the overall system of Cu homeostasis in *C. jejuni* based on results of this chapter. Cj1161 and Cj1163 are the transmembrane Cu translocating proteins, whose functions are to pump out Cu from cytoplasm to periplasm delivered to them by Cu chaperones. Cj1162 and j1164 are the cytoplasmic Cu chaperones,

whose role is to collect unwanted excess Cu from cytoplasm and transporting them to Cj1161 and Cj1163, respectively. Cj1165 and Cj1166 are the inner membrane proteins with unknown functions. Therefore, in short, Cj1162 and Cj1164 capture unwanted excess Cu before it turns toxic in the cytoplasm and transport it to Cj1161 and Cj1163, where it gets pumped out, hence maintaining the intracellular Cu homeostasis. This pumped out Cu may be captured by multicopper oxidase, Cu chaperones working for some metalloproteins, etc in periplasm.

Chapter 5: Bacterial periplasmic nitrate and trimethylamine-N-oxide respiration coupled to menaquinol-cytochrome c reductase (Qcr): Implications for electrogenic reduction of alternative electron acceptors.

Garg N., Taylor A.J., and Kelly D.J. (2018). Scientific Reports. 8(1), 15478. doi: 10.1038/s41598-018-33857-2.

Supplementary information for this published manuscript can be found online at: https://static-content.springer.com/esm/art%3A10.1038%2Fs41598-018-33857-2/MediaObjects/41598_2018_33857_MOESM1_ESM.pdf

Preface:

Reduction of TMAO to TMA and nitrate to nitrite by TorA and NapA reductases, respectively, is known to occur in *C. jejuni*. Previously it was supposed that the Tor and Nap systems receive electrons directly from the quinone pool but with little experimental evidence. It is widely known that the quinol-cytochrome *c* reductase complex (QcrABC) mediates the transfer of electrons from the menaquinone pool to cytochrome *c* to be further delivered to the terminal *cbb₃*-type cytochrome *c* oxidase. In this paper, it is shown that the QcrABC also mediates the transfer of electrons from the menaquinone pool to Nap and Tor reductases in an electrogenic, energy-conserving manner and supports growth of *C. jejuni* in oxygen limited conditions.

Author contribution:

Mutagenesis for construction of *qcrABC* deletion mutant followed by total membrane preparation, SDS-PAGE and haem blotting for verification of *qcrABC* deletion mutant were performed by Nitanshu Garg (N.G.). RT-PCR to verify expression of *cfa* gene and absence of *qcr* gene transcription in the *qcrABC* mutant was performed by Aidan J. Taylor (A.J.T.). Measurement of rate of respiration, growth curves and measurement of accumulation of ROS for phenotypic analysis of a *qcrABC* deletion mutant grown under microaerobic conditions were performed by N.G. Comparison of growth of wild-type and *qcrABC* strains on fumarate, nitrate and TMAO under oxygen-limited conditions were performed by N.G. Measurement of

nitrite concentration and sample preparation for measurement of TMA accumulation by NMR were done by N.G. and NMR was performed by Mrs. Andrea Hounslow in the departmental biomolecular NMR facility. CccB (Cj1020) and CccC (Cj0037) knock out mutants were made by Dr. Yang Wei Liu. The oxygen-limited growth curves for *c*-type cytochromes CccB (Cj1020) and CccC (Cj0037) knock out mutants with fumarate, nitrate and TMAO were performed by N.G. David J. Kelly (D.J.K.) wrote the manuscript with N.G. and A.J.T. contributing the material and methods section. N.G., A.J.T. and D.J.K. edited and reviewed the text.

SCIENTIFIC REPORTS



OPEN

Bacterial periplasmic nitrate and trimethylamine-N-oxide respiration coupled to menaquinol-cytochrome *c* reductase (Qcr): Implications for electrogenic reduction of alternative electron acceptors

Nitanshu Garg, Aidan J. Taylor & David J. Kelly

The periplasmic reduction of the electron acceptors nitrate ($E_m +420$ mV) and trimethylamine-N-oxide (TMAO; $E_m +130$ mV) by Nap and Tor reductases is widespread in Gram-negative bacteria and is usually considered to be driven by non-energy conserving quinol dehydrogenases. The *Epsilonproteobacterium Campylobacter jejuni* can grow by nitrate and TMAO respiration and it has previously been assumed that these alternative pathways of electron transport are independent of the proton-motive menaquinol-cytochrome *c* reductase complex (QcrABC) that functions in oxygen-linked respiration. Here, we show that a *qcrABC* deletion mutant is completely deficient in oxygen-limited growth on both nitrate and TMAO and is unable to reduce these oxidants with physiological electron donors. As expected, the mutant grows normally on fumarate under oxygen-limited conditions. Thus, the periplasmic Nap and Tor reductases receive their electrons via QcrABC in *C. jejuni*, explaining the general absence of NapC and TorC quinol dehydrogenases in *Epsilonproteobacteria*. Moreover, the specific use of menaquinol ($E_m -75$ mV) coupled with a Qcr complex to drive reduction of nitrate or TMAO against the proton-motive force allows the process to be electrogenic with a $H^+/2e^-$ ratio of 2. The results have general implications for the role of Qcr complexes in bacterial oxygen-independent respiration and growth.

The cytochrome *bc*₁ complex (referred to as Complex III in eukaryotic mitochondria) is a highly conserved proton-translocating, quinol-cytochrome *c* reductase (Qcr) that has a major role in oxygen-linked respiration in phylogenetically diverse prokaryotes¹. The core of the complex consists of the membrane bound Rieske Fe-S protein and a dihaem *b* containing cytochrome, combined with a membrane anchored *c*-type cytochrome facing the extracytoplasmic side of the cytoplasmic membrane. The complex functions via an electron bifurcating proton-motive Q-cycle that couples electron transfer from the quinol pool to periplasmic electron acceptors with proton translocation across the cytoplasmic membrane². In one cycle, for every two electrons transferred, four protons are released to the extracytoplasmic side (p-phase) of the membrane and two protons are taken up from the cytoplasmic side (n-phase). The mechanistically similar cytochrome *b*₆*f* complex operates in chloroplasts and cyanobacteria, and connects the two photosystems of oxygenic photosynthesis¹.

In mitochondria, and most lineages of Gram-negative bacteria where it is present, including the *Alpha- Beta-* and *Gamma*proteobacteria, the *c*-type cytochrome associated with the Qcr complex is a monohaem protein in the *c*₁ family, that donates electrons to small soluble periplasmic *c*-type cytochromes which act to shuttle electrons to the terminal cytochrome *c* oxidase. However, uniquely in *Epsilonproteobacteria*, including the pathogens *Campylobacter jejuni* and *Helicobacter pylori* and the rumen bacterium *Wolinella succinogenes*, this cytochrome is a dihaem protein, a member of the cytochrome *c*₄ family³. Phylogenetic and sequence/structure analysis suggests

Department of Molecular Biology and Biotechnology, The University of Sheffield, Firth Court, Western Bank, Sheffield, S10 2TN, UK. Correspondence and requests for materials should be addressed to D.J.K. (email: d.kelly@sheffield.ac.uk)

a mutational induced collapse of the dihaem structure during evolution has resulted in the cytochrome c_1 type of molecule³. High GC Gram-positive bacteria also have a dihaem cytochrome c associated with the Rieske/cytochrome b core. In these latter bacteria, soluble c -type cytochromes are absent; instead the oxidase interacts directly to form a “super-complex” that couples quinol oxidation with oxygen reduction^{4–6}.

There are a few important examples where, in addition to its role in cytochrome c oxidase linked oxygen respiration, the bc_1 complex can mediate electron transport to periplasmic reductases. The best studied of these are in denitrifying bacteria, such as *Paracoccus denitrificans*, where the nitrous oxide reductase (Nos), nitric oxide reductase (Nor) and the copper- or cd_1 -type of nitrite reductases all receive their electrons by a cytochrome bc_1 dependent route, via either cytochrome c or a small copper protein acting as an electron shuttle^{7–9}. In addition, many Gram-negative bacteria have a periplasmic cytochrome c peroxidase that is commonly dependent on the cytochrome bc_1 complex¹⁰. Genomic studies have revealed that some bacteria have genes for multiple separate Qcr type complexes, although their physiological roles are largely unknown¹¹.

The presence of a Rieske/cytochrome b core complex containing the atypical dihaem cytochrome c_4 in *Epsilonproteobacteria*³ is of interest in relation to possible alternative functions of this complex in this group of bacteria. Recently, it was shown that in *W. succinogenes*, nitrate respiration via the periplasmic Nap reductase was unexpectedly severely inhibited in a mutant missing the Qcr complex¹². This conflicts with the current model of nitrate reduction by the active site subunit NapA, which is based on electron transfer from menaquinol through the membrane associated NapGH subunits acting as a quinol dehydrogenase^{13,14}.

In this study, we sought to clarify the role of the Qcr complex in the important *Epsilonproteobacterium C. jejuni*, which is the commonest cause of bacterial food-borne gastroenteritis in many countries¹⁵. This bacterium has a microaerophilic lifestyle and colonises the caeca of chickens to high levels; it infects humans mainly through consumption of undercooked poultry¹⁶. In addition to the use of oxygen as a preferred electron acceptor, various strains of *C. jejuni* can reduce fumarate, nitrate, nitrite, TMAO/DMSO, tetrathionate and hydrogen peroxide and many of these can support growth under severely oxygen-limited conditions^{17–20}. Whether completely anaerobic growth occurs is controversial^{17,21} but due to the presence of a single oxygen-requiring ribonucleotide reductase essential for DNA synthesis¹⁷, a small amount of oxygen seems necessary for viability.

Although the assembly, composition and functions of the electron transport chains of *C. jejuni* have been clarified in recent years^{22–24}, it has been assumed, based on models developed in other bacteria, that the major function of the proton-translocating Qcr complex is in oxygen-linked respiration. Here, we provide evidence from mutant studies for a hitherto unappreciated role for QcrABC in both nitrate and TMAO respiration. The results provide a rationale for the puzzling absence of the membrane bound quinol dehydrogenases NapC and TorC, that are essential for periplasmic nitrate and TMAO reduction respectively, in many other bacteria (e.g. *E. coli*), that lack a Qcr complex. Moreover, we show that by the use of menaquinol ($E_m -75$ mV) as the electron donor to Qcr, the periplasmic reduction of nitrate, TMAO and certain other electron acceptors e.g. tetrathionate, can be an electrogenic process.

Results

Isolation and characterisation of a *qcrABC* deletion mutant. The genes *cj1186c-cj1184c* are operonic and encode the Rieske FeS subunit, the dihaem cytochrome b subunit and the dihaem cytochrome c subunit, respectively, of the Qcr complex in *C. jejuni* (Fig. 1A). Although currently annotated as *petABC* (due to their homology with the *Rhodobacter* photosynthetic electron transport genes encoding a typical cytochrome bc_1 complex), we propose that the *qcrABC* designation be used, as this more accurately reflects their function in this non-photosynthetic bacterium. QcrA and QcrB are similar to many other related homologues, with one transmembrane helix and nine transmembrane helices respectively, while QcrC is predicted to have two transmembrane helices and is significantly larger (41.4 kDa) than the *W. succinogenes* homologue (31.7 kDa).

The *qcrABC* genes were deleted from the chromosome of *C. jejuni* NCTC 11168 using allelic exchange via a plasmid containing upstream and downstream flanking regions for recombination and where the coding regions were replaced with a non-polar kanamycin resistance cassette with an outward reading promoter²⁵ (Fig. 1A). Small colonies that developed on selective plates were shown to have the correct genotype by PCR with flanking primers (Table 1). Despite repeated attempts, we were unable to obtain a complemented strain with the wild-type *qcrABC* genes integrated at a distal locus. However, RT-PCR showed that transcription of the *qcrA*, *qcrB* and *qcrC* genes was absent in the mutant, and that the *cfa* gene, immediately downstream of the *qcrABC* operon, was not significantly altered in expression in the mutant compared to wild-type (Fig. 1B). To further confirm the phenotype of the *qcrABC* mutant, total membranes were prepared by differential centrifugation and subjected to haem blotting as described in Experimental Procedures, to specifically detect c -type cytochromes. Figure 1C shows a band of ~42 kDa consistent with size of QcrC (41.4 kDa) is present in wild-type membranes but missing in the *qcrABC* strain (the full size blot can be viewed in Supplementary Fig. 1).

Comparison of oxygen respiration and microaerobic growth phenotypes of *qcrABC* and *ccoNOQP* mutants: Deletion of *qcrABC* causes accumulation of ROS. Cells of WT, *qcrABC* and a *ccoNOQP* deletion strain²⁴, were grown in complex media under standard microaerobic conditions and the specific rate of oxygen consumption in cell suspensions compared, with formate as electron donor. Figure 2A shows that the *qcrABC* and *ccoNOQP* strains had similar rates of formate-linked oxygen respiration but these were 58% and 68% lower respectively compared to the wild-type parent. These results are consistent with electron flux proceeding through the Qcr complex to CcoNOQP, thus giving a similar rate when the cognate genes of either complex are deleted, with the remaining rate being due to oxygen reduction by the alternative Qcr-independent CioAB menaquinol oxidase.

Figure 2B shows growth curves for wild-type, *qcrABC* and *ccoNOQP* strains under microaerobic conditions in complex media with no added exogenous electron acceptors. It is clear that the *qcrABC* strain has a severe

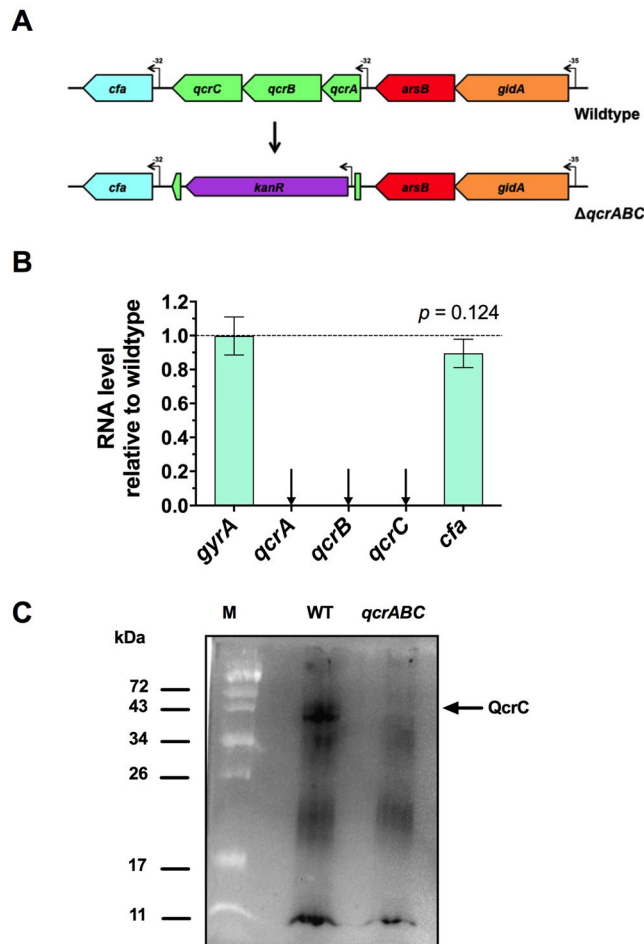


Figure 1. Construction and verification of a *qcrABC* deletion mutant. **(A)** Mutagenesis strategy. The majority of the coding regions of the *qcrA-C* genes were replaced with a kanamycin resistance cassette with its own promoter. The downstream *cfa* gene has its own promoter, but the cassette has no terminator and so should be non-polar on *cfa*. **(B)** RT-PCR to verify expression of *cfa* gene and absence of *qcr* gene transcription in the *qcrABC* mutant. Fold-change in the mutant is shown relative to the wild type strain, using *gyrA* gene as a control. The difference between expression of the *cfa* gene in mutant and wild-type was not significant by t-test. **(C)** shows a comparison of the membrane associated *c*-type cytochromes revealed after a total membrane preparation was subjected to SDS-PAGE and electroblotting to a nitrocellulose membrane, followed by staining for haem-associated peroxidase activity using the chemiluminescence technique described in Methods. 20 μ g total protein was run per lane. The Image shown is a cropped version of the full-size blot that can viewed in Supplementary Fig. 1, and was obtained using a ChemiDoc XRS system (BioRad Inc) with an exposure time of 2 min. A band corresponding to the expected size of QcrC is missing in the *qcrABC* deletion mutant.

growth defect, with a low final cell yield and doubling time of ~6 h in exponential phase compared to ~3.5 h for the wild-type. Interestingly, this is much slower than the *ccoNOQP* deletion mutant (~4.5 h doubling time), which receives electrons from the Qcr complex. We hypothesised that major disruption to the electron transport chain by removal of the Qcr complex might cause an accumulation of reactive oxygen species (ROS), particularly because the two periplasmic cytochrome *c* peroxidases in *C. jejuni* (Cj0020 and Cj0358) are thought to be dependent on the Qcr complex^{10,22}. This was tested using the fluorescent ROS sensitive dye 2',7'-dihydrochlorofluorescein diacetate (H2DCFDA). We found much higher levels of ROS production in the *qcrABC* strain compared to wild-type when cells were resuspended and incubated in oxygenated buffer (Fig. 2C). Our previous studies using the same method have shown that the same *ccoNOQP* deletion mutant used here does not accumulate ROS above WT levels under these conditions²⁴.

Nitrate and TMAO dependent oxygen-limited growth and respiration requires the QcrABC complex. Under oxygen-limited conditions in static broth cultures, we have previously shown that growth of *C. jejuni* NCTC 11168 is dependent on the addition of a range of alternative electron acceptors including fumarate ($E_m + 30$ mV), nitrate ($E_m + 420$ mV) or TMAO ($E_m + 130$ mV)^{17,18}, although growth yields under these conditions are poor compared to microaerobic growth. There are two fumarate reductases present in *C. jejuni*, a menaquinol:fumarate reductase (FrdABC complex) and a methylmenaquinol:fumarate reductase (MfrABE complex) and thus electrons pass directly from the (methyl)menaquinol pool to fumarate via these enzymes^{19,26}. Figure 3A

Name	Sequence 5'–3'
qcrABC_ISA_F1F	GAGCTCGGTACCCGGGGATCCTCTAGAGTCTGGAGTTTGCTTTTGTAGTTTG
qcrABC_ISA_F1R	AAGCTGTCAAACATGAGAACCAAGGAGAATGCTTCGTCTACTCTCAGATGTAGC
qcrABC_ISA_F2F	GAATTGTTTTAGTACCTAGCCAAGGTGTGCGCGTTCGTGGTCTAAATTAC
qcrABC_ISA_F2R	AGAATACTCAAGCTTGCATGCCTGCAGGTCATAAAAATCATTACCTATATCATAATGACTTTT
Kan_F	ATTCTCCTTGGTTCTCATGTTTGACAGCTTAT
Kan_R	GCACACCTTGGCTAGGTACTAAAACAATTCAT
qcr_Screen_F	TTAAAATAAGTTTTTTTGCTTTGCT
qcr_Screen_R	AGTTTTTTAAGGGTATGTTCTATTTTGT
RT1186F	GAGAGTAGACGAAGCTTTATG
RT1186R	GTTCTAAGCTCTCCATCTTG
RT1185F	GTAGATTGGCTTGATCAAA
RT1185R	CAAGTGCAGTATCTGGTTT
RT1184F	GCTGTTGAAGATACTACTTTTG
RT1184R	CGATCTTTGCAACATCTAC
RT1183F	GAAACAAACCTGCTAAATTT
RT1183R	CCTTAGCCATTTTCATCATA
RTgyrAF	ATGCTCTTTGCAGTAACCAAAAAA
RTgyrAR	GGCCGATTTACGCACCTTA

Table 1. Primers used in this study. For RT-PCR primers the designation refers to the relevant gene (e.g. RT1186F is the forward primer for *cj1186c*).

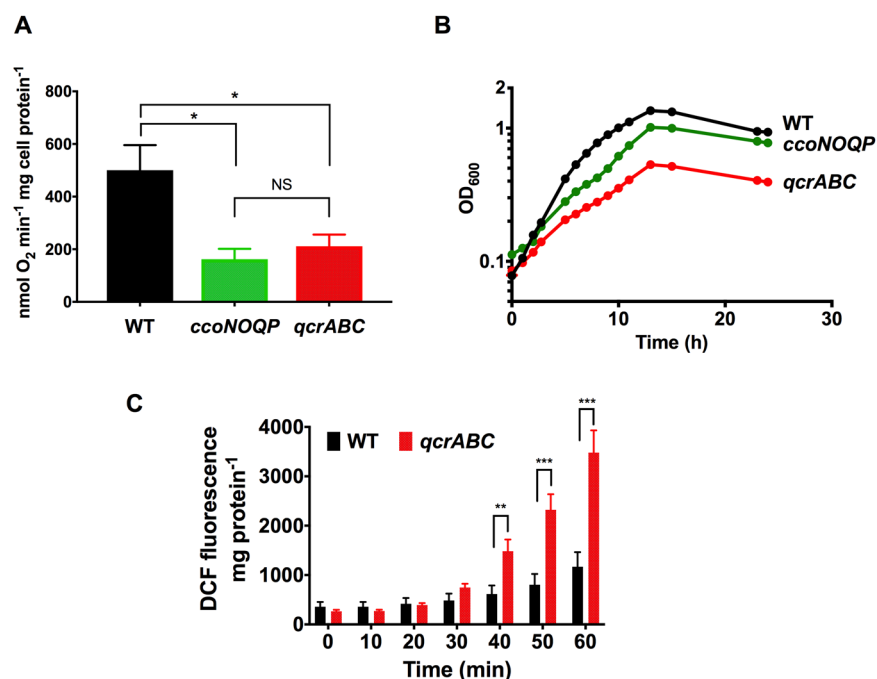


Figure 2. Phenotypic analysis of a *qcrABC* deletion mutant grown under microaerobic conditions. (A) shows the specific rate of formate dependent oxygen consumption measured by an oxygen electrode in cell suspensions of the strains indicated. About 68% of the electron flux to oxygen proceeds through the cytochrome *c* oxidase (*CcoNOQP*) and, as expected, this is similar in the *qcrABC* mutant, which is the source of electrons for *CcoNOQP*. The alternative oxidase (*CioAB*) accounts for the remaining electron flux. The data shown are means and standard deviation of triplicate determinations (* $P < 0.05$ by one way ANOVA. NS, not significant). (B) Growth curves of the strains indicated under microaerobic conditions. The *qcrABC* strain shows a larger reduction in growth rate and cell yield compared to the *ccoNOQP* mutant. The data shown are the means and standard deviations of triplicate growth curves; in most cases the error bars are too small to be seen. (C) Accumulation of ROS in microaerobically incubated cells suspensions of wild-type and *qcrABC* mutant strains. The fluorescence emission of 2',7' dihydrodichlorofluorescein diacetate (H₂D₂CFDA) added to 10 μ M final concentration is shown, normalized to total cell protein. Data are means and standard deviations of triplicate experiments. (** $P < 0.01$, *** $P = 0.001$ by multiple t-tests).

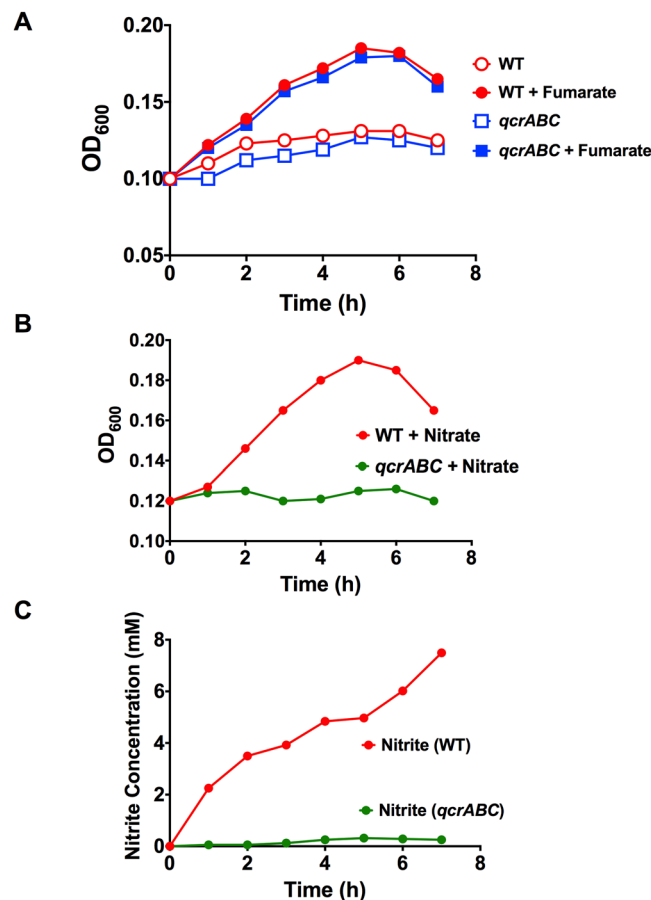


Figure 3. Comparison of growth of wild-type and *qcrABC* strains on fumarate and nitrate under oxygen-limited conditions. **(A)** growth of wild-type (red lines and symbols) and *qcrABC* mutant (blue lines and symbols) in the absence (open symbols) or presence (closed symbols) of 20 mM sodium fumarate. The mutant does not have a growth defect on fumarate, consistent with the two fumarate reductases present in *C. jejuni* deriving electrons directly from the (methyl)menaquinol pool. **(B)** growth of wild-type (red line and closed symbols) and *qcrABC* mutant (green line and closed symbols) in the presence of 20 mM sodium nitrate. **(C)** nitrite concentrations were measured in samples taken from the same growth curve as in **(B)** as described in Experimental Procedures. The data shown are single representative growth curves from several that have been performed with independent inocula. In each case similar results were obtained.

shows that growth of the *qcrABC* mutant under oxygen-limited conditions with fumarate is identical to that of the parental wild-type strain and that neither strain grows in the absence of fumarate, showing that as expected, fumarate reduction is not dependent on the Qcr complex. This is an important control and the similar growth rate of both mutant and wild-type strains under these conditions, in contrast to the marked aerobic growth defect shown in Fig. 2B, further supports the view that the *qcrABC* mutant experiences significant oxidative stress in the presence of sufficient oxygen.

However, similar experiments with nitrate (Fig. 3B) or TMAO (Fig. 4A) as exogenous electron acceptors show that, in contrast to the wild-type, the *qcrABC* mutant is unable to grow with either of these oxidants. Nitrite accumulation from nitrate (Fig. 3C) and TMA accumulation from TMAO (Fig. 4B,C) only occur to any significant extent in wild-type cells and is closely correlated with growth. Taken together, the data indicate that the Qcr complex is required for both nitrate and TMAO-dependent growth and respiration. TMAO reduction was quantified as TMA accumulation at a chemical shift of 2.88–2.89 ppm using $^1\text{H-NMR}$ spectroscopy of culture supernatants (Fig. 4B,C). During these experiments, we noted a resonance at 2.39 ppm increasing in intensity in the mutant cell supernatants, but much less in the wild-type (Fig. 4D). This peak has a natural abundance ^{13}C resonance at 36.8 ppm, which matches succinate; it accumulated to ~ 1.2 mM after 7 h in the mutant, compared to ~ 0.5 mM in the wild-type. A peak at 2.36 ppm, increased in both WT and mutant (Fig. 4D) and had a natural abundance ^{13}C peak at 29.2 ppm, matching pyruvate (~ 2 mM in both strains after 7 h).

The soluble c-type cytochromes CccB (Cj1020) and CccC (Cj0037) are not required for nitrate or TMAO reduction. Electron transfer from the Qcr complex to the Nap or Tor enzymes in the periplasm could occur either directly from QcrC, for example, or via additional periplasmic cytochromes. In *C. jejuni*, we previously identified and characterised three major periplasmic c-type cytochromes; two monohaem proteins, CccA and CccB, and the dihaem CccC²⁴. Deletion mutants in *cccB* or *cccC* show only the loss of the cognate

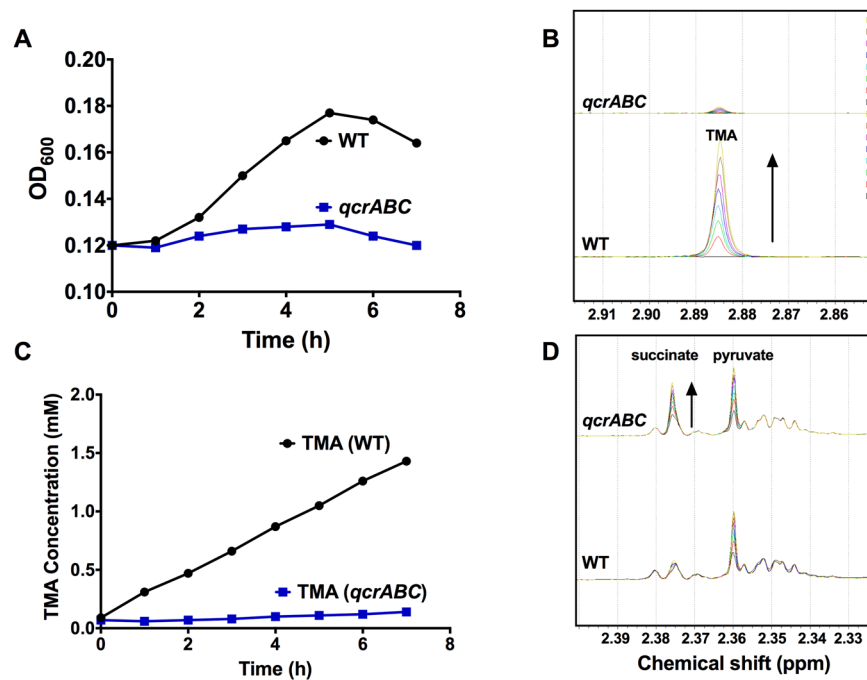


Figure 4. Growth of wild-type and *qcrABC* strains on TMAO under oxygen-limited conditions and measurement of TMA accumulation. **(A)** growth of wild-type (black line and closed symbols) and *qcrABC* mutant (blue line and closed symbols) in the presence of 20 mM TMAO. Representative growth curve of several performed which all gave similar results. **(B)** ¹H-NMR measurement of TMA accumulation during the growth curve shown in panel A. The region of chemical shift between 2.85 and 2.92 ppm is shown, with the TMA resonance at 2.885 ppm used for quantification. The different coloured spectra are media supernatants from samples taken every hour from time 0 (black spectra) to 7 h (yellow spectra), showing progressive TMA accumulation in the wild-type cells (black arrow) but no significant accumulation in the *qcrABC* mutant. The actual TMA concentrations are plotted in panel (C). Panel (D) shows the region of chemical shift between 2.32 and 2.40 ppm from the same spectra as in panel B, to illustrate the excretion of succinate (black arrow) in the *qcrABC* mutant.

cytochromes, but deletion of *cccA* leads to an unusual pleiotropic phenotype involving the loss of all detectable periplasmic *c*-type cytochromes²⁴. Therefore, we could not determine if electron transport to nitrate or TMAO requires CccA by mutant phenotypic studies. However, as Fig. 5 shows, a double *cccB cccC* mutant grows on fumarate, nitrate and TMAO under oxygen-limited conditions just as well as the wild-type, showing that neither of the soluble *c*-type cytochromes CccB or CccC are involved in electron transport to any of these electron acceptors.

Discussion

Until very recently, examples of the role of bacterial Qcr complexes in electron transport to a wider range of oxidants than just molecular oxygen was limited to hydrogen peroxide and the reduction of certain nitrogen oxides in denitrifying bacteria. The results presented here clearly show that nitrate and TMAO reduction and growth depend on electron transport through the Qcr complex in *C. jejuni*. Our data support recent experiments in the related *Epsilonproteobacterium* *W. succinogenes*, which also unexpectedly showed a dependency of nitrate reduction on the Qcr complex¹². Both bacteria possess a single periplasmic nitrate reductase of the Nap type, with the catalytic NapA subunit receiving electrons via a dihem cytochrome *c* subunit, NapB (Fig. 6). The periplasmic Nap class of nitrate reductases are very widespread in many phylogenetically diverse groups of bacteria and have been thought to be obligately coupled to quinol oxidation through the intermediacy of either the NapC class of tetrahaem quinol dehydrogenases or, in bacteria like *C. jejuni* and *W. succinogenes*, where NapC is absent, the NapGH proteins (Fig. 6), which have been proposed to form an alternative quinol dehydrogenase module^{13,14,27}. In either case, because quinol oxidation (and thus proton release) occurs on the periplasmic side of the membrane, into the same cellular compartment that nitrate reduction (and thus proton consumption) occurs, electron transfer from quinol to nitrate by this mechanism is not energy conserving^{14,28}.

The midpoint redox potential of the nitrate/nitrite couple is highly positive ($E_m + 420$ mV) and in principle nitrate reduction could be driven by either ubiquinol oxidation ($E_m + 90$ mV) with a ΔE of 330 mV, or menaquinol oxidation ($E_m - 75$ mV) with a ΔE of 495 mV. Indeed, in *E. coli*, it is thought that NapC catalyses electron transfer from menaquinol to NapB, whereas NapGH is more specific for ubiquinol²⁹. For a proton-motive Qcr-dependent mechanism of nitrate reduction, however, the redox potential of the quinol used becomes more critical as a pre-existing proton-motive force of ~ 180 mV, positive outside, exists across the cytoplasmic membrane, against which the Q-cycle mechanism has to operate. *C. jejuni* synthesises menaquinones but not ubiquinone, and so employs the energetically more favourable menaquinol dependent reduction of nitrate which, via

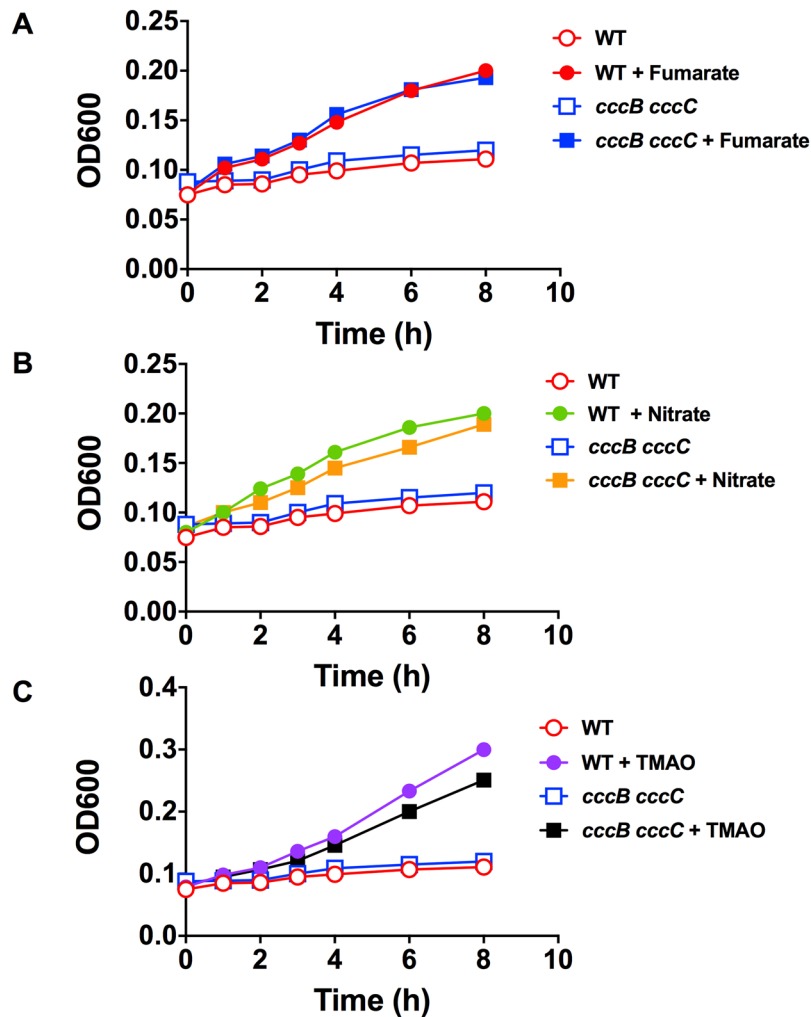


Figure 5. The *c*-type cytochromes CccB (Cj1020) and CccC (Cj0037) are not required for oxygen-limited growth on fumarate, nitrate or TMAO. Panels (A–C) show representative growth curves of wild-type and the *cccB cccC* double mutant in static MHS media alone (open symbols) or in the presence of 20 mM sodium fumarate (closed symbols in A), 20 mM sodium nitrate (closed symbols in B) or 20 mM TMAO (closed symbols in C). The open symbol data are controls for the electron acceptor dependent growth and are the same in each panel.

the Qcr mechanism, would be electrogenic with a net $H^+/2e$ ratio of 2 (Fig. 6). Note that recent measurements of Δp in *C. jejuni*, using a permeant cation redistribution method, gave values of ~ 100 – 120 mV³⁰, but this is an underestimate of the actual value expected for an energy transducing membrane.

Our results, and those of Hein *et al.*¹² provide a rationale for the absence of NapC in *Epsilonproteobacteria*, but call into question the proposed role of NapGH as a quinol dehydrogenase in these and other bacteria employing a Qcr-complex for nitrate reduction. Nevertheless, from previous mutant studies in *W. succinogenes*³¹ it has been established that NapG and NapH are essential for NapA dependent nitrate reduction. In *C. jejuni* *napH* is also essential for nitrate respiration and deletion of *napG* is highly deleterious¹⁸, with residual growth thought to be due to the ability of the quinol dehydrogenase of the nitrite reductase (NrfH) to donate electrons to NapB¹⁸. NapG and NapH are possibly involved after electrons leave the Qcr complex, but the route by which electrons might be transferred to them requires investigation. NapG is membrane bound but facing the periplasm, with several FeS redox centres and so direct transfer from the quinol oxidase site in QcrB or the periplasmically located *c*-haems in QcrC are both possible. However, in the light of our current results, we think it more likely that QcrC can donate electrons directly to NapB and that NapGH has some other role (Fig. 6), for example in the reductive maturation of NapA, as has been discussed previously³². Irrespective of their precise function in the process, the key bioenergetic consequence of nitrate reduction being dependent on the Qcr complex is that electron transfer from menaquinol to nitrate will be energy conserving. It should be noted that in addition to the Nap-type of nitrate reductase, evidence is also emerging for a role for the Qcr complex in nitrate reduction in *Streptomyces*, which uses the membrane bound Nar-type of enzyme³³, possibly suggesting direct Qcr-Nar electron transfer in this case.

That TMAO reduction is also Qcr dependent in *C. jejuni* now explains the long-standing puzzling observation that there is no homologue of the membrane bound pentahaem quinol dehydrogenase TorC in this bacterium^{17,22}, and it has hitherto been unclear how quinol oxidation is coupled to TMAO reduction. TorC has been

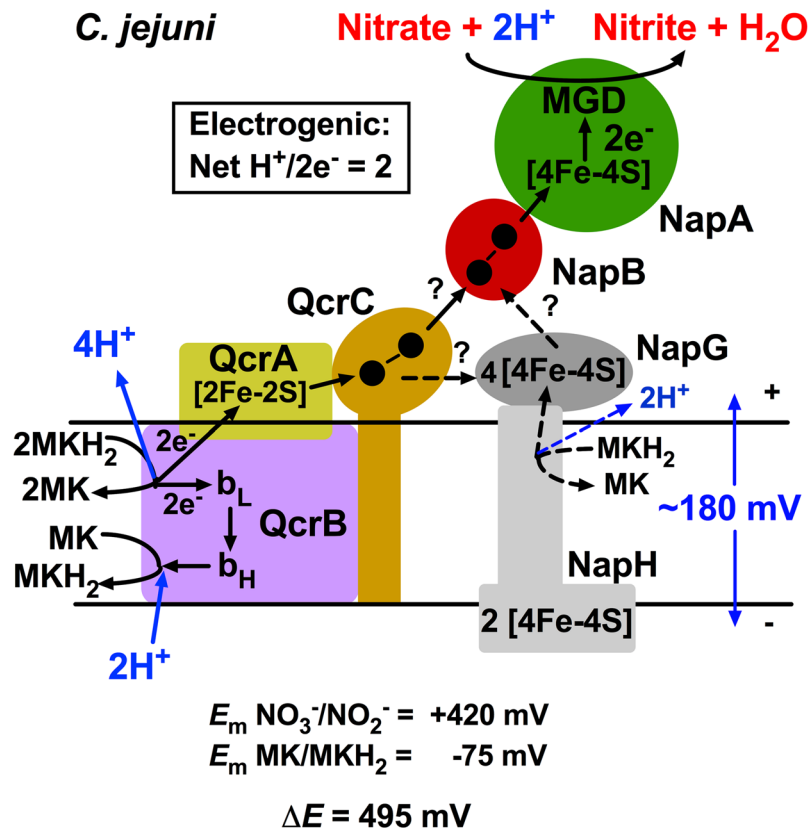


Figure 6. Model for electrogenic nitrate reduction in *C. jejuni*. The redox potential span between the MK/MKH₂ and the nitrate/nitrite couple is large enough to allow for a Qcr dependent electrogenic mechanism, given a typical transmembrane Δp of $\sim 180 \text{ mV}$. The operation of the Qcr complex directly coupled to the NapAB enzyme gives a net transmembrane proton translocation of 2 H^+ per 2 e^- transferred from menaquinol. There is uncertainty about the precise route of electron transfer from the Qcr complex to NapB (dashed arrows) but the simplest mechanism would be direct transfer from haem 2 of QcrC to haem 1 of NapB. The role of NapG and NapH, which are known to be essential for nitrate respiration, is unclear. NapG may act in the electron transfer pathway itself or NapGH may act as a quinol dehydrogenase involved in a reductive maturation process e.g. for NapA. Black filled circles in QcrC and NapB represent the haems.

characterised best in *E. coli*³⁴ and is a member of the widespread NapC/NrfH family, which are commonly tetra-haem proteins. It consists of an N-terminal membrane anchored domain, a central periplasmic domain containing the four core haem c centres and an additional C-terminal periplasmic domain containing a fifth c-type haem (Supplementary Fig. 2 and Fig. 7A). Electron transfer from TorC to the catalytic molybdoenzyme subunit TorA occurs via this fifth haem in the C-terminal domain³⁴ (Fig. 7A). Interestingly, in *C. jejuni*, TorA (Cj0264) is associated with a small soluble monohaem c-type cytochrome (TorB; Cj0265), which is absent from *E. coli*, but which is homologous to the C-terminal domain of TorC (see the alignment in Supplementary Fig. 2 and Fig. 7B). Thus, we suggest that the functions of TorB and the C-terminal domain of TorC are equivalent and that this domain has been retained as a soluble protein in bacteria like *C. jejuni* that use a Qcr-dependent mechanism of TMAO reduction, presumably to specifically receive electrons from QcrC.

What are the bioenergetic implications of a Qcr-dependent mechanism of TMAO reduction? While it is clearly unfavourable thermodynamically for ubiquinol oxidation ($E_m + 90 \text{ mV}$) to drive the reduction of TMAO ($E_m + 130 \text{ mV}$) against a typical Δp across the membrane of $\sim 180 \text{ mV}$, TMAO reduction by menaquinol ($E_m - 75 \text{ mV}$) has a ΔE of 205 mV . Although this would seemingly be close to the limit of electrogenic function for a Qcr-dependent, Q-cycle mechanism across an energised membrane, the product of TMAO reduction is TMA, which is a water soluble gas which would tend to diffuse out of the system. This could help shift the equilibrium and provide a thermodynamic pull that would effectively increase the ΔE available to drive the reaction. It should be noted that *C. jejuni* also synthesises methylmenaquinone (MMK) with an E_m of -125 mV for the MMK/MMKH₂ couple; if MMKH₂ could be used to drive TMAO reduction then the ΔE increases to 255 mV . Thus, the model of TMAO reduction in *C. jejuni* we now propose (Fig. 7B) is, like nitrate reduction, electrogenic with a net $\text{H}^+/2\text{e}^-$ ratio from menaquinol oxidation of 2, whereas in *E. coli* it is 0, because TorC is a non proton-motive menaquinol dehydrogenase releasing protons into the periplasm (Fig. 7A); in the latter case, it is only at the level of the primary dehydrogenases that energy can be conserved during TMAO (or indeed Nap dependent nitrate) reduction.

We noted that ~ 2 -fold more succinate was excreted during oxygen-limited growth of the *qcrABC* mutant on TMAO, which might be a compensatory mechanism to maintain redox balance by disposing of electrons through a Qcr independent route, i.e. fumarate reduction, although the low rate did not allow any significant growth. Both

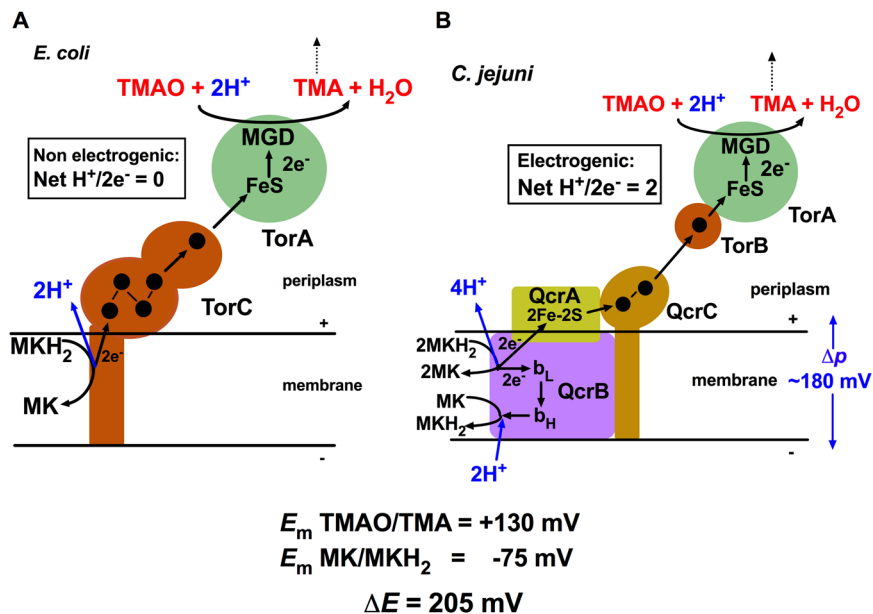


Figure 7. Comparison of the mechanism of TMAO reduction in *E. coli* and *C. jejuni*. (A) shows how quinol oxidation on the periplasmic side of the membrane in *E. coli* is coupled to electron transfer (black arrows) through the five haems in TorC (black filled circles) and the [4Fe-4S] and molybdopterin guanine dinucleotide (MGD) cofactors in TorA, ultimately reducing TMAO to TMA. Note that this mechanism is not energy-conserving ($\text{H}^+/\text{2e}^-$ transferred is 0) because proton release from quinol oxidation and proton uptake during TMAO reduction occur in the same compartment (the periplasm). (B) shows the proposed energy-conserving mechanism of TMAO reduction in *C. jejuni* coupled to the proton-motive Q cycle in the Qcr complex, which gives an overall net $\text{H}^+/\text{2e}^-$ ratio of 2. Although the redox span between menaquinol and TMAO is 205 mV, close to the typical value of $\sim 180 \text{ mV}$ for Δp , continued diffusion of TMA away from the system (dashed black arrow) would shift the equilibrium and favour electrogenic TMAO reduction. TorB (Cj0265), homologous to the C-terminal domain of TorC (see Supplementary Fig. 2), most likely receives electrons directly from QcrC (black arrows), before transfer to the redox centres in TorA. b_L , low-potential haem b ; b_H , high-potential haem b in the QcrB subunit.

wild-type and mutant excreted some pyruvate under these oxygen-limited conditions, and this has been noted previously in *C. jejuni* grown under very low oxygen availability³⁵.

Although we have focussed on the clear phenotypes of the *qcrABC* mutant in relation to nitrate and TMAO reduction under oxygen-limited growth conditions, we also noted that this mutant grew far more poorly with oxygen as electron acceptor compared to a mutant deficient in the cytochrome *c* oxidase, CcoNOQP. We hypothesised that a growth inhibiting build-up of ROS might result from removal of the Qcr complex, because of its role as electron donor to the two periplasmic cytochrome *c* peroxidases (Cj0020 and Cj0358). Measurements using a ROS sensitive dye suggested a much higher accumulation of ROS was indeed occurring in the *qcr* mutant compared to the wild-type. There may also be other reasons why ROS would accumulate in this mutant, for example if there is a reduction in its ability to properly oxidise the quinol pool and electrons are transferred to oxygen by non-physiological routes.

These new results concerning the reduction of nitrate and TMAO in *C. jejuni* not only change our overall view of the bioenergetics of this pathogen but, more generally, help to rationalise the use of menaquinol in electrogenic Qcr-dependent electron transport pathways to alternative acceptors of moderate redox potential. For example, the recent discovery of the TsdA type of bidirectional tetrathionate reductase in some strains of *C. jejuni* and many other bacteria²⁰, which is a soluble periplasmic dihaem cytochrome *c*, also suggests the involvement of the Qcr complex in this mode of tetrathionate reduction. The recent experimental determination of the midpoint redox potential of the tetrathionate/thiosulphate couple as $+198 \text{ mV}$ ³⁶ rather than the previously assumed value of $+24 \text{ mV}$, means that the redox span using menaquinol to reduce tetrathionate is 273 mV, allowing the Qcr complex to operate electrogenically against the Δp , as with TMAO and nitrate.

Nitrate, TMAO and tetrathionate are present in the mammalian host intestinal environment and there is evidence that *Salmonella* uses nitrate reduction via the Nap system³⁷ and tetrathionate reduction (in this case via the molybdoenzyme Ttr³⁸) to gain a competitive advantage in host infection. While *torA* deletion mutants of *C. jejuni* do not show gross colonisation defects in a chicken model of colonisation, a *napA* mutant colonised at lower levels than the wild-type²¹. Given the conservation of Qcr-dependent pathways to electron acceptors other than oxygen in many *C. jejuni* strains, we suggest they are important in the infection biology of this pathogen.

Experimental Procedures

Bacterial strains, media and general culture conditions. *Campylobacter jejuni* strain NCTC 11168 was the wild-type strain used in this study. An isogenic *ccoNOQP* deletion mutant was previously constructed and described²⁴. Individual deletion mutants in *cccB* (*cj1020c::cat*) and *cccC* (*cj0037::kan*) have also been previously described and characterised²⁴; a double mutant was made by transformation of the deletion mutant plasmid pGEM1020CAT²⁴ into the *cccC* mutant. Construction of the *qcrABC* deletion mutant is described below. All strains were routinely grown on Columbia Blood Agar base CM0331 (Oxoid, Basingstoke, UK) containing 5% (v/v) lysed horse blood (SR0050C, Thermo Scientific) and 10 µg/ml each of amphotericin B and vancomycin (referred to as CBA media) at 42 °C under microaerobic conditions [10% (v/v) O₂, 5% (v/v) CO₂ and 85% (v/v) N₂] in a MACS growth cabinet (Don Whitley Scientific, Shipley, UK). Selective antibiotics (either kanamycin or chloramphenicol) were added where appropriate to a final concentration of 50 µg ml⁻¹. From plates, bacterial cells were inoculated in 50–100 ml Mueller-Hinton broth (Oxoid) plus 20 mM L-Serine (MHS) in 250 ml conical flasks. Liquid cultures for microaerobic growth were shaken at 200 rpm on a KS125 IKA-labortechnik shaker (IKA, Staufen, Germany) at 42 °C in the MACS growth cabinet as above. For oxygen-limited growth, cells were grown in 200 ml MHS in 250 ml conical flasks in the MACS growth cabinet as above, but without shaking. Where required, the electron acceptors sodium fumarate, sodium nitrate or TMAO were added to a final concentration of 20 mM from filter-sterilised stocks.

DNA manipulation and construction of a *qcrABC* deletion mutant. Chromosomal DNA of *C. jejuni* was extracted by using the wizard genomic DNA purification kit (Promega). Standard techniques were employed for the cloning, transformation, preparation and restriction analysis of plasmid DNA from *E. coli*³⁹. A plasmid vector (pGEMQCR) for allelic exchange mutagenesis of *qcrABC* was assembled using pGEM3zf (Promega), 500 bp upstream and downstream fragments flanking *qcrABC* and a kanamycin resistance cassette derived from pJM30²⁵ using the Gibson isothermal assembly method, as previously described²⁴. The two flanking fragments were PCR amplified using primers *qcr_ISA_F1F/F1R* and *qcr_ISA_F2F/F2R* (Table 1) with adapters homologous to 30 bp around the *HincII* site of the pGEM3zf multiple cloning site and 30 bp at the start or end of the kanamycin resistance cassette, which was amplified using primers *Kan_F* and *Kan_R* (Table 1). An isothermal assembly reaction was carried out at 50 °C for 1 h with equimolar amounts of both flanking fragments, kanamycin cassette and *HincII* digested pGEM3zf in a reaction master mix containing isothermal assembly buffer, T5 Exonuclease, Phusion polymerase and Taq ligase²⁴. The mixture was then transformed directly into competent *E. coli* DH5a cells with selection for kanamycin resistance. Plasmid pGEMQCR was checked by automated DNA sequencing using standard vector M13 primers. *C. jejuni* cells were grown in MHS overnight, pelleted and washed in 1 ml of ice cold wash buffer (9% (w/v) sucrose and 15% (w/v) glycerol in water), 3–4 times and finally resuspended in 200–300 µl of ice cold wash buffer. pGEMQCR was electrotransformed into these cells (2.5 kV, 200 Ohms, 25 µF; Bio-Rad Gene Pulser), which were then spread onto non-selective CBA plates. After overnight incubation, cell growth was transferred to CBA plates containing kanamycin. Colonies appeared within 2–4 days, which were PCR screened with primers *qcr_screen_F* and *qcr_screen_R* (Table 1) that anneal approximately 100 bp upstream and downstream of the *qcr* operon respectively.

RT-PCR. Aliquots (5 ml) of mid-log microaerobically grown cultures (OD_{600 nm} ~0.6) were pelleted and washed in 1 ml 20 mM sodium phosphate buffer, pH 7.4, then 5 µl phenol and 50 µl ethanol mixed in before re-pelleting. Phenol-pellets were stored at –80 °C. RNA was purified from phenol-pellets using the TRIzol Max Bacterial RNA Isolation Kit (Thermo Fisher) and subsequently DNase treated using the TURBO DNase Kit (Invitrogen), following the manufacturers protocols. The absence of contaminating DNA was confirmed by PCR screening using MyTaq Red Mix (Bioline). RT-PCR was performed using the SensiFAST SYBR kit (Bioline), with 20 µl reactions contained in 96-well plates following the manufacturers recommendations. Genomic DNA serial dilution controls were performed for each primer set to generate a standard CT curve. The RT-PCR was performed in an Mx3005P cyclor, controlled by MxPro software (Stratagene). CT values generated by the software were manually processed to generate fold RNA changes, relative to wildtype, using *gyrA* as the housekeeping control gene. DNA controls were performed in duplicate, while RNA screening reactions were performed in quadruplicate. Primers used for RT-PCR are listed in Table 1.

Microaerobic and oxygen-limited growth curves, and determination of nitrite. For comparisons of microaerobic growth, cells from overnight starter cultures in the MACS cabinet were inoculated in 200 ml MHS in 500 ml conical flasks with appropriate antibiotics to a final OD (600 nm) of 0.1 and grown at 42 °C until an OD 600 nm of approximately 0.4–0.5. They were then back diluted to an OD 600 nm of 0.1 in fresh 100 ml MHS in shaken 250 ml conical flasks and the OD 600 nm monitored every hour using Jenway 6705 UV spectrophotometer. All Growth curves were done in triplicates. For growth and supernatant sample collection under oxygen-limited conditions, cells grown microaerobically as above, were back diluted to an OD of 0.1 in fresh 200 ml MHS in 250 ml conical flasks, with and without TMAO, nitrate or fumarate, and OD 600 nm monitored every hour. Cells in 1 ml samples were separated from the media supernatant by centrifugation (13,800 × g, 5 min) and the supernatants removed and stored frozen at –20 °C until ready for analysis. For nitrite determination, diluted culture supernatants (50 µl) from oxygen-limited growth experiments were added to 850 µl of 1% (w/v) sulphanilamide (Sigma) dissolved in 1 M HCl and 100 µl of 0.02% (w/v) naphthylethylenediamine (Sigma). After 15 min, the absorbance at 540 nm was measured and nitrite concentrations were determined by reference to a standard curve.

¹H and ¹³C-NMR. For analysis of TMAO reduction, trimethylamine (TMA) concentrations in supernatant samples were quantified by ¹H-NMR. To 800 µl of sample 10 µl of 100 mM trimethylsilyl propionate (TSP) was added as a 0 ppm chemical shift and quantitation reference. 450 µl of the mixture was transferred to NMR tubes,

50 μ l of D₂O was added and spectra acquired as described by Sellars *et al.*¹⁷. Integration of the single peak of TMA at 2.88–2.89 ppm and comparison with the TSP peak allowed TMA concentrations to be calculated. The ¹³C chemical shifts of succinate and pyruvate were obtained from a 2D ¹H–¹³C HSQC spectrum, acquired with the standard Bruker pulse program, hsqcetgpsisp2, on an 800 MHz Avance I NMR spectrometer. The data were acquired with 2048 points in the direct dimension and 300 complex points in the indirect dimension, 64 transients per indirect point and a SW of 100 ppm for ¹³C.

Total membrane protein isolation and detection of c-type cytochromes. Cell cultures were grown overnight in 500 ml MHS, harvested by centrifuging at 8,000 \times g, 4 °C for 20 min and resuspended in 5 ml of 10 mM HEPES buffer (pH 7.4). Cells were broken by sonication for 6 \times 20 s at a frequency of 16 microns amplitude (MSE sonicator). Unbroken cells and debris were removed by centrifuging at 15,000 \times g, 4 °C for 30 min. The supernatant was then centrifuged at 100,000 \times g, 4 °C for 1 h in a benchtop ultracentrifuge (Beckman). The supernatant was discarded and the membrane pellet was washed and resuspended in 1 ml 25 mM phosphate buffer (pH 7.4). Total protein concentration was determined by Lowry assay. Proteins were denatured gently by incubating for 1 h at 37 °C in SDS-PAGE sample buffer but without β -mercaptoethanol. Proteins were separated by SDS-PAGE on 10% acrylamide gels and either stained with Coomassie blue G250 or electroblotted onto nitrocellulose membrane (Hybond-C extra, GE Healthcare). Covalently bound haem was detected as haem-associated peroxidase activity⁴⁰, using the enhanced chemiluminescence (ECL) kit from GE Healthcare. Images were obtained using a ChemiDoc XRS system (BioRad Inc) with an exposure time of 2 min.

Measurement of substrate respiration rate in intact cells. Respiration rates were measured as the rate of oxygen consumption of cell suspensions in a Clark-type oxygen electrode using 10 mM sodium formate as electron donor, calibrated using air-saturated 25 mM phosphate buffer (pH 7.4) (200 nmol dissolved O₂ ml⁻¹ at 42 °C). Total protein concentration of the cell suspension was determined by Lowry assay at 600 nm and the specific rate of oxidation was calculated as nmol oxygen produced min⁻¹ mg⁻¹ total protein.

Measurement of Reactive Oxygen Species (ROS). Cells were grown microaerobically in MHS and harvested at mid-exponential growth phase by centrifugation (8,000 \times g, for 3 min). Cell pellets were washed and resuspended in 5 ml of 25 mM phosphate buffer (pH 7.4). Cells were added to 6 ml of 25 mM phosphate buffer (pH 7.4) in 6-well plates to a final OD 600 nm of 0.2. 2',7'-dihydrodichlorofluorescein diacetate (H2DCFDA; Life Technologies, USA), dissolved in 1% DMSO, was added to a final concentration of 10 μ M at time zero and the plates incubated microaerobically at 42 °C. Samples (1 ml) were removed every 10 min and fluorescence emission at 538 nm measured on a Cary Eclipse (Agilent), fluorimeter, with excitation at 485 nm. Total protein concentration of the cell suspension was determined by Lowry assay and the data expressed as fluorescence intensity per mg protein.

Data Availability

All data generated or analysed during this study are included in this published article.

References

- Dibrova, D. V., Cherepanov, D. A., Galperin, M. Y., Skulachev, V. P. & Mulkidjanian, A. Y. Evolution of cytochrome *bc* complexes: From membrane-anchored dehydrogenases of ancient bacteria to triggers of apoptosis in vertebrates. *Biochim Biophys Acta* **1827**, 1407–1427 (2013).
- Xia, D. *et al.* Structural analysis of cytochrome *bc*₁ complexes: implications to the mechanism of function. *Biochim Biophys Acta* **1827**, 1278–1294 (2013).
- Baymann, F., Lebrun, E. & Nitschke, W. Mitochondrial cytochrome *c*₁ is a collapsed di-heme cytochrome. *Proc Natl Acad Sci USA* **101**, 17737–17740 (2004).
- Niebisch, A. & Bott, M. Molecular analysis of the cytochrome *bc*₁-*aa*₃ branch of the *Corynebacterium glutamicum* respiratory chain containing an unusual diheme cytochrome *c*₁. *Arch Microbiol* **174**, 282–294 (2001).
- Graf, S. *et al.* Rapid Electron Transfer within the III-IV Supercomplex in *Corynebacterium glutamicum*. *Sci Rep.* **6**, 34098, <https://doi.org/10.1038/srep34098> (2016).
- Kao, W. C. *et al.* The obligate respiratory supercomplex from *Actinobacteria*. *Biochim Biophys Acta.* **1857**, 1705–1714 (2016).
- Alefounder, P. R. & Ferguson, S. J. Electron transport-linked nitrous oxide synthesis and reduction by *Paracoccus denitrificans* monitored with an electrode. *Biochem Biophys Res Commun.* **104**, 1149–1155 (1982).
- Carr, G. J., Page, M. D. & Ferguson, S. J. The energy-conserving nitric-oxide-reductase system in *Paracoccus denitrificans*. Distinction from the nitrite reductase that catalyses synthesis of nitric oxide and evidence from trapping experiments for nitric oxide as a free intermediate during denitrification. *Eur J Biochem.* **179**, 683–692 (1989).
- Pearson, I. V., Page, M. D., van Spanning, R. J. & Ferguson, S. J. A mutant of *Paracoccus denitrificans* with disrupted genes coding for cytochrome *c*₅₅₀ and pseudoazurin establishes these two proteins as the *in vivo* electron donors to cytochrome *cd*₁ nitrite reductase. *J Bacteriol.* **185**, 6308–6315 (2003).
- Atack, J. M. & Kelly, D. J. Structure, mechanism and physiological roles of bacterial cytochrome *c* peroxidases. *Adv Microb Physiol.* **52**, 73–106 (2007).
- ten Brink, F., Schoepp-Cothenet, B., van Lis, R., Nitschke, W. & Baymann, F. Multiple Rieske/cyt *b* complexes in a single organism. *Biochim Biophys Acta.* **1827**, 1392–406 (2013).
- Hein, S., Witt, S. & Simon, J. Clade II nitrous oxide respiration of *Wolinella succinogenes* depends on the *NosG*, *-C*₁, *-C*₂, *-H* electron transport module, *NosB* and a Rieske/cytochrome *bc* complex. *Environ Microbiol.* **19**, 4913–4925 (2017).
- Kern, M. & Simon, J. Characterization of the NapGH quinol dehydrogenase complex involved in *Wolinella succinogenes* nitrate respiration. *Mol Microbiol.* **69**, 1137–1152 (2008).
- Kern, M. & Simon, J. Electron transport chains and bioenergetics of respiratory nitrogen metabolism in *Wolinella succinogenes* and other *Epsilonproteobacteria*. *Biochim Biophys Acta.* **1787**, 646–656 (2009).
- O'Brien, S. J. & Sarah, J. The consequences of *Campylobacter* infection. *Curr Opin Gastroenterol.* **33**, 14–20 (2017).
- Sheppard, S. K. *et al.* *Campylobacter* genotyping to determine the source of human infection. *Clin Infect Dis* **48**, 1072–1078 (2009).
- Sellars, M. J., Hall, S. J. & Kelly, D. J. Growth of *Campylobacter jejuni* supported by respiration of fumarate, nitrate, nitrite, trimethylamine-N-oxide, or dimethyl sulfoxide requires oxygen. *J Bacteriol.* **184**, 4187–4196 (2002).
- Pittman, M. S. *et al.* Growth of *Campylobacter jejuni* on nitrate and nitrite: electron transport to NapA and NrfA via NrfH and distinct roles for NrfA and the globin Cgb in protection against nitrosative stress. *Mol Microbiol.* **63**, 575–590 (2007).

19. Weingarten, R. A., Taveirne, M. E. & Olson, J. W. The dual-functioning fumarate reductase is the sole succinate: quinone reductase in *Campylobacter jejuni* and is required for full host colonization. *J Bacteriol.* **191**, 5293–52300 (2009).
20. Liu, Y. W., Denkmann, K., Kosciow, K., Dahl, C. & Kelly, D. J. Tetrathionate stimulated growth of *Campylobacter jejuni* identifies a new type of bi-functional tetrathionate reductase (TsdA) that is widely distributed in bacteria. *Mol Microbiol.* **88**, 173–188 (2013).
21. Weingarten, R. A., Grimes, J. L. & Olson, J. W. Role of *Campylobacter jejuni* respiratory oxidases and reductases in host colonization. *Appl Environ Microbiol.* **74**, 1367–1375 (2008).
22. Myers, J. D. & Kelly, D. J. Respiratory electron transport in *Helicobacter* and *Campylobacter*, (ed. Zannoni, D.) 63–80 (*Respiration in Archaea and Bacteria*, 2004) Springer, Netherlands.
23. Kelly, D. Complexity and Versatility in the Physiology and Metabolism of *Campylobacter jejuni*, (ed. In Nachamkin, I., Szymanski, C. & Blaser, M.) 41–61 (*Campylobacter*, Third Edition. 2008) ASM Press, Washington, DC., <https://doi.org/10.1128/9781555815554.ch3>.
24. Liu, Y. W. & Kelly, D. J. Cytochrome *c* biogenesis in *Campylobacter jejuni* requires cytochrome *c*₆ (CccA; Cj1153) to maintain apocytochrome cysteine thiols in a reduced state for haem attachment. *Mol Microbiol.* **96**, 1298–1317 (2015).
25. van Vliet, A. H., Wooldridge, K. G. & Ketley, J. M. Iron-responsive gene regulation in a *Campylobacter jejuni* *fur* mutant. *J Bacteriol.* **180**, 5291–5298 (1998).
26. Guccione, E. *et al.* Reduction of fumarate, mesaconate and crotonate by Mfr, a novel oxygen-regulated periplasmic reductase in *Campylobacter jejuni*. *Environ Microbiol.* **12**, 576–591 (2010).
27. Cole, J. A. & Richardson, D. J. Respiration of Nitrate and Nitrite. *EcoSal Plus.* **3**, <https://doi.org/10.1128/ecosal.3.2.5>. (2008).
28. Simon, J., van Spanning, R. J. & Richardson, D. J. The organisation of proton motive and non-proton motive redox loops in prokaryotic respiratory systems. *Biochim Biophys Acta.* **1777**, 1480–1490 (2008).
29. Brondijk, T. H., Nilavongse, A., Filenko, N., Richardson, D. J. & Cole, J. A. NapGH components of the periplasmic nitrate reductase of *Escherichia coli* K-12: location, topology and physiological roles in quinol oxidation and redox balancing. *Biochem J.* **379**, 47–55 (2004).
30. van der Stel, A.-X. *et al.* Generation of the membrane potential and its impact on the motility, ATP production and growth in *Campylobacter jejuni*. *Mol Microbiol.* **105**, 637–651 (2017).
31. Kern, M., Mager, A. M. & Simon, J. Role of individual *nap* gene cluster products in NapC-independent nitrate respiration of *Wolinella succinogenes*. *Microbiology.* **153**, 3739–3747 (2007).
32. Kern, M. & Simon, J. Periplasmic nitrate reduction in *Wolinella succinogenes*: cytoplasmic NapF facilitates NapA maturation and requires the menaquinol dehydrogenase NapH for membrane attachment. *Microbiology.* **155**, 2784–94 (2009).
33. Sawers, R. G., Falke, D. & Fischer, M. Oxygen and Nitrate Respiration in *Streptomyces coelicolor* A₃(2). *Adv Microb Physiol.* **68**, 1–40 (2016).
34. Gon, S., Giudici-Ortoni, M. T., Méjean, V. & Iobbi-Nivol, C. Electron transfer and binding of the *c*-type cytochrome TorC to the trimethylamine N-oxide reductase in *Escherichia coli*. *J Biol Chem.* **276**, 11545–11551 (2001).
35. Guccione, E. *et al.* Transcriptome and proteome dynamics in chemostat culture reveal how *Campylobacter jejuni* modulates metabolism, stress responses and virulence factors upon changes in oxygen availability. *Environ Microbiol.* **19**, 4326–4348 (2017).
36. Kurth, J. M., Dahl, C. & Butt, J. N. Catalytic protein film electrochemistry provides a direct measure of the tetrathionate/thiosulfate reduction potential. *J Am Chem Soc.* **137**, 13232–13235 (2015).
37. Lopez, C. A., Rivera-Chávez, F., Byndloss, M. X. & Bäuml, A. J. The Periplasmic Nitrate Reductase NapABC Supports Luminal Growth of *Salmonella enterica* Serovar Typhimurium during Colitis. *Infect Immun.* **83**, 3470–3478 (2015).
38. Winter, S. E. *et al.* Gut inflammation provides a respiratory electron acceptor for *Salmonella*. *Nature.* **467**, 426–429 (2010).
39. Sambrook, J., Fritsch, E. F. & Maniatis, T. Molecular cloning: a laboratory manual, (ed. Sambrook, J.) 1–1546 (*Molecular cloning: a laboratory manual, Second Edition*, 1989) Cold Spring Harbor Laboratory Press, New York.
40. Feissner, R., Xiang, Y. & Kranz, R. G. Chemiluminescent-based methods to detect subpicomole levels of *c*-type cytochromes. *Anal Biochem.* **315**, 90–94 (2003).

Acknowledgements

This work was funded by a University of Sheffield Vice Chancellors Indian Scholarship to NG and a UK Biotechnology and a Biological Sciences Research Council (BBSRC) grant (BB/R003491/1) to DJK for AJT. We thank Dr. Jörg Simon for insightful discussions on the role of the Qcr complex in epsilonproteobacteria. We acknowledge Yang Wei Liu for construction of the *cccB cccC* mutant and Mrs. Andrea Hounslow for performing the NMR in the departmental biomolecular NMR facility. This paper is dedicated to the memory of J. Baz Jackson, an inspirational mentor.

Author Contributions

N.G. and A.J.T. performed all experiments. D.J.K. wrote the manuscript and N.G., A.J.T. and D.J.K. edited and reviewed the text.

Additional Information

Supplementary information accompanies this paper at <https://doi.org/10.1038/s41598-018-33857-2>.

Competing Interests: The authors declare no competing interests.

Publisher's note: Springer Nature remains neutral with regard to jurisdictional claims in published maps and institutional affiliations.



Open Access This article is licensed under a Creative Commons Attribution 4.0 International License, which permits use, sharing, adaptation, distribution and reproduction in any medium or format, as long as you give appropriate credit to the original author(s) and the source, provide a link to the Creative Commons license, and indicate if changes were made. The images or other third party material in this article are included in the article's Creative Commons license, unless indicated otherwise in a credit line to the material. If material is not included in the article's Creative Commons license and your intended use is not permitted by statutory regulation or exceeds the permitted use, you will need to obtain permission directly from the copyright holder. To view a copy of this license, visit <http://creativecommons.org/licenses/by/4.0/>.

© The Author(s) 2018

Chapter 6

General conclusions and future work

Findings of this study can be summarised according to figure 6.1. It was already established at the start of this study that the activity of *cbb₃*-type cytochrome *c* oxidase in *C. jejuni* is essential for its optimum growth and host colonisation (Weerakoon et al., 2008; Liu and Kelly, 2015). This study provides evidence supporting that Cj0911 and Cj0909 in *C. jejuni* are copper chaperones homologous to Sco1 and PCu_AC, respectively, and responsible for Cu assembly to CcoN. Genes encoding Cj0911 and Cj0909, along with genes encoding Cj0908 and Cj0910, potentially form an operon in *C. jejuni* as they have the same promoter. Cj0908 and Cj0910 are membrane bound novel proteins containing a thioredoxin-like motif and potentially responsible for reducing Cu(II) to Cu (I) in the highly oxidised periplasm because CcoN binds Cu in Cu(I) form. Clearly, these proteins require further study. The first thing to verify is whether Cj0908 and Cj0910 are actually working as thioredoxins for CcoNOQP activity and what is the need for two thioredoxins. Are the functions of Cj0909 and Cj0911 unique or redundant? Further work should include analysing the oxidase activities of individual mutants and the overexpression and purification of proteins to derive the protein structure and understand the protein-protein and Cu-protein interactions *in vitro*. Cj0911 and Cj0909 have to be purified and analysed for their affinity for binding Cu(I) and Cu(II). Cj0908 and Cj0910 have to be analysed for their potential to reduce Cu(II) to Cu(I). For these assays, the pET21a protein overexpression vectors for each individual protein have been designed with strepII-tag for purification but time constraints didn't allow us to further investigate them for this study. None of these proteins, though handling Cu in the periplasm, showed any role in intracellular Cu homeostasis (section 3.2.7). Further analysis is also required to see the influence of these proteins on the biogenesis of the CcoNOQP complex. The best possible way is to raise antibodies against each of these (CcoNOQP) proteins and check their presence in each of the individual assembly mutant but this procedure is practically less feasible as CcoNOQP are inner membrane proteins. CcoN can be detected with the help of flag tagging the protein. CcoO can be visualised on heme blots. Strategies for CcoP and CcoQ detection are still to be derived.

In many bacteria, the presence of a gene cluster *ccoGHIS* downstream to *ccoNOQP* has been observed. These gene products were reported necessary for

CcoNOQP biogenesis and maturation in *Rhodobacter capsulatus* (Koch *et al.*, 2000). In *C. jejuni*, genes encoding CcoGHIS does not form a cluster and do not lie next to *ccoNOQP*. They are scattered throughout the genome. The bioinformatics results (section 3.2.2), cytochrome *c* oxidase activity results (section 3.2.10) and Cu sensitivity assay result (section 3.2.9) showed in this study provides evidence that Cj0369 in *C. jejuni* is CcoG, Cj1483 is CcoH, Cj1155 is CcoI and Cj1154 is CcoS (See section 3.3 for further details). $\Delta cj1484c$ also showed reduced cytochrome *c* oxidase and interestingly, it further reduced on adding excess Cu. This unique observation needs further analysis. The similar G+C content in *ccoP* and *cj1486c* also suggest that *cj1486c* might be evolutionarily associated with *ccoP*. The process of biogenesis of the CcoNOQP complex and its coordination with CcoGHIS proteins is still not well understood in any bacteria. Several potential models of biogenesis of CcoNOQP complex and role of CcoGHIS in its biogenesis exist (discussed in section 3.3), but need more evidence. Future work should include protein-protein interaction studies of CcoGHIS proteins with each other and the oxidase subunits. In particular, is CcoG a reductase that passes copper to CcoI? And is CcoI also required for other processes? The exact roles of Cj1146, Cj1485 and Cj1484 are not clear from this study. Purification of an active oxidase complex would be interesting to see if any of these proteins are associated with it as extra subunits, for example. Based on the findings in this study, a potential working model of cytochrome *c* oxidase with Cu assembly proteins, CcoGHIS and Cj1486, Cj1485 and Cj1484 has been shown in section 3.4 (Fig. 3.26).

The fact that Cu is both essential and toxic for the *C. jejuni* cells, requires careful Cu homeostasis. In many bacteria, including Gram-negative *Rhodobacter sphaeroides*, it was reported that the CcoNOQP Cu assembly proteins had some role in maintaining the Cu homeostasis as well (Thompson *et al.*, 2012). However, it was not observed in *C. jejuni* (see section 3.2.7). *C. jejuni* contains a separate CopA homologous protein, Cj1161, having Cu translocating function (Hall *et al.*, 2008). It was observed that in *C. jejuni* genome, genes *cj1161* to *cj1164* are transcribed by the same promotor and potentially making an operon. On further bioinformatics analysis, it was found that Cj1162 is homologous to CopZ, Cj1163 to potential Zn-Co-Ni transporters and Cj1164c to Zn finger proteins. Based on bioinformatics results (section 4.2.2), Cu toxicity assay (section 4.2.5), growth curve assay (section 4.2.6),

RT-PCT (section 4.2.7) and ICP-MS (section 4.2.8) results, this study provides evidence suggesting that Cj1161, Cj1162, Cj1163 and Cj1164 proteins are responsible for maintaining intracellular Cu homeostasis in *C. jejuni* (See section 4.3 for further details). Interestingly, Zn toxicity assay and ICP-MS result (section 4.2.10) shows that Cj1163 is involved in Zn homeostasis as well. This study also attempted to see the connection of these Cu homeostasis genes on cytochrome *c* oxidase activity as it is a metalloprotein, which uses Cu as co factor. The reduction in oxidase activity in Cu homeostasis mutants suggests that intracellular Cu homeostasis has direct connection with oxidase activity, but this needs further investigation, in particular, it is not known how copper is taken up by the cells, as there is no CcoA transporter homologue in *C. jejuni*, so identification of additional copper transporters is important. Future work thus includes establishing the role of Cu homeostasis in cytochrome *c* oxidase activity and discovering the pathway of Cu entry and exit of the cells.

Finally, this study also focused on the wider role of the Qcr complex in the electron transport chain in *C. jejuni* and obtained evidence showing that the Qcr complex mediates electron transport between the menaquinone pool and nitrate and TMAO reductase, supporting growth in oxygen-limited environments (Garg *et al.*, 2018). These results show for the first time that periplasmic nitrate and TMAO reduction can be energy conserving, broaden our view of the role of bacterial Qcr complexes and have general implications for other bacteria. Both, nitrate and TMAO are present in the mammalian host intestinal environment. Therefore, Qcr complex mediated respiration in *C. jejuni* may provide a competitive advantage *in vivo*. Unanswered questions here include the exact electron transport route from the Qcr complex to NapB; is this direct or does it include NapG? What is the role of the NapGH quinol dehydrogenase? Biochemical studies on the electron transfer pathway are needed but this will require purification of these membrane bound complexes with cofactors assembled, which is technically challenging.

Chapter 7

References

- Abriata, L. A., Banci, L., Bertini, I., Ciofi-Baffoni, S., Gkazonis, P., Spyroulias, G. A., Vila, A. J. and Wang, S. (2008). Mechanism of Cu(A) assembly. *Nature chemical biology*. 4(10), 599-601.
- Al-Haideri, H., White, M.A., and Kelly, D.J. (2016). Major contribution of the type II beta carbonic anhydrase CanB (Cj0237) to the capnophilic growth phenotype of *Campylobacter jejuni*. *Environ. Microbiol.* 18, 721–735.
- Allos, B.M., and Blaser, M.J. (1995). *Campylobacter jejuni* and the expanding spectrum of related infections. *Clin. Infect. Dis.* 20, 1092–1101.
- Allos, B.M. (1998). *Campylobacter jejuni* infection as a cause of the Guillain-Barré syndrome. *Infect Dis Clin North Am.* 12(1):173-84.
- Allos, B.M. (2011). Microbiology, pathogenesis, and epidemiology of *Campylobacter* infection. In: UpToDate, Calderwood SB (Ed), UpToDate, Waltham, MA, 2013.
- Altekruse, S.F., Stern, N.J., Fields, P.I., and Swerdlow, D.L. (1999). *Campylobacter jejuni*-an emerging foodborne pathogen. *Emerg Infect Dis.* 5(1), 28-35.
- Amieva, M., & Peek, R. M. (2015). Pathobiology of *Helicobacter pylori*-Induced Gastric Cancer. *Gastroenterology*, 150(1), 64-78.
- Anbar, A.D., and Knoll, A.H. (2002). Proterozoic ocean chemistry and evolution: a bioinorganic bridge? *Science*. 297(5584), 1137-1142.
- Ashgar, S. S., Oldfield, N. J., Wooldridge, K. G., Jones, M. A., Irving, G. J., Turner, D. P. and Ala'Aldeen, D. A. (2007). CapA, an autotransporter protein of *Campylobacter jejuni*, mediates association with human epithelial cells and colonization of the chicken gut. *Journal of bacteriology*. 189, 1856-1865.
- Atack, J.M., and Kelly, D.J. (2008). Contribution of the stereospecific methionine sulphoxide reductases MsrA and MsrB to oxidative and nitrosative stress resistance in the food-borne pathogen *Campylobacter jejuni*. *Microbiology*. 154, 2219–2230.
- Atack, J. M., Harvey, P., Jones, M. A., and Kelly, D. J. (2008). The *Campylobacter jejuni* thiol peroxidases Tpx and Bcp both contribute to aerotolerance and peroxide-mediated stress resistance but have distinct substrate specificities. *Journal of bacteriology* 190, 5279-5290.
- Baar, C., Eppinger, M., Raddatz, G., and other authors (2003). Complete genome sequence and analysis of *Wolinella succinogenes*. *Proceedings of the National Academy of Sciences of the United States of America*. 100, 11690-11695.
- Bacon, D. J., Szymanski, C. M., Burr, D. H., Silver, R. P., Alm, R. A., and Guerry, P. (2001). A phase-variable capsule is involved in virulence of *Campylobacter jejuni* 81-176. *Molecular microbiology*. 40, 769-777.

Bacon, D. J., Alm, R. A., Hu, L., Hickey, T. E., Ewing, C. P., Batchelor, R. A., Trust, T. J., and Guerry, P. (2002). DNA sequence and mutational analyses of the pVir plasmid of *Campylobacter jejuni* 81-176. *Infection and immunity*. *70*, 6242-6250.

Baillon, M. L., van Vliet, A.H., Ketley, J.M., Constantinidou, and Penn, C.W. (1999). An iron-regulated alkyl hydroperoxide reductase (Ahpc) confers aerotolerance and oxidative stress resistance to the microaerophilic pathogen *Campylobacter jejuni*. *J Bacteriol*. *181(16)*, 4798-4804.

Banci, L., Bertini, I., Ciofi-Baffoni, S., Huffman, D.L., and O'Halloran, T.V. (2001). Solution structure of the yeast copper transporter domain Ccc2a in the apo and Cu(I)-loaded states. *J. Biol. Chem*. *276*, 8415–8426.

Banci, L., Bertini, I., Cantini, F., Migliardi, M., Rosato, A., and Wang, S. (2005). An atomic-level investigation of the disease-causing A629P mutant of the Menkes protein, ATP7A. *J. Mol. Biol*. *352*, 409–417.

Bannister, J.V., Bannister, W.H., and Rotilio, G. (1987). Aspects of the structure, function, and applications of superoxide dismutase. *CRC Crit Rev Biochem*. *22(2)*,111-80.

Barnes, I. H., Bagnall, M. C., Browning, D. D., Thompson, S. A., Manning, G., and Newell, D. G. (2007). Gamma-glutamyl transpeptidase has a role in the persistent colonization of the avian gut by *Campylobacter jejuni*. *Microbial pathogenesis*. *43*, 198-207.

Barondeau, D.P., and Getzoff, E.D., (2004). Structural insights into protein-metal ion partnerships. *Curr Opin Struct Biol*. *14(6)*, 765-74.

Bayliss, C.D., Bidmos, F.A., Anjum, A., Manchev, V.T., Richards, R.L., Grossier, J.P., Wooldridge, K.G., Ketley, J.M., Barrow, P.A., and Jones, M.A. (2012). Phase variable genes of *Campylobacter jejuni* exhibit high mutation rates and specific mutational patterns but mutability is not the major determinant of population structure during host colonization. *Nucleic Acids Res*. *40*, 5876–5889.

BBC News UK. (2014). <https://www.bbc.co.uk/news/business-30227342>.

BBC News UK. (2015). <https://www.bbc.co.uk/news/uk-32911228>

Beery, J. T., Hugdahl, M. B., and Doyle, M.P. (1988). Colonization of gastrointestinal tracts of chicks by *Campylobacter jejuni*. *Appl Environ Microbiol* *54(10)*, 2365-2370.

Bilous, P. T., and Weiner, J. H. (1988). Molecular cloning and expression of the *Escherichia coli* dimethyl sulfoxide reductase operon. *Journal of bacteriology*. *170*, 1511-1518.

Bingham-Ramos, L. K., and Hendrixson, D. R. (2008). Characterization of two putative cytochrome *c* peroxidases of *Campylobacter jejuni* involved in promoting commensal colonization of poultry. *Infection and immunity*. *76*, 1105-1114.

- Biswas, D., Fernando, U., Reiman, C., Willson, P., Potter, A., and Allan, B. (2006). Effect of cytolethal distending toxin of *Campylobacter jejuni* on adhesion and internalization in cultured cells and in colonization of the chicken gut. *Avian diseases*. 50, 586-593.
- Blaser, M.J., and Engberg, J. (2008). Clinical aspects of *Campylobacter jejuni* and *Campylobacter coli* Infections. In: *Campylobacter*. Third edition. Nachamkin, I., Szymanski, C.M., and Blaser, M.J. Eds. ASM Press, Washington D.C.
- Bolton, F. J., and Coates, D. (1983). A comparison of microaerobic systems for the culture of *Campylobacter jejuni* and *Campylobacter coli*. *European journal of clinical microbiology*. 2, 105-110.
- Brondijk, T. H., Fiegen, D., Richardson, D. J., and Cole, J. A. (2002). Roles of NapF, NapG and NapH, subunits of the *Escherichia coli* periplasmic nitrate reductase, in ubiquinol oxidation. *Molecular microbiology*. 44, 245-255.
- Brondijk, T. H., Nilavongse, A., Filenko, N., Richardson, D. J., and Cole, J. A. (2004). NapGH components of the periplasmic nitrate reductase of *Escherichia coli* K-12: location, topology and physiological roles in quinol oxidation and redox balancing. *The Biochemical journal* 379, 47-55.
- Burns, B. P., Hazell, S. L., and Mendz, G. L. (1995). Acetyl-CoA carboxylase activity in *Helicobacter pylori* and the requirement of increased CO₂ for growth. *Microbiology*. 141 (Pt. 12), 3113-3118.
- Buschmann, S., Warkentin, E., Xie, H., Langer, J.D., Ermler, U., and Michel, H. (2010). The structure of *ccb₃* cytochrome oxidase provides insights into proton pumping. *Science*. 329(5989), 327-30.
- Butzler, J.P., Dekeyser, P., Detrain, M., and Dehaen, F. (1973). Related vibrio in stools. *J. Pediatr*. 82, 493-495.
- Byran, F.L., and Doyle M.P. (1995). Health Risks and Consequences of *Salmonella* and *Campylobacter jejuni* in Raw Poultry. *J Food Prot*. 58 (3),326-344.
- Campbell, B.J., Engel, A.S., Porter, M.L., and Takai, K. (2006). The versatile ϵ -proteobacteria: key players in sulphidic habitats. *Nat. Rev. Microbiol*. 4, 458-468.
- Carlone, G. M., and Lascelles, J. (1982). Aerobic and anaerobic respiratory systems in *Campylobacter fetus subsp. jejuni* grown in atmospheres containing hydrogen. *Journal of bacteriology*. 152, 306-314.
- Carlone, G. M., and Anet, F. A. (1983). Detection of menaquinone-6 and a novel methyl-substituted menaquinone-6 in *Campylobacter jejuni* and *Campylobacter fetus subsp. fetus*. *Journal of general microbiology*. 129, 3385-3393.
- Chan, C. S., Chang, L., Winstone, T. M., and Turner, R. J. (2010). Comparing system-specific chaperone interactions with their Tat dependent redox enzyme substrates. *FEBS letters*. 584, 4553-4558.

- Chang, C., and Miller, J.F. (2006) *Campylobacter jejuni* colonization of mice with limited enteric flora. *Infect Immun.* 74, 5261-5271.
- Chantarapanont, W., Berrang, M.E., and Frank, J.F. (2004). Direct microscopic observation of viability of *Campylobacter jejuni* on chicken skin treated with selected chemical sanitizing agents. *J. Food Prot.* 67, 1146–1152.
- Cobine P., Wickramasinghe W.A., Harrison M.D., Weber T., Solioz M., and Dameron C.T. (1999). The *Enterococcus hirae* copper chaperone CopZ delivers copper(I) to the CopY repressor. *FEBS Lett.* 445(1), 27-30.
- Collins, M.D., Costas, M., and Owen, R.J. (1984) Isoprenoid quinone composition of representatives of the genus *Campylobacter*. *Arch Microbiol.* 137, 168-170.
- Cosseau, C., and Batut, J. (2004). Genomics of the ccoNOQP-encoded cbb3 oxidase complex in bacteria. *Arch Microbiol.* 181(2), 89-96.
- Costa, C., Macedo, A., Moura, I., Moura, J.J., Le Gall, J., Berlier, Y., Liu, M.Y., and Payne, W.J. (1990). Regulation of the hexaheme nitrite/nitric oxide reductase of *Desulfovibrio desulfuricans*, *Wolinella succinogenes* and *Escherichia coli*. A mass spectrometric study. *FEBS Lett.* 276(1-2), 67-70.
- Dasti, J.I., Tareen, A.M., Lugert, R., Zautner, A.E., and Groß, U. (2010). *Campylobacter jejuni*: A brief overview on pathogenicity-associated factors and disease-mediating mechanisms. *Int. J. Med. Microbiol.* 300, 205–211.
- Day, W. A., Jr., Sajecki, J.L., Pitts, T.M., and Joens, L.A. (2000). Role of catalase in *Campylobacter jejuni* intracellular survival. *Infect Immun.* 68(11), 6337-6345.
- De la Cerda, B., Navarro, J.A., Hervás, M., and De la Rosa, M.A. (1997). Changes in the reaction mechanism of electron transfer from plastocyanin to photosystem I in the cyanobacterium *Synechocystis* sp. PCC 6803 as induced by site-directed mutagenesis of the copper protein. *Biochemistry.* 36(33), 10125-30.
- Debruyne, L., Gevers, D., and Vandamme, P. (2008). Taxonomy of the Family *Campylobacteraceae*. In: *Campylobacter*. Third edition. Nachamkin, I., Szymanski, C.M., and Blaser, M.J. Eds. ASM Press, Washington D.C.
- Debruyne, L., Broman, T., Bergström, S., Olsen, B., On, S.L., and Vandamme, P. (2010). *Campylobacter volucris* sp. nov., isolated from black-headed gulls (*Larus ridibundus*). *Int J Syst Evol Microbiol.* 60(Pt 8),1870-5.
- Dibrova, D.V., Cherepanov, D.A., Galperin, M.Y., Skulachev, V.P., and Mulkidjanian, A.Y. (2013). Evolution of cytochrome *bc* complexes: from membrane-anchored dehydrogenases of ancient bacteria to triggers of apoptosis in vertebrates. *Biochim Biophys Acta.* 1827(11-12),1407-27.

- Dickinson, E.K., Adams, D.L., Schon, E.A., and Glerum, D.M. (2000). A human SCO2 mutation helps define the role of Sco1p in the cytochrome oxidase assembly pathway. *J Biol Chem.* 275(35), 26780-5.
- Djoko, K.Y., Franiek, J.A., Edwards, J.L., Falsetta, M.L., Kidd, S.P., Potter, A.J., Chen, N.H., Apicella, M.A., Jennings, M.P., and McEwan A.G. (2012). Phenotypic characterization of a copA mutant of *Neisseria gonorrhoeae* identifies a link between copper and nitrosative stress. *Infect Immun.* 80(3),1065-71.
- Doku, R.T., Park, G., Wheeler, K.E., and Splan, K.E. (2013). Spectroscopic characterization of copper(I) binding to apo and metal-reconstituted zinc finger peptides. *J Biol Inorg Chem.* 18(6), 669-78.
- Dollwet, H.H.A., and Sorenson, J.R.J. (1985). Historic uses of copper compounds in medicine. *Trace Elem Med.* 2, 80–87.
- Du, X., Kong, K., Tang, H., Tang, H., Jiao, X., and Huang, J. (2018). The Novel Protein Cj0371 Inhibits Chemotaxis of *Campylobacter jejuni*. *Front Microbiol.* 9,1904.
- Durand, A., Azzouzi, A., Bourbon, M.L., Steunou, A.S., Liotenberg, S., Maeshima, A., Astier, C., Argentini, M., Saito, S., and Ouchane, S. (2015). c-type Cytochrome Assembly Is a Key Target of Copper Toxicity within the Bacterial Periplasm. *MBio.* 6(5), e01007-15.
- Ekici, S., Turkarslan, S., Pawlik, G., Dancis, A., Baliga, N.S., Koch, H.G., and Daldal, F. (2014). Intracytoplasmic copper homeostasis controls cytochrome c oxidase production. *MBio.* 5(1), e01055-13.
- Elharrif, Z., and Mégraud, F. (1986) Characterization of thermophilic *Campylobacter*. II. enzymatic profiles. *Curr. Microbiol.* 13(6), 317-322.
- Elliott, K.T., and DiRita, V.J. (2008). Characterization of CetA and CetB, a bipartite energy taxis system in *Campylobacter jejuni*. *Mol. Microbiol.* 69, 1091–1103.
- Elmi, A., Watson, E., Sandu, P., Gundogdu, O., Mills, D.C., Inglis, N.F., Manson, E., Imrie, L., Bajaj-Elliott, M., Wren, B.W., Smith D.G., and Dorrell N. (2012). *Campylobacter jejuni* outer membrane vesicles play an important role in bacterial interactions with human intestinal epithelial cells. *Infect Immun.* 80(12), 4089-98.
- Henry, R. (2013). Etymologia: *Campylobacter*. *Emerg Infect Dis.* 19(8), 1313. doi: 10.3201/eid1908.ET-1908.
- Evans, S.J., and Sayers, A.R. (2000). A longitudinal study of *campylobacter* infection of broiler flocks in Great Britain. *Prev. Vet. Med.* 46, 209–223.
- Faundez, V., Hartzell, H.C., and Adler, E.M. (2004). Teaching resources. Chloride concentration and pH along the endosomal pathway. *Sci STKE.* 234, tr2.

Feissner, R. E., Richard-Fogal, C.L., Frawley, E.R., and Kranz, R.G. (2006). ABC transporter-mediated release of a haem chaperone allows cytochrome *c* biogenesis. *Mol Microbiol.* 61(1), 219-231.

Ferguson, S. J. (2001). Keilin's cytochromes: how bacteria use them, vary them and make them. *Biochemical Society transactions.* 29, 629-640.

Flanagan, R. C., Neal-McKinney, J. M., Dhillon, A. S., Miller, W. G., and Konkel, M. E. (2009). Examination of *Campylobacter jejuni* putative adhesins leads to the identification of a new protein, designated FlpA, required for chicken colonization. *Infection and immunity.* 77, 2399-2407.

Fouts, D.E., Mongodin, E.F., Mandrell, R.E., Miller, W.G., Rasko, D.A., Ravel, J., Brinkac, L.M., Deboy, R.T., Parker, C.T., Daugherty, S.C. (2005). Major structural differences and novel potential virulence mechanisms from the genomes of multiple campylobacter species. *PLoS Biol.* 3.

Friedrich, T. (1998). The NADH:Ubiquinone oxidoreductase (complex I) from *Escherichia coli*. *Biochim Biophys Acta.* 1364(2), 134-146.

Gaasbeek, E.J., Wagenaar, J.A., Guilhabert, M.R., Van Putten, J.P.M., Parker, C.T., and Van Der Wal, F.J. (2010). Nucleases encoded by the integrated elements CJIE2 and CJIE4 inhibit natural transformation of *Campylobacter jejuni*. *J. Bacteriol.* 192, 936–941.

Gardner, S.P., and Olson, J.W. (2018). Interaction of Copper Toxicity and Oxidative Stress in *Campylobacter jejuni*. *J Bacteriol.* 200(21).

Garg N., Taylor A.J., and Kelly D.J. (2018). Bacterial periplasmic nitrate and trimethylamine-N-oxide respiration coupled to menaquinol-cytochrome *c* reductase (Qcr): Implications for electrogenic reduction of alternative electron acceptors. *Sci Rep.* 8(1), 15478.

Gaynor, E.C., Cawthraw, S., Manning, G., MacKichan, J.K., Falkow, S., and Newell, D.G. (2004). The Genome-Sequenced Variant of *Campylobacter jejuni* NCTC 11168 and the Original Clonal Clinical Isolate Differ Markedly in Colonization, Gene Expression, and Virulence-Associated Phenotypes. *J. Bacteriol.* 186, 503–517.

Genest, O., Ilbert, M., Mejean, V., and Iobbi-Nivol, C. (2005) TorD, an essential chaperone for TorA molybdoenzyme maturation at high temperature. *J Biol Chem.* 280, 15644-15648.

Gennis, R.B., and Stewart, V. (1996). Respiration. In: Neidhardt, F. *et al.* (ed.), *Escherichia coli* and *Salmonella*: Cellular and molecular biology. 2nd ed. 1: 217-261. ASM Press, Washington, DC.

Gibson, D.G., Young, L., Chuang, R., Venter, J.C., Hutchison, C.A., Smith, H.O., Iii, C.A.H., and America, N. (2009). Enzymatic assembly of DNA molecules up to several hundred kilobases. *Nat. Methods.* 6, 343–345.

- Gilbreath, J.J., Cody, W.L., Merrell, D.S., and Hendrixson, D.R. (2011). Change is good: variations in common biological mechanisms in the epsilonproteobacterial genera *Campylobacter* and *Helicobacter*. *Microbiol. Mol. Biol. Rev.* 75, 84–132.
- Giner-Lamia, J., López-Maury, L., and Florencio, F.J. (2015). CopM is a novel copper-binding protein involved in copper resistance in *Synechocystis* sp. PCC 6803. *Microbiologyopen*. 4(1), 167-85.
- Golden, N.J., and Acheson, D.W.K. (2002). Identification of motility and autoagglutination *Campylobacter jejuni* mutants by random transposon mutagenesis. *Infect. Immun.* 70, 1761–1771.
- Gon, S., Giudici-Orticoni, M. T., Mejean, V., and Iobbi-Nivol, C. (2001). Electron transfer and binding of the *c*-type cytochrome TorC to the trimethylamine N-oxide reductase in *Escherichia coli*. *The Journal of biological chemistry*. 276, 11545-11551.
- Gong, C., Liu, X., and Jiang, X. (2014). Application of bacteriophages specific to hydrogen sulfide-producing bacteria in raw poultry by-products. *Poult Sci.* 93(3), 702-10.
- Goodhew, C. F., elKurdi, A. B., and Pettigrew, G. W. (1988). The microaerophilic respiration of *Campylobacter mucosalis*. *Biochimica et biophysica acta*. 933, 114-123.
- Goon, S., Kelly, J. F., Logan, S. M., Ewing, C. P., and Guerry, P. (2003). Pseudaminic acid, the major modification on *Campylobacter* flagellin, is synthesized via the *Cj1293* gene. *Molecular microbiology*. 50, 659-671.
- Gosset, G. (2005). Improvement of *Escherichia coli* production strains by modification of the phosphoenolpyruvate: Sugar phosphotransferase system. *Microb Cell Fact.* 4(1), 14.
- Grant, C. C., Konkel, M.E., Cieplak, W. Jr., and Tompkins, L.S. (1993). Role of flagella in adherence, internalization, and translocation of *Campylobacter jejuni* in nonpolarized and polarized epithelial cell cultures. *Infect Immun.* 61(5), 1764-1771.
- Gripp, E., Hlahla D., Didelot, X., Kops, F., Maurischat, S., Tedin, K., Alter, T., Ellerbreek, L., Schreiber, K., Schomburg, D., Janssen, T., Bartholomaeus, P., Hofreuter, D., Woltemate, S., Uhr, M., Brenneke, B., Gruning, P., Gerlach, G., Wieler, L., Suerbaum, S., and Josenhans, C. (2011). Closely related *Campylobacter jejuni* strains from different sources reveal a generalist rather than a specialist lifestyle. *BMC Genomics*. 12, 584.
- Guccione, E., Leon-Kempis, Mdel R., Pearson B.M., Hitchin, E., Mulholland, F., van Diemen, P.M., Stevens, M.P., and Kelly, D.J. (2008). Amino acid-dependent growth of *Campylobacter jejuni*: Key roles for aspartase (aspa) under microaerobic and oxygen-limited conditions and identification of aspb (cj0762), essential for growth on glutamate. *Mol Microbiol.* 69(1), 77-93.
- Guccione, E., Hitchcock, A., Hall, S.J., Mulholland, F., Shearer, N., van Vliet, A.H., and Kelly, D.J. (2010). Reduction of fumarate, mesaconate and crotonate by mfr, a

novel oxygen-regulated periplasmic reductase in *Campylobacter jejuni*. *Environ Microbiol.* *12*(3), 576-591.

Guccione, E.J., Kendall, J.J., Hitchcock, A., Garg, N., White, M.A., Mulholland, F., Poole, R.K., and Kelly, D.J. (2017). Transcriptome and proteome dynamics in chemostat culture reveal how *Campylobacter jejuni* modulates metabolism, stress responses and virulence factors upon changes in oxygen availability. *Environ Microbiol.* *19*(10), 4326-4348.

Guerry, P., Alm, R.A., Power, M.E., Logan, S.M., and Trust, T.J. (1991). Role of Two Flagellin Genes in *Campylobacter* Motility. *J. Bacteriol.* *173*, 4757-4764.

Gundogdu, O., Bentley, S. D., Holden, M. T., Parkhill, J., Dorrell, N., and Wren, B.W. (2007). Re-annotation and re-analysis of the *Campylobacter jejuni* nctc11168 genome sequence. *BMC Genomics.* *8*, 162.

Gundogdu, O., Mills, D.C., Elmi, A., Martin, M.J., Wren, B.W., and Dorrell, N. (2011). The *Campylobacter jejuni* transcriptional regulator Cj1556 plays a role in the oxidative and aerobic stress response and is important for bacterial survival in vivo. *J. Bacteriol.* *193*, 4238-4249.

Gundogdu, O., da Silva, D.T., Mohammad, B., Elmi, A., Mills, D.C., Wren, B.W., and Dorrell, N. (2015). The *Campylobacter jejuni* MarR-like transcriptional regulators RrpA and RrpB both influence bacterial responses to oxidative and aerobic stresses. *Front. Microbiol.* *6*, 1-12.

Hall, S. J., Hitchcock, A., Butler, C.S., and Kelly, D.J. (2008). A multicopper oxidase (Cj1516) and a CopA homologue (Cj1161) are major components of the copper homeostasis system of *Campylobacter jejuni*. *J Bacteriol.* *190*(24), 8075-8085.

Hanahan, D. (1983). Studies on transformation of *Escherichia coli* with plasmids. *J Mol Biol.* *166*(4), 557-580.

Hassani, B.K., Astier, C., Nitschke, W., and Ouchane, S. (2010). CtpA, a copper-translocating P-type ATPase involved in the biogenesis of multiple copper-requiring enzymes. *J Biol Chem.* *285*(25), 19330-7.

He, G., Shankar, R.A., Chzhan, M., Samouilov, A., Kuppusamy, P., and Zweier, J.L. (1999). Noninvasive measurement of anatomic structure and intraluminal oxygenation in the gastrointestinal tract of living mice with spatial and spectral EPR imaging. *Proc Natl Acad Sci U S A.* *96*(8), 4586-4591.

Hendrixson, D. R., Akerley, B.J., and DiRita, V.J. (2001). Transposon mutagenesis of *Campylobacter jejuni* identifies a bipartite energy taxis system required for motility. *Mol Microbiol.* *40*(1), 214-224.

Hendrixson, D. R., and DiRita V.J. (2004). Identification of *Campylobacter jejuni* genes involved in commensal colonization of the chick gastrointestinal tract. *Mol Microbiol.* *52*(2), 471-484.

- Hernández-Montes, G., Argüello, J.M., and Valderrama, B. (2012). Evolution and diversity of periplasmic proteins involved in copper homeostasis in gamma proteobacteria. *BMC Microbiol.* *12*, 249.
- Heywood, W., Henderson, B., and Nair, S.P. (2005). Cytolethal distending toxin: Creating a gap in the cell cycle. *J. Med. Microbiol.* *54*, 207–216.
- Hinton, A., Jr. (2006). Growth of *Campylobacter* in media supplemented with organic acids. *J Food Prot.* *69*(1), 34-38.
- Hoffman, P. S. and Goodman, T.G. (1982). Respiratory physiology and energy conservation efficiency of *Campylobacter jejuni*. *J Bacteriol.* *150*(1), 319-326.
- Hofreuter, D., Tsai, J., Watson, R.O., Novik, V., Altman, B., Benitez, M., Clark, C., Perbost, C., Jarvie, T., Du, L., and Galan J.L. (2006). Unique features of a highly pathogenic *Campylobacter jejuni* strain. *Infect Immun.* *74*(8), 4694-4707.
- Hofreuter, D., Novik, V., and Galan, J.E. (2008). Metabolic diversity in *Campylobacter jejuni* enhances specific tissue colonization. *Cell Host Microbe.* *4*(5), 425-433.
- Hofreuter, D. (2014). Defining the metabolic requirements for the growth and colonization capacity of *Campylobacter jejuni*. *Front Cell Infect Microbiol.* *4*, 137.
- Hornig, Y.C., Cobine, P.A., Maxfield, A.B., Carr, H.S., and Winge, D.R. (2004). Specific copper transfer from the Cox17 metallochaperone to both Sco1 and Cox11 in the assembly of yeast cytochrome C oxidase. *J Biol Chem.* *279*(34), 35334-40.
- Hugdahl, M. B., Beery, J.T., and Doyle, M.P. (1988). Chemotactic behavior of *Campylobacter jejuni*. *Infect Immun.* *56*(6), 1560-1566.
- Hughes, N. J., Chalk, P.A., Clayton, C.L., and Kelly, D.J. (1995). Identification of carboxylation enzymes and characterization of a novel four-subunit pyruvate:flavodoxin oxidoreductase from *Helicobacter pylori*. *J Bacteriol.* *177*(14), 3953-3959.
- Hughes, N. J., Clayton, C.L., Chalk, P.A., and Kelly, D.J. (1998). *Helicobacter pylori* porCDAB and oorDABC genes encode distinct pyruvate:flavodoxin and 2-oxoglutarate:acceptor oxidoreductases which mediate electron transport to NADP. *J Bacteriol.* *180*(5), 1119-1128.
- Ingledeu, W. J. and Poole, R.K. (1984). The respiratory chains of *Escherichia coli*. *Microbiol Rev.* *48*(3), 222-271.
- Iwata, S. (1998). Structure and function of bacterial cytochrome *c* oxidase. *J Biochem.* *123*(3), 369-75.
- Jackson, R. J., Elvers, K.T., Lee, L.J., Gidley, M.D., Wainwright, L.M., Lightfoot, J., Park, S.F., and Poole R.K. (2007). Oxygen reactivity of both respiratory oxidases in *Campylobacter jejuni*: The *cydAB* genes encode a cyanide-resistant, low-affinity oxidase that is not of the cytochrome *bd* type. *J Bacteriol.* *189*(5), 1604-1615.

Jacobs, B. C., van Belkum, A., and Endtz, H.P., (2008). Guillain-Barre Syndrome and *Campylobacter* Infection. In: *Campylobacter*. Third edition. Nachamkin, I., Szymanski, C.M. and Blaser, M.J. Eds. ASM Press, Washington D.C.

Jiang, X. and Doyle, M.P. (2000). Growth supplements for *Helicobacter pylori*. *J Clin Microbiol.* 38(5), 1984-1987.

Jin, S., Joe, A., Lynett, J., Hani, E.K., Sherman, P., and Chan, V.L. (2001). JlpA, a novel surface-exposed lipoprotein specific to *Campylobacter jejuni*, mediates adherence to host epithelial cells. *Mol Microbiol.* 39(5), 1225-1236.

Joslin, S.N., and Hendrixson, D.R. (2009). Activation of the *Campylobacter jejuni* FlgSR two-component system is linked to the flagellar export apparatus. *J. Bacteriol.* 191, 2656–2667.

Juhnke, H. D., Hiltcher, H., Nasiri, H. R., Schwalbe, H., and Lancaster, C. R. (2009). Production, characterization and determination of the real catalytic properties of the putative 'succinate dehydrogenase' from *Wolinella succinogenes*. *Molecular microbiology.* 71, 1088-1101.

Kaakoush, N.O., Deshpande, N.P., Man, S.M., Burgos-Portugal, J.A., Khattak, F.A., Raftery, M.J., Wilkins, M.R., and Mitchell, H.M. (2015). Transcriptomic and proteomic analyses reveal key innate immune signatures in the host response to the gastrointestinal pathogen *Campylobacter concisus*. *Infect Immun.* 83(2), 832-45.

Kanungpean, D., Kakuda, T., and Takai, S. (2011). Participation of CheR and CheB in the chemosensory response of *Campylobacter jejuni*. *Microbiology.* 157, 1279-1289.

Karlin, K.D. (1993). Metalloenzymes, structural motifs, and inorganic models. *Science.* 261(5122), 701-8.

Karlyshev, A. V., Everest, P., Linton, D., Cawthraw, S., Newell, D. G. & Wren, B. W. (2004). The *Campylobacter jejuni* general glycosylation system is important for attachment to human epithelial cells and in the colonization of chicks. *Microbiology.* 150, 1957-1964.

Karlyshev, A. V. & Wren, B. W. (2005). Development and application of an insertional system for gene delivery and expression in *Campylobacter jejuni*. *Applied and environmental microbiology.* 71, 4004-4013.

Kassem, I.I., Candelero-Rueda, R.A., Esseili, K.A., and Rajashekara, G. (2017). Formate simultaneously reduces oxidase activity and enhances respiration in *Campylobacter jejuni*. *Sci Rep.* 7, 40117.

Kather, B., Stingl, K., van der Rest, M. E., Altendorf, K., and Molenaar, D. (2000). Another unusual type of citric acid cycle enzyme in *Helicobacter pylori*: the malate:quinone oxidoreductase. *Journal of bacteriology.* 182, 3204-3209.

- Kelle, K., Pages, J. M., and Bolla, J. M. (1998). A putative adhesin gene cloned from *Campylobacter jejuni*. *Research in microbiology*. *149*, 723-733.
- Kelly, D. J. (2001). The physiology and metabolism of *Campylobacter jejuni* and *Helicobacter pylori*. *Journal of applied microbiology*. *90*, 16S-24S.
- Kelly, D. J. (2008). Complexity and versatility in the physiology and metabolism of *Campylobacter jejuni*. In: *Campylobacter*. Third edition. Nachamkin, I., Szymanski, C.M. and Blaser, M.J. Eds. ASM Press, Washington D.C.
- Kendall, J.J., Barrero-Tobon, A.M., Hendrixson, D.R., and Kelly, D.J. (2014). Hemerythrins in the microaerophilic bacterium *Campylobacter jejuni* help protect key iron-sulphur cluster enzymes from oxidative damage. *Environ. Microbiol.* *16*, 1105–1121.
- Kern, M., Mager, A. M., and Simon, J. (2007). Role of individual *nap* gene cluster products in NapC-independent nitrate respiration of *Wolinella succinogenes*. *Microbiology*. *153*, 3739-3747.
- Kern, M., and Simon, J. (2008). Characterization of the NapGH quinol dehydrogenase complex involved in *Wolinella succinogenes* nitrate respiration. *Molecular microbiology*. *69*, 1137-1152.
- Kern, M., and Simon, J. (2009a). Electron transport chains and bioenergetics of respiratory nitrogen metabolism in *Wolinella succinogenes* and other Epsilonproteobacteria. *Biochimica et biophysica acta*. *1787*, 646-656.
- Kern, M., Winkler, C., and Simon, J. (2011a) Respiratory nitrogen metabolism and nitrosative stress defence in ϵ -proteobacteria: the role of NssR-type transcription regulators. *Biochemical Society transactions*. *39*, 299-302.
- Knablein, J., Dobbek, H., and Schneider, F. (1997) Organization of the DMSO respiratory operon of *Rhodobacter capsulatus* and its consequences for homologous expression of DMSOR/TMAOR. *Biol Chem*. *378*, 303-308.
- Koch, H.G., Winterstein, C., Saribas, A.S., Alben, J.O., and Daldal, F. (2000). Roles of the *ccoGHIS* gene products in the biogenesis of the *ccb₃*-type cytochrome c oxidase. *J Mol Biol*. *297*(1), 49-65.
- Konkel, M. E., Garvis, S.G., Tipton, S.L., Anderson, D.E. Jr., and Cieplak, W. Jr. (1997). Identification and molecular cloning of a gene encoding a fibronectin-binding protein (CadF) from *Campylobacter jejuni*. *Mol Microbiol*. *24*(5), 953-963.
- Konkel, M. E., Klena, J.D., Rivera-Amill, V., Monteville, M.R., Biswas, D., Raphael, B., and Mickelson, J., (2004). Secretion of virulence proteins from *Campylobacter jejuni* is dependent on a functional flagellar export apparatus. *J Bacteriol*. *186*(11), 3296-3303.

Korolik, V., and Ketley, J. (2008). Chemosensory Signal Transduction Pathway of *Campylobacter jejuni*. Third edition. Nachamkin, I., Szymanski, C.M. and Blaser, M.J. Eds. ASM Press, Washington D.C.

Korshunov, S., Imlay, K.R., and Imlay, J.A. (2016). The cytochrome *bd* oxidase of *Escherichia coli* prevents respiratory inhibition by endogenous and exogenous hydrogen sulfide. *Mol Microbiol.* *101*(1), 62-77.

Kowarik, M., Numao, S., Feldman, M.F., Schulz, B.L., Callewaert, N., Kiermaier, E., Catrein, I., and Aebi, M. (2006). N-linked glycosylation of folded proteins by the bacterial oligosaccharyltransferase. *Science.* *314*, 1148–1150.

Koyanagi, S., Nagata, K., Tamura, T., Tsukita, S., and Sone, N. (2000). Purification and characterization of cytochrome *c-553* from *Helicobacter pylori*. *Journal of biochemistry.* *128*, 371-375.

Krieg, N. R. and Hoffman, P.S. (1986). Microaerophily and oxygen toxicity. *Annu Rev Microbiol.* *40*, 107-130.

Kröger, A., Biel, S., Simon, J., Gross, R., Unden, G., and Lancaster, C.R.D. (2002). Fumarate respiration of *Wolinella succinogenes*: Enzymology, energetics and coupling mechanism. *Biochim. Biophys. Acta - Bioenerg.* *1553*, 23–38.

Kulajta, C., Thumfart, J.O., Haid, S., Daldal, F., and Koch, H.G. (2006). Multi-step assembly pathway of the *cbb3*-type cytochrome *c* oxidase complex. *J Mol Biol.* *355*(5), 989-1004.

Kusters, J.G., Van Vliet, A.H.M., and Kuipers, E.J. (2006). Pathogenesis of *Helicobacter pylori* infection. *Clin. Microbiol. Rev.* *19*, 449–490.

Lai, C.K., Chen, Y.A., Lin, C.J., Lin, H.J., Kao, M.C., Huang, M.Z., Lin, Y.H., Chiang-Ni, C., Chen, C.J., Lo, U.G., Lin, L.C., Lin, H., Hsieh, J.T., and Lai, C.H. (2016). Molecular Mechanisms and Potential Clinical Applications of *Campylobacter jejuni* Cytolethal Distending Toxin. *Front Cell Infect Microbiol.* *6*, 9.

Lancaster, C. R. (2002). Succinate:quinone oxidoreductases: An overview. *Biochim Biophys Acta.* *1553*(1-2), 1-6.

Lara-Tejero, M., and Galan, J.E. (2001). CdtA, CdtB, and CdtC form a tripartite complex that is required for cytolethal distending toxin activity. *Infect Immun.* *69*(7), 4358-4365.

Leach, S., Harvey, P., and Wali, R. (1997). Changes with growth rate in the membrane lipid composition of and amino acid utilization by continuous cultures of *Campylobacter jejuni*. *J Appl Microbiol.* *82*(5), 631-640.

Lee, A., O'Rourke, J.L., Barrington, P.J., and Trust, T.J. (1986). Mucus colonization as a determinant of pathogenicity in intestinal infection by *Campylobacter jejuni*: A mouse cecal model. *Infect Immun.* *51*(2), 536-546.

- Leon-Kempis, Mdel, R., Guccione, E., Mulholland, F., Williamson, M.P., and Kelly, D.J. (2006). The *Campylobacter jejuni* PEB1a adhesin is an aspartate/glutamate-binding protein of an ABC transporter essential for microaerobic growth on dicarboxylic amino acids. *Mol Microbiol.* 60(5), 1262-1275.
- Linder, M.C., and Hazegh-Azam, M. (1996). Copper biochemistry and molecular biology. *Am J Clin Nutr.* 63(5), 797S-811S.
- Lindmark, B., Rompikuntal, P.K., Vaitkevicius, K., Song, T., Mizunoe, Y., Uhlin, B.E., Guerry, P., and Wai, S.N. (2009). Outer membrane vesicle-mediated release of cytolethal distending toxin (CDT) from *Campylobacter jejuni*. *BMC Microbiol.* 9, 220.
- Line, J. E., Hiatt, K.L., Guard-Bouldin J., and Seal, B.S. (2010). Differential carbon source utilization by *Campylobacter jejuni* 11168 in response to growth temperature variation. *J Microbiol Methods.* 80(2), 198-202.
- Liochev, S.I. (1999). The mechanism of "Fenton-like" reactions and their importance for biological systems. A biologist's view. *Met Ions Biol Syst.* 36, 1-39.
- Liu, Y.W., and Kelly, D.J. (2015). Cytochrome *c* biogenesis in *Campylobacter jejuni* requires cytochrome *c6* (CccA; Cj1153) to maintain apocytochrome cysteine thiols in a reduced state for haem attachment. *Mol Microbiol.* 96(6), 1298-317.
- Liu, Y. W., Denkmann, K., Kosciow, K., Dahl, C., and Kelly, D.J. (2013). Tetrathionate stimulated growth of *Campylobacter jejuni* identifies a new type of bi-functional tetrathionate reductase (TsdA) that is widely distributed in bacteria. *Mol Microbiol.* 88(1), 173-188.
- Macomber, L., and Imlay, J.A. (2009). The iron-sulfur clusters of dehydratases are primary intracellular targets of copper toxicity. *Proc Natl Acad Sci U S A.* 106(20), 8344-9.
- Manning, G., Duim, B., Wassenaar, T., Wagenaar, J.A., Ridley, A., and Newell, D.G. (2001). Evidence for a Genetically Stable Strain of *Campylobacter jejuni*. *Appl. Environ. Microbiol.* 67, 1185–1189.
- Marchant, J., Wren, B., and Ketley, J. (2002). Exploiting genome sequence: Predictions for mechanisms of *Campylobacter* chemotaxis. *Trends Microbiol.* 10, 155–159.
- Marshall, B., Warren, J.R., Blincow, E., Phillips, M., Goodwin, C.S., Murray, R., Blackbourn, S., Waters, T., and Sanderson, C. (1988). PROSPECTIVE DOUBLE-BLIND TRIAL OF DUODENAL ULCER RELAPSE AFTER ERADICATION OF *CAMPYLOBACTER PYLORI*. *Lancet.* 332, 1437–1442.
- Mattatall, N.R., Jazairi, J., and Hill, B.C. (2000). Characterization of YpmQ, an accessory protein required for the expression of cytochrome *c* oxidase in *Bacillus subtilis*. *J Biol Chem.* 275(37), 28802-9.
- McCrindle, S. L., Kappler, U., and McEwan, A.G. (2005). Microbial dimethylsulfoxide and trimethylamine-*N*-oxide respiration. *Adv Microb Physiol.* 50, 147-198.

- McNally, D. J., Hui, J.P., Aubry, A.J., Mui, K.K., Guerry, P., Brisson, J.R., Logan, S.M., and Soo, E.C. (2006). Functional characterization of the flagellar glycosylation locus in *Campylobacter jejuni* 81-176 using a focused metabolomics approach. *J Biol Chem*, 281(27), 18489-18498.
- McSweegan, E. and Walker, R.I. (1986). Identification and characterization of two *Campylobacter jejuni* adhesins for cellular and mucous substrates. *Infect Immun*. 53(1), 141-148.
- Méjean, V., Iobbi-Nivol, C., Lepelletier, M., Giordano, G., Chippaux, M., and Pascal, M.C. (1994). TMAO anaerobic respiration in *Escherichia coli*: Involvement of the *tor* operon. *Mol Microbiol*. 11(6), 1169-1179.
- Meydan, S., Klepacki, D., Karthikeyan, S., Margus, T., Thomas, P., Jones, J.E., Khan, Y., Briggs, J., Dinman, J.D., Vázquez-Laslop, N., and Mankin, A.S. (2017). Programmed Ribosomal Frameshifting Generates a Copper Transporter and a Copper Chaperone from the Same Gene. *Mol Cell*. 65(2), 207-219.
- Miller, W. G., Bates, A.H., Horn, S.T., Brandl, M.T., Wachtel M.R., and Mandrell R.E. (2000). Detection on surfaces and in Caco-2 cells of *Campylobacter jejuni* cells transformed with new *gfp*, *yfp*, and *cfp* marker plasmids. *Appl Environ Microbiol*. 66(12), 5426-5436.
- Mohammed, K. A., Miles R.J., and Halablab, M.A. (2004). The pattern and kinetics of substrate metabolism of *Campylobacter jejuni* and *Campylobacter coli*. *Lett Appl Microbiol*. 39(3), 261-266.
- Moss, C. W., Kai, A., Lambert, M. A., and Patton, C. (1984). Isoprenoid quinone content and cellular fatty acid composition of *Campylobacter* species. *Journal of clinical microbiology*. 19, 772-776.
- Moss, C. W., Lambert-Fair, M. A., Nicholson, M. A., and Guerrant, G. O. (1990). Isoprenoid quinones of *Campylobacter cryaerophila*, *C. cinaedi*, *C. fennelliae*, *C. hyointestinalis*, *C. pylori*, and "*C. upsaliensis*". *Journal of clinical microbiology*. 28, 395-397.
- Müller, A., Thomas, G.H., Horler, R., Brannigan, J.A., Blagova, E., Levdivkov, V.M., Fogg, M.J., Wilson, K.S., and Wilkinson, A.J. (2005). An ATP-binding cassette-type cysteine transporter in *Campylobacter jejuni* inferred from the structure of an extracytoplasmic solute receptor protein. *Mol Microbiol*. 57(1), 143-155.
- Muraoka, W. T., and Zhang, Q. (2011). Phenotypic and genotypic evidence for L-fucose utilization by *Campylobacter jejuni*. *J Bacteriol*. 193(5), 1065-1075.
- Myers, J. D. & Kelly, D. J. (2005). A sulphite respiration system in the chemoheterotrophic human pathogen *Campylobacter jejuni*. *Microbiology*. 151, 233-242.

- Nachamkin, I., Yang, X. H. & Stern, N. J. (1993). Role of *Campylobacter jejuni* flagella as colonization factors for three-day-old chicks: analysis with flagellar mutants. *Applied and environmental microbiology*. 59, 1269-1273.
- Naikare, H., Butcher, J., Flint, A., Xu, J., Raymond, K.N., and Stintzi, A. (2013). *Campylobacter jejuni* ferric-enterobactin receptor CfrA is TonB3 dependent and mediates iron acquisition from structurally different catechol siderophores. *Metallomics*. 5(8), 988-996.
- Nakamura, K., and GO, N. (2005). Function and molecular evolution of multicopper blue proteins. *Cell Mol Life Sci*. 62(18), 2050-66.
- Nicholls, D.G., and Ferguson, J.S. (2002). In *Bioenergetics 3*, Academic Press, London/San Diego.
- Nothhaft, H., and Szymanski, C.M. (2010). Protein glycosylation in bacteria: sweeter than ever. *Nat. Rev. Microbiol*. 8, 765–778.
- Novik, V., Hofreuter, D., and Galan, J.E. (2010). Identification of *Campylobacter jejuni* genes involved in its interaction with epithelial cells. *Infect Immun*. 78(8), 3540-3553.
- Oelschlaeger, T. A., Guerry, P., and Kopecko, D.J. (1993). Unusual microtubule-dependent endocytosis mechanisms triggered by *Campylobacter jejuni* and *Citrobacter freundii*. *Proc Natl Acad Sci U S A*. 90(14), 6884-6888.
- Oh, J.I., and Kaplan, S. (2002). Oxygen adaptation. The role of the CcoQ subunit of the cbb 3 cytochrome c oxidase of *Rhodobacter sphaeroides* 2.4.1. *J Biol Chem*. 277, 16220–16228.
- Okoli, A.S., Wadstrom, T., and Mendz, G.L. (2007). MiniReview: Bioinformatic study of bile responses in *Campylobacterales*. *FEMS Immunol. Med. Microbiol*. 49, 101–123.
- Olson, C.K., Ethelberg, S., van Pelt, W., and Tauxe, R.V. (2008). Epidemiology of *Campylobacter jejuni* Infections in Industrialized Nations. In: *Campylobacter*. Third edition. Nachamkin, I., Szymanski, C.M. and Blaser, M.J. Eds. ASM Press, Washington D.C.
- Olson, J. W. and Maier, R.J. (2002). Molecular hydrogen as an energy source for *Helicobacter pylori*. *Science*. 298(5599), 1788-1790.
- Onder O., Verissimo A.F., Khalfaoui-Hassani B., Peters A., Koch H.G., and Daldal F. (2017). Absence of Thiol-Disulfide Oxidoreductase DsbA Impairs *cbb₃*-Type Cytochrome *c* Oxidase Biogenesis in *Rhodobacter capsulatus*. *Front Microbiol*. 8, 2576.
- Osman, D., and Cavet, J.S. (2008). Copper homeostasis in bacteria. *Adv Appl Microbiol*. 65, 217-47.

Pajaniappan, M., Hall, J.E., Cawthraw, S.A., Newell, D.G., Gaynor, E.C., Fields, J.A., Rathbun, K.M., Agee, W.A., Burns, C.M., Hall, S.J., Kelly, D.J., and Thompson, S.A. (2008). A temperature-regulated *Campylobacter jejuni* gluconate dehydrogenase is involved in respiration-dependent energy conservation and chicken colonization. *Mol Microbiol.* 68(2), 474-491.

Palumaa, P. (2013). Copper chaperones. The concept of conformational control in the metabolism of copper. *FEBS Lett.* 587(13), 1902-10.

Palyada, K., Sun, Y.Q., Flint, A., Butcher, J., Naikare, H., and Stintzi, A., (2009). Characterization of the oxidative stress stimulon and PerR regulon of *Campylobacter jejuni*. *BMC Genomics.* 10, 481.

Pang, W.L., Kaur, A., Ratushny, A.V., Cvetkovic, A., Kumar, S., Pan, M., Arkin, A.P., Aitchison, J.D., Adams, M.W., and Baliga, N.S. (2013). Metallochaperones regulate intracellular copper levels. *PLoS Comput Biol.* 9(1), e1002880.

Parkhill, J., Wren, B.W., Mungall, K., Ketley, J.M., Churcher, C., Basham, D., Chillingworth, T., Davies, R.M., Feltwell, T., and Holroyd, S. (2000). The genome sequence of the food-borne pathogen *Campylobacter jejuni* reveals hypervariable sequences. *Nature.* 403, 665–668.

Parsons, C.M., Potter, L.M., and Brown, J.R.D. (1982). Effects of dietary protein and intestinal microflora on excretion of amino-acids in Poultry. *Poultry Science.* 61, 939-946.

Pawlik G., Kulajta C., Sachelaru I., Schröder S., Waidner B., Hellwig P., Daldal F., and Koch H.G. (2010). The putative assembly factor CcoH is stably associated with the *cbb₃*-type cytochrome oxidase. *J Bacteriol.* 192(24), 6378-89.

Pearson, B.M., Gaskin, D.J.H., Segers, R.P.A.M., Wells, J.M., Nuijten, P.J.M., and Van Vliet, A.H.M. (2007). The complete genome sequence of *Campylobacter jejuni* strain 81116 (NCTC11828). *J. Bacteriol.* 189, 8402–8403.

Pei, Z., Burucoa, C., Grignon, B., Baqar, S., Huang, X. Z., Kopecko, D. J., Bourgeois, A. L., Fauchere, J. L., and Blaser, M. J. (1998). Mutation in the *peb1A* locus of *Campylobacter jejuni* reduces interactions with epithelial cells and intestinal colonization of mice. *Infection and immunity.* 66, 938-943.

Pesci, E. C., Cottle, D.L., and Pickett, C.L. (1994). Genetic, enzymatic, and pathogenic studies of the iron superoxide dismutase of *Campylobacter jejuni*. *Infect Immun.* 62(7), 2687-2694.

Peterson, J. H., Woolhead, C.A., and Bernstein, H.D. (2003). Basic amino acids in a distinct subset of signal peptides promote interaction with the signal recognition particle. *J Biol Chem.* 278(46), 46155-46162.

Pitcher, R.S., and Watmough, N.J. (2003). The bacterial cytochrome *cbb₃* oxidases. *Biochim Biophys Acta.* 1655(1-3), 388-99.

- Pittman, M. S., Elvers, K. T., Lee, L., Jones, M. A., Poole, R. K., Park, S. F. & Kelly, D. J. (2007). Growth of *Campylobacter jejuni* on nitrate and nitrite: electron transport to NapA and NrfA via NrfH and distinct roles for NrfA and the globin Cgb in protection against nitrosative stress. *Molecular microbiology*. 63, 575-590.
- Poly, F., Threadgill, D., and Stintzi, A. (2004). Identification of *Campylobacter jejuni* ATCC 43431-specific genes by whole microbial genome comparisons. *J Bacteriol*. 186(14), 4781-95.
- Poly, F., Read, T., Tribble, D. R., Baqar, S., Lorenzo, M., and Guerry, P. (2007). Genome sequence of a clinical isolate of *Campylobacter jejuni* from Thailand. *Infection and immunity*. 75, 3425-3433.
- Potter, L. C. and Cole, J.A. (1999). Essential roles for the products of the *napABCD* genes, but not *napFGH*, in periplasmic nitrate reduction by *Escherichia coli* K-12. *Biochem J*. 344 Pt 1, 69-76.
- Potter, L. C., Millington, P., Griffiths, L., Thomas, G.H. and Cole, J.A. (1999). Competition between *Escherichia coli* strains expressing either a periplasmic or a membrane-bound nitrate reductase: Does Nap confer a selective advantage during nitrate-limited growth? *Biochem J*. 344 Pt 1, 77-84.
- Potter, L., Angove, H., Richardson, D., and Cole, J. (2001). Nitrate reduction in the periplasm of Gram-negative bacteria. *Adv Microb Physiol*. 45, 51-112.
- Power, M. E., Guerry, P., McCubbin, W. D., Kay, C. M., and Trust, T. J. (1994). Structural and antigenic characteristics of *Campylobacter coli* FlaA flagellin. *Journal of bacteriology*. 176, 3303-3313.
- Preisig, O., Zufferey, R., and Hennecke, H. (1996). The *Bradyrhizobium japonicum fixGHIS* genes are required for the formation of the high-affinity *cbb₃*-type cytochrome oxidase. *Arch Microbiol*. 165(5), 297-305.
- Prendergast, M.M., Tribble, D.R., Baqar, S., Scott, D.A., Ferris, J.A., Walker, R.I., and Moran, A.P. (2004). In vivo phase variation and serologic response to lipooligosaccharide of *Campylobacter jejuni* in experimental human infection. *Infect Immun*. 72(2), 916-22.
- Purdy, D., Buswell, C.M., Hodgson, A.E., McAlpine, K., Henderson, I., and Leach, S.A. (2000). Characterisation of cytolethal distending toxin (CDT) mutants of *Campylobacter jejuni*. *J Med Microbiol*. 49(5), 473-479.
- Purves, J., Thomas, J., Riboldi, G.P., Zapotoczna, M., Tarrant, E., Andrew, P.W., Londoño, A., Planet, P.J., Geoghegan, J.A., Waldron, K.J., and Morrissey, J.A. (2018). A horizontally gene transferred copper resistance locus confers hyper-resistance to antibacterial copper toxicity and enables survival of community acquired methicillin resistant *Staphylococcus aureus* USA300 in macrophages. *Environ Microbiol*. 20(4), 1576-1589.

- Quintana J., Novoa-Aponte L., and Argüello J.M. (2017). Copper homeostasis networks in the bacterium *Pseudomonas aeruginosa*. *J Biol Chem.* 292(38), 15691-15704.
- Rahman, H., King, R.M., Shewell, L.K., Semchenko, E.A., Hartley-Tassell, L.E., Wilson, J.C., Day, C.J., and Korolik, V. (2014). Characterisation of a multi-ligand binding chemoreceptor CcmL (Tlp3) of *Campylobacter jejuni*. *PLoS Pathog.* 10(1), e1003822.
- Rensing C., and Grass, G. (2003). *Escherichia coli* mechanisms of copper homeostasis in a changing environment. *FEMS Microbiol Rev.* 27(2-3), 197-213.
- Rensing, C., Ghosh, M., and Rosen, B.P. (1999). Families of soft-metal-ion-transporting ATPases. *J Bacteriol.* 181(19), 5891-7.
- Rensing, C., Fan, B., Sharma, R., Mitra, B., and Rosen, B.P. (2000). CopA: An *Escherichia coli* Cu(I)-translocating P-type ATPase. *Proc Natl Acad Sci U S A.* 97(2), 652-6.
- Ribardo, D. A., and Hendrixson, D.R. (2011). Analysis of the LIV system of *Campylobacter jejuni* reveals alternative roles for LivJ and LivK in commensalism beyond branched-chain amino acid transport. *J Bacteriol.* 193(22), 6233-6243.
- Richardson, D. J., and Ferguson, S.J. (1995). Competition between hydrogenperoxide and nitrate for electrons from the respiratory chains of *Thiosphaera pantotropha* and *Rhodobacter capsulatus*. *FEMS Microbiol. Lett.* 132, 125–129.29.
- Rivera-Amill, V., Kim, B.J., Seshu, J., and Konkel, M.E. (2001). Secretion of the Virulence-Associated *Campylobacter* Invasion Antigens from *Campylobacter jejuni* Requires a Stimulatory Signal. *J. Infect. Dis.* 183, 1607–1616.
- Sałaszyńska-Guz, A. and Klimuszko, D. (2008). Functional analysis of the *Campylobacter jejuni* *cj0183* and *cj0588* genes. *Curr Microbiol.* 56(6), 592-596.
- Schaible, U.E., and Kaufmann, S.H. (2005). A nutritive view on the host-pathogen interplay. *Trends Microbiol.* 13(8), 373-80.
- Schroder, W. and Moser, I. (1997). Primary structure analysis and adhesion studies on the major outer membrane protein of *Campylobacter jejuni*. *FEMS Microbiol Lett.* 150(1), 141-147.
- Sebald, M., and Veron, M. (1963). Teneur en Bases de l'ADN et Classification des Vibrions. *Ann. l'Institut Pasteur.* 105, 897–910.
- Sellars, M.J., Hall, S.J., and Kelly, D.J. (2002). Growth of *Campylobacter jejuni* supported by respiration of fumarate, nitrate, nitrite, trimethylamine-N-oxide, or dimethyl sulfoxide requires oxygen. *J. Bacteriol.* 184, 4187–4196.

- Shen, Z., Patil, R.D., Sahin, O., Wu, Z., Pu, X., Dai, L., Plummer, P.J., Yaeger, M.J., and Zhang, Q. (2016). Identification and functional analysis of two toxin-antitoxin systems in *Campylobacter jejuni*. *Mol. Microbiol.* *101*, 909–923.
- Silva J., Leite, D., Fernandes, M., Mena, C., Gibbs, P.A., and Teixeira, P. (2011). *Campylobacter* spp. as a Foodborne Pathogen: A Review. *Front Microbiol.* *2*, 200.
- Singh, K., Senadheera, D.B., Lévesque, C.M., and Cvitkovitch, D.G. (2015). The copYAZ Operon Functions in Copper Efflux, Biofilm Formation, Genetic Transformation, and Stress Tolerance in *Streptococcus mutans*. *J Bacteriol.* *197*(15), 2545-57.
- Sitthisak S., Knutsson, L., Webb, J.W., and Jayaswal, R.K. (2007). Molecular characterization of the copper transport system in *Staphylococcus aureus*. *Microbiology.* *153*(Pt 12), 4274-83.
- Skirrow, M.B. (2006). John McFadyean and the centenary of the first isolation of *Campylobacter* species. *Clin Infect Dis.* *43*(9), 1213-7.
- Smaldone, G.T., and Helmann, J.D. (2007). CsoR regulates the copper efflux operon copZA in *Bacillus subtilis*. *Microbiology.* *153*(Pt 12), 4123-8.
- Smart, J. P., Cliff, M.J. and Kelly, D.J. (2009). A role for tungsten in the biology of *Campylobacter jejuni*: Tungstate stimulates formate dehydrogenase activity and is transported via an ultra-high affinity ABC system distinct from the molybdate transporter. *Mol Microbiol.* *74*(3), 742-757.
- Smith, K.S., and Ferry, J.G. (2000). Prokaryotic carbonic anhydrases. *FEMS Microbiol. Rev.* *24*, 335–366.
- Smith, M. A., Finel, M., Korolik, V., and Mendz, G. L. (2000). Characteristics of the aerobic respiratory chains of the microaerophiles *Campylobacter jejuni* and *Helicobacter pylori*. *Archives of microbiology.* *174*, 1-10.
- Smith, T. (1918). SPIRILLA ASSOCIATED WITH DISEASE OF THE FETAL MEMBRANES IN CATTLE (INFECTIOUS ABORTION). *J. Exp. Med.* *28*, 701–719.
- Song, Y. C., Jin, S., Louie, H., and other authors. (2004). FlaC, a protein of *Campylobacter jejuni* TGH9011 (ATCC43431) secreted through the flagellar apparatus, binds epithelial cells and influences cell invasion. *Molecular microbiology.* *53*, 541-553.
- Sparacino-Watkins, C., Stolz, J.F., and Basu, P. (2014). Nitrate and periplasmic nitrate reductases. *Chem Soc Rev.* *43*(2), 676-706.
- St Maurice, M., Cremades, N., Croxen, M.A., Sisson, G., Sancho, J., and Hoffman, P.S. (2007). Flavodoxin:quinone reductase (FqrB): A redox partner of pyruvate:ferredoxin oxidoreductase that reversibly couples pyruvate oxidation to NADPH production in *Helicobacter pylori* and *Campylobacter jejuni*. *J Bacteriol.* *189*(13), 4764-4773.

- Stadtman, E.R. (1990). Metal ion-catalyzed oxidation of proteins: biochemical mechanism and biological consequences. *Free Radic Biol Med.* 9(4), 315-25.
- Stahl, M., Butcher, J., and Stintzi, A. (2012). Nutrient acquisition and metabolism by *Campylobacter jejuni*. *Front Cell Infect Microbiol.* 2, 5.
- Stahl, M., Friis, L.M., Nothaft, H., Liu, X., Li, J., Szymanski, C.M., and Stintzi, A. (2011). L-fucose utilization provides *Campylobacter jejuni* with a competitive advantage. *Proc Natl Acad Sci U S A.* 108(17), 7194-7199.
- Storz, G., and Imlay, J.A. (1999). Oxidative stress. *Curr. Opin. Microbiol.* 2, 188–194.
- Straw, M.L., Chaplin, A.K., Hough, M.A., Paps, J., Bavro, V.N., Wilson, M.T., Vijgenboom, E., and Worrall, J.A.R. (2018). A cytosolic copper storage protein provides a second level of copper tolerance in *Streptomyces lividans*. *Metallomics.* 10(1), 180-193.
- Szymanski, C.M., Yao, R., Ewing, C.P., Trust, T.J., and Guerry, P. (1999). Evidence for a system of general protein glycosylation in *Campylobacter jejuni*. *Mol. Microbiol.* 32, 1022–1030.
- Szymanski, C. M., Burr, D. H., and Guerry, P. (2002). *Campylobacter* protein glycosylation affects host cell interactions. *Infection and immunity.* 70, 2242-2244.
- Takai, K., Inagaki, F., Nakagawa, S., Hirayama, H., Nunoura, T., Sako, Y., Neilson, K.H., and Horikoshi, K. (2003). Isolation and phylogenetic diversity of members of previously uncultivated epsilon-Proteobacteria in deep-sea hydrothermal fields. *FEMS Microbiol. Lett.* 218, 167–174.
- Tareen, A. M., Dasti, J.I., Zautner, A.E., Gross, U., and Lugert R. (2011). Sulphite : cytochrome *c* oxidoreductase deficiency in *Campylobacter jejuni* reduces motility, host cell adherence and invasion. *Microbiology.* 157(Pt 6), 1776-1785.
- Taveirne, M. E., Sikes, M.L., and Olson, J.W. (2009). Molybdenum and tungsten in *Campylobacter jejuni*: Their physiological role and identification of separate transporters regulated by a single ModE like protein. *Mol Microbiol.* 74(3), 758-771.
- Thibault, P., Logan, S. M., Kelly, J. F., Brisson, J. R., Ewing, C. P., Trust, T. J. & Guerry, P. (2001). Identification of the carbohydrate moieties and glycosylation motifs in *Campylobacter jejuni* flagellin. *The Journal of biological chemistry.* 276, 34862-34870.
- Thomas, M. T., Shepherd, M., Poole, R.K., van Vliet, A.H., Kelly, D.J., and Pearson, B.M. (2011). Two respiratory enzyme systems in *Campylobacter jejuni* NCTC 11168 contribute to growth on L-lactate. *Environ Microbiol.* 13(1), 48-61.
- Thompson, A.K., Gray, J., Liu, A., and Hosler, J.P. (2012). The roles of *Rhodobacter sphaeroides* copper chaperones PCu(A)C and Sco (PrrC) in the assembly of the copper centers of the *aa₃*-type and the *cbb₃*-type cytochrome *c* oxidases. *Biochim Biophys Acta.* 1817(6), 955-64.

ThönyMeyer, L. (1997). Biogenesis of respiratory cytochromes in bacteria. *Microbiol Mol Biol Rev.* 61(3), 337-376.

Trasnea, P.I., Utz, M., Khalfaoui-Hassani, B., Lagies, S., Daldal, F., and Koch, H.G. (2016). Cooperation between two periplasmic copper chaperones is required for full activity of the *cbb₃*-type cytochrome *c* oxidase and copper homeostasis in *Rhodobacter capsulatus*. *Mol Microbiol.* 100(2), 345-61.

Trasnea, P.I., Andrei, A., Marckmann, D., Utz, M., Khalfaoui-Hassani, B., Selamoglu, N., Daldal, F., and Koch, H.G. (2018). A Copper Relay System Involving Two Periplasmic Chaperones Drives *cbb₃*-Type Cytochrome *c* Oxidase Biogenesis in *Rhodobacter capsulatus*. *ACS Chem Biol.* 13(5), 1388-1397

Trumpower, B. L. (1990). Cytochrome *bc₁* complexes of microorganisms. *Microbiological reviews.* 54, 101-129.

Trust, T.J., Logan, S.M., Gustafson, C.E., Romaniuk, P.J., Kim, N.W., Chan, V.L., Ragan, M.A., Guerry, P. and Gutell, R.R. (1994). Phylogenetic and molecular characterization of a 23S rRNA gene positions the genus *Campylobacter* in the epsilon subdivision of the Proteobacteria and shows that the presence of transcribed spacers is common in *Campylobacter* spp. *J Bacteriol.* 176(15), 4597-609.

Untergasser, A., Nijveen, H., Rao, X., Bisseling, T., Geurts, R., and Leunissen, J.A. (2007). Primer3Plus, an enhanced web interface to Primer3. *Nucleic Acids Res.* 35(Web Server issue):W71-4.

van Mourik, A., Bleumink-Pluym, N.M., van Dijk, L., van Putten, J.P., and Wosten, M.M. (2008). Functional analysis of a *Campylobacter jejuni* alkaline phosphatase secreted via the Tat export machinery. *Microbiology.* 154(Pt 2), 584-592.

van Sorge, N. M., Bleumink, N. M., van Vliet, S. J., Saeland, E., van der Pol, W. L., van Kooyk, Y., and van Putten, J. P. (2009). N-glycosylated proteins and distinct lipooligosaccharide glycoforms of *Campylobacter jejuni* target the human *c*-type lectin receptor MGL. *Cellular microbiology.* 11, 1768-1781.

van Vliet, A.H., and Ketley, J.M. (2001) Pathogenesis of enteric *Campylobacter* infection. *Symp Ser Soc Appl Microbiol.* 45S-56S.

Vandamme, P., Debruyne, L., De Brandt, E., and Falsen, E. (2010). Reclassification of *Bacteroides ureolyticus* as *Campylobacter ureolyticus* comb. nov., and emended description of the genus *Campylobacter*. *Int J Syst Evol Microbiol.* 60(Pt 9), 2016-22.

Vandamme, P., Harrington, C.S., Jalava, K., and On, S.L. (2000). Misidentifying *helicobacters*: the *Helicobacter cinaedi* example. *J Clin Microbiol.* 38(6), 2261-6.

Vargas, C., McEwan, A.G., and Downie, J.A. (1993). Detection of *c*-type cytochromes using enhanced chemiluminescence. *Anal Biochem.* 209(2), 323-326.

Vegge, C. S., Brondsted, L., Li, Y.P., Bang, D.D., and Ingmer, H. (2009). Energy taxis drives *Campylobacter jejuni* toward the most favorable conditions for growth. *Appl Environ Microbiol.* 75(16), 5308-5314.

Velayudhan, J. and Kelly, D.J. (2002). Analysis of gluconeogenic and anaplerotic enzymes in *Campylobacter jejuni*: An essential role for phosphoenolpyruvate carboxykinase. *Microbiology.* 148(Pt 3), 685-694.

Velayudhan, J., Jones, M.A., Barrow, P.A. and Kelly, D.J. (2004). L-serine catabolism via an oxygen-labile L-serine dehydratase is essential for colonization of the avian gut by *Campylobacter jejuni*. *Infect Immun.* 72(1), 260-268.

Véron, M., Lenoisé-Furet, A., and Beaune, P. (1981). Anaerobic respiration of fumarate as a differential test between *Campylobacter fetus* and *Campylobacter jejuni*. *Curr. Microbiol.* 6, 349-354.

Wassenaar, T.M., and Blaser, M.J. (1999). Pathophysiology of *Campylobacter jejuni* infections of humans. *Microbes Infect.* 1(12), 1023-33.

Wassenaar, T. M., Bleumink-Pluym, N.M., and van der Zeijst, B.A. (1991). Inactivation of *Campylobacter jejuni* flagellin genes by homologous recombination demonstrates that *flaA* but not *flaB* is required for invasion. *EMBO J.* 10(8), 2055-2061.

Wassenaar, T.M., Van Der Zeijst, B.A., Ayling, R., and Newell, D.G. (1993). Colonization of chicks by motility mutants of *Campylobacter jejuni* demonstrates the importance of flagellin A expression. *J. Gen. Microbiol.* 139, 1171–1175.

Watson, R.O. and Galán, J.E. (2008a). Interaction of *Campylobacter jejuni* with Host Cells. In: Nachamkin, I. *et al.* (ed.) *Campylobacter*. 3rd ed. Chapter 16. ASM Press, Washington, DC.

Watson, R.O., and Galan, J.E. (2008b) *Campylobacter jejuni* survives within epithelial cells by avoiding delivery to lysosomes. *PLoS Pathog.* 4, e14.

Weerakoon, D.R. and Olson, J.W. (2008). The *Campylobacter jejuni* NADH:ubiquinone oxidoreductase (complex I) utilizes flavodoxin rather than NADH. *J Bacteriol.* 190(3), 915-925.

Weerakoon, D. R., Borden, N.J., Goodson, C.M., Grimes, J., and Olson, J.W. (2009). The role of respiratory donor enzymes in *Campylobacter jejuni* host colonization and physiology. *Microb Pathog.* 47(1), 8-15.

Weiner, J. H., Rothery, R. A., Sambasivarao, D., and Trieber, C. A. (1992). Molecular analysis of dimethylsulfoxide reductase: a complex iron-sulfur molybdoenzyme of *Escherichia coli*. *Biochimica et biophysica acta.* 1102, 1-18.

Weingarten, R. A., Grimes, J. L., and Olson, J. W. (2008). Role of *Campylobacter jejuni* respiratory oxidases and reductases in host colonization. *Applied and environmental microbiology.* 74, 1367-1375.

- Weingarten, R. A., Taveirne, M. E., and Olson, J. W. (2009). The dual-functioning fumarate reductase is the sole succinate:quinone reductase in *Campylobacter jejuni* and is required for full host colonization. *Journal of bacteriology*. *191*, 5293-5300.
- Westfall, H. N., Rollins, D.M., and Weiss, E. (1986). Substrate utilization by *Campylobacter jejuni* and *Campylobacter coli*. *Appl Environ Microbiol*. *52*(4), 700-705.
- Whitehouse, C.A., Balbo, P.B., Pesci, E.C., Cottle, D.L., Mirabito, P.M., and Pickett, C.L. (1998) *Campylobacter jejuni* cytolethal distending toxin causes a G2-phase cell cycle block. *Infect Immun*. *66*, 1934-1940.
- Williams, C.L., Neu, H.M., Gilbreath, J.J., Michel, S.L., Zurawski, D.V., and Merrell, D.S. (2016). Copper Resistance of the Emerging Pathogen *Acinetobacter baumannii*. *Appl Environ Microbiol*. *82*(20), 6174-6188.
- Winter, S. E., Winter, M.G., Xavier, M.N., Thiennimitr, P., Poon, V., Keestra, A.M., Laughlin, R.C., Gomez, G., Wu, J., Lawhon, S.D., Popova, I.E., Parikh, S.J., Adams, L.G., Tsois, R.M., Stewart, V.J., and Baumler, A.J. (2013). Host-derived nitrate boosts growth of *E. coli* in the inflamed gut. *Science*. *339*(6120), 708-711.
- Woodall, C. A., Jones, M.A., Barrow, P.A., Hinds, J., Marsden, G.L., Kelly, D.J., Dorrell, N., Wren B.W., and Maskell, D.J. (2005). *Campylobacter jejuni* gene expression in the chick cecum: Evidence for adaptation to a low-oxygen environment. *Infect Immun*. *73*(8), 5278-5285.
- Wösten, M.M.S.M., Wagenaar, J.A., and Van Putten, J.P.M. (2004). The FlgS/FlgR Two-component Signal Transduction System Regulates the *fla* Regulon in *Campylobacter jejuni*. *J. Biol. Chem*. *279*, 16214–16222.
- Wright, J. A., Grant, A.J., Hurd, D., Harrison, M., Guccione, E., Kelly, D.J. and Maskell, D.J. (2009). Metabolite and transcriptome analysis of *Campylobacter jejuni* *in vitro* growth reveals a stationary-phase physiological switch. *Microbiology*. *155*(Pt 1), 80-94.
- Yamamoto, K., and Ishihama, A. (2005). Transcriptional response of *Escherichia coli* to external copper. *Mol Microbiol*. *56*(1), 215-27.
- Yamaoka, Y. (2008). Roles of *Helicobacter pylori* BabA in gastroduodenal pathogenesis. *World J Gastroenterol*. *14*(27), 4265-72.
- Yamasaki, M., Igimi, S., Katayama, Y., Yamamoto, S., and Amano, F. (2004). Identification of an oxidative stress-sensitive protein from *Campylobacter jejuni*, homologous to rubredoxin oxidoreductase/rubrerhythrin. *FEMS microbiology letters*. *235*, 57-63.
- Yao, R., Burr, D.H., Doig, P., Trust, T.J., Niu, H., and Guerry, P. (1994). Isolation of motile and non-motile insertional mutants of *Campylobacter jejuni*: The role of motility in adherence and invasion of eukaryotic cells. *Mol Microbiol*. *14*(5), 883-893.

Young, K.T., Davis, L.M., and Dirita, V.J. (2007). *Campylobacter jejuni*: molecular biology and pathogenesis. *Nat. Rev. Microbiol.* 5, 665–679.

Young, N.M., Brisson, J.R., Kelly, J., Watson, D.C., Tessier, L., Lanthier, P.H., Jarrell, H.C., Cadotte, N., St. Michael, F., Aberg, E., *et al.* (2002). Structure of the N-linked glycan present on multiple glycoproteins in the gram-negative bacterium, *Campylobacter jejuni*. *J. Biol. Chem.* 277, 42530–42539.

Young, R. (2014). Phage lysis: Three steps, three choices, one outcome. *J. Microbiol.* 52, 243–258.

Zautner, A.E., Lugert, R., Masanta, W.O., Weig, M., Groß, U., and Bader, O. (2016). Subtyping of *Campylobacter jejuni* ssp. *doylei* Isolates Using Mass Spectrometry-based PhyloProteomics (MSPP). *J Vis Exp.* (116).

Zhao, X., Norris, S.J., and Liu, J. (2014). Molecular architecture of the bacterial flagellar motor in cells. *Biochemistry.* 53(27), 4323-33.

Zilbauer, M., Dorrell, N., Wren, B.W., and Bajaj-Elliott, M. (2008). *Campylobacter jejuni*-mediated disease pathogenesis: an update. *Trans R Soc Trop Med Hyg.* 102(2), 123-9.

Ziprin, R. L., Young, C.R., Byrd, J.A., Stanker, L.H., Hume, M.E., Gray, S.A., Kim, B.J., and Konkel, M.E. (2001). Role of *Campylobacter jejuni* potential virulence genes in cecal colonization. *Avian Dis.* 45(3), 549-557.

Ziprin, R.L., Young, C.R., Byrd, J.A., Stanker, L.H., Hume, M.E., Gray, S.A., Kim, B.J., and Konkel, M.E. (2014). Role of *Campylobacter jejuni* potential virulence genes in cecal colonization. *Avian Dis.* 45, 549–557.

Appendix

